Regulatory elements in the terpenoid biosynthesis of defensive secretions in leaf beetle larvae

Dissertation

To Fulfill the
Requirements for the Degree of „doctor rerum naturalium“
(Dr. rer. nat.)

Submitted to the Council of the Faculty
of Biology and Pharmacy
of the Friedrich Schiller University Jena

by Dipl. Biol. Sindy Frick
born on 06.02.1981
in Jena

1. Gutachter: Prof. Dr. Wilhelm Boland, Max Planck Institute for Chemical Ecology, Jena

2. Gutachter: Prof. Dr. Jonathan Gershenzon, Max Planck Institute for Chemical Ecology, Jena

3. Gutachter: Prof. Dr. Monika Hilker, Freie Universität Berlin

Tag der öffentlichen Disputation: 08.01.2014

For me and you!

CONTENTS

1 INTRODUCTION

Terpenoids are one of the most structurally and stereochemically diverse family of natural products. They are often cyclized and rearranged in a complex manner resulting in more than 55.000 known structures present in Eukaryota, Bacteria and Archaea (1). The imposing numbers of compounds come along with a multitude of different functions and are part of primary as well as secondary metabolism. For instance, they are essential compounds of membranes, e.g. sterols (eukaryotes), hopanoids (Bacteria) and prenyllipids (Archaea) (2-4) or serve as modifications for membrane components (5, 6). Plastoquinone, phylloquinone and ubiquinone are associated with the electron transport chains (7, 8), while carotenoids and the phytol side chain of chlorophyll are essential for photosynthesis (9, 10). Other terpenoids function as hormones like gibberellins in plants (11), juvenile hormones (JH) in insects (12) and steroid hormones in animals (13). Nevertheless, most terpenoids are secondary metabolites and predominantly shape the pleasant smell or spicy taste of e.g. citrus fruits, eucalyptus, lemon grass, rosemary, sage, and peppermint species - acting thereby as toxins, repellents or attractants to other organisms. This leads to the assumption that they have ecological roles in antagonistic or mutualistic interactions (14, 15).

Terpenes are named after the isolated hydrocarbon from the conifer secretion called turpentine. The chemical compositions of turpentine are mainly compounds with the molecular formula $C_{10}H_{16}$ which laid the foundation for further terminology. Wallach proposed 1887 that *mono*terpenoids are constructed by two isoprene units, each considered as *hemi*terpene, which are the basal building block for all terpenes (16, 17). Following this formal logic Ruzicka approved the proposed “isoprenic rule” of Wallach also for longer terpenoid compounds. Later, Lynen and Bloch completed this terminology and discover the biosynthesis of terpenes. Due to all this, terpenes are classified by the number of constituent isoprene units. Products which contain three units are named *sesqui*terpenes, those containing four units *di*terpenes and so on (18-20). In nature, macromolecular structures with more than 30 isoprene units are found ubiquitary in the primary metabolism and classified as *poly*terpenes (21). The first two carbon skeletons precisely identified are those of the sesquiterpenes α-santalen (1910) and farnesol (1913) (22-24).

1.1 TERPENE BIOSYNTHESIS

Despite their structural diversity, terpenes derive from the universal C_5 isoprene units isopentenyl diphosphate (IDP) and dimethylallyl diphosphate (DMADP) synthesized *via* the mevalonate (MVA) pathway or the methylerythritol phosphate (MEP) pathway (25-27). While Gram-negative bacteria exclusively use the MEP pathway, Archaea and Eukaryota (except plants) exhibit only the enzymes of the MVA pathways (28, 29). Plants are able to produce isoprenes *via* both pathways although both of them are localized in different cell compartments (30). The precursor of the MVA derived isoprene units is activated acetic acid, the so called acetyl-coenzyme A (Fig. 1). Two equivalents of acetyl-CoA couple to acetoacetyl-CoA, similar to a Claisen condensation. The acetoacetyl-CoA reacts further with another acetyl-CoA to form 3-hydroxy-3-methylglutaryl-CoA (HMG). These reactions are followed by an enzymatic reduction with NADPH + H^+ and catalyzed by the 3-hydroxy-3-methylglutaryl-CoA reductase (HMGR) to generate (R)-mevalonic acid. Afterwards, three enzymatic reactions consuming adenosine triphosphate (ATP) phosphorylate mevalonic acid. Decarboxylation and elimination of H_2O generate activated IDP which can easily be isomerized by an isoprenyl diphosphate isomerase (IDI) to DMADP. Both compounds are kept in equilibrium (31-36).

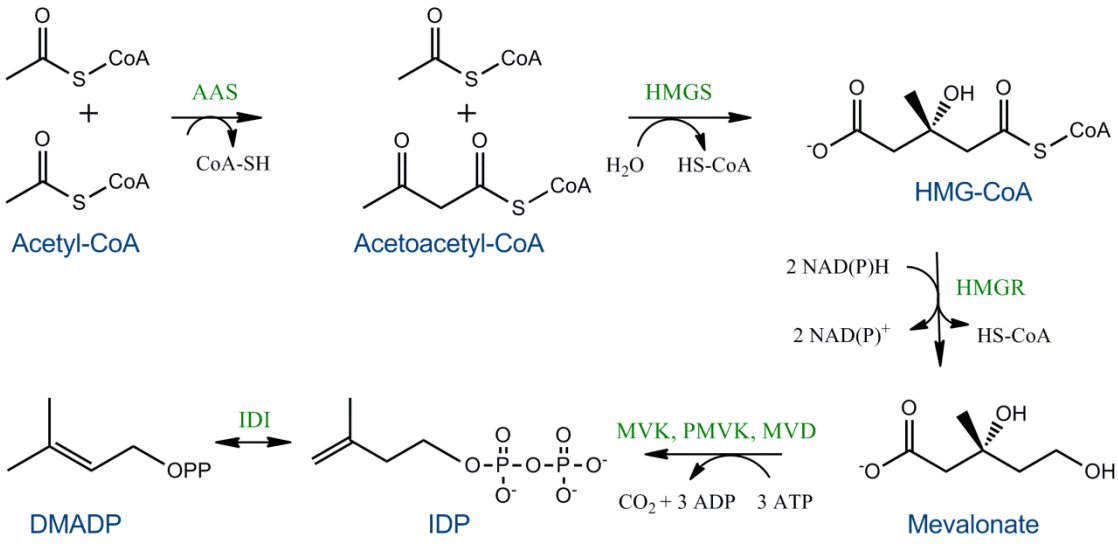

Fig. 1: Biosynthesis of IDP and DMADP *via* the mevalonate pathway. AAS, acetoacetyl-CoA synthase; HMGS, HMG-CoA synthase; HMGR, HMG-CoA reductase; MVK, mevalonate kinase; PMVK, phosphomevalonate kinase; MVD, mevalonate diphosphate decarboxylase; IDI, isoprenyl diphosphate isomerase; IDP, isopentenyl diphosphate; DMADP, dimethylallyl diphosphate.

DMADP and IDP are further condensed to linear diphosphate intermediates resulting in C_{10} (geranyl diphosphate; GDP), C_{15} (farnesyl diphosphate; FDP), C_{20} (geranylgeranyl diphosphate; GGDP) or even much larger carbon skeletons (Fig. 2).

The alkylation reaction is catalyzed by isoprenyl diphosphate synthases (IDSs) belonging to the terpenoid synthase superfamily (29, 37-40). They are additionally classified as *cis*- or *trans*-IDSs depending on the stereochemistry of the double-bond in their formed products (41, 42). In general, *cis*-IDSs synthesize long-chain products (C_{50} – $C_{\sim 5000}$) although some short-chain producing enzymes are known (43-46). *Trans*-IDSs usually synthesize products up to C_{50}. Most of these acyclic precursors are further modified by subsequent cyclization and/or rearrangements catalyzed by terpene synthases to produce the huge variety of terpene metabolites (47, 48).

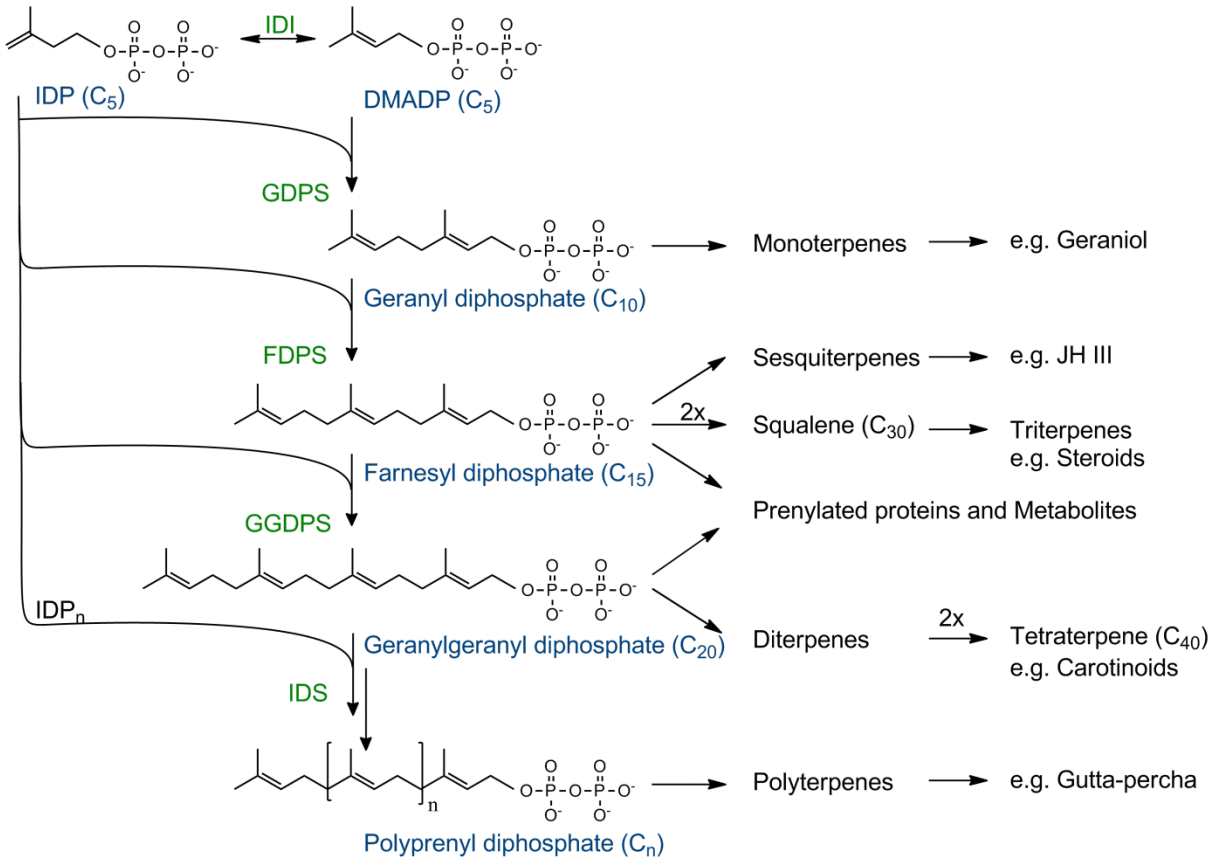

Fig. 2: Biosynthesis of various terpene classes. IDI, isoprenyl diphosphate isomerase; IDP, isopentenyl diphosphate; DMADP, dimethylallyl diphosphate; GDPS, *trans*-geranyl diphosphate synthase; FDPS, *trans*-farnesyl diphosphate synthase; GGDPS, *trans*-geranylgeranyl diphosphate synthase; JH III, juvenile hormone III.

1.2 Branch point enzymes within MVA pathway

1.2.1 3-Hydroxy-3-MethylGlutaryl-CoA Reductase (HMGR)

IDP and DMADP can originate from the MVA pathway (12). An important rate-limiting enzyme within this pathway is HMGR (EC 1.1.1.34). It catalyzes the four-electron reduction of (S)-HMG-CoA to the carboxylic acid (R)-mevalonate utilizing two molecules of NADPH (49) (Fig. 3). Homologs of these highly conserved enzymes are found in eukaryotes, prokaryotes and Archaea. *Via* sequence comparisons of the catalytic center two distinct classes can be identified. The sequence identities within one class are around 33-65% whereas the classes compared to each other represent only 14-22% identical residues (50). Class II enzymes are primarily present as soluble proteins in the cytoplasm of Eubacteria and some Archaea utilizing NADH as electron donor. The HMGR of *Pseudomonas mevalonii* was the first structurally and biochemically characterized enzyme of the class II proteins (51-53).

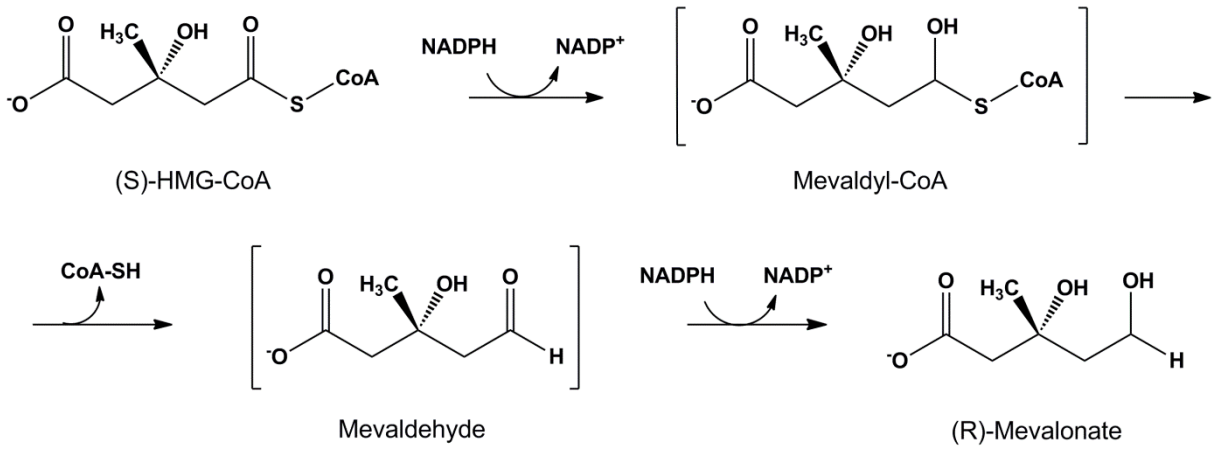

Fig. 3: Reaction mechanism of the biosynthesis of (R)-Mevalonate catalyzed by HMGR.

HMGRs of eukaryotes and most archaea are glucoproteins belonging to the class I enzymes. They typically utilize NADPH as electron donor. Class I enzymes consist of two distinct domains, a hydrophobic NH_2-terminal membrane anchor and a COOH-terminal catalytic domain extending into the cytoplasm (50, 54, 55). The poorly conserved N-terminus anchors the enzyme with 2 to 8 transmembrane α-helices, specifically for each species, in the membrane of the endoplasmatic reticulum (56). The membrane

domain and the highly conserved catalytic domain are connected *via* a non-conserved hydrophilic linker region. The crystal structure of the human HMGR catalytic domain (PDB DQ8, 1DQ9, 1DQA) comprises a homotetrameric structure with asymmetrically arranged monomers (54, 55). The C-terminal domains of two monomers form a dimeric structure to build the active site in which each monomer-unit contributes residues necessary for catalysis (54, 57, 58). This reaction takes place in two sequential hydride transfers from NADPH, in which HMG-CoA is reduced to mevalonate. A protonated histidine residue plays a critical role in this catalysis by donating a proton to the thiol anion after the first reduction. The substrate binding induces closure of the C-terminal helix, moving the catalytic histidine in an optimal position completing the active site (49, 57, 59).

REGULATORY PROCESSES CONCERNING HMGR ACTIVITY

HMGR is uniquely suited as a primary branch point within terpene biosynthesis catalyzing a costly and irreversible reaction. Thus, HMGR activity influences the output of the MVA pathway regulation of this enzyme is highly important to prevent surplus production of intermediate. This occurs indeed by several regulatory mechanisms on transcriptional (60-62), translational as well as post-translational level (63-65).

For instance, the N-terminal membrane anchor usually includes a regulatory sterol-sensing domain (SSD) which binds lipids and plays an important role in HMGR-activity regulation (59, 66-68). Mammalian HMGR displays a sterol-mediated feedback inhibition at transcriptional levels and *via* degradation of the enzyme. This ensures that sterol synthesis does not exceed requirements (66). Additionally, in both mammals and yeast a non-sterol isoprenoid signal positively regulates the rate of HMGR degradation under high concentrations of the intermediate FDP (69, 70). Moreover, AMP-activated protein kinase (AMPK) phosphorylates a conserved amino residue in the active center which decreases the affinity for NADPH due to the interference with the closure flap of the C-terminal site. Along with AMPK, protein phosphatase 2A (PP2A) plays an important role in HMGR regulation since its ability to fully restore HMGR activity by dephosphorylation (49, 59, 71). Furthermore, HMGR can be influenced on the level of translation by non-sterol isoprenoids and may involve the 5′- untranslated region of the HMGR-mRNA. However, this aspect of regulation has received limited attention and the mechanism is not clear yet (63, 66).

1.2.2 Isoprenyl Diphosphate Synthases (IDSs)

Although HMGR constitutes a key enzyme of the early steps of terpenoid biosynthesis, IDSs can act further downstream as regulatory branch points (Fig. 2) (47). IDSs produce prenyl diphosphates - the general backbones for the biosynthesis of the whole variety of terpenes. Therefore, a stringent regulation of these reactions has to be coordinated.

REGULATORY PROCESSES CONCERNING IDS ACTIVITY

In plants, the transcriptional regulation of IDSs genes within different developmental stages or tissues was observed in various species (72-75). For example, the transcript level of *fdps,* which is involved in the withanolide biosynthesis of *Withania somnifera,* was significantly elevated in response to salicylic acid, methyl jasmonate and mechanical wounding. The accumulation of corresponding mRNA was detected in most organs but showed maximum expression in flowers and young leafs which indicates differential regulation (76). In Norway spruce, the formation of traumatic resin ducts correlated with higher amounts of terpenes and an upregulation of IDSs genes producing GDP or GGDP after treatment with methyl jasmonate (77). Differential expression of IDSs genes was also observed in Lepidoptera larvae for two FPDSs homologs. Genes of type-I IDSs were demonstrated to be ubiquitously expressed in all tissues, whereas the type-II transcripts were nearly 20 times more abundant and essentially restricted to the JH producing glands of insect larvae (78). Nevertheless, the mechanisms of transcriptional and translational regulation are not well investigated yet.

Regulation of IDS activity, especially product and substrate specificity, is not well understood in detail right now. In *Artemisia tridentata ssp. Spiciformis*, three FDPS isoforms were identified with sequence similarity greater than 89%. Biochemical characterization revealed that FDPS1 and FDPS2 synthesized FDP, whereas their kinetic behavior and substrate specificity varied. In contrast, FDPS5 synthesized GDP when incubated with IDP and DMADP but also produced two irregular monoterpenoids, namely chrysanthemyl diphosphate and lavandulyl diphosphate, when incubated only with DMADP (72). Two isolated FDPS enzymes from *Myzus persicae* showed 82% sequence similarity but revealed altered functionality. Amino acid exchanges with different hydrophobicity resulted in conformational change of the catalytic pocket (79).

Aphid enzymes often displayed a dual GDPS/FDPS activity. Increasing concentrations of DMADP led to increasing proportions of the GDP product (80-83).

Additional alteration of enzymatic activity in case of different co-factors was observed. Literature describes Mg^{2+} and Mn^{2+} as the common co-factors for IDSs but analysis showed that both co-factors are not eqivalent and altered the prenyl coupling in insects like *Myzus persicae* or *Choristoneura fumiferana* (80-85). Although it has been shown that Zn^{2+}, Ni^{2+} or Co^{2+} influence enzyme activity in microorganisms (86, 87) and plants, e.g. *Abies grandis* (88), but the mechanisms behind these effects are not known. Summing up, these results of coordinated regulation on transcriptional as well as post-translational level (e.g. product specificity) indicate that the enzymes conduct the biosynthesis and the metabolic flux of terpenes.

STRUCTURAL CHARACTERISTICS OF IDSS

Further explanations will focus on *trans*-scIDSs due to the more detailed knowledge and ubiquitous appearance in all living organisms. *Trans*-IDSs can be divided into enzymes generating short-chain (scIDS, C_{10}-C_{20}), medium-chain (C_{25}-C_{35}), and long-chain (C_{40}-C_{50}) products (89). These enzymes remarkably differ in their selectivity to the chain-length of their substrates and products (37, 90, 91) and are further classified according to the chain-length of their main product. For instance, geranyl diphosphate synthases (GDPSs; EC 2.5.1.1) catalyze the coupling of the homoallylic IDP with the allylic DMADP resulting in GDP, the ubiquitous C_{10}-building block of monoterpenes. Farnesyl diphosphate synthases (FDPSs; EC 2.5.1.10) produce FDP, the C_{15} precursor of sequiterpenes and triterpenes (C_{30}), and geranylgeranyl diphosphate synthases (GGDPSs; EC 2.5.1.29) produce GGDP, the C_{20} backbone of diterpenes and the precursors for tetraterpenes (C_{40}). FDPS and GGDPS are typical representatives of scIDSs since their products are apparently required by all living organisms (92).

In 1994, the first crystallized scIDS, an a*via*n FDPS, shed light onto the protein structure and catalytic activity of this enzyme class (93). Members of the scIDS family share a common protein fold and appear typically as homodimers (94) at which each monomer possesses a fully equipped catalytic center. This is nested within an α-helical bundle, regularly built up by 12 helices, containing allylic binding regions. All identified enzymes show characteristic and highly conserved motifs, so they may have evolved from a common ancestor (93). The obvious conserved regions are the first aspartate rich motif (FARM) with the amino acid sequence DDxx(xx)D and the second aspartate rich

motif (SARM) with the sequence DDxxD. These motifs are crucial for the direct enzyme's catalytic effect due to the binding of the substrates and co-factors. While FARM represents the binding site of the allylic substrate, SARM is known to bind IDP. Both motifs are located on opposite walls within the active cavity and facing each other (1, 21, 40, 81, 82). IDSs need a trinuclear metal cluster for activation, usually Mg^{2+} or Mn^{2+}, which complex with the aspartates as well as with IDP (95). Two pairs of aspartates from FARM and SARM coordinate the corresponding diphosphate of the substrates for catalytic cleavage.

ALKYLATION MECHANISM OF *TRANS*-IDS

Generally, catalysis by scIDSs follows a sequential mechanism named "head-to-tail alkylation" (Fig. 4).

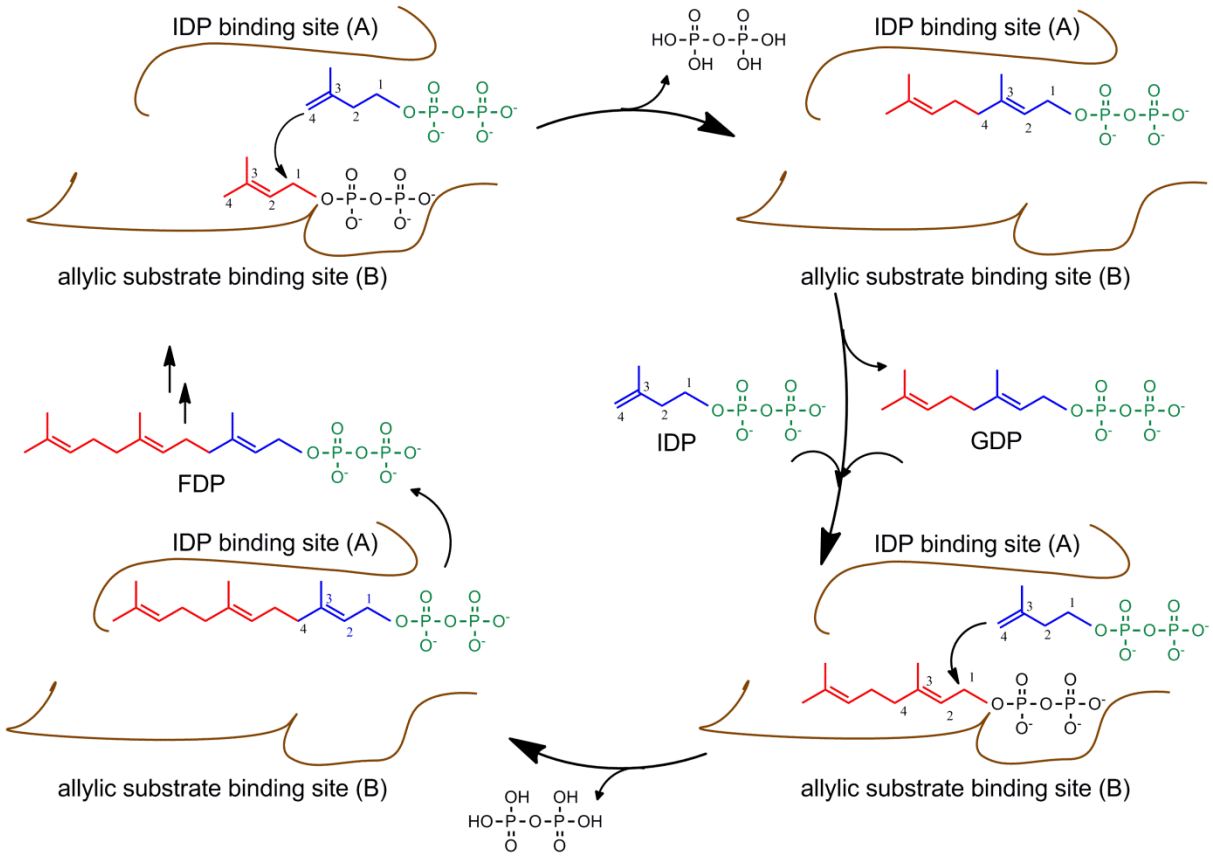

Fig. 4: Principle catalytic mechanism of the "head-to-tail alkylation" of scIDS (modified by (96)).

The coupling is generated by ionization of the allylic diphosphate precursor followed by cleavage of the carbon–oxygen bond of DMADP. The carbocation attacks the C3–C4 double bond of IDP to form a tertiary carbocationic intermediate that loses a proton

from C2 whereby generating an allylic product. This dissociative electrophilic alkylation forms a new carbon-carbon double bond between the C1 of the allylic carbocation and the C4 of IDP (1, 94-96). The hydrocarbon tail of DMADP extends into the active cavity that accommodates the growing carbon chain. The IDP binding region (A) positions the C4 of IDP close to the C1 of the allylic substrate located at binding site (B). The sequential addition of IDP to the growing chain proceeds through the release of the cleaved diphosphate from (B), rearrangement of the formed product from (A) to (B), binding of another IDP in (A) and followed by the same reactions as before (94).

A substantial and also intriguing question is how IDSs regulate and determine chain-length and thereby product specificity. Studies on IDSs using data acquired by sequence comparison, site-directed mutagenesis and crystallography resulted in the common idea of the "molecular-ruler-theory". In principle, amino acids located upstream and downstream of FARM have been assigned as the main chain-length determination region (CLD). These residues limit the deepness/size by building a bottom within the catalytic cavity which accommodates the growing carbon chain and therefore restricts the final product length (24, 63-65). Depending on the position upstream of the FARM region, the lengths of the cavity differ. For FDPS residues located at the fourth and fifth position mainly regulate C_{15} chain-length (Fig. 5) (42, 47, 80-82, 97-106).

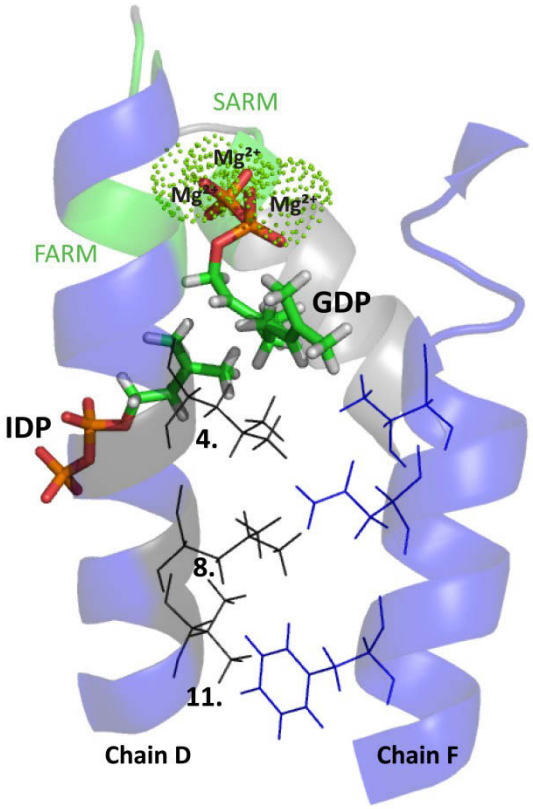

Fig. 5: Homology model of *sc*IDS displaying chain-length-determination (CLD) region. Chain D housing the DDxxD motif of FARM (green). SARM (green) is located at the gray helix in the background. Dotted spheres are the trinuclear metal cluster generated by Mg^{2+}. The blue helices are determined as the main CLD area. IDP and GDP are displayed as possible substrates for *sc*IDS. Chain elongation to form FDP would be oriented downwards. Amino acids of chain D at position 4, 8 and 11 as well as residues of chain F are shown to illustrate the possible steric conflict with a growing carbon chain.

With increasing number of 3D structures for prenyltransferases, the mechanism of chain-length determination has just begun to emerge. Newer findings showed that besides these residues also amino acids located at the dimer interface influence chain-length specificity. Mutation studies clearly indicated that the monomers have an impact on each other and therefore also regulate chain-length specificity (98, 107).
Furthermore, early studies described the role of metal co-factors on IDS activity. They displayed a significant influence on enzyme activity and chain-length of the product (108-111). In using different divalent metals co-factors like Co^{2+}, Mn^{2+} and Zn^{2+} besides the common Mg^{2+}, they observed products which were shifted by one to two units longer than those obtained with Mg^{2+} (86, 87, 110, 111). These results depict clearly, that chain lengths specificity can not only be influenced by steric hindrance of interacting residues, the general statement of the "molecular-ruler-theory", but also by metal co-factors itself. However, the final mechanism is not clarified yet.

1.3 TERPENES IN INSECTS

Most of the knowledge regarding terpene metabolism resulted from extensively investigated plants. But also insects synthesize terpenes, such as hormones, pheromones or allomones. Juvenile hormones, for instance, are a group of essential acyclic sesquiterpenoids produced by all insects to regulate development, reproduction and diapause. Pheromones and allomones are signal compounds in order to communicate intra- and interspecifically to find mating partners, to warn, to mark food sources, to aggregate or to defend themselves against predators. Aggregation pheromones like the monoterpenoid ipsdienol produced by bark beetles coordinate the colonization of coniferous trees (112-114). Furthermore, different aphid species produce the sex pheromones nepetalactone and nepetalactol (cyclopentanoid monoterpenes) to find possible mating partners (115-117). The sesquiterpenoid alarm pheromone *(E)*-β-farnesene warns the aphid community in case of an attack (118).

1.3.1 Defense strategies of Chrysomelidae larvae

Many insects reside at the bottom of the food chain and are highly exposed to predators. Therefore, protection against natural enemies is indispensable, especially in early developmental stages, to reach fertility and to produce offspring to ensure the evolutionary survival of the species. Especially Chrysomelina larvae possess sophisticated strategies in terms of chemical defense (119). Besides isoxazolinones derivates, salicin, benzaldehyde and conjugated acetates they use cyclopentanoic monoterpenes like plagiodial and chrysomelidial for defense (120-122). In order to discharge the deterrent molecules, the larvae developed specialized pair-wise exocrine glands on their dorsal thoracal and abdominal segments. These glands are attached to an impermeable reservoir which stores the deterrent compound. In case of predatory attack, the reservoirs release droplets of secretion containing defensive compounds (Fig. 6) (123-126).

Fig. 6: *Phaedon cochleariae* larvae show upended gland reservoirs containing a defensive secretion which is released after a predatory attack.

The source of the deterrent compound in the larval secretions depends on different strategies (Fig. 7). *Chrysomela* species as well as *Phratora vitellinae* for instance developed an energy-saving but highly host plant specific defense strategy. This depends on the secondary metabolites of salicaceaous plants which restricts the larvae in their forage. These species sequester the phenolic glucoside salicin and convert it to the biological active salicylaldehyde in the glandular reservoir (127-131). A second approach evolved in the so called interrupta group of the Chrysomelina species (e.g. *Chrysomela lapponica*). They developed a mixed-mode mechanism to produce butyrate-esters in addition to salicylaldehyde. For this purpose they sequester simultaneously a variety of glucosidically bound leaf alcohols. Their agluca are esterified

with *de-novo* produced isobutyric acid and 2-methylbutyric acid derived from the insects' internal pool of amino acids (132-136). However, the third approach in the subtribe Chrysomelina, considered as the most ancestral strategy of larval defense, is the *de-novo* production of cyclopentanoic monoterpenes (iridoids) in tremendous quantities (121, 137-139). The larvae of the leaf beetle *P. cochleariae* synthesize the iridoid Chrysomelidial (119, 121, 140).

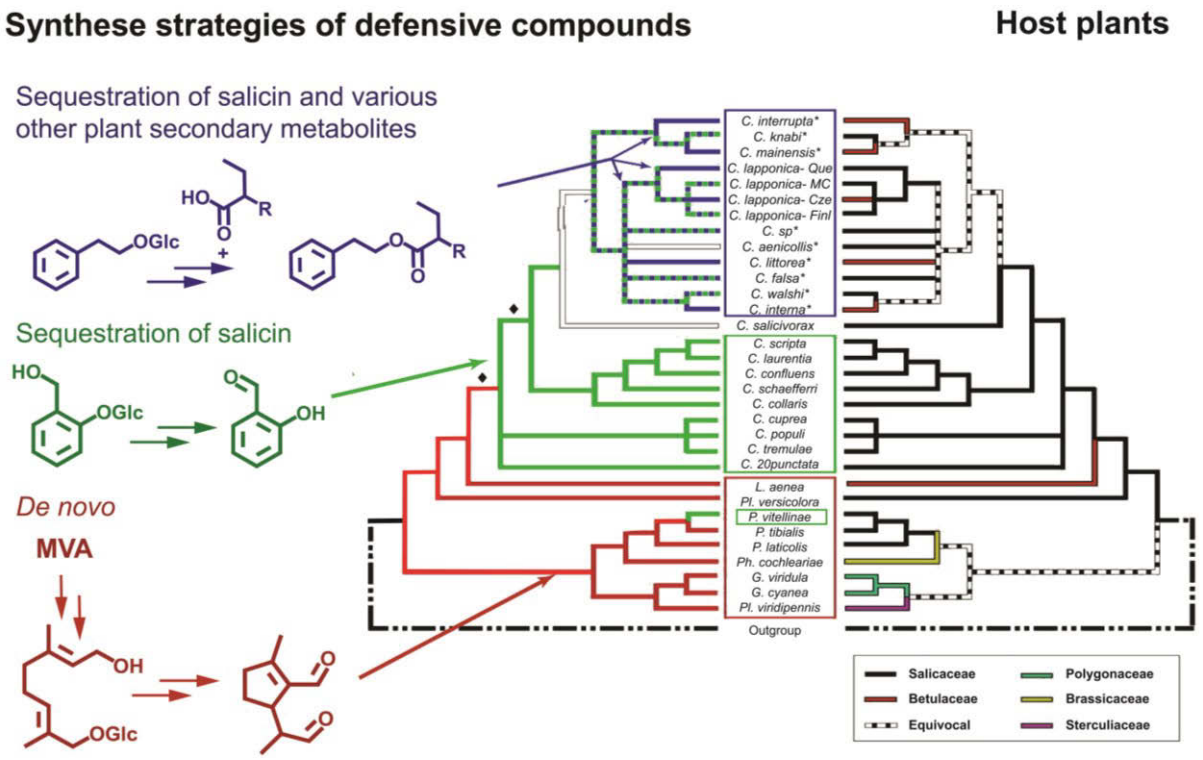

Fig. 7: Maximum parsimony reconstruction of the evolutionary relationship of Chrysomelina species considering the biosynthesis of deterrent compounds in the larval glands and host plant affiliation. Abbre*via*tions: *Pl.: Plagiodera; G.: Gastophysa; Ph.: Phaedon; P.: Phratora; L.: Linaeidea; C.: Chrysomela* (apted and modified from (119))

1.3.2 Origin and biosynthesis of de-novo produced terpenoids

A natural advantage of the *de-novo* group is their ability to defend themselves independent of host plant derived metabolites. They do not need to sequester compounds but do produce the glucosidically bound precursor 8-hydroxygeraniol glucoside (Ger-8-*O*-Glc) *de-novo* in the fat body tissue. The production of terpenoid precursors as well as regulatory mechanisms of involved branch point enzymes received limited attention so far. It is known, that biosynthesis of Chrysomelidial is most likely compartmented into different tissues of the larval body and therefore subjected to

different regulatory elements. Enhanced HMGR and GDPS activity, only detected in fat body tissue of iridoid producing larvae, indicate high biosynthetic activity of this tissue due to *de novo* production of iridoid precursor Ger-8-*O*-Glc (141, 142).

The isoprene units IDP and DMADP, provided by the MVA pathway, serve as substrates for *sc*IDSs to synthesize the monoterpenoid precursor GDP (12, 141). After dephosphorylation of GDP, the intermediate geraniol is produced by an up to now unknown enzyme. Subsequently, a ω-hydroxylation converts geraniol into 8-hydroxygeraniol (Ger-8-OH) presumably catalyzed by a P450 cytochrome oxidase. A final glucosylation step results in formation of Ger-8-*O*-Glc. Thereafter, Ger-8-O-Glc is exported into the hemolymph and further transferred to the glandular reservoir where the final steps in iridoid formation (chrysomelidial) occur (Fig. 8) (119, 126, 141-149). The enzymatic reactions in the glandular reservoir from Ger-8-*O*-Glc to the iridoid chrysomelidial have been studied in detail. Selective transport proteins take up the glucoside. Subsequently, an unspecific *β*-glucosidase cleaves off the sugar moiety to achieve Ger-8-OH. An oxygen dependent oxidase stereospecifically removes the hydrogen atoms from the terminal $-CH_2OH$ group yielding 8-oxogeranial. Afterwards, chrysomelidial is formed by a predicted cyclase (121, 126, 141-146, 150, 151).

Due to their independence of plant derived precursors, *de-novo* producers can overcome evolutionary host plant shifts without losing defense. This autonomy is nicely reflected also by the manifoldness of their host plants reaching from Polygonaceae (e.g. *G. viridula*), Brassicaceae (e.g. *P. cochleariae*), Betulaceae (*L. aenea*) to Salicaceae (*Pl. versicolora*) (Fig. 7). However, a high disadvantage of *de-novo* producers are higher metabolic costs compared to more evolved Chrysomelina species which sequester the glucosidic precursors directly from their host plants.

Interestingly, feeding experiments with deuterated precursors or the *S*-analogs of the natural *O*-glucoside (Ger-8-*O*-Glc) elucidated that *de-novo* producers already possess the ability to sequester. After feeding for a certain time on impregnated forage, the secretions contained the thioglucoside or deuterated chrysomelidial, respectively. These findings demonstrate that larvae of the ancestral Chrysomelina species already possess a transport system which principally supports sequestration. Therefore, the larvae may employ both, endogenous and exogenous pools of precursors if supplied by their host plant (130, 131, 136, 139, 152, 153).

However, to gain a benefit of sequestered plant derived glucosides the regulatory mechanism of terpenoid biosynthesis had to evolve. These regulatory processes have to be understood to investigate evolutionary processes from the ancestral *de-novo* producing strategy to the evolved and energy-saving sequestering approach

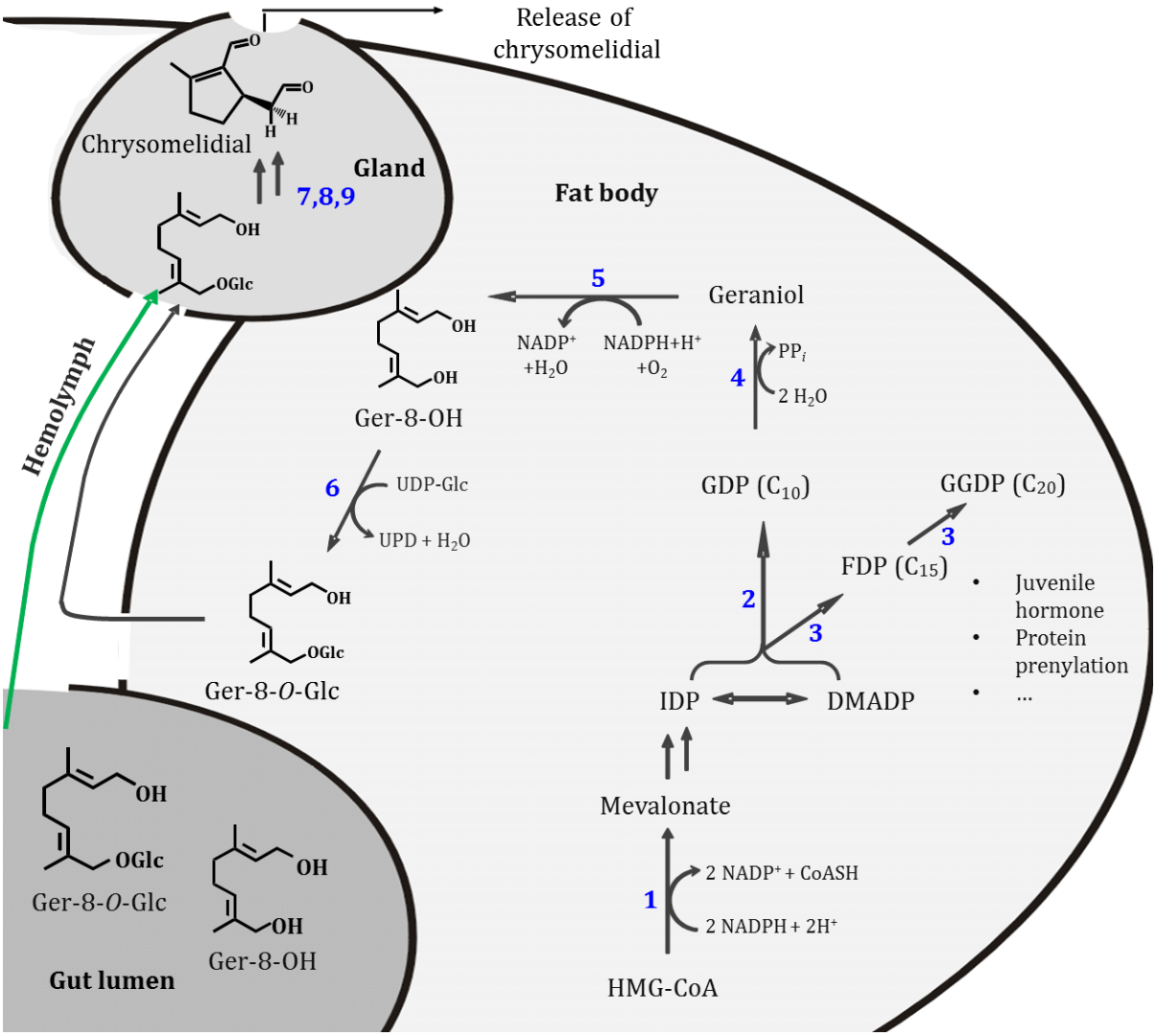

Fig. 8 Biosynthesis of the defensive secretions in the larvae of *Phaedon cochleariae*. 1, HMGR; 2, GDPS; 3, *sc*IDS; 4, Phosphatase; 5, Cytochrome P-450 mixed function Oxygenase; 6, Glycosyltransferase; 7, *β*-D-Glucosidase; 8, Oxidase; 9, Cyclase. Green arrow indicate the possibility of sequestration (adapted from (58))

2 AIMS OF THE THESIS

Chrysomelina larvae exhibit a biochemically self-contained defense metabolism, whereby they display an excellent research object in studying regulatory mechanisms and the evolutionary development of the defensive systems. The proposed development of the chemical defense in Chrysomelina leaf beetle larvae proceeded *via* different biosynthetic steps. *De-novo* production of terpenoid compounds are declared as the most ancestral strategy which finally developed to the sequestration of plant derived phenolic glucosides. The most evolved strategy is the combination of sequestration and *de-novo* production of compounds. However, all larvae show common principles. Besides the uniform morphology they generally use glucosidically bound precursors which are transferred *via* the hemolymph to the glandular reservoir. This suggests a common transport mechanism. However, all species show a highly selective and substrate specific uptake of the precursors into the glandular system - adapted to their genuine precursor of defensive compound.

The observations that even *de-novo* producers are able to sequester further implicate the existence of regulatory mechanisms to gain a benefit from plant derived substrates. To ensure an efficient chrysomelidial production besides other terpenoid compounds regulatory mechanisms have to exist. Consequently, to control and channel different terpenoid fluxes within the larval metabolism, defined regulatory processes had to be developed.

My objectives were to identify and characterize enzymes essentially involved in the *de-novo* biosynthesis of the defensive compound chrysomelidial. I especially focused on their regulatory impact and the corresponding requirements to fulfill their controlling function.

Manuscript one focuses on the hypothesis that the larvae benefit from plant derived metabolites. Therefore, geraniol, Ger-8-OH and Ger-8-*O*-Glc were analyzed regarding their regulatory impact on the activity of HMGR as it represents the key enzyme of the MVA pathway.

Manuscript two provides an overview of the studies concerning sequestration processes of plant-derived compounds by leaf beetle larvae. The route of ingested compounds is investigated and linked to different transport networks. The impact of these substances as shown in the first manuscript is linked to the question of the relevance of sequestration processes regarding adaptive radiation observed for the Chrysomelina subtribe.

Manuscript three explains the development of a reliable RNAi method to analyze biochemical pathways. It is shown that RNAi is approved to interrupt the biosynthesis of deterrent specifically *in-vivo*. This in turn elucidated the *in-vivo* function of newly identified enzymes.

Manuscript four focuses on the identification and characterization of a *sc*IDS from *Phaedon cochleariae* (*Pc*IDS1). RNAi experiments targeting *Pc*IDS1 revealed participation of this enzyme in the *de-novo* biosynthesis of defensive iridoids. Profound analysis of *Pc*IDS1 elucidated an up to now undiscovered regulatory mechanism for this enzyme class. There, the products of *Pc*IDS1 differ in their chain lengths depending on the present divalent metal co-factor. This influence of product specificity represents an additional level of regulation of branch point enzymes within terpenoid metabolism besides the HMGR regulation shown in the first manuscript. Since GDP and FDP serve as precursor for various metabolites, the larvae may control the systemic flux simply by changing the co-factor.

3 OVERVIEW OF MANUSCRIPTS

4.1 MANUSCRIPT 1: IMPLICATION OF HMGR IN HOMEOSTASIS OF SEQUESTERED AND DE-NOVO PRODUCED PRECURSORS OF THE IRIDOID BIOSYNTHESIS IN LEAF BEETLE LARVAE

Antje Burse, Sindy Frick, Axel Schmidt, Rita Buechler, Maritta Kunert, Jonathan Gershenzon, Wolfgang Brandt, Wilhelm Boland

Insect Biochemistry and Molecular Biology (2008)

Summary

Former studies revealed that *de-novo* producers possess the ability to sequester plant derived glucosides. Here we tested the glucoside, its aglucon (Ger-8-OH) and geraniol regarding their impact on HMGR, the key enzyme of the MVA-pathway. Profound analyzes of the recombinant catalytic portion of HMGR regarding enzyme activity were carried out. Data display a significant inhibitory impact of Ger-8-OH on HMGR. Homology modeling of the catalytic domain and docking experiments indicated binding of Ger-8-OH in the active site indicating a possible competitive inhibitor function. These data emphasize that HMGR may represent a regulatory element maintaining homeostasis between *de-novo* produced and sequestered precursors.

Author contributions:

S.F. and A.B. performed research, interpreted data substantially and contributed in writing the manuscript.
A.S. helped with the Radio-GC measurements.
R.B. helped in purification process of the heterologous expressed protein.
M.K. synthesized 8-hydroxygeraniol and its thioglucoside.
W. Brandt performed protein modeling and docking studies and wrote the first draft of the corresponding part in the paper.
A.B. and W. Boland contributed substantially to the interpretation of all data.
A.B., A.S., J.G. and W. Boland supervised the work and revised the manuscript.

4.2 MANUSCRIPT 2: ALWAYS BEING WELL PREPARED FOR DEFENSE: THE PRODUCTION OF DETERRENTS BY JUVENILE CHRYSOMELINA BEETLES (CHRYSOMELIDAE)

Antje Burse, Sindy Frick, Sabrina Discher, Karla Tolzin-Banasch, Roy Kirsch, Anja Strauss, Maritta Kunert, Wilhelm Boland

Phytochemistry (2009)

Summary

A general overview is provided on the deterrent biosynthesis by juvenile chrysomelina species. It was demonstrated that most likely all species possess the ability to sequester plant-derived glucosides, which in turn requires a highly efficient and complex transport system. Various feeding studies explain the selectivity of involved transport mechanisms located at the gut barrier, the glandular system and the excretion tissue. Elucidations of fundamental biosynthetic steps explain the importance of HMGR and GDPS within the *de-novo* production of chrysomelidial. The regulatory influences of sequestered precursors on branch point enzymes of the *de-novo* biosynthesis provide further aspects for co-evolutionary correlations based on plant insect interactions.

Author contributions:

S.F. performed research, contributed to the interpretation and writing of the manuscript related to the studies of HMGR and IDS.

S.D., A.S., R.K., M.K. performed research, interpreted data and wrote parts of the manuscript related to transport system and sequestration process of plant derived glucosides.

K.T-B. performed research, interpreted data and wrote parts of the manuscript concerning chemical defense of *C. lapponica.*

A.B. and W.B. contributed substantially to the interpretation of all data.

A.B. wrote first draft of the manuscript and all authors contributed substantially in terms of their research part.

4.3 MANUSCRIPT 3: PRECISE RNAI-MEDIATED SILENCING OF METABOLICALLY ACTIVE PROTEINS IN THE DEFENSE SECRETIONS OF JUVENILE LEAF BEETLES

René Roberto Bodemann, Peter Rahfeld, Magdalena Stock, Maritta Kunert, Natalie Wielsch, Marco Groth, Sindy Frick, Wilhelm Boland, Antje Burse

Proceedings of the Royal Society B: Biological Sciences (2012)

Summary:

RNAi methodology was established in juvenile *Chrysomela populi* and *Phaedon cochleariae* to analyze *in-vivo* function of proteins involved in the biosynthesis of deterrent compound. In particular the salicyl alcohol synthase (SAO) of *C. populi* and a novel protein from *P. cochleariae*, annotated as JH-binding protein (JHBP), were studied. Both proteins, located in the glandular secretions, were successfully silenced. In case of JHPB a function could be addressed to the protein in terms of the cyclization of 8-oxogeranial to form chrysomelidial. Altogether, the approach demonstrates clearly that RNAi is a suitable method to selectively annihilate transcripts of enzymes belonging to a distinct biosynthetic pathway.

Author contributions:

S.F. generated transcriptome libraries of *P. cochleariae* and performed research to a small proportion.

R.R.B. and P.R. established RNAi approach in leaf beetle larvae and performed research on *Cpop*SAO and *Pc*To-like.

M.S. established and performed off-target prediction and contributed to the interpretation of LC/MSE output data.

M.K. designed GC/MS assays, synthesized standards and contributed to the interpretation of output data.

N.W. performed LC/MSE analysis collected and contributed to interpretation of output data.

W.B. and A.B. contributed substantially to the interpretation of all data.

R.R.B., P.R. and A.B. wrote first draft of the manuscript and all authors contributed substantially to revisions.

4.4 MANUSCRIPT 4: METAL IONS CONTROL PRODUCT SPECIFICITY OF ISOPRENYL DIPHOSPHATE SYNTHASES IN THE INSECT TERPENOID PATHWAY

Sindy Frick, Raimund Nagel, Axel Schmidt, René R. Bodemann, Peter Rahfeld, Gerhard Pauls, Wolfgang Brandt, Jonathan Gershenzon, Wilhelm Boland and Antje Burse

Proceedings of the National Academy of Sciences of the United States of America (2013)

Summary:

The identification and intense characterization of an isoprenyl diphosphate synthase (*Pc*IDS1) isolated from the juvenile leaf beetle *Phaedon cochleariae* is described. Profound studies of parameters, influencing the enzyme activity of *Pc*IDS1, elucidated an undiscovered carbon chain-length determination mechanism. There, the product specificity of *Pc*IDS1, concerning the chain-length of the final product, can be shifted depending on the present divalent metal co-factor. RNAi experiments targeting *Pc*IDS1 revealed the participation of this enzyme in the *de-novo* biosynthesis of the defensive monoterpene chrysomelidial.

Author contributions:

S.F. designed and performed research, analyzed and interpreted data and wrote manuscript to a bigger part.
R.N. and G.P. helped with HPLC MS/MS measurements
R.R.B. performed RNAi injection and helped to collect samples.
P.R. helped with size exclusion chromatography.
W. Brandt designed and performed research of protein modeling and thermodynamic calculations and wrote the corresponding part of the paper.
A.B., A.S., J.G. and W. Boland supervised the work and revised the manuscript

5 Manuscripts

5.1 MANUSCRIPT 1

IMPLICATION OF HMGR IN HOMEOSTASIS OF SEQUESTERED AND *DE-NOVO* PRODUCED PRECURSORS OF THE IRIDOID BIOSYNTHESIS IN LEAF BEETLE LARVAE

Available online at www.sciencedirect.com
ScienceDirect
Insect Biochemistry and Molecular Biology 38 (2008) 76–88
Insect Biochemistry and Molecular Biology
www.elsevier.com/locate/ibmb

Implication of HMGR in homeostasis of sequestered and *de novo* produced precursors of the iridoid biosynthesis in leaf beetle larvae

Antje Burse[a,*], Sindy Frick[a], Axel Schmidt[b], Rita Buechler[a], Maritta Kunert[a], Jonathan Gershenzon[b], Wolfgang Brandt[c], Wilhelm Boland[a]

[a]*Department of Biochemistry, Max Planck Institute for Chemical Ecology, Hans-Knoell-Str. 8, D-07745 Jena, Germany*
[b]*Department of Bioorganic Chemistry, Max Planck Institute for Chemical Ecology, Hans-Knoell-Str. 8, D-07745 Jena, Germany*
[c]*Leibniz Institute of Plant Biochemistry, Department of Bioorganic Chemistry, Weinberg 3, D-06120 Halle/Saale, Germany*

Received 20 August 2007; received in revised form 14 September 2007; accepted 20 September 2007

Abstract

Insects employ iridoids to deter predatory attacks. Larvae of some Chrysomelina species are capable to produce those cyclopentanoid monoterpenes *de novo*. The iridoid biosynthesis proceeds via the mevalonate pathway to geranyl diphospate (GDP) subsequently converted into 8-hydroxygeraniol-8-*O*-β-D-glucoside followed by the transformation into the defensive compounds. We tested whether the glucoside, its aglycon or geraniol has an impact on the activity of 3-hydroxy-3-methylglutaryl-CoA reductase (HMGR), the key regulatory enzyme of the mevalonate pathway and also the iridoid biosynthesis. To address the inhibition site of the enzyme, initially a complete cDNA encoding full length HMGR was cloned from *Phaedon cochleariae*. Its catalytic portion was then heterologously expressed in *Escherichia coli*. Purification and characterization of the recombinant protein revealed attenuated activity in enzyme assays by 8-hydroxygeraniol whereas no effect has been observed by addition of the glucoside or geraniol. Thus, the catalytic domain is the target for the inhibitor. Homology modeling of the catalytic domain and docking experiments demonstrated binding of 8-hydroxygeraniol to the active site and indicated a competitive inhibition mechanism. Iridoid producing larvae are potentially able to sequester glucosidically bound 8-hydroxygeraniol whose cleavage of the sugar moiety results in 8-hydroxygeraniol. Therefore, HMGR may represent a regulator in maintenance of homeostasis between *de novo* produced and sequestered intermediates of iridoid metabolism. Furthermore, we demonstrated that HMGR activity is not only diminished in iridoid producers but most likely prevalent within the Chrysomelina subtribe and also within the insecta.

Keywords: Leaf beetle; Chemical defense; Iridoids; 3-Hydroxy-3-methylglutaryl-CoA reductase; 8-Hydroxygeraniol; Fat body; Sequestration

1. Introduction

Production of toxins to deter predators is widely distributed within the leaf beetle (Chrysomelidae) family (Pasteels et al., 1982, 1990, 1994; Pasteels, 1993; Blum, 1994; Laurent et al., 2003, 2005). In the subtribe Chrysomelina not only adults, but also the larvae are chemically protected (Blum, 1994; Termonia and Pasteels, 1999; Termonia et al., 2001). They possess pair-wise exocrine glands (composed of a reservoir with adhered glandular cells) on their dorsal thoracal and abdominal segments (Renner, 1970). Disturbed larvae release droplets of secretion from these glands containing the defensive compounds which range from iridoids (cyclopentanoid monoterpenes) to aromatic aldehydes and ester derivatives. They are produced either *de novo* or acquired by sequestration of secondary metabolites from host plants (Pasteels et al., 1982, 1986; Schulz, 1998; Termonia and Pasteels, 1999; Termonia et al., 2001).

In leaf beetle larvae iridoids are shown to be synthesized *de novo* (Meinwald et al., 1977; Blum et al., 1978; Pasteels et al., 1982; Oldham et al., 1996; Soe et al., 2004). In our previous work we demonstrated that the biosynthesis is most likely compartmented into different tissues of the larval body (Burse et al., 2007). In the defensive glands, the

*Corresponding author. Tel.: +49 3641 571265; fax: +49 3641 571202.
E-mail address: aburse@ice.mpg.de (A. Burse).

0965-1748/$ - see front matter © 2007 Elsevier Ltd. All rights reserved.
doi:10.1016/j.ibmb.2007.09.006

intermediate 8-hydroxygeraniol-8-*O*-β-D-glucoside is converted into the cyclopentanoid monoterpenes (Fig. 1) (Pasteels et al., 1990; Soetens et al., 1993; Daloze and Pasteels, 1994). More detailed, an unspecific β-glucosidase removes the sugar moiety from the glucoside, and an oxidase possessing a defined substrate spectrum subsequently catalyzes the formation of an acyclic dialdehyde (Pasteels et al., 1990; Veith et al., 1996; Brueckmann et al., 2002). The final transformation into the iridoids is achieved by cyclization and isomerization reactions (Lorenz et al., 1993; Veith et al., 1994). Endogenous, glucosidically bound 8-hydroxygeraniol is not produced in the defensive glands, but according to previous results this compound can be synthesized in the fat body tissue from where it has to be transferred via the hemolymph into the glands by still unknown mechanisms (Burse et al., 2007). Feeding experiments with *S*-analogs of the natural *O*-glucoside demonstrated that these larvae are principally able to sequester 8-hydroxygeraniol-8-*O*-β-D-glucoside (Feld et al., 2001; Kuhn et al., 2004). After transfer from gut lumen into the glandular reservoir, this glucosidically bound compound can be converted into the iridoids by the same

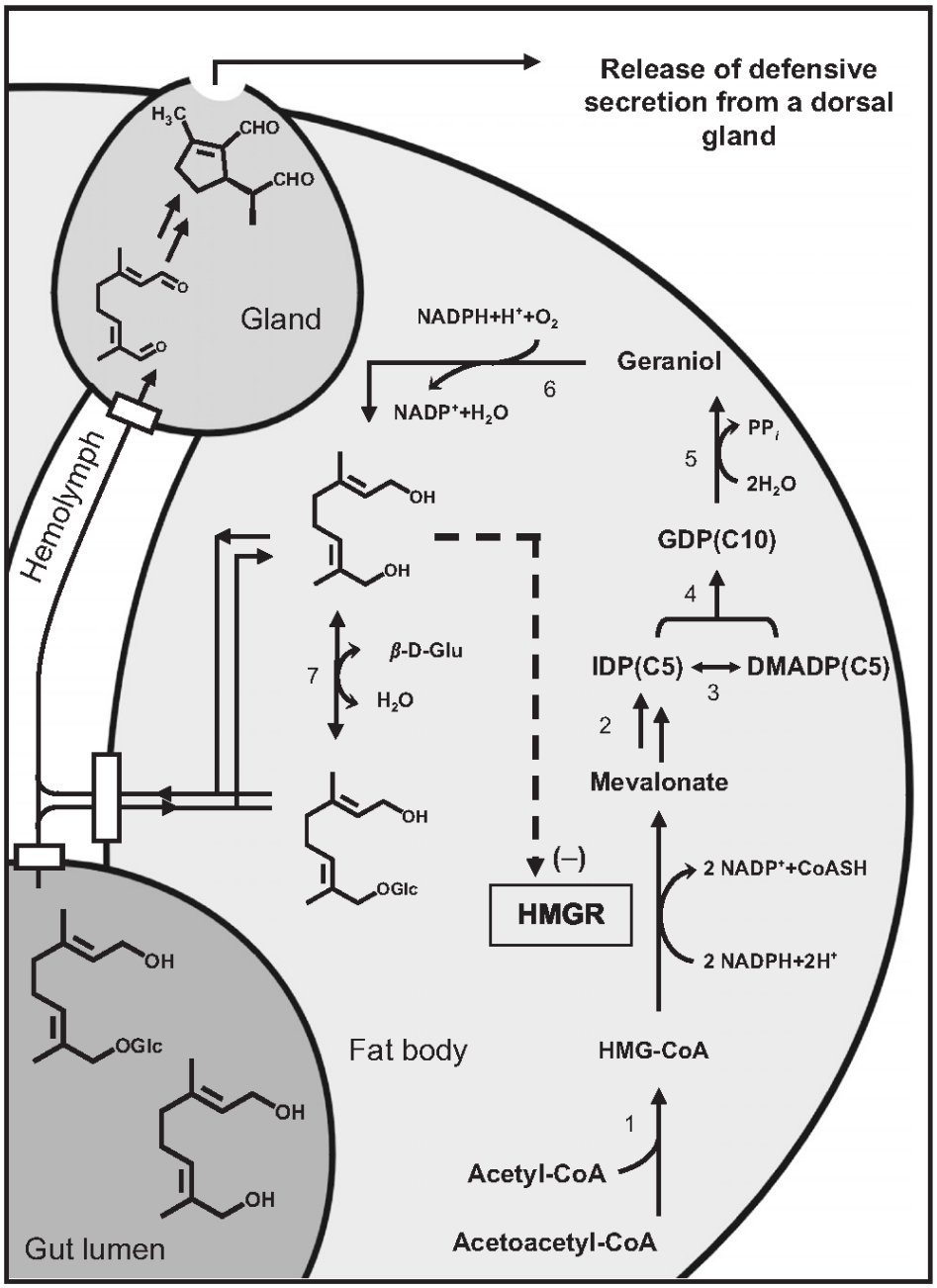

Fig. 1. Biosynthesis of deterrent iridoids in the larvae of *P. cohlleariae*. 1, 3-hydroxy-3-methylglutaryl CoA synthetase; 2, mevalonate kinase, phosphomevalonate kinase, diphosphomevalonate decarboxylase; 3, isopentenyl-diphosphate Δ-isomerase; 4, geranyl-diphosphate synthase; 5, phosphatase; 6, cytochrome P-450 mixed-function oxygenase; 7, β-glucosidase. (adapted from Pasteels et al., 1990; Burse et al., 2007).

enzymatic reactions already described for *de novo* synthesis (Pasteels et al., 1990; Lorenz et al., 1993; Daloze and Pasteels, 1994; Veith et al., 1994, 1996, 1997; Oldham et al., 1996; Laurent et al., 2003). Therefore, the larvae may employ both, endogenous or exogenous pools of the iridoid precursor depending on need or supply by the host plant.

The *de novo* synthesis of 8-hydroxygeraniol-8-*O*-β-D-glucoside in the larvae utilizes geranyl diphospate (GDP) (Lorenz et al., 1993; Veith et al., 1994). GDP originates from the mevalonate pathway whose committed step is catalyzed by 3-hydroxy-3-methylglutaryl-CoA reductase (HMGR; EC 1.1.1.34) (Friesen and Rodwell, 2004). The enzyme utilizes two molecules of NADPH to mediate the four-electron reduction of HMG-CoA to the carboxylic acid mevalonate.

Because HMGR is one of the most regulated enzymes known (Goldstein and Brown, 1990), its regulatory features may be also important for the biosynthesis of iridoids in the chrysomelids. In bark beetles for example, HMGR expression analyses provided evidence for localization of the *de novo* synthesis of monoterpenoid aggregation pheromones (Seybold and Tittiger, 2003). Increased mRNA levels corresponded in the anterior midgut to pheromone production in male bark beetles of different species (Ivarsson et al., 1998; Tittiger et al., 1999, 2003; Hall et al., 2002a, b; Nardi et al., 2002; Keeling et al., 2004; Tillman et al., 2004).

According to the primary structure alignments of Bochar et al. (1999) two classes of HMGRs can be distinguished. Class I includes the enzymes from eukaryotes and most archaea and class II those from prokaryotes and archaea. Eukaryotic HMGRs are glucoproteins and anchored with a variable number of membrane spanning domains in the endoplasmatic reticulum. They possess a linker region and a conserved C-terminal catalytic domain which extends out into the cytoplasm. The crystal structure of the catalytic portion of human HMGR revealed that the enzyme functions as homotetramer (PDB codes: 1DQ8, 1DQ9, 1DQA) (Istvan and Deisenhofer, 2000; Istvan et al., 2000). The homotetramer is composed of two functional dimers each of which has two active sites. Residues at the interface of both monomers participate in substrate binding and catalysis.

HMGR transcription and translation is modulated by the abundance of sterols and non-steroid mevalonate-derived compounds causing changes of over 200-fold in intracellular levels of the enzyme (Goldstein and Brown, 1990). In mammalian and yeast cells the network controlling HMGR activity is under extensive investigation (Hampton, 2002; Rawson, 2003; Bengoechea-Alonso and Ericsson, 2007). In insects, however, only fragmentary knowledge is available about HMGR regulation (Brown et al., 1983). Whereas in human and yeast sterol regulatory element binding proteins (SREBPs) control HMGR transcription, in *Drosophila melanogaster* the SREBP-pathway is involved only in non-sterol lipid synthesis (Rawson, 2003). In fruit fly phosphatidylethanolamine triggers the proteolytic release of SREBP from intracellular membranes and not cholesterol as in mammals (Dobrosotskaya et al., 2002; Seegmiller et al., 2002). Insects lack the enzymes necessary to convert farnesyl diphosphate to squalene and sterols (Clark and Bloch, 1959). Instead, they generate lower-molecular weight compounds participating in essential cellular functions and inter-organismic communication (Edwards and Ericsson, 1999). In insects HMGR transcription is affected by juvenile hormones (Belles et al., 2005), sesquiterpenoid compounds that regulate embryogenesis, metamorphosis, reproduction and pheromone synthesis (Dubrovsky, 2005). Extensive studies in bark beetles support the paradigm that juvenile hormone stimulates *de novo* aggregation pheromone synthesis via HMGR induction in concert with other enzymes of the mevalonate pathway (Ivarsson et al., 1998; Tillman et al., 1998, 2004; Tittiger et al., 1999, 2003; Keeling et al., 2006). However, the mechanism behind this transcriptional regulation of this pathway is still an enigma.

Catalytic efficiency of vertebrate HMGR can be post-translationally modulated by phosphorylation and isoprenoid-mediated degradation accelerating the decrease of active enzyme (Gil et al., 1985; Sato et al., 1993). No information on the effects of post-translational modification is available for insects. Generally, HMGR is modulated indirectly by sterols and other terpenoids. Inhibition of the enzyme is effected by statins (Corsini et al., 1995). Statins are potent competitive inhibitors sharing a HMG moiety and a rigid hydrophobic group linked to it. Crystallization revealed interaction of these compounds with the active site of HMGR (Istvan and Deisenhofer, 2001). Suppression of HMGR activity is also observed by diverse mevalonate-derived secondary plant products, especially in terms of the impact of mevalonate pathway suppression by dietary isoprenoids in carcinogenesis (Elson et al., 1999; Mo and Elson, 2004). Plant-derived monoterpenes including limonene, geraniol or ionone decrease mammalian HMGR activity by unknown mechanisms of lowering enzyme mass.

In the present paper we report for the first time that HMGR is negatively regulated by 8-hydroxygeraniol, a non-sterol metabolite of iridoid biosynthesis proceeding in leaf beetle larvae. Purification of the catalytic domain revealed that inhibition by 8-hydroxygeraniol is subject to the catalytic domain which was corroborated by docking analyses on the modeled HMGR catalytic portion suggesting competitive inhibition by this monoterpene. *De novo* producing larvae possess the potential to sequester glucosidically bound 8-hydroxygeraniol. After cleavage of the sugar moiety the aglucon may interfere with HMGR and consequently, the enzyme may represent a key regulator to maintain homeostasis of endo- and exogenous metabolites of the iridoid synthesis. Inhibition was also observed for other insect HMGRs including *D. melanogaster*.

2. Materials and methods

2.1. Leaf beetles

Phaedon cochleariae and *Gastrophysa viridula* were reared as continuous cultures in the laboratory (20 °C and 16:8 L:D period) on leaves of *Brassica rapa spp. chinensis* and *Rumex obtusifolia*, respectively. *Chrysomela populi* (feeding on *Populus canadensis*) was collected in Furth im Wald (Germany), *Chrysomela lapponica* (feeding on *Salix myrsinifolia)* in the Parc Naturel Régional du Queyras (France), and *Agelastica alni* (feeding on *Alnus glutinosa*) in Greiz (Germany).

2.2. Tissue samples

Fat body tissue was dissected in modified Ringer solution from third-instar larvae (14–16 d) of all leaf beetle species (von Nickisch-Rosenegk et al., 1990). Samples for HMGR activity assay were suspended in 2× assay buffer (400 mM mops, 10% sucrose, 80 mM EGTA) and macerated on ice by a Polytron homogenizer with subsequent freeze-thawing at −20 °C. For each experiment, tissue of 10 larvae of *P. cochleariae* and *G. viridula*, and of five larvae of *C. populi*, *C. lapponica,* and *A. alni* were pooled. Non-dissected fruit flies were completely macerated for the enzyme assays. Data were collected from three independent experiments. Fat body tissue samples for RNA isolation were either freshly processed or kept at −80 °C until needed.

2.3. Chemicals and radiochemicals

D,L-3-[glutaryl-3-^{14}C]-hydroxy-3-methylglutaryl CoA (^{14}C HMG CoA) and (*R,S*)-[5-^{3}H]-mevalonolactone were purchased from Biotrend. 8-Hydroxygeraniol and its thioglucoside were synthesized as described by Feld et al. (2001). Fluvastatin was purchased from Calbiochem. If not otherwise stated, all other chemicals were purchased from Sigma.

2.4. HMG-CoA reductase activity

In vitro assays were essentially carried out as described by Burse et al. (2007). Briefly, HMRG activity was monitored in a final volume of 50 µl containing 200 mM mops, 40 mM EGTA, 5% (w/v) sucrose, 0.1% (w/v) BSA, 40 mM EDTA, 1 mM DTT, 1 mM NADPH, and crude protein extract or purified enzyme. Inhibition was tested by adding the compounds at desired concentrations to this mixture. The enzymatic reaction was started by the addition of unlabeled HMG CoA and 0.5 µl ^{14}C-HMG CoA (specific activity 55 mCi/mmol) to obtain a final substrate concentration of 200 µM. The mixture was incubated for 30 min at 30 °C. Addition of 10 µl of 10 N HCl terminated the reaction; subsequent incubation for 1 h completed the spontaneous cyclization of ^{14}C-mevalonate to ^{14}C-mevalonolactone. After adding of internal standard (*R,S*)-[5-^{3}H]-mevalonolactone (specific activity 20 Ci/mmol) and 250 µl of a saturated solution of K_2HPO_4/KH_2PO_4, pH 6.8, the mixture was extracted with ethyl acetate. Organic phases were assayed for total radioactivity by liquid scintillation counting. Radio-GC demonstrated ^{14}C-mevalonolactone as the only metabolite of ^{14}C-HMG-CoA conversion under the assay conditions (Burse et al., 2007). The amount of the produced mevalonate was calculated by using the recovery rate of the internal standard and by subtracting the denatured protein control of the corresponding tissue sample relative to the protein content.

2.5. RNA extraction and cDNA synthesis

Total RNA was extracted from dissected tissues with the RNeasy Micro Kit (Qiagen) according to the manufacturer's instructions. Complete removal of DNA was achieved by using the RNase-Free DNase Set (Qiagen). The quality of the RNA was evaluated by measuring the 260:280 nm absorbance ratio, and the integrity of 18 and 28 S ribosomal RNA bands was assessed by electrophoresis on RNA 6000 Nano labchips (Agilent Technologies). RNA concentrations were determined from absorbance values at a wavelength of 260 nm. cDNA fragments to determine the HMGR in different leaf beetle larvae were generated as described previously (Burse et al., 2007). Sequence information of the cDNA fragments was used to generate gene-specific primers for rapid amplification of cDNA ends (RACE).

2.6. Determination of HMGR cDNA ends

Total RNA was extracted from fat body tissue of larvae of *P. cochleariae* and used as starting material for 5′- and 3′- RACE performed with the BD SMART RACE cDNA Amplification Kit (BD Bioscinence Clontech). Identification of the 5′-end of *HMGR* was carried out according to manufacturer's instructions using the following gene-specific primer designed from PCR fragment sequences: 5′-CCC AGG ATC TTC CTT CTG ATC CCC ACC C-3′. The sequence of the 3′-end of *HMGR* was obtained from of *P. cochleariae* using the gene-specific primer 5′-CGC GCA CGC CGG CAA CAT CGT GAC CGC C-3′ and for subsequent nested PCR the primer 5′-GGA CCC CGC GCA GAA CAT CGG GAG CAG C-3′. PCR products were cloned using the TOPO TA Cloning Kit (Invitrogen) and sequenced.

2.7. Sequenzing and sequence analyses

Nucleotide sequencing was carried out by MWG-Biotech AG, Ebersberg (Germany). Nucleotide sequence data were aligned and processed with Lasergene sequence analysis software version 5.07 (DNASTAR Inc., Madison, WI). DNA and protein sequence similarity

searches in databases were performed with programs based on the BLAST algorithm (Altschul et al., 1997) provided by the National Center for Biotechnology Information, Bethesda, MD. Topology analyses of deduced amino acid sequences were done by using the dense alignment surface (DAS) method (Cserzo et al., 1997) supplied by the DAS server of the Department of Biochemistry, Stockholm University, Sweden. Protein family motifs and post-translational modifications were searched with programs provided by the ExPASy (Expert Protein Analysis System) proteomics server from the Swiss Institute of Bioinformatics, Switzerland.

2.8. Construction of the expression plasmid

The catalytic portion of the *HMGR* gene was amplified by PCR from *P. cochleariae* cDNA by using Platinum *Pfx* DNA Polymerase (Invitrogen), a forward primer (5′-CAC CGA AGG CTC CCC ATC CTC C) and a reverse primer containing the stop codon (5′-TCA AAA ATT GTC CTT GCA AGG CGG ACT GAG). The resulting 1.5-kb fragment was gel purified and ligated into pET100/D-TOPO (Invitrogen). The resulting Plasmid pETPcHRcat, isolated from transformed *E. coli* TOP10F' cells, was sequenced to confirm the presence of unaltered *HMGR*. *E. coli* Rosetta-gami 2 (DE3) cells (Novagen) were transformed with the plasmid construct to express the N-terminally 6-His-tagged protein.

2.9. Expression and purification of the gene product

Initially, Rosetta-gami 2 (DE3) cells transformed with pETPcHRcat were inoculated in Overnight Express Autoinduction System 1 medium (Novagen) and grown at 18 °C to midlog phase. To obtain the desired volume, pre-culture was staged and the final fermentation continued at 18 °C to stationary phase. Harvested cells were lysed by BugBuster Protein Extraction Reagent (Novagen) according to manufacturer's instruction. After removal of the insoluble cell debris and adding of 20 mM imidazole, the soluble fraction was applied to a HisTrap HP column (GE Healthcare) prepacked with precharged Ni-sepharose. Affinity chromatography was performed by the liquid chromatography system ÄKTAexplorer (GE Healthcare). After column equilibration with 20 mM imidazole elution was achieved at a flow rate at 1 ml/min by using buffer A (20 mM sodium phosphate, 0.5 M NaCl, pH 7.4) and buffer B (500 mM imidazole; 20 mM sodium phosphate, 0.5 M NaCl, pH 7.4). After two holds at 10% and 20% B, the gradient increased linearly from 20% to 100% B.

Fractions containing purified recombinant protein were verified by 10% SDS-PAGE (Sambrook and Russell, 2000). Buffer exchange was carried out by using Zeba Desalt Spin columns (Pierce) according to the manufacturer's protocol. HMGR activity was assayed and fractions with high activity were combined and stored at −20 °C. Protein concentrations in enzyme assays were measured by Bradford assay using the Pierce reagent with bovine serum albumin as standard according to the manufacturers' instruction.

2.10. Homology modeling of HMGR and docking of 8-hydroxygeraniol

The catalytic portion of HMGR including E416-F887 from *P. cochleariae* (Fig. 3) which has been heterologously expressed in *E. coli* was also subject to a homology-based modeling. A BLASTP data base search of this protein domain revealed except for the first 33 and last 30 amino acid residues for which no alignment could be obtained, homology to the complex of the catalytic portion of human HMGR with HMG and CoA (PDB code 1DQ8) (Istvan et al., 2000) with a score of 567, an *e*-value of *e*-162, and a sequence identity of 64%. Using the molecular modeling program MOE (molecular operating environment, Chem. Comp. Group Inc., Montreal, Canada) the leaf beetle HMGR structure was built by alignment with the crystallographic structure of 1dq8 using the BLOSOM65-substitution matrix (Henikoff and Henikoff, 1992, 1993). Ten structures were generated with subsequent energy minimization using Charmm22 (MacKerell et al., 1998) and Born-Sovation (Pellegrini and Field, 2002). All structures were validated with respect to their stereochemical quality with PROCHECK (Laskowski et al., 1993) and for native folding with PROSA II (Sippl, 1990). All parameters for an appropriate stereochemical quality of the structures were fulfilled by PROCHECK (90.8% in most favoured region, 8.6% in additionally allowed regions and 0.3% in generously allowed regions, 0.3, i.e. 1 outlier). All other values, such as peptide bond planarity, overall G-factor, side chain dihedral angles are inside or even better than expected for a corresponding high-resolution X-ray structure.

Except for two small loops of some 10 residues, the PROSA analysis showed all residues in negative energy area, an almost identical energy graph to the template protein, and a combined energy *z*-score of −9.41 (template *z*-score = −9.82 for 417 amino acids), which is in the expected range for a protein with 408 amino acid residues and native fold.

The ligand 8-hydroxygeraniol was docked using the automatic docking program GOLD (Genetic Optimized Ligand Docking, Cambridge Crystallographic Data Centre, Cambridge, UK) (Jones et al., 1995, 1997; Nissink et al., 2002; Verdonk et al., 2003) with standard values given by the program. Initially, by the site finder option of MOE 14 potential sites for docking of small ligands were identified. To capture all these sites by docking with GOLD, a radius of 50 Å around an atom in the center of the model protein was applied. Subsequently 50 docking runs were performed. Since residues at the interface of both monomers participate in substrate binding and catalysis, which is shown by the docked 3-hydroxy-3-methyl-glutaric acid (HMG) in the X-ray structure of 1DQ8 close to CoA,

a dimeric structure of the modeled proteins was formed by superposition of the backbone atoms of two monomers with two units of the template X-ray structure and accordingly merged to each other to form the dimeric structure of the modeled protein. Using the dimeric structure of the model new docking runs were performed to inspect putative binding of 8-hydroxygeraniol in a similar position as HMG in the X-ray structure.

3. Results

3.1. Inhibition of HMGR from tissue samples

The iridoid precursor 8-hydroxygeraniol-8-*O*-β-D-glucoside can be *de novo* synthesized by the larvae of *P. cochleariae* via the MVA pathway. These larvae possess also the potential to sequester the compound from host plants (Feld et al., 2001; Kuhn et al., 2004). HMGR is one of the most highly regulated enzymes of the MVA pathway (Goldstein and Brown, 1990) and presumably also of the glucoside synthesis. Therefore, this key enzyme may control the equilibrium of iridoid precursors supplied by uptake and endogenous synthesis. Impact on HMGR activity has been analyzed for the glucoside and its aglucon and geraniol, respectively. Because the *O*-β-D-glucoside of 8-hydroxygeraniol can easily be hydrolyzed, instead, the stable *S*-analogon has been used.

HMGR activity was assayed with crude enzyme extract of fat body tissue from *P. cochleariae* larvae. Incubation with 8-hydroxygeraniol revealed a significant decrease of HMGR activity, 50% inhibition was achieved with a concentration of approx. 2 mM (Fig. 2). By geraniol the enzyme activity declined only of 25–35% at concentrations ⩾5 mM. Almost no inhibition was detectable by incubation with the thioglucoside of 8-hydroxygeraniol. Consequently, HMGR activity can be modulated by an intermediate of the iridoid biosynthesis.

3.2. Expression and purification of the catalytic domain of the P. cochleariae HMGR

In order to validate the results from crude enzyme extracts and to examine whether the catalytic domain is subject to inhibitor interaction, the HMGR catalytic domain from *P. cochleariae* has been heterologously expressed and purified from *E. coli* cells.

First, we identified a 2664-bp open reading frame encoding the entire putative HMGR by using RACE method. The deduced protein possesses a predicted molecular mass of 97.1 kDa and a pI of 6.9. Comparison of the 888-amino acid sequence with data base entries employing BLASTP revealed significant similarity to the insects HMGRs (Altschul et al., 1997). With 76% identity, the putative enzyme shows the highest homology to the sequence of *Tribolium castaneum*. Comparison to the HMGR of the bark beetles *Ips paraconfusus*, *Ips pini*, and *Dendroctonus jeffreyi* as well as to *Anthonomus grandis*

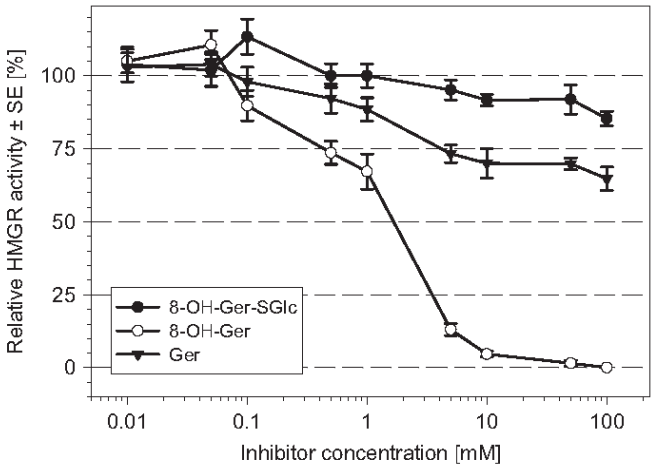

Fig. 2. Inhibition of HMGR in crude enzyme extract from fat body tissue of *P. cochleariae* larvae.

showed more than 60% identity. *Blattella germanica* and *D. melanogaster* revealed an identity of 68% and 52%, respectively. To human HMGR the identity is 50%.

Prediction programs and motif searches were employed to gain insights into the topology of *P. cochleariae* HMGR. The N-terminal 332 amino acid residues are calculated to anchor the enzyme with eight membrane-spanning helices in the endoplasmatic reticulum (Fig. 3). N-glucosylation between helix 7 and 8 was predicted for the residue N295. A hydrophilic linker region (residues 333–450) connects the membrane-spanning and catalytic domain. The highly conserved catalytic portion (residues 451–887) possesses amino acids involved in dimerization (e.g. the key dimerization element ENVIG at position 515–519), binding of NADPH (e.g. DAMGMN at position 639–644) and HMG-CoA (residues of the putative cis-loop) and catalysis. Residue S858 was calculated to be site of phosphorylation in *P. cochleariae* HMGR. This modification may reduce the enzyme activity by decreasing the affinity for NADPH according to observations from the crystal structure of the human HMGR (Istvan and Deisenhofer, 2000; Istvan et al., 2000). Although the ubiquitin-dependent proteasomal degradation triggered by sterols and non-sterols in vertebrates has not been reported from insect HMGRs, a sterol sensing domain is predicted for the leaf beetle HMGR (residues 63–220).

The catalytic portion (E416-F887) of *P. cochleariae* HMGR was N-terminal fused to a His-peptide for purification (Fig. 3). Heterologous expression of the recombinant protein in *E. coli* yielded a single-soluble protein band at 54.5 kDa (Fig. 4). The overall yield was approx. 2 mg/l culture.

Highest activity of purified enzyme was determined in the temperature range from 25 to 35 °C with its optimum at 30 °C (data not shown). The optimal pH was determined in different buffer systems (Fig. 5). The enzyme was most active in phosphate buffer at pH 7.5 and in mops at pH 7.4. Using the reductions equivalent NADH utilized by

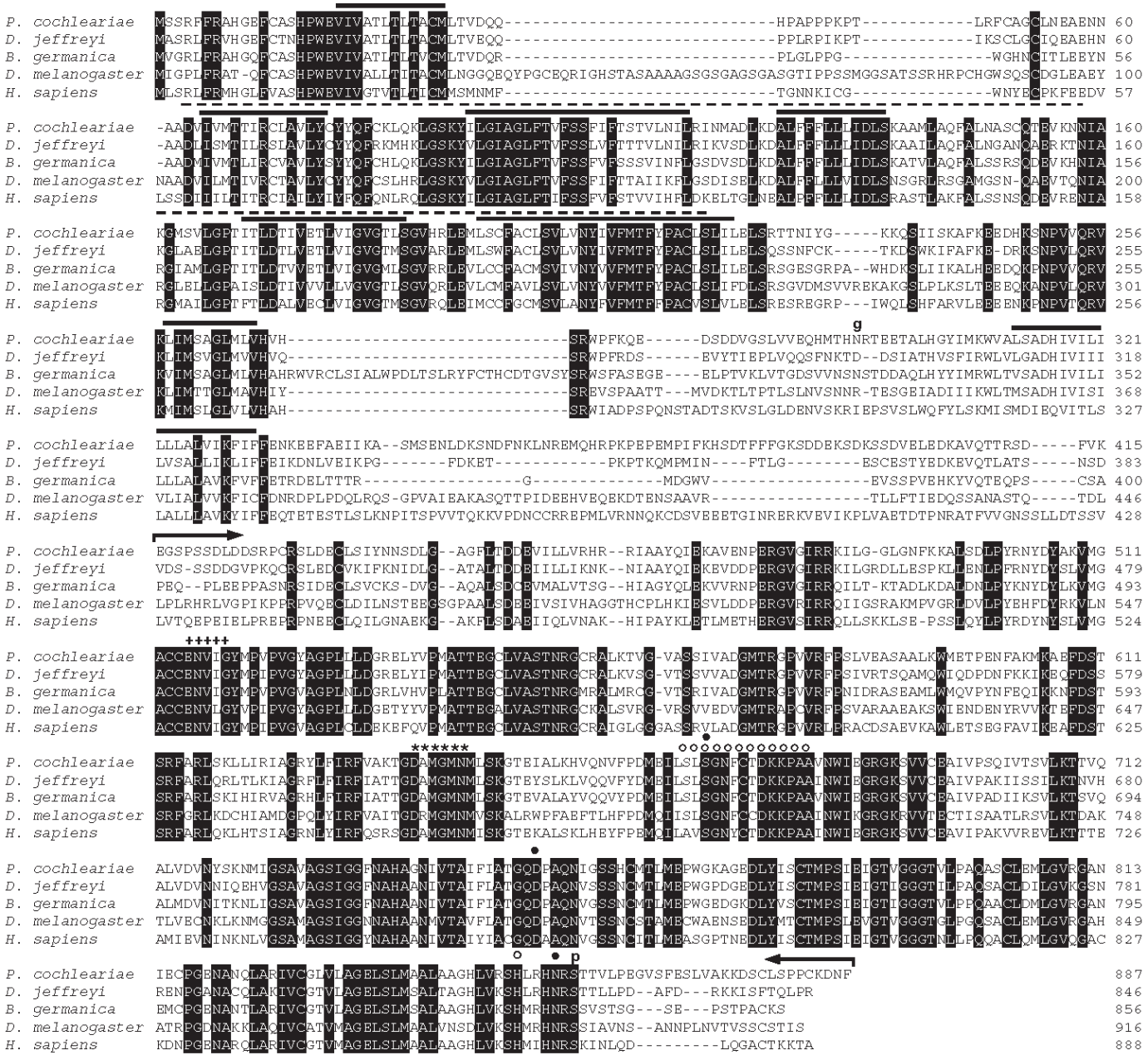

Fig. 3. Alignment of *P. cochleariae* HMGR with insect (*Dendroctonus jeffreyi*, AF159136; *Blatella germanica*, X70034; *D. melanogaster*, M21329) and human (M11058) HMGRs. Alignment was generated by ClustalW method. Similar residues are white against black. Putative transmembrane segments are marked with black bars above the alignment. A dashed bar indicates the predicted sterol sensing domain. Conserved motifs implicated in dimerization (+), binding of NADPH (*), HMG-CoA (°), and 8-hydroxygeraniol (●) are shown. Arrows illustrate primer binding sites for amplification of the catalytic domain for heterologous expression and homology modeling. g, glucosylation site; p, phosphorylation site.

prokaryotic class II HMGRs no activity was detectable at the tested concentrations of 0.1 and 10 mM (data not shown).

3.3. Inhibition of the purified catalytic domain of HMGR

Inhibition of the catalytic domain of beetle HMGR was tested with the statin fluvastatin and the intermediates of iridoid synthesis. Statins are drugs widely used to control the cholesterol level in patients with hyperlipidemia (Pahan, 2006). These structural analogues of HMG-CoA inhibit the enzyme competitively with an affinity of about 1000 10,000 times greater than that of the natural substrate (Pahan, 2006). The fully synthetic fluvastatin features a fluorobenzol substituted indol linked to the HMG-like moiety (Fig. 6A) The crystalline structure of human HMGR in complex with statins, including fluvastatin (PDB code 1HWI), revealed that the binding site of HMG-CoA is occupied whereas binding of NADPH is unaffected by the drugs (Istvan and Deisenhofer, 2001).

Insect HMGR was inhibited by fluvastatin with an IC_{50} of about 220 nM. In human an $IC_{50} = 28$ nM has been reported (Holdgate et al., 2003). Clear inhibition of activity of the catalytic domain was shown for 8-hydroxygeraniol. The IC_{50} was about 1.2 mM. Neither the thioglucoside nor geraniol inhibited the enzyme activity at the tested concentrations (Fig. 6B).

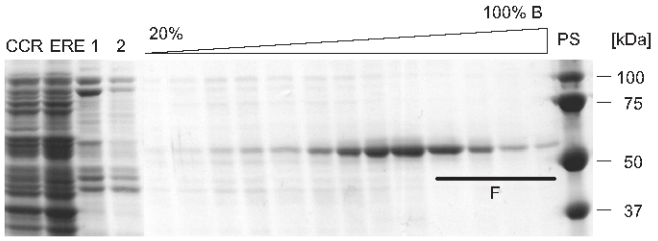

Fig. 4. SDS-PAGE of the recombinant catalytic domain of HMGR from *P. cochleariae* purified by nickel affinity chromatography employing the liquid chromatography system ÄKTAexplorer. PS, standards of the indicated mass. C, control (*E. coli* row enzyme extract with empty vector). RE, *E. coli* row enzyme extract expressing HMGR. 1, elution with 10% B. 2, elution with 20% B. Lane 5–13, elution by the gradient 20% B to 100% B. F, fractions combined and used in enzyme assays.

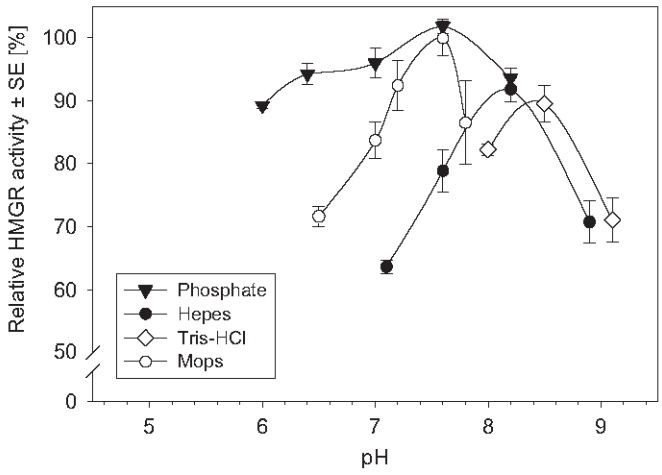

Fig. 5. Enzymatic activity of the purified catalytic domain of HMGR from *P. cochleariae* in different buffer systems.

3.4. Homology modeling of the leaf beetle HMGR and docking of 8-hydroxygeraniol

Based on the three-dimensional structure of the catalytic portion of human HMGR (PDB code 1DQ8 containing HMG and CoA) a high-quality model (indicated by a PROCHECK and PROSA II analysis) of the corresponding region (E416-F887) of the HMGR from *P. cochleariae* was developed. The secondary structure of the homodimeric protein is shown in Fig. 7 illustrating an overall identical fold to the template protein. Starting with extensive docking studies of 8-hydroxygeraniol to one monomer using GOLD including almost the complete protein (see method section) only one site with high fitness-value of 31 (value of a scoring function for docking arrangements, the higher the value the higher is the expected affinity of the ligand) was detected. In this case 8-hydroxygeraniol is recognized by the formation of a hydrogen bond of the 8-hydroxy-function with the side chain of N644 and of the geraniol-hydroxy group with Q756. Since this docking position is far away from the catalytic active center an allosteric modulation of the structure would be the only explanation for the observed inhibitory effect of 8-hydroxygeraniol. However, in human the catalytic active site is formed by the participation of two monomeric subunits of the protein which operates as a homotetramer. Therefore, a corresponding model of a homodimeric protein was build and docking studies were performed close to the active site (Fig. 7). The resulting most preferred docking arrangement of 8-hydroxygeraniol appeared in a position almost identical to the position of HMG in the X-ray structure of the template in direct

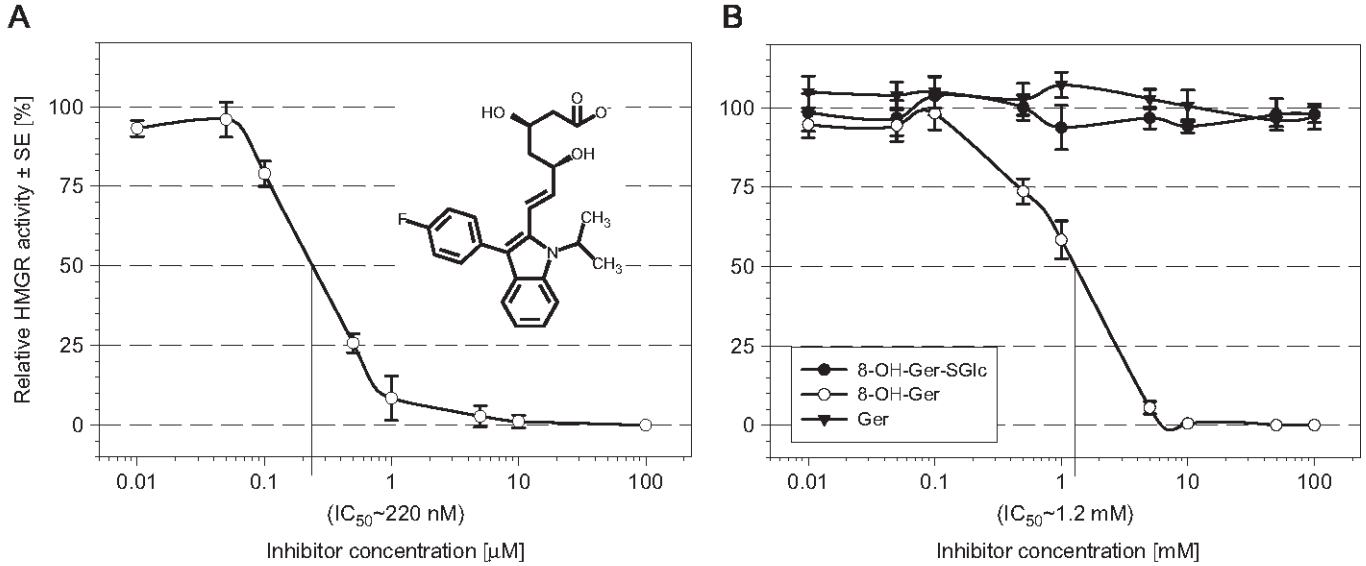

Fig. 6. Inhibition of the purified catalytic domain of HMGR from *P. cochleariae* by (A) fluvastatin, and (B) intermediates of the iridoid metabolism.

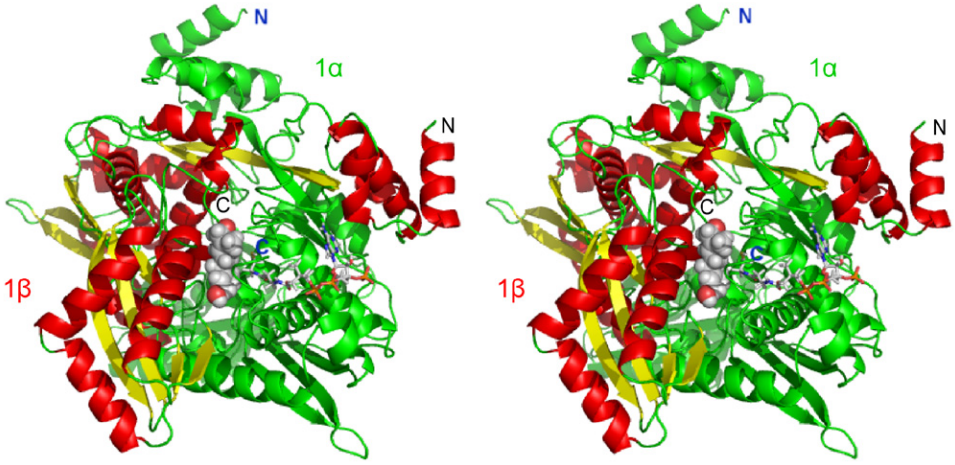

Fig. 7. Stereo representation of the secondary structure of the homodimer of HMGR from *P. cochleariae*. For clarity, the secondary structure of subunit 1α is colored uniform in green. Within the center of the protein the location of the ligand 8-hydroxygeraniol (space filled) is displayed.

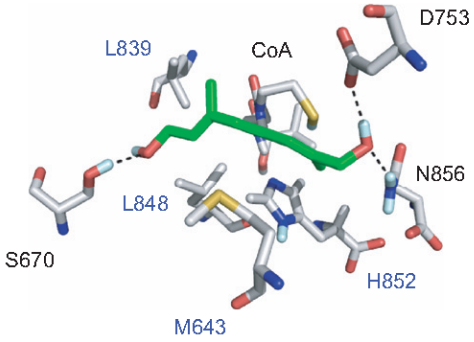

Fig. 8. Interaction of 8-hydroxygeraniol with the catalytic active site of HMGR. Black labeled residues indicate interactions with chain A and blue labeled with chain B of the homodimeric protein. Dotted black lines represent hydrogen bonds between the ligand and the protein.

neighborhood to CoA (Fig. 7). Since the obtained fitness value of 41 is considerably higher than the former one, this position is the most favored docking position of 8-hydroxygeraniol. This docking position in the active site clearly defines 8-hydroxygeraniol as a competitive inhibitor. The interaction of 8-hydroxygeraniol with the protein is characterized by the formation of hydrogen bonds to S670 and D753 from chain A and to N856 from chain B (Figs. 3 and 8). Furthermore, hydrophobic interactions with L839, L848, H852, and M643 stabilize the docking arrangement.

3.5. *Inhibition of HMGR from other insects*

To address the question whether HMGR inhibition by 8-hydroxygeraniol is restricted to iridoid producing species, crude enzyme extracts obtained from Chrysomelina larvae which do not produce iridoids *de novo*, extracts from larvae of Galerucinae and extracts from adults of *D. melanogaster* were assayed. In fact, the activity of the HMGR was attenuated in all species at the tested 5 mM 8-hydroxygeraniol (Fig. 9). This concentration reduced HMGR activity of the two iridoid producers *P. cochleariae* and *G. viridula* by ⩾80%, of the two sequestering Chrysomelina species *C. populi* and *C. lapponica* by 60 75%, of the Galerucinae *A. alni* by 75% and of *D. melanogaster* by 55%. Thus, inhibition by 8-hydroxygeraniol is most likely more widespread across the insects than limited to terpenoid producers.

4. Discussion

Larvae of some Chrysomelina species are capable of iridoid *de novo* production which is localized in different compartments of the larval body (Pasteels et al., 1990; Oldham et al., 1996; Soe et al., 2004; Burse et al., 2007). The larvae are also potentially capable to sequester precursors of the biosynthesis from host plants; hence, iridoid production is not exclusively governed by endogenous metabolites and the incorporated compounds may also modulate *de novo* synthesis (Feld et al., 2001; Kuhn et al., 2004). Recent data (unpublished results) support that sequestration of terpenoid precursors occurs, indeed, in nature.

Up to now, all tested iridoid producing Chrysomelina larvae have the potential to sequester 8-hydroxygeraniol-8-*O*-β-D-glucoside as shown by the successful import of the corresponding thioglucoside from treated leaves into the defensive system (Feld et al., 2001; Kuhn et al., 2004). We studied the impact of this glucoside as well as its aglycon and geraniol on the activity of HMGR providing precursors for 8-hydroxygeraniol-8-*O*-β-D-glucoside synthesis. With the *S*-analog of the natural *O*-glucoside of 8-hydroxygeraniol no effect on HMGR activity has been observed. Instead, only the aglycon clearly inhibited enzyme activity. Geraniol slightly decreased the activity of HMGR, but only in assays containing crude enzyme extracts and not in experiments with purified catalytic domain. Peffley and Gayen (2003) demonstrated that plant-derived geraniol lowered HMGR activity in hamster kidney cells by affecting the translation and also the

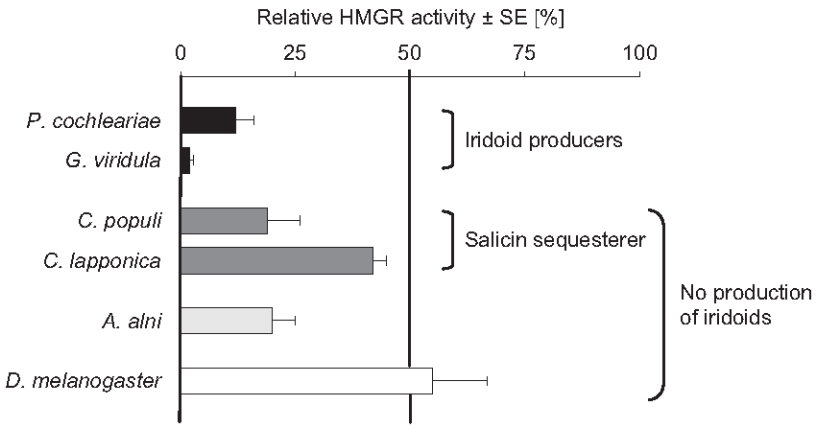

Fig. 9. Inhibition of the HMGR in a crude enzyme extracts from leaf beetle larvae and *D. melanogaster* in the presence of 5 mM 8-hydroxygeraniol.

mRNA levels. It remains to be determined whether the same can be observed on insect HMGR after geraniol treatment. A reduced HMGR activity after geraniol treatment was not detectable in our tissue incubation experiments.

8-Hydroxygeraniol modulates HMGR activity and with this also the iridoid production in chrysomelid larvae. HMGR activity may be affected not only by the endogenous level of 8-hydroxygeraniol but also by the sequestered glucoside (Fig. 1). We assume that the glucose moiety could be hydrolytically cleaved off by glucosidases, and that the resulting aglycon can than attenuate HMGR activity. Cleavage may occur after uptake into the fat body cells or already in the hemolymph or in both. Moreover, due to the activity of glucosidases in the gut lumen (Pasteels et al., 1983, 1990) 8-hydroxygeraniol can be liberated from the plant-derived glucoside already during the gut passage. A successful import of this compound through the gut membrane to the hemolymph and finally into the defensive secretion has been demonstrated (Lorenz et al., 1993). Incubation of dissected fat body tissue in 8-hydroxygeraniol solution resulted in decreased HMGR activity indicating transfer of this compound. But recent findings indicate that the glucoside also can pass the fat body membrane (unpublished data). The sugar moiety serves most likely for the transfer of the poor soluble aglucon in the hemolymph suggesting major impact of the glucoside on HMGR regulation (Feld et al., 2001). It seems reasonable to assume that HMGR represents one of the key regulators in maintaining homeostasis between sequestered and *de novo* produced metabolites in iridoid synthesis. To what extend other enzymes of this metabolism are also regulated by iridoid precursors is subject to future work.

Inhibition of mammalian HMGR has not only been reported from geraniol but also from the cyclic monoterpens *d*-limonene, menthol, perillyl alcohol and *β*-ionone in the context of chemoprevention of carcinogenesis (Elson et al., 1999; Mo and Elson, 2004). In tumor cells HMGR activity is several-fold more sensitive than normal cells to isoprenoid-mediated post-transcriptional downregulation. Menthol and *β*-ionone lower HMGR mass (Clegg et al., 1982; Yu et al., 1994). Limonene and perillyl alcohol attenuate HMGR activity through a mechanism regulating the efficiency of translation initiation (Qureshi et al., 1988; Peffley and Gayen, 2003). HMGR possesses different domains which are subject to different post-transcriptional regulation mechanisms (Friesen and Rodwell, 2004). The membrane-spanning domain is involved in accelerated degradation of the enzyme (Gil et al., 1985; Chun and Simoni, 1992). Phosphorylation of the catalytic domain results also in activity loss (Sato et al., 1993; Omkumar and Rodwell, 1994). However, in insects besides the transcriptional regulation triggered by juvenile hormones, this modulation of HMGR activity received only limited attention (Belles et al., 2005). Heterologous expression of the catalytic domain from the leaf beetle HMGR resulted in an active recombinant protein which is inhibited by 8-hydroxygeraniol in our assays. Thus, the compound interacts directly with the catalytic domain like the competitive statin inhibitors (Brown et al., 1978; Istvan and Deisenhofer, 2001) rather than down-regulating the enzyme activity by lowered enzyme mass. Unlike the statin inhibitor, the IC50 of 8-hydroxygerniol is in the mM-range which may be attributed to the use of the truncated protein. The results may be different in studies with the holoenzyme which are in progress. Docking studies of 8-hydroxygeraniol to a model of the homodimer of the catalytic portion of *P. cochleariae* HMGR revealed that the compound interacts with the enzyme in a position almost identical to the position of HMG in the three-dimensional structure of the human HMGR in direct neighborhood to CoA defining 8-hydroxygeraniol as a competitive inhibitor. These theoretical analyses substantiate our experimentally attained results. As a consequence, the larvae have a tool to fine-tune HMGR activity rapidly in response to changing biosynthetic demands, like increased *de novo* biosynthesis of iridoids after secretion release or during larval development, or like plasticity in the metabolite content of host plants in dependence on biotic and abiotic factors. HMGR

is regulated by negative feed-back inhibition by an intermediate of the defensive compound biosynthesis which is not essential for the cellular function but for inter-organismic communication.

Inhibition of HMGR by 8-hydroxygeraniol is not limited to Chrysomelina larvae which produce iridoids *de novo*. Enzyme activity is also diminished in insects that do not produce iridoids *de novo*. According to phylogenetic analyses of the Chrysomelina (Termonia et al., 2001), iridoid producers are considered to be the most ancestral branch, whereas the salicin sequestering species including the tested *C. populi* are more evolved (Pasteels et al., 1983; Kuhn et al., 2004). The most developed species like the analyzed *C. lapponica* esterify *de novo*-synthesized butyric acids with a variety of glucosidically bound leaf alcohols (Hilker and Schulz, 1994; Schulz et al., 1997; Termonia and Pasteels, 1999; Kuhn et al., 2007). Apparently, inhibition is retained during Chrysomelina evolution but its relevance in HMGR modulation *in vivo* remains to be elucidated. Decreased activity detected in the galerucine species *A. alni* as well as in the fruit fly points to an inhibition mechanism presumably more widespread across insects.

Acknowledgments

This study was supported by grants from the Max Planck Society and the Deutsche Forschungsgemeinschaft (SPP1152: Evolution of metabolic diversity). We gratefully acknowledge Jacques M. Pasteels for providing leaf beetles and for his creativity and helpful advice which supported this project. We thank Angelika Berg for taking care of the beetles.

References

Altschul, S.F., Madden, T.L., Schaffer, A.A., Zhang, J.H., Zhang, Z., Miller, W., Lipman, D.J., 1997. Gapped BLAST and PSI-BLAST: a new generation of protein database search programs. Nucleic Acids Res. 25, 3389–3402.

Belles, X., Martin, D., Piulachs, M.-D., 2005. The mevalonate pathway and the synthesis of juvenile hormone in insects. Annu. Rev. Entomol. 50, 181–199.

Bengoechea-Alonso, M.T., Ericsson, J., 2007. SREBP in signal transduction: cholesterol metabolism and beyond. Curr. Opin. Cell Biol. 19, 215–222.

Blum, M.S., 1994. Antipredatory devices in larvae of the Chrysomelidae: a unidentified synthesis for defensive electicism. In: Jolivet, P.H., Cox, M.L., Petitpierre, E. (Eds.), Novel Aspects of the Biology of the Chrysomelidae. Kluwer Academics Publishers, Doderecht, The Netherlands, pp. 277–288.

Blum, M.S., Wallace, J.B., Duffield, R.M., Brand, J.M., Fales, H.M., Sokoloski, E.A., 1978. Chrysomelidial in the defensive secretion of the leaf beetle *Gastrophysa cyanea* Melsheimer. J. Chem. Ecol. 4, 47–53.

Bochar, D.A., Stauffacher, C.V., Rodwell, V.W., 1999. Sequence comparisons reveal two classes of 3-hydroxy-3-methylglutaryl coenzyme A reductase. Mol. Genet. Metab. 66, 122–127.

Brown, M.S., Faust, J.R., Goldstein, J.L., Kaneko, I., Endo, A., 1978. Induction of 3 hydroxy-3-methyl glutaryl Coenzyme A reductase activity in human fibroblasts incubated with compactin Ml-236b a competitive inhibitor of the reductase. J. Biol. Chem. 253, 1121–1128.

Brown, K., Havel, C.M., Watson, J.A., 1983. Isoprene synthesis in isolated embryogenic *Drosophila* cells. J. Biol. Chem. 258, 8512–8518.

Brueckmann, M., Termonia, A., Pasteels, J.M., Hartmann, T., 2002. Characterization of an extracellular salicyl alcohol oxidase from larval defensive secretions of *Chrysomela populi* and *Phratora vitellinae* (Chrysomelina). Insect Biochem. Mol. Biol. 32, 1517–1523.

Burse, A., Schmidt, A., Frick, S., Kuhn, J., Gershenzon, J., Boland, W., 2007. Iridoid biosynthesis in Chrysomelina larvae: fat body produces early terpenoid precursors. Insect Biochem. Mol. Biol. 37, 255–265.

Chun, K.T., Simoni, R.D., 1992. The role of the membrane domain in the regulated degradation of 3- hydroxy-3-methylglutaryl coenzyme A reductase. J. Biol. Chem. 267, 4236–4246.

Clark, A.J., Bloch, K., 1959. The absence of sterol synthesis in insects. J. Biol. Chem. 234, 2578–2582.

Clegg, R.J., Middleton, B., Bell, G.D., White, D.A., 1982. The mechanism of cyclic mono terpene inhibition of hepatic 3-hydroxy-3-methyl glutaryl Coenzyme A reductase Ec-1.1.1.34 *in-vivo* in the rat. J. Biol. Chem. 257, 2294–2299.

Corsini, A., Maggi, F.M., Catapano, A.L., 1995. Pharmacology of competitive inhibitors of hmg-CoA reductase. Pharmacol. Res. 31, 9–27.

Cserzo, M., Wallin, E., Simon, I., von Heijne, G., Elofsson, A., 1997. Prediction of transmembrane alpha-helices in procariotic membrane proteins: the Dense Alignment Surface method. Prot. Eng. 10, 673–676.

Daloze, D., Pasteels, J.M., 1994. Isolation of 8-hydroxygeraniol-8-O-beta-D-glucoside, a probable intermediate in biosynthesis of iridoid monoterpenes, from defensive secretions of *Plagiodera versicolora* and *Gastrophysa viridula* (coleoptera, chrysomelidae). J. Chem. Ecol. 20, 2089–2097.

Dobrosotskaya, I.Y., Seegmiller, A.C., Brown, M.S., Goldstein, J.L., Rawson, R.B., 2002. Regulation of SREBP processing and membrane lipid production by phospholipids in *Drosophila*. Science 296, 879–883.

Dubrovsky, E.B., 2005. Hormonal cross talk in insect development. Trends Endocrin. Met. 16, 6–11.

Edwards, P.A., Ericsson, J., 1999. Sterols and isoprenoids: signaling molecules derived from the cholesterol biosynthetic pathway. Annu. Rev. Biochem. 68, 157–185.

Elson, C.E., Peffley, D.M., Hentosh, P., Mo, H.B., 1999. Isoprenoid-mediated inhibition of mevalonate synthesis: potential application to cancer. P. Soc. Exp. Biol. Med. 221, 294–311.

Feld, B.K., Pasteels, J.M., Boland, W., 2001. *Phaedon cochleariae* and *Gastrophysa viridula* (Coleoptera:Chrysomelidae) produce defensive iridoid monoterpenes *de novo* and are able to sequester glycosidically bound terpenoid precursors. Chemoecology 11, 191–198.

Friesen, J., Rodwell, V., 2004. The 3-hydroxy-3-methylglutaryl coenzyme-A (HMG-CoA) reductases. Genome Biol. 5, 248.

Gil, G., Faust, J.R., Chin, D.J., Goldstein, J.L., Brown, M.S., 1985. Membrane-bound domain of HMG CoA reductase is required for sterol-enhanced degradation of the enzyme. Cell 41, 249–258.

Goldstein, J.L., Brown, M.S., 1990. Regulation of the mevalonate pathway. Nature 343, 425–430.

Hall, G.M., Tittiger, C., Andrews, G.L., Mastick, G.S., Kuenzli, M., Luo, X., Seybold, S.J., Blomquist, G.J., 2002a. Midgut tissue of male pine engraver, *Ips pini*, synthesizes monoterpenoid pheromone component ipsdienol *de novo*. Naturwissenschaften 89, 79–83.

Hall, G.M., Tittiger, C., Blomquist, G.J., Andrews, G.L., Mastick, G.S., Barkawi, L.S., Bengoa, C., Seybold, S.J., 2002b. Male Jeffrey pine beetle, *Dendroctonus jeffreyi*, synthesizes the pheromone component frontalin in anterior midgut tissue. Insect. Biochem. Mol. Biol. 32, 1525–1532.

Henikoff, S., Henikoff, J.G., 1992. Amino acid substitution matrices from protein blocks. Proc. Natl. Acad. Sci. USA 89, 10915–10919.

Henikoff, S., Henikoff, J.G., 1993. Performance evaluation of amino acid substitution matrices. Proteins 17, 49–61.

Hilker, M., Schulz, S., 1994. Composition of larval secretion of *Chrysomela lapponica* (Coleoptera, Chrysomelidae) and its dependence on host plant. J. Chem. Ecol. 20, 1075–1093.

Holdgate, G.A., Ward, W.H.J., McTaggart, F., 2003. Molecular mechanism for inhibition of 3-hydroxy-3-methylglutaryl CoA (HMG-CoA) reductase by rosuvastatin. Biochem. Soc. T. 31, 528–531.

Istvan, E.S., Deisenhofer, J., 2000. The structure of the catalytic portion of human HMG-CoA reductase. BBA-Mol. Cell Biol. L. 1529, 9–18.

Istvan, E.S., Deisenhofer, J., 2001. Structural mechanism for statin inhibition of HMG-CoA reductase. Science 292, 1160–1164.

Istvan, E.S., Palnitkar, M., Buchanan, S.K., Deisenhofer, J., 2000. Crystal structure of the catalytic portion of human HMG-CoA reductase: insights into regulation of activity and catalysis. EMBO J. 19, 819–830.

Ivarsson, P., Tittiger, C., Blomquist, C., Borgeson, C.E., Seybold, S.J., Blomquist, G.J., Hogberg, H.E., 1998. Pheromone precursor synthesis is localized in the metathorax of *Ips paraconfusus* Lanier (Coleoptera, Scolytidae). Naturwissenschaften 85, 507–511.

Jones, G., Willett, P., Glen, R.C., 1995. Molecular recognition of receptor sites using a genetic algorithm with a description of desolvation. J. Mol. Biol. 245, 43–53.

Jones, G., Willett, P., Glen, R.C., Leach, A.R., Taylor, R., 1997. Development and validation of a genetic algorithm for flexible docking. J. Mol. Biol. 267, 727–748.

Keeling, C.I., Blomquist, G.J., Tittiger, C., 2004. Coordinated gene expression for pheromone biosynthesis in the pine engraver beetle, *Ips pini* (Coleoptera:Scolytidae). Naturwissenschaften 91, 324–328.

Keeling, C.I., Bearfield, J.C., Young, S., Blomquist, G.J., Tittiger, C., 2006. Effects of juvenile hormone on gene expression in the pheromone-producing midgut of the pine engraver beetle, *Ips pini*. Insect Mol. Biol. 15, 207–216.

Kuhn, J., Pettersson, E.M., Feld, B.K., Burse, A., Termonia, A., Pasteels, J.M., Boland, W., 2004. Selective transport systems mediate sequestration of plant glucosides in leaf beetles: a molecular basis for adaptation and evolution. Proc. Natl. Acad. Sci. USA 101, 13808–13813.

Kuhn, J., Pettersson, E.M., Feld, B.K., Nie, L., Tolzin-Banasch, K., Machkour M'Rabet, S., Pasteels, J.M., Boland, W., 2007. Sequestration of plant-derived phenolglucosides by larvae of the leaf beetle *Chrysomela lapponica*: thioglucosides as mechanistic probes. J. Chem. Ecol. 33, 5–24.

Laskowski, R.A., MacArthur, M.W., Moss, D.S., Thornton, J.M., 1993. PROCHECK: a program to check the stereochemical quality of protein structures. J. Appl. Cryst. 26, 283–291.

Laurent, P., Braekman, J.C., Daloze, D., Pasteels, J., 2003. Biosynthesis of defensive compounds from beetles and ants. Eur. J. Org. Chem., 2733–2743.

Laurent, P., Braekman, J.C., Daloze, S., 2005. Insect chemical defense. Chem. Pheromones Other Semiochem. II 240, 167–229.

Lorenz, M., Boland, W., Dettner, K., 1993. Biosynthesis of iridodials in the defense glands of beetle larvae (Chrysomelinae). Angew. Chem. Int. Edit. 32, 912–914.

MacKerell, A.D., Bashford, D., Bellott, M., Dunbrack, R.L., Evanseck, J.D., Field, M.J., Fischer, S., Gao, J., Guo, H., Ha, S., Joseph-McCarthy, D., Kuchnir, L., Kuczera, K., Lau, F.T.K., Mattos, C., Michnick, S., Ngo, T., Nguyen, D.T., Prodhom, B., Reiher, W.E., Roux, B., Schlenkrich, M., Smith, J.C., Stote, R., Straub, J., Watanabe, M., Wiorkiewicz-Kuczera, J., Yin, D., Karplus, M., 1998. All-atom empirical potential for molecular modeling and dynamics studies of proteins. J. Phys. Chem. B 102, 3586–3616.

Meinwald, J., Jones, T.H., Eisner, T., Hicks, K., 1977. New methylcyclopentanoid terpenes from the larval defensive secretion of a chrysomelid beetle (*Plagiodera versicolora*). Proc. Natl. Acad. Sci. USA 74, 2189–2193.

Mo, H.B., Elson, C.E., 2004. Studies of the isoprenoid-mediated inhibition of mevalonate synthesis applied to cancer chemotherapy and chemoprevention. Exp. Biol. Med. 229, 567–585.

Nardi, J.B., Young, A.G., Ujhelyi, E., Tittiger, C., Lehane, M.J., Blomquist, G.J., 2002. Specialization of midgut cells for synthesis of male isoprenoid pheromone components in two scolytid beetles, *Dendroctonus jeffreyi* and *Ips pini*. Tissue Cell 34, 221–231.

Nissink, J.W.M., Murray, C., Hartshorn, M., Verdonk, M.L., Cole, J.C., Taylor, R., 2002. A new test set for validating predictions of protein–ligand interaction. Proteins Struct. Func. Gen. 49, 457–471.

Oldham, N.J., Veith, M., Boland, W., Dettner, K., 1996. Iridoid monoterpene biosynthesis in insects-evidence for a *de novo* pathway occurring in the defensive glands of *Phaedon armoraciae* (Chrysomelidae) leaf beetle larvae. Naturwissenschaften 83, 470–473.

Omkumar, R.V., Rodwell, V.W., 1994. Phosphorylation of ser(871) impairs the function of his(865) of syrian hamster 3-hydroxy-3-methylglutaryl-coa reductase. J. Biol. Chem. 269, 16862–16866.

Pahan, K., 2006. Lipid-lowering drugs. Cell. Mol. Life Sci. 63, 1165–1178.

Pasteels, J.M., 1993. The value of defensive compounds as taxonomic characters in the classification of leaf beetles. Biochem. Syst. Ecol. 21, 135–142.

Pasteels, J.M., Braekman, J.C., Daloze, D., Ottinger, R., 1982. Chemical defence in chrysomelid larvae and adults. Tetrahedron 38, 1891–1897.

Pasteels, J.M., Rowell-Rahier, M., Braekman, J.C., Dupont, A., 1983. Salicin from host plant as precursor of salicyl aldehyde in defensive secretion of Chrysomeline larvae. Physiol. Entomol. 8, 307–314.

Pasteels, J.M., Daloze, D., Rowell-Rahier, M., 1986. Chemical defense in chrysomelid eggs and neonate larvae. Physiol. Entomol. 11, 29–38.

Pasteels, J.M., Duffey, S., Rowell-Rahier, M., 1990. Toxins in chrysomelid beetles, possible evolutionary sequence from *de novo* synthesis to derivation from food–plant chemicals. J. Chem. Ecol. 16, 211–222.

Pasteels, J.M., Rowell-Rahier, M., Braekman, J.-C., Daloze, D., 1994. Chemical defence of adult leaf beetles updated. In: Jolivet, P.H., Cox, M.L., Petitpierre, E. (Eds.), Novel Aspects of the Biology of Chrysomelidae, 50. Kluwer Academic Publisher, Dordrecht, The Netherlands, pp. 289–301.

Peffley, D.M., Gayen, A.K., 2003. Plant-derived monoterpenes suppress hamster kidney cell 3-hydroxy-3-methylglutaryl coenzyme A reductase synthesis at the transcriptional level. J. Nutr. 133, 38–44.

Pellegrini, E., Field, M.J., 2002. A generalized-born solvation model for macromolecular hybrid-potential calculations. J. Phys. Chem. A 106, 1316–1326.

Qureshi, A. A., Mangels, W. R., Din, Z. Z., Elson, C. E., 1988. Inhibition of hepatic mevalonate biosynthesis by the monoterpene D-limonene. J. Agr. Food Chem. 36, 1220–1224.

Rawson, R.B., 2003. The SREBP pathway–insights from insigs and insects. Nat. Rev. Mol. Cell Bio. 4, 631–640.

Renner, K., 1970. Über die ausstülpbaren Hautblasen der Larven von *Gastroidea viridula* De Geer und ihre ökologische Bedeutung (Coleoptera: Chrysomelidae). Beitäge zur Entomologie 20, 527–533.

Sambrook, J., Russell, D.W., 2000. Molecular Cloning. A Laboratory Manual. Cold Spring Harbor Laboratory Press, US.

Sato, R., Goldstein, J.L., Brown, M.S., 1993. Replacement of serine-871 of hamster 3-hydroxy-3-methylglutaryl-CoA reductase prevents phosphorylation by AMP-activated kinase and blocks inhibition of sterol synthesis induced by ATP depletion. Proc. Natl. Acad. Sci. USA 90, 9261–9265.

Schulz, S., 1998. Insect–plant interactions-metabolism of plant compounds to pheromones and allomones by lepidoptera and leaf beetles. Eur. J. Org. Chem., 13–20.

Schulz, S., Gross, J., Hilker, M., 1997. Origin of the defensive secretion of the leaf beetle *Chrysomela lapponica*. Tetrahedron 53, 9203–9212.

Seegmiller, A.C., Dobrosotskaya, I., Goldstein, J.L., Ho, Y.K., Brown, M.S., Rawson, R.B., 2002. The SREBP pathway in *Drosophila*: regulation by palmitate, not sterols. Dev. Cell 2, 229–238.

Seybold, S.J., Tittiger, C., 2003. Biochemistry and molecular biology of *De Novo* Isoprenoid pheromone production in the Scolytidae. Annu. Rev. Entomol. 48, 425–453.

Sippl, M.J., 1990. Calculation of conformational ensembles from potentials of mean force. An approach to the knowledge-based prediction of local structures in globular proteins. J. Mol. Biol. 213, 859–883.

Soe, A., Bartram, S., Gatto, N., Boland, W., 2004. Are iridoids in leaf beetle larvae synthesized *de novo* or derived from plant precursors? A methodological approach. Isot. Environ. Health Stud. 40, 175–180.

Soetens, P., Pasteels, J.M., Daloze, D., 1993. A simple method for *in vivo* testing of glandular enzymatic activity on potential precursors of larval defensive compounds in *Phratora* species (Coleoptera: Chrysomelinae). Experientia 49, 1024–1026.

Termonia, A., Pasteels, J.M., 1999. Larval chemical defence and evolution of host shifts in *Chrysomela* leaf beetles. Chemoecology 9, 13–23.

Termonia, A., Hsiao, T.H., Pasteels, J.M., Milinkovitch, M.C., 2001. Feeding specialization and host-derived chemical defense in Chrysomeline leaf beetles did not lead to an evolutionary dead end. Proc. Natl. Acad. Sci. USA 98, 3909–3914.

Tillman, J.A., Holbrook, G.L., Dallara, P.L., Schal, C., Wood, D.L., Blomquist, G.J., Seybold, S.J., 1998. Endocrine regulation of *de novo* aggregation pheromone biosynthesis in the pine engraver, *Ips pini* (Say) (Coleoptera, Scolytidae). Insect Biochem. Mol. 28, 705–715.

Tillman, J.A., Lu, F., Goddard, L.M., Donaldson, Z.R., Dwinell, S.C., Tittiger, C., Hall, G.M., Storer, A.J., Blomquist, G.J., Seybold, S.J., 2004. Juvenile hormone regulates *de novo* isoprenoid aggregation pheromone biosynthesis in pine bark beetles, *Ips* spp., through transcriptional control of HMG-CoA reductase. J. Chem. Ecol. 30, 2459–2494.

Tittiger, C., Blomquist, G.J., Ivarsson, P., Borgeson, C.E., Seybold, S.J., 1999. Juvenile hormone regulation of HMG-R gene expression in the bark beetle *Ips paraconfusus* (Coleoptera: Scolytidae): implications for male aggregation pheromone biosynthesis. Cell. Mol. Life Sci. 55, 121–127.

Tittiger, C., Barkawi, L.S., Bengoa, C.S., Blomquist, G.J., Seybold, S.J., 2003. Structure and juvenile hormone-mediated regulation of the HMG-CoA reductase gene from the Jeffrey pine beetle, *Dendroctonus jeffreyi*. Mol. Cell. Endocrinol. 199, 11–21.

Veith, M., Lorenz, M., Boland, W., Simon, H., Dettner, K., 1994. Biosynthesis of iridoid monoterpenes in insects-defensive secretions from larvae of leaf beetles (Coleoptera, Chrysomelidae). Tetrahedron 50, 6859–6874.

Veith, M., Dettner, K., Boland, W., 1996. Stereochemistry of an alcohol oxidase from the defensive secretion of larvae of the leaf beetle *Phaedon armoraciae* (Coleoptera, Chrysomelidae). Tetrahedron 52, 6601–6612.

Veith, M., Oldham, N.J., Dettner, K., Pasteels, J.M., Boland, W., 1997. Biosynthesis of defensive allomones in leaf beetle larvae-stereochemistry of salicylalcohol oxidation in *Phratora vitellinae* and comparison of enzyme substrate and stereospecificity with alcohol oxidases from several iridoid producing leaf beetles. J. Chem. Ecol. 23, 429–443.

Verdonk, M.L., Cole, J.C., Hartshorn, M.J., Murray, C.W., Taylor, R.D., 2003. Improved protein–ligand docking using GOLD. Proteins Struct. Funct . Gen. 52, 609–623.

von Nickisch-Rosenegk, E., Detzel, A., Wink, M., Schneider, D., 1990. Carrier-mediated uptake of digoxin by larvae of the cardenolide sequestering moth, *Syntomeida epilais*. Naturwissenschaften 77, 336–338.

Yu, S.G., Abuirmeileh, N.M., Qureshi, A.A., Elson, C.E., 1994. Dietary beta-ionone suppresses hepatic 3-hydroxy-3-methylglutaryl coenzyme a reductase activity. J. Agr. Food Chem. 42, 1493–1496.

5.2 MANUSCRIPT 2

ALWAYS BEING WELL PREPARED FOR DEFENSE: THE PRODUCTION OF DETERRENTS BY JUVENILE CHRYSOMELINA BEETLES (CHRYSOMELIDAE)

Phytochemistry 70 (2009) 1899–1909

Contents lists available at ScienceDirect

Phytochemistry

journal homepage: www.elsevier.com/locate/phytochem

Review

Always being well prepared for defense: The production of deterrents by juvenile *Chrysomelina* beetles (Chrysomelidae)

Antje Burse *, Sindy Frick, Sabrina Discher, Karla Tolzin-Banasch, Roy Kirsch, Anja Strauß, Maritta Kunert, Wilhelm Boland

Max Planck Institute for Chemical Ecology, Department of Bioorganic Chemistry, Hans-Knöll-Str. 8, D-07745 Jena, Germany

ARTICLE INFO

Article history:
Received 9 April 2009
Received in revised form 3 August 2009
Available online 4 September 2009

Keywords:
Chemical ecology
Co-evolution
Secondary metabolites
Leaf beetles
Chemical defense
Sequestration
Transport protein
Thioglucosides
Fat body
Iridoid synthesis

ABSTRACT

In response to herbivores, plants produce a variety of natural compounds. Many beetle species have developed ingenious strategies to cope with these substances, including colonizing habitats not attractive for other organisms. Leaf beetle larvae of the subtribe Chrysomelina, for example, sequester plant-derived compounds and use them for their own defense against predators. Using systematically modified structural mimics of plant-derived glucosides, we demonstrated that all tested Chrysomelina larvae channel compounds from the gut lumen into the defensive glands, where they serve as intermediates in the synthesis of deterrents. Detailed studies of the sequestration process revealed a functional network of transport processes guiding phytochemicals through the larval body. The initial uptake by the larvae's intestine seems to be fairly unspecific, which contrasts sharply with the specific import of precursors into the defensive glands. The Malpighian tubules and hind-gut organs facilitate the rapid clearing of body fluid from excess or unusable compounds. The network exists in both sequestering species and species producing deterrents *de novo*. Transport proteins are also required for *de novo* synthesis to channel intermediates from the fat body to the defensive glands for further conversion. Thus, all the tools needed to exploit host plants' chemistry by more derived Chrysomelina species are already developed by iridoid–*de novo* producers. Early intermediates from the iridoid–*de novo* synthesis which also can be sequestered are able to regulate the enzyme activity in the iridoid metabolism.

Contents

1. Introduction

Beetles have used plants as a food source for about 230 million years, which has contributed to reciprocal adaptation and the enormous biodiversity that is found today in both organism groups (Farrell, 1998). Phytophagous species account for more than double the non-herbivorous taxa. This disparity became especially pronounced with the increasing diversity of angiosperms in the Post-Cretaceous period. In response to herbivores, plants developed several morphological and biochemical adaptations which allowed them to wage a kind of chemical warfare; one strategy of this war was based on toxic secondary metabolite production, storage and eventually release (Macias et al., 2007). As some insects became adapted to these metabolites, interactions between the two organism groups occasionally led to highly specific relationships.

The sequestration of poisonous phytochemicals and their use for defense purposes or as building blocks for toxins or

* Corresponding author. Tel.: +49 3641 571265; fax: +49 3641 57120.
E-mail address: aburse@ice.mpg.de (A. Burse).

0031-9422/$ - see front matter © 2009 Elsevier Ltd. All rights reserved.
doi:10.1016/j.phytochem.2009.08.002

pheromones is a widespread phenomenon observed in Coleoptera (Duffey, 1980). Leaf beetles (Chrysomelidae) in particular are known for their ability to import structurally different allelochemicals, such as β-amyrin (Laurent et al., 2003b), cucurbitacins (Gillespie et al., 2003), pyrrolizidin alkaloids (Hartmann, 2004), phenolglucosides (Pasteels et al., 1983), naphthaleneglucoside (Pasteels et al., 1990), glucosidically bound aliphatic alcohols (Schulz et al., 1997) or iridoid glucosides (Willinger and Dobler, 2001). The sequestered compounds often have to be further transformed to become biologically active. Altering the metabolite profile of the plant may entail modifications in the deterrent pattern of the insect. Consequently, co-evolution plays a crucial role in explaining secondary metabolite diversity in plants and their grazers.

We provide an overview of our studies on sequestration processes of plant-derived compounds by leaf beetles. After we followed the route of incorporated phytochemicals and their conversion within insects on the molecular level, we explored the impact of the sequestered compounds on the endogenous biosynthesis of deterrents. Finally, we discuss our results in the context of development of metabolite diversity in chrysomelids as well as the relevance of sequestration as a process for enhancing the adaptive radiation observed in plants and beetles.

2. Chemical defense in leaf beetle larvae

Within the Chrysomelidae are many species in which not only the adults but also the larvae produce deterrents from plant-derived compounds (Pasteels et al., 1982; Blum, 1994; Schulz, 1998; Laurent et al., 2003a, 2005). In certain cases, the defensive compounds are stored in specialized structures of the body and used to repel predators, such as in the larvae of the leaf beetle subtribe Chrysomelina. The larvae possess nine pairs of defensive glands on the last two thoracic and first seven abdominal tergites (Renner, 1970; Pasteels and Rowell-Rahier, 1989). Each of the exocrine glands is composed of many secretory cells which are attached to a large reservoir. When the larvae are stimulated, they emit secretions from the tips of the glandular tubercles. As soon as the disturbance is over, the secretions are sucked back into the reservoir. The anti-predatory effect of the secretions can be attributed either to autogenously synthesized defensive compounds or to sequestered plant-derived glucosides converted within the reservoir by a few enzymatic reactions into deterrents.

According to phylogenetic analyses of Chrysomelina species by Termonia et al. (2001), the *de novo* production of deterrent iridoids (monoterpenoids with the iridane skeleton) is considered the ancestral strategy (Meinwald et al., 1977; Blum et al., 1978; Pasteels et al., 1982; Soe et al., 2004) (Fig. 1A). More derived species acquired the ability to sequester compounds, which made the biosynthesis of deterrent substances more economical. Larvae of the Chrysomelina species feeding on Salicaceae sequester phenolglucosides such as salicin and salicortin (Pasteels et al., 1983; Brueckmann et al., 2002; Michalski et al., 2008) (Fig. 1B). The glucosides serve as precursors for the odiferous and repellent salicylaldehyde. In contrast to the incorporation of a few plant-derived compounds, larvae of the most evolved Chrysomelina species are able to take up a wide variety of glucosidically bound leaf alcohols. Their aglucons are further esterified with butyric acids derived from the insects' internal pools of amino acids, which can result in a cocktail of at least 70 deterrent esters (Hilker and Schulz, 1994; Schulz et al., 1997; Termonia and Pasteels, 1999; Kuhn et al., 2007) (Fig. 1C).

A combination of the above-described strategies of allomone production with the host plant families mirrors the reciprocal adaptation of Chrysomelina beetles to their hosts (Termonia et al., 2001; Fernandez and Hilker, 2007) (Fig. 1D). Species synthesizing the deterrents *de novo* feed on different plant families, such as Brassicaceae or Polygonaceae. In contrast, Chrysomelina members whose larvae sequester salicin are adapted exclusively to Salicaceae. Larvae of *Chrysomela lapponica* sequester a blend of glucosidically bound leaf alcohols; it is remarkable that this species has developed allopatric populations which colonize salicaceous and betulaceaous plants. Populations on *Salix* spec., rich in salicin, have been reported to produce almost exclusively salicylaldehyde, whereas populations on birches synthesize a completely dissimilar pattern of defensive compounds due to the lack of or strongly reduced level of salicin in the plant (Hilker and Schulz, 1994; Schulz et al., 1997).

To sequester and use new plant-derived metabolites for self-defense, not only the transport mechanisms but also the following enzymatic reactions must be modified. Basically the same enzymatic reactions convert sequestered or *de novo* produced compounds into allomons in the larval defensive glands of all Chrysomelina species. A β-glucosidase removes the sugar moiety from the glucosides. Subsequently, an oxidase whose substrate spectrum is likely defined catalyzes the formation of (di)aldehydes (Veith et al., 1996; Brueckmann et al., 2002; Michalski et al., 2008). Pasteels et al. (1990) postulated the *de novo* synthesis of defensive compounds as the primitive state which harbors the set of enzymes that allows plant-derived glucosides to evolve the capacity to be used for defense. In many respects, the sequestration of glucosides is beneficial. The compounds are abundant in the leaves of the food plant. *A priori* they are mostly non-toxic but can be readily cleaved into deterrent aglycons or compounds that can be enzymatically converted into deterrents or even toxins. The catabolism of the glucose moiety supplies additional energy equivalents (Pasteels et al., 1983). Not least, the polar glycosides are non-diffusible through membranes unless functional transport systems mediate their passage.

3. A network of transporters mediates sequestration and the excretion of glucosides

Numerous publications postulate that selective transport systems facilitate the sequestration of secondary metabolites from plants into insects. Within the order Coleoptera, for example, the transport processes of the strongly deterrent pyrrolizidine alkaloids (PAs) are exploited by some leaf beetle species for their own predator defense; these alkaloids have been studied extensively in the last decade (for review see Hartmann (1999, 2004), Hartmann and Ober (2000, 2008)). Plants store PAs mostly as non-toxic *N*-oxides. Their reduction during the intestinal passage results in lipophilic pro-toxic free bases which can pass through membranes by diffusion. Incorporated free bases can then be converted into the toxic pyrrolic intermediates. Species of the genus *Oreina* which are adapted to feed on PA-containing plants have evolved a special sequestration mechanism to avoid self-poisoning. The beetles suppress the reduction of the PA *N*-oxides in the gut and directly absorb the polar compound (Hartmann et al., 1997, 1999). Feeding experiments using ^{14}C-labeled senecionine and its *N*-oxide, suggested carrier-mediated transport of the polar *N*-oxide from gut into hemolymph in larvae and adults and from hemolymph into exocrine glands in adults of *Oreina cacaliae* (Hartmann et al., 1999). Direct evidence for membrane transport was provided by feeding double-labeled [^{14}C]senecionine [^{18}O] *N*-oxide as a tracer to *O. cacaliae* and *Oreina speciosissima*: the ^{18}O-label was retained after passage from gut into the defensive secretions of adult beetles (Narberhaus et al., 2004a, b). The same tracer has also shown that transport proteins are responsible for incorporating polar senecionine-type *N*-oxides in adults of *Longitarsus jacobaeae*.

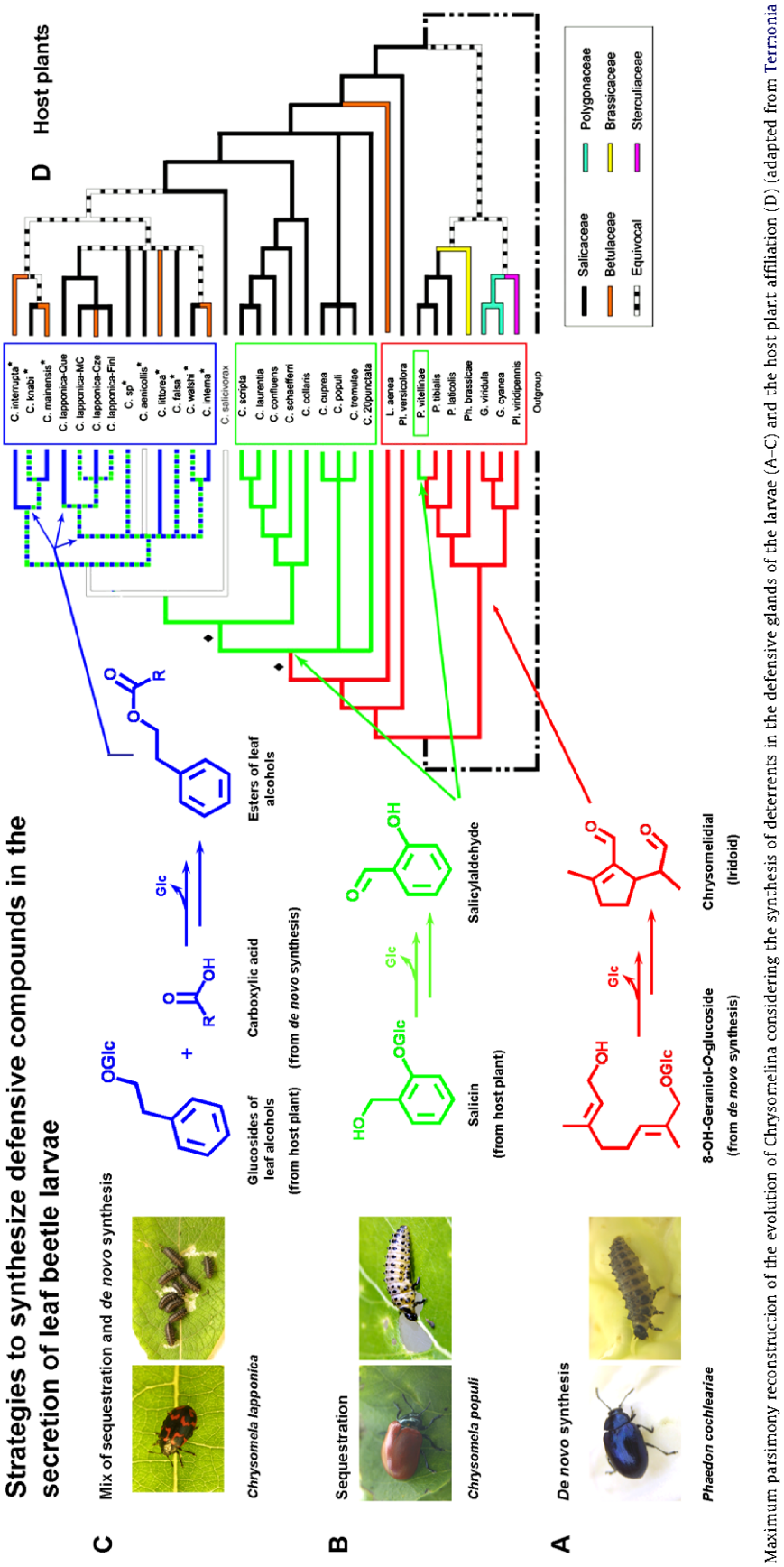

Fig. 1. Maximum parsimony reconstruction of the evolution of Chrysomelina considering the synthesis of deterrents in the defensive glands of the larvae (A–C) and the host plant affiliation (D) (adapted from Termonia et al. (2001)).

Larvae and adults of another PA-adapted species, *Platyphora boucardi*, absorb the lipophilic pro-toxic free bases and transfer them highly efficiently into the defensive glands, thus preventing them from accumulating in the hemolymph (Hartmann et al., 2001, 2003; Pasteels et al., 2001, 2003). The concentration difference of >1000 between hemolymph and the secretions of the easily diffusible lipophilic tertiary alkaloids also suggests the participation of carriers; this, however, has yet to be proven experimentally.

Radio-labeled traces are suitable to study transport processes. But in Chrysomelina species which sequester glucosides, *S*-analogs instead of the natural plant-derived *O*-glucosides were used to follow the route of incorporated compounds (Feld et al., 2001; Kuhn et al., 2004, 2007). The glycomimics are stable against the glucosidases in the gut and the gland, and they accumulate in the defensive secretions where they can be easily quantified by high-performance liquid chromatography mass-spectrometry.

To understand the selection criteria for the sequestered compounds, thioglucosides of salicin isomers, along with aliphatic and aromatic *S*-glucosides were tested (Fig. 2). The chrysomeline larvae were allowed to feed on individual compounds and assessed their passage through the intestinal and glandular system by analyzing their secretions. The feeding experiments not only revealed the existence of transport systems that channel the hydrophilic plant-derived glucosides through the gut membrane into the defensive gland *via* hemolymph transfer but also demonstrated the varied selectivity of glucoside uptake in the analyzed Chrysomelina species. For example, larvae of *Chrysomela populi* and *Phratora vitellinae* which secrete almost exclusively salicylaldehyde import predominantly the *S*-mimic (6) of the genuine precursor salicin (Kuhn et al., 2004, 2007) (Fig. 2). Iridoid-producing larvae of the four tested species *Phaedon cochleariae*, *Gastrophysa virdula*, *Hydrothassa marginella*, and *Phratora laticollis* seem to possess transporters mediating the selective uptake of the *S*-mimic of

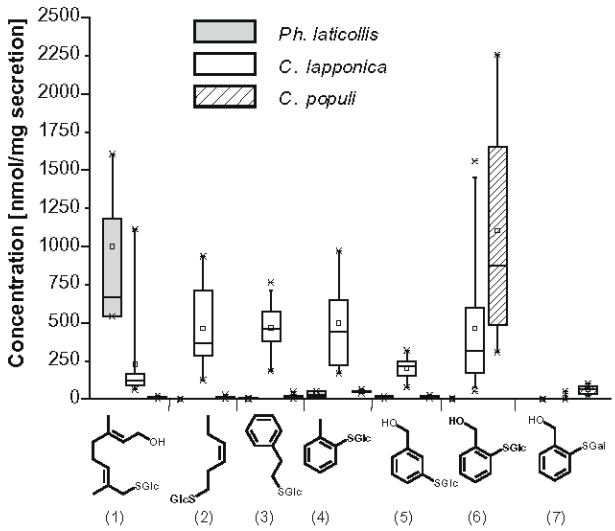

Fig. 2. Uptake of thioglucosides from gut lumen into the defensive secretions after larvae fed on the single compounds. For all experiments, the upper surfaces of host plant leafs were impregnated with methanolic solutions of the test compounds (0.5 μmol/cm leaf). Secretions samples were taken after 48 h feeding on 25–35 cm^2 leaf material. Five to seven larvae were fed for each replication ($n = 3–10$ depending on compound). In all experiments, post hoc multiple comparisons (Tamhane's T2 test, SPSS) were carried out to evaluate significant differences ($P < 0.05$). **1**, (2*E*,6*E*)-8-hydroxy-2,6-dimethyl-octa-2,6-dienyl-1′-thio-β-D-glucopyranoside (8-OH-Ger-*S*-glucoside); **2**, (3*Z*)-hex-3-en-1-yl-1′-thio-β-D-glucopyranoside; **3**, 2-phenylethyl-1′-thio-β-D-glucopyranoside (phenylethyl-*S*-glucoside); **4**, 2-tolyl-1′-thio-β-D-glucopyranoside; **5**, 3-hydroxymethyl-phenyl-1′-thio-β-D-glucopyranoside; **6**, 2-hydroxymethyl-phenyl-1′-thio-β-D-glucopyranoside (*S*-salicin); **7**, 2-hydroxymethyl-phenyl-1′-thio-β-D-galactopyranoside.

glucosidically bound 8-hydroxygeraniol (1), an early intermediate in iridoid metabolism (Feld et al., 2001; Kuhn et al., 2004) (Fig. 2). The uptake systems even differentiated between stereoisomers such as Ger-8-*S*-Glc and Ger-1-*S*-Glc; the former was favored by a factor of 10 over the 1-*S*-Glc (Feld et al., 2001). In all cases, the preference for a single glucoside corresponds to the composition of the secretions that contain one or few deterrent substances.

These results sharply contrast with those from experiments in which *C. lapponica* larvae fed on willow and birch. Regardless of the host plant, all larvae can incorporate similarly efficiently a broad range of structurally altered thioglucosides in addition to *S*-salicin (Kuhn et al., 2007) (Fig. 2). The final concentration of each tested thioglucoside in the secretions of *C. lapponica* larvae did not exceed 200–450 nmol mg^{-1}, a concentration which clearly differs from that of the secretions of *C. populi*, where *S*-salicin accumulated to about 1100 nmol mg^{-1}. But in total the glucoside content was similar to that of *C. populi*.

In the hemolymph of all studied species, only traces of the ingested thioglucosides were detected; this indicates the body fluid is rapidly cleaned from the imported substances (Feld et al., 2001; Kuhn et al., 2004, 2007). Consequently, the intestinal transport systems most likely work with a gradient from high to low substance concentrations. In contrast, the putative carriers in the defensive glands must transfer compounds against a steep gradient. From our results, it seems reasonable to assume that different transport systems facilitate the sequestration process.

Analyses carried out with isomers of *S*-salicin and *S*-cresol showed that the putative transporter seemed to select their glucosidically bound substrates by matching the orientation of the hydroxyl groups, in particular by embedding them into a network of hydrogen bonds inside the protein (Kuhn et al., 2007). For example, the transport systems of *C. populi* responded to the structural modifications of salicin, such as *para*-, and *meta*-position of the hydroxyl groups by reducing the import by about 90%. Also, *ortho*-, *para*-, and *meta*-cresol lacking only the hydroxyl group of the salicin side chain were not significantly accumulated in the secretions. A mechanistic model postulating hydrogen bonds between substituents of the glucosides and a putative carrier would also explain why the galactoside was not sequestered in lavae of either *C. populi* or *C. lapponica* (Fig. 2). Because the alglycons rely on the import of glucosidically bound compounds, their structural features and those of the sugar are important (Kuhn et al., 2007).

Apparently *C. lapponica* evolved transport mechanisms with a broad substrate spectrum, allowing changes in host plants that were even contrary to the "phytochemical bridge" postulated by Ehrlich and Raven (1964). Ecological studies carried out on the different *C. lapponica* populations revealed that willow inhabitants are frequently exposed to specialized parasitoids and predators (Zvereva and Rank, 2003, 2004; Gross et al., 2004). For example, syrphid species learned to use salicylaldehyde in the defensive secretions of larvae feeding on willow as a way to locate their prey. Grazing on birch, indeed, lowers the mortality of the larvae, suggesting that the presence of natural enemies is one of the important driving forces behind host plant shifts.

Our feeding experiments demonstrated selective glucoside incorporation into Chrysomelina larvae but did not address the localization of the selective barrier(s) and the route of glucosides within the larval body. Therefore, we carried out *in vitro* studies with dissected gut tissue and Malpighian tubules as well as *in vivo* microinjection into the larval hemolymph using equimolar mixtures of *S*-analogs; these mixtures were both similar and dissimilar to the natural glucosidic precursors of the defensive compounds (Discher et al., 2009). 8-OH-Ger-*S*-glucoside (1) mimics an early intermediate in the iridoid synthesis, phenylethyl-*S*-glucoside (3) resembles a precursor for esters produced by *C. lapponica*, and *S*-salicin (6) corresponds to the genuine precursor

for salicylaldehyde (Fig. 3). In the test series we compared larvae of two Chrysomelina species: the iridoid producer *P. cochleariae* (feeding on *Brassica rapa chinensis*) and the obligate salicin-sequestering species *C. populi* (feeding on *Populus canadensis*).

First, in feeding experiments using the thioglucoside mixture, we corroborated the results of the feeding experiments with individual thioglucosides (Discher et al., 2009). Larvae of both *P. cochleariae* and *C. populi* selectively imported the genuine precursor from food treated with the *S*-glucoside mix into the defensive secretions. In the hemolymph, only traces of all three compounds were detectable. Analysis of the feces revealed both non-precursors as well as precursors had been excreted.

Interestingly, the *in vitro* incubation of gut tissue with the thioglucoside mixture demonstrated that all compounds had been taken up into the epithelial cells regardless of the precursor function of the glucosides in either species (Discher et al., 2009) (Fig. 3A illustrates results from *P. cochleariae*). Consequently, the intestinal carriers most likely allow a broad substrate spectrum to enter the hemolymph.

In contrast, microinjecting the compound mixture into the hemocoel showed that only the genuine precursor of the deterrent compound was selectively imported into the defensive glands in both tested Chrysomelina species (Discher et al., 2009) (Fig. 3B illustrates results from *P. cochleariae*). Similar observations were made in the genus *Oreina*. After unspecific uptake of host plant PAs into the hemolymph of larvae and adults, certain macrocyclic PAs are selectively sequestered by adult beetles into their defensive glands (Hartmann et al., 1997).

Analyses of samples taken at different time points after injection showed the rapid clearance of the thioglucosides from the hemolymph (Discher et al., 2009). In both Chrysomelina species, the genuine glucoside selectively accumulated after 1 h and only traces of all three glucosides were detectable in the hemolymph at the same time point. The glucoside content within the secretions did not change significantly over a period of 48 h.

Injected thioglucosides not transferred into the defensive glands and an excess of the precursor glucoside were found in the feces after these were excreted by the Malpighian tubules and presumably also the hind gut (O'Donnell and Rheault, 2005). The *in vitro* incubation of dissected Malpighian tubules with the thioglucoside mixture also demonstrated that all compounds were taken up into this tissue, indicating their role in clearing the hemolymph from non-useful substances (Discher et al., 2009).

In contrast to the experimentally used thioglucosides, the natural *O*-glucosides entering the gut can be hydrolyzed by glucosidases. The aglucons are also able to pass through the gut membrane most likely by diffusion and reach the defensive system as demonstrated by larvae feeding of labeled d_5-8-hydroxygeraniol which was converted into the deterrent iridoid plagiodial (Kunert et al., 2008). Interestingly, after injecting the deuterated aglucon, d_5-8-hydroxygeraniol-8-*O*-β-D-glucoside was detected in the hemolymph as well as in the feces. Apparently, the compound was glucosylated by the larvae to prevent their self-poisoning. That underlines the importance of sugars as a form of transport during sequestration. Detoxification by *O*-glucosylation is a mechanism also reported from *O. cacaliae* (Hartmann et al., 1999). Typically this species incorporates the non-toxic PA *N*-oxides, but traces of the lipophilic tertiary alkaloid are also absorbed; these can be rendered innocuous by glucosylation. Although the *N*-oxidation of PAs is the most prevalent detoxification strategy known from insects, it seems inefficient in this *Oreina* species.

A complex network of different transport systems seems to control the supply of precursors that synthesize defensive compounds in both sequestering and deterrent-*de novo* producing Chrysomelina larvae (Fig. 4). First, the plant-derived metabolites have to pass through the highly polarized gut epithel cells; as transport proteins

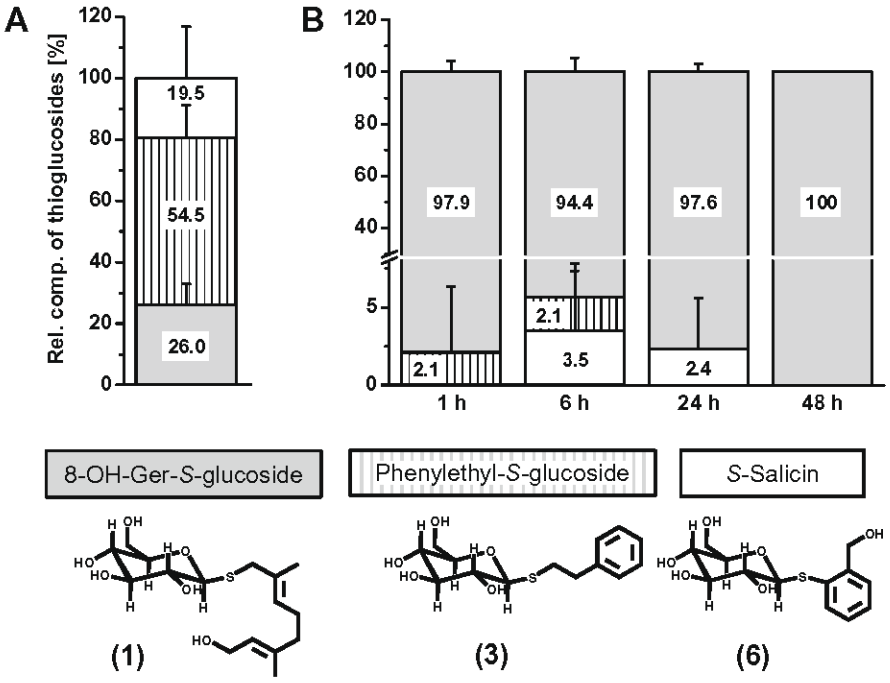

Fig. 3. Relative distribution of thioglucosides 1, 3, 6 in gut tissue and secretions of third-instar larvae of *Phaedon cochleariae*. *In vitro* uptake into gut cells was determined 1 h after incubating the dissected tissue in an equimolar mixture of thioglucosides (0.1 mM each, eight guts per sample) in physiological saline ($n = 9$). Absolute values [nmol substance/mg tissue]: **1**, 0.13 ± 0.06; **3**, 0.30 ± 0.12; **6**, 0.20 ± 0.19 (95% convidence interval) (A). Uptake into the secretions was measured at different time points after microinjecting an equimolar mixture of thioglucosides (1.47 nmol per larva, 20 larvae per sample) into the hemolymph of the larvae ($n = 5$). Absolute values [nmol substance/mg secretion]: 1 h, **1**, 2.83 ± 0.83; **3**, 0.08 ± 0.16; **6**, n.d.; 6 h, **1**, 3.32 ± 1.27; **3**, 0.10 ± 0.09; **6**, 0.30 ± 0.36; 24 h, **1**, 2.68 ± 1.11; **3**, n.d.; **6**, 0.15 ± 0.19; 48 h, **1**, 2.63 ± 0.74, **3**, n.d.; **6**, n.d. (B). n.d. = not detected (95% convidence interval) (adapted from Discher et al. (2009)).

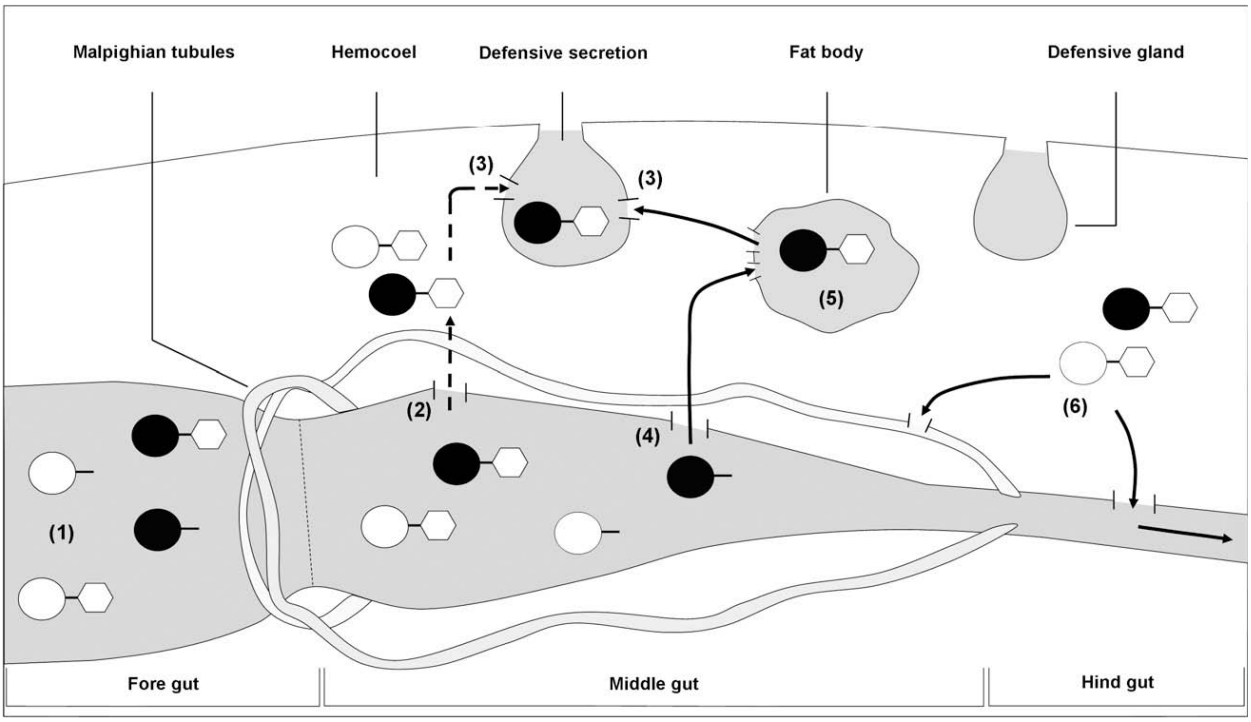

Fig. 4. A network of transport processes are implicated in the sequestration of secondary metabolites from the host plant. Glucosides and aglucons reach the gut lumen with the food (1). Carriers mediate the uptake of glucosides into the hemolymph (2). From there they are either transferred into the defensive glands, from which transporters selectively channel progenitors of deterrents into the secretions (3) or unused or excessive glucosides are excreted by the Malpighian tubules and hind-gut organs (6). Agluca may reach the hemocoel by diffusion (4) and precursors of the deterrents are most likely glucosylated in the fat body (5) from where they are channeled via the hemolymph either into the defensive secretion (3) or to the excretory tissue (6) (adapted from Kunert et al. (2008)).

are distributed in the plasma membrane somewhat unevenly, different types could mediate the trans-cellular transport of glucosides. The broad spectrum of metabolite transfer into the hemocoel allows the entrance of structurally unrelated glucosides; these circulate in the hemolymph until they reach the defensive glands via active transport or are excreted. To date it remains unknown which carrier types are implicated in the sequestration phenomenon. Most likely, the relationship between uptake into the gland and the excretion process is dynamic and depends on the capacity of the defensive system; this can change during larval development and as a result of disturbance by predators. Recently, we partly sequenced cDNA libraries generated from defensive glands and gut tissue to identify putative transporters involved in the sequestration process. Considering the broad substrate spectrum of putative carriers in the gut and the Malpighian tubules, we suggest that only minor modifications in the highly selective import mechanisms of the defensive glands and adaptations of the subsequent enzymatic reactions to the new precursors are required for beetles to use structurally different plant metabolites for chemical defense.

4. Iridoid–*de novo* biosynthesis and sequestration

The chemical defense of some beetles is often based on both the sequestration of metabolites from host plant and endogenous synthesis. In the genus *Oreina*, for example, some species produce cardenolides *de novo* and additionally take up plant-derived PAs (Dobler et al., 1996). Feeding experiments with *S*-analogs of the natural *O*-glucoside(s) demonstrated that the larvae of all tested iridoid–*de novo* producing Chrysomelina species should be able to sequester the precursor 8-hydroxygeraniol-8-*O*-*β*-D-glucoside (Feld et al., 2001; Kuhn et al., 2004). However, it has never been established that these larvae effectively take up the compound *in vivo*. This should be possible if the food plants provide metabolites matching the transport capacity and corresponding to an intermediate in the iridoid biosynthesis.

First, host plants were incubated with labeled 1-deoxy-[1-^{13}C,5,5-2H2]-D-xylulose (^{13}C-DOX), an intermediate in the methylerythriol-4-phosphate pathway which supplies precursors mainly to produce monoterpenes in plants (Kunert et al., 2008; Soe et al., 2004). Because insects cannot use ^{13}C-DOX to synthesize terpenoids, it can be used to determine the biosynthetic origin of iridoids in larval secretions. Additional treatment with jasmonic acid elicited the *de novo* biosynthesis of terpenoids and generated a broad spectrum of labeled compounds that may include precursors for iridoid biosynthesis in leaf beetle larvae. Moreover, the labeling of terpenoid volatiles emitted by the treated plants ensured the successful incorporation of ^{13}C-DOX.

The iridoid–producing larvae of *Plagiodera versicolora* (feeding on *Salix fragilis*) and *Ph. laticollis* (feeding on *P. canadensis*) fed on the ^{13}C-DOX-pretreated plant material for defined periods and then their defensive secretions were collected. The extensive incorporation of the label in the deterrent iridoid plagiodial in the two tested species indicated the uptake of iridoid precursors from the food plant (Kunert et al., 2008). In contrast, no clear evidence for the import and transformation of plant-derived precursors was found for the iridoid–*de novo* producing larvae of *P. cochleariae* (feeding on *Brassica rapa*, *Brassica oleracea* var. *gemmifera*, *Amoracia rusticana*) and *Gastrophysa viridula* (feeding on *Rumex obtusifolia*), although uptake of the 8-OH-Ger-*S*-glucoside (1) has been demonstrated for all four tested species.

In analyses of the glucosidically bound terpenoids of food plants, specifically *S. fragilis* and *P. canadensis*, we identified 8-hydroxygeraniol-8-*O*-*β*-D-glucoside, indicating that the compound can be sequestered by *Pl. versicolora* and *Ph. laticollis* larvae feeding on these plants (Table 1) (Kunert et al., 2008). The ability to sequester a plant-derived precursor represents a cost-saving strat-

Table 1
Identification of 8-hydroxygeraniol-8-*O*-*β*-D-glucoside in food plants of iridoid producing Chrysomelina larvae.

Leaf beetle species	Food plant	8-Hydroxygeraniol (μg g $^{-1}$ FW)
Plagiodera versicolora	*Salix fragilis*	2.3 ± 0.1
Phratora laticollis	*Populus canadensis*	1.1 ± 0.03
Gastrophysa viridula	*Rumex obtusifolius*	0.08 ± 0.01
Phaedon cochleariae	*Brassica oleracae var. gemmifera*	Not detectable
	Brassica rapa	Not detectable
	Amoraciae rusticana	Not detectable

Glucosidically bound 8-hydroxygeraniol was extracted and cleaved enzymatically followed by derivatisation (Kunert et al., 2008). The aglucon was unambiguously identified by comparison with authentic references. Data represent the mean ± SE ($n = 3$).

egy that allows insects to reduce their metabolic investment in *de novo* biosynthesis (Pasteels et al., 1983, 1990). In contrast to the *Salicaceae*, only traces of 8-hydroxygeraniol-8-*O*-*β*-D-glucoside were found in *R. obtusifolius* and the glucoside was not detected in the tested Brassicaceae species, namely the food plants of *G. viridula* and *P. cochleariae*. Although this is consistent with the lack of labeling in the defensive secretions, it remains unclear why these species possess the capability to sequester the glucoside if the ability is not required *in vivo*.

5. Localization of the iridoid–*de novo* synthesis

After transfer from gut lumen to the glandular reservoir, glucosidically bound 8-hydroxygeraniol is processed by enzymatic reactions described for *de novo* iridoid synthesis (Pasteels et al., 1990; Lorenz et al., 1993; Daloze and Pasteels, 1994; Veith et al., 1994, 1996, 1997; Oldham et al., 1996; Laurent et al., 2003a). An unspecific *β*-glucosidase removes the sugar moiety from the glucoside, and an oxidase possessing a defined substrate spectrum subsequently catalyzes the formation of an acyclic dialdehyde (Pasteels et al., 1990; Veith et al., 1996; Brueckmann et al., 2002; Michalski et al., 2008). The final transformation is achieved by cyclization and isomerization reactions (Lorenz et al., 1993; Veith et al., 1994). Although the glucoside was detected in the secretions, the enzymes catalyzing its formation have not been identified there (Pasteels et al., 1990; Daloze and Pasteels, 1994).

Glucosidically bound 8-hydroxygeraniol is assembled from isopentenyl diphosphate (IDP) and dimethylallyl diphosphate (DMADP) derived from the mevalonate pathway (Oldham et al., 1996; Belles et al., 2005) (Fig. 5). An important rate-limiting enzyme of this pathway is 3-hydroxy-3-methylglutaryl-CoA reductase (HMGR; EC 1.1.1.34), which catalyzes the four-electron reduction of HMG-CoA to the carboxylic acid mevalonate using two molecules of NADPH (Friesen and Rodwell, 2004). HMGR belongs to the most highly regulated enzymes known, and it can be modulated on the transcriptional, translational and post-translational level (Goldstein and Brown, 1990). Analyses of HMGR expression and enzyme activity have been used to locate the *de novo* biosynthesis of monoterpenoids in bark beetles (Seybold and Tittiger, 2003). To localize the early steps of the iridoid synthesis in leaf beetle larvae, we compared two iridoid–*de novo* producers, *P. cochleariae* and *G. viridula*, with the salicin-sequestering *C. populi*, hoping to identify the key larval enzymes of the biosynthesis of 8-hydroxygeraniol-8-*O*-*β*-D-glucoside.

Employing quantitative real-time PCR, we found an obvious increase in transcripts of *HMGR* in the fat body of the iridoid-producing species (Burse et al., 2007). The level was approx. 1000- and 100-fold higher in *P. cochleariae* and *G. viridula*, respectively, relative to the gut tissue. In contrast, the level of *HMGR* mRNA level in the fat body of *C. populi* larvae was not significantly different from that of the gut tissue. Also, the transcript levels for *HMGR* in the Malpighian tubules, glands and head of the three examined species corresponded to the general levels observed in the gut tissue. The basal *HMGR* transcript abundance detected in all tested tissues traces back to the fact that the enzyme supplies the precursor for molecules involved in essential metabolic processes in all cells, such as dolichol, required for glycoprotein synthesis, and haem A and ubiquinone, implicated in electron transport or isopentyladenine, present in some tRNAs (Edwards and Ericsson, 1999).

Since HMGR is regulated not only on the transcriptional level but also during translation and post-translationally, the activity of the enzyme was monitored in dissected tissues of larvae of *P. cochleariae*, *G. viridula* and *C. populi*. Enzyme assays were carried out with radio-labled HMG-CoA and revealed a correlation between HMGR transcript abundance and activity (Burse et al., 2007). In the fat bodies of the iridoid producers *P. cochleariae* and *G. viridula*, HMGR activity was approx. 30 and 5 times, respectively, greater than in their gut tissue. However, the striking difference found on the transcript level could not be detected in the assays, indicating that HMGR activity is indeed modulated after transcription. The HMGR activity in the fat body of *C. populi* larvae did not differ significantly from that measured in gut tissue. Activity in guts and Malpighian tubules of all three species did not vary significantly from each other.

Whereas HMGR constitutes a key enzyme only of the early steps, isoprenyl diphosphate synthases (IDS) act as later regulatory and branch point enzymes in terpenoid biosynthesis (Liang et al., 2002). They catalyze the sequential condensation reactions of IDP and DMADP. IDS are named for their main products such as geranyl-diphosphate synthases (GDPS; EC 2.5.1.1), which catalyze the single condensation of IDP and DMADP; this single condensation results in geranyl diphosphate (GDP), the C_{10} backbone component of monoterpenes. Recently, it has been demonstrated that a GDPS from the male bark beetle *Ips pini* supplies the precursor in the *de novo* synthesis of the monoterpenoid aggregation pheromone (Gilg et al., 2005). In iridoid-producing Chrysomelina larvae, 8-hydroxygeraniol-8-*O*-*β*-D-glucoside is derived from GDP, implying that GDPS participates in the *de novo* synthesis of the deterrent compounds (Veith et al., 1994). GDP is converted into 8-hydroxygeraniol by *ω*-hydroxylation followed by glucosylation to obtain 8-hydroxygeraniol-8-*O*-*β*-D-glucoside (Daloze and Pasteels, 1994; Veith et al., 1994, 1996).

To detect the accumulation of isoprenoids which could serve as potential precursors for iridoids, we performed IDS assays where the overall product pattern differed in the fat body of the iridoid-producing larvae from that of the *C. populi* larvae (Burse et al., 2007). In the tissue of *P. cochleariae* and *G. viridula,* approx. 90% of all the identified isoprenoids was geraniol and only 10% farnesol. Geranylgeraniol was not found. In contrast, the enzymes of the fat body of *C. populi* produced only ca. 20% geraniol, 60% farnesol and 20% geranylgeraniol. Unlike assays with the fat body, assays with gut tissue of the iridoid-producing larvae showed an accumulation of 50% geraniol, 40% farnesol and 10% geranylgeraniol. The gut tissue of *C. populi* larvae produced the same compounds in the ratio of ca. 40% geraniol, 50% farnesol and 10% geranylgeraniol.

Moreover, 8-hydroxygeraniol-8-*O*-*β*-D-glucoside, the end product of the early terpenoid biosynthesis, was extracted only from the fat body tissue of the two iridoid producers (Burse et al., 2007). According to our data, it seems reasonable that the fat body – the most prominent tissue in the larvae performing myriad metabolic functions throughout insects' development – is implicated in the *de novo* production of the glucosidically bound iridoid precursor (Fig. 5). Hence, all of the required enzymes including an oxidase, which converts geraniol into 8-hydroxygeraniol, and a glucosyltransferase should be present in

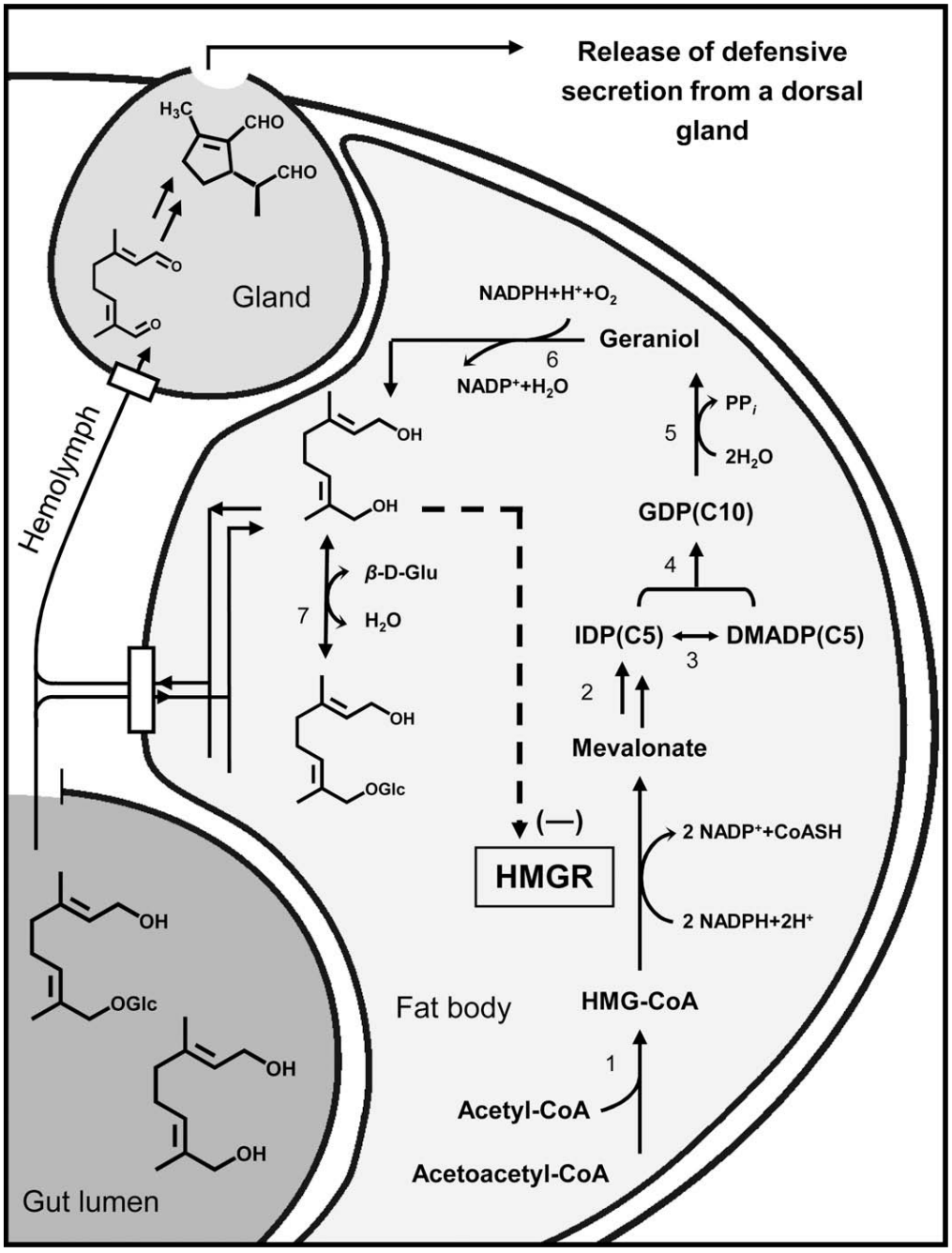

Fig. 5. Biosynthesis of deterrent iridoids in the larvae of *P. cochleariae*. (1) 3-hydroxy-3-methylglutaryl CoA synthetase; (2) mevalonate kinase, phosphomevalonate kinase, diphosphomevalonate decarboxylase; (3) isopentenyl-diphosphate Δ-isomerase; (4) geranyl-diphosphate synthase; (5) phosphatase; (6) cytochrome P-450 mixed-function oxygenase; (7) β-glucosidase (adapted from Pasteels et al. (1990) and Burse et al. (2007)).

the fat body. This would correlate with observations by Veith et al. (1994), who postulated the existence of at least two different oxidative processes in iridoid-releasing larvae according to the substrate specificity of the enzymes. One enzyme type converts natural geraniol into 8-hydroxygeraniol, most likely localized in fat body tissue. The second type produces 8-oxocitral from the diol in the glandular reservoir.

The iridoid biosynthesis seems to be compartmentalized into different tissues of the larval body. According to these observations, the glucoside must be released from fat body tissue into the hemolymph before being transported into the defensive glands for further conversion. The larvae may employ endogenous or exogenous pools of the iridoid precursor, depending on needs or host plant's supply.

6. Do sequestered compounds have an impact on iridoid–*de novo* synthesis?

In our previous studies of iridoid–*de novo* synthesis, the HMGR transcript level and enzyme activity indicated that the fat body tissue is implicated in the *de novo* production of the glucosidically bound iridoid precursor (Burse et al., 2007). Furthermore, we tested whether 8-hydroxygeraniol-8-*O*-β-D-glucoside, its aglycon

or geraniol has an effect on the activity of HMGR. Because the β-D-glucoside of 8-hydroxygeraniol can be easily hydrolyzed, the stable *S*-analogon has been used. HMGR activity was assayed with the crude enzyme extract of fat body tissue from *P. cochleariae* larvae (Burse et al., 2008). Incubation with 8-hydroxygeraniol revealed that HMGR activity decreased significantly; 50% inhibition was achieved with a concentration of approx. 2 mM. geraniol (⩾5 mM) reduced the enzyme activity only by 25–35%. Almost no inhibition was detectable by incubation with the thioglucoside of 8-hydroxygeraniol. Consequently, HMGR activity can be modulated by an intermediate of the iridoid biosynthesis.

To address the inhibition site of the enzyme, we initially cloned a complete cDNA fragment that encoded the full-length HMGR from *P. cochleariae* (Burse et al., 2008). Its catalytic portion was then heterologously expressed in *Escherichia coli* cells. Purification and characterization of the recombinant protein revealed attenuated activity in enzyme assays by 8-hydroxygeraniol, whereas no effect has been observed by adding the glucoside or geraniol (Fig. 6A). The three-dimensional structure of the catalytic portion of human HMGR (PDB code 1DQ8 containing HMG and CoA) was the basis for a high-quality model of the corresponding region (E416-F887, catalytic domain) of the HMGR from *P. cochleariae* (Burse et al., 2008). The resulting most preferred docking arrangement of 8-hydroxygeraniol appeared in a position almost identical

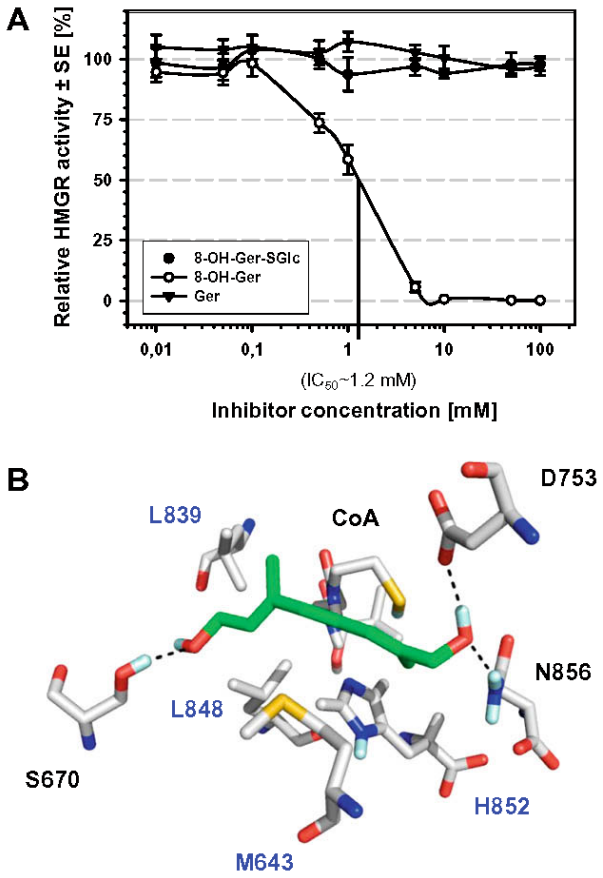

Fig. 6. Inhibition of the recombinant catalytic domain of HMGR from *P. cochleariae* by geraniol, 8-hydroxygeraniol and its thioglucoside. The enzyme was purified by nickel affinity chromatography from *E. coli* cells (A). Homology model of the interaction of 8-hydroxygeraniol with the catalytic active site of HMGR (B). Black labeled residues indicate interactions with chain A and blue labeled with chain B of the homodimeric protein. Dotted black lines represent hydrogen bonds between the ligand and the protein (adapted from Burse et al. (2008)). (For interpretation of the references to colour in this figure legend, the reader is referred to the web version of this article.)

to the position of HMG in the X-ray structure of the template, directly adjacent to CoA, which defined 8-hydroxygeraniol as a competitive inhibitor. The interaction of 8-hydroxygeraniol with the protein is characterized by the formation of hydrogen bonds to S670 and D753 from chain A and to N856 from chain B (Fig. 6B). Furthermore, hydrophobic interactions with L839, L848, H852, and M643 stabilize the docking arrangement. Thus, the compound interacts directly with the catalytic domain, as do the competitive statin inhibitors (Brown et al., 1978; Istvan and Deisenhofer, 2001), rather than down-regulating the enzyme activity by lowering the enzyme mass. As a consequence, the larvae have a tool for fine-tuning HMGR activity rapidly in response to changing biosynthetic demands, such as the increased *de novo* biosynthesis of iridoids after the release of secretions or during larval development. HMGR is regulated through feedback inhibition by an intermediate in the defensive compound biosynthesis which is essential not for the cellular function but for inter-organismic communication.

HMGR activity may be affected not only by the endogenous level of 8-hydroxygeraniol but also by the sequestered glucoside. We assume that the glucose moiety could be hydrolytically cleaved off by glucosidases, and that the resulting aglycon can then attenuate HMGR activity. Due to the activity of glucosidases in the gut lumen (Pasteels et al., 1983, 1990), 8-hydroxygeraniol can be liberated from the plant-derived glucoside during the gut passage. This compound has been successfully imported through the gut membrane to the hemolymph and finally into the defensive secretion (Lorenz et al., 1993; Kunert et al., 2008). Incubating dissected fat body tissue in a solution of 8-hydroxygeraniol decreased HMGR activity, indicating that this compound had been transferred. Accordingly, HMGR represents one of the key regulators in maintaining homeostasis between metabolites that are sequestered and those that are produced *de novo* in iridoid synthesis.

7. Final remarks

We have demonstrated that the larvae of most likely all Chrysomelina species possess the ability to sequester plant-derived glucosides regardless of the extent of *de novo* synthesis of the defensive compounds. However, sequestration seems to become relevant *in vivo* for iridoid–*de novo* producers which feed on plants from the salicaceous family. The most ancestral species, those adapted, for example, to Brassicacae or Polygonaceae, are capable of incorporating glucosides but do not use the compounds for iridoid synthesis, perhaps due to the absence or very low amounts of iridoid precursors in the host plant. Interestingly, the basis for the evolution of sequestration was established in ancestral species such as *G. viridula* or *P. cochleariae*. With the distribution of the *de novo* synthesis into different tissues, they had to develop transport mechanisms into the defensive gland which can be recruited in the more evolved species for secondary metabolite uptake from the host plants. Furthermore, *de novo* producers harbor a set of enzymes in their defensive glands that can adapt to convert sequestered compounds. In fact, establishing the sequestration process did not depend on the invention of new protein functions during Chrysomelina evolution.

Although the entire sequestration process including uptake and excretion obviously requires a large number of transport mechanisms, few proteins have to be altered to adapt to a different substrate spectrum. Taking into account that import by the intestines and export by excretory tissue are fairly unspecific, only the specialized transporters and the following enzymes in the defensive glands have to be modified. Evidently, the glandular carriers representing the bottleneck tightly control the metabolite uptake. They may influence host plant affiliation as well as the diversity of deterrents in the secretions and, thus, become one of the causal

factors manipulating the co-evolutionary events between plants and Chrysomelina beetles. Finally, due to the complexity of the sequestration process emphasized in our recent studies, the Chrysomelina taxon is shown here to be a fascinating model system which provides diverse starting points for exploring the mutual reactions of beetles and plants.

Acknowledgments

This study was supported by grants from the Deutsche Forschungsgemeinschaft (SPP 1152: Evolution of metabolic diversity) and from the Max Planck Society. We wish to thank Prof. Dr. Stefan H. Heinemann, Friedrich Schiller University Jena, for the microinjection experiments, Dr. Wolfgang Brand, Leibniz Institute of Plant Biochemistry Halle/Saale, for modeling the HMGR, Dr. Axel Schmidt, MPI for Chemical Ecology Jena, for the IDS assays. Also we are very grateful to all the chemists who synthesized the compounds used in the feeding experiments. We also thank Dr. Rita Büchler for help during protein purification, Angelika Berg for taking care of the beetles, Andrea Lehr, Anja David, Marion Stäger, and Angela Roßner for technical assistance as well as Kerstin Ploss for the high-resolution MS analyses. We gratefully acknowledge Prof. Dr. Jacques M. Pasteels, Université Libre de Bruxelles, for providing leaf beetles and for his creativity and helpful advice which improved this project considerably.

References

Belles, X., Martin, D., Piulachs, M.-D., 2005. The mevalonate pathway and the synthesis of juvenile hormone in insects. Annu. Rev. Entomol. 50, 181–199.

Blum, M.S., 1994. Antipredatory devices in larvae of the *Chrysomelidae*: a unidentified synthesis for defensive electricism. In: Jolivet, P.H., Cox, M.L., Petitpierre, E. (Eds.), Novel Aspects of the Biology of the *Chrysomelidae*. Kluwer Academics Publishers, Doderecht, The Netherlands, pp. 277–288.

Blum, M.S., Wallace, J.B., Duffield, R.M., Brand, J.M., Fales, H.M., Sokoloski, E.A., 1978. Chrysomelidial in the defensive secretion of the leaf beetle *Gastrophysa cyanea* Melsheimer. J. Chem. Ecol. V4, 47–53.

Brown, M.S., Faust, J.R., Goldstein, J.L., Kaneko, I., Endo, A., 1978. Induction of 3-hydroxy-3-methyl glutaryl coenzyme A reductase activity in human fibroblasts incubated with compactin MI-236b: a competitive inhibitor of the reductase. J. Biol. Chem. 253, 1121–1128.

Brueckmann, M., Termonia, A., Pasteels, J.M., Hartmann, T., 2002. Characterization of an extracellular salicyl alcohol oxidase from larval defensive secretions of *Chrysomela populi* and *Phratora vitellinae* (*Chrysomelina*). Insect Biochem. Mol. Biol. 32, 1517–1523.

Burse, A., Schmidt, A., Frick, S., Kuhn, J., Gershenzon, J., Boland, W., 2007. Iridoid biosynthesis in *Chrysomelina* larvae: fat body produces early terpenoid precursors. Insect Biochem. Mol. Biol. 37, 255–265.

Burse, A., Frick, S., Schmidt, A., Buechler, R., Kunert, M., Gershenzon, J., Brandt, W.G., Boland, W., 2008. Implication of HMGR in homeostasis of sequestered and *de novo* produced precursors of the iridoid biosynthesis in leaf beetle larvae. Insect Biochem. Mol. Biol. 38, 76–88.

Daloze, D., Pasteels, J.M., 1994. Isolation of 8-hydroxygeraniol-8-*O*-β-D-glucoside, a probable intermediate in biosynthesis of iridoid monoterpenes, from defensive secretions of *Plagiodera versicolora* and *Gastrophysa viridula* (*Coleoptera*: *Chrysomelidae*). J. Chem. Ecol. 20, 2089–2097.

Discher, S., Burse, A., Tolzin-Bansch, K., Heinemann, S.H., Pasteels, J.M., Boland, W., 2009. A versatile transport network for sequestering and excreting plant glycosides in leaf beetles provides an evolutionary flexible defense strategy. ChemBioChem. doi:10.1002/cbic.200900226.

Dobler, S., Mardulyn, P., Pasteels, J.M., Rowell-Rahier, M., 1996. Host-plant switches and the evolution of chemical defense and life history in the leaf beetle genus *Oreina*. Evolution 50, 2373–2386.

Duffey, S.S., 1980. Sequestration of plant natural products by insects. Annu. Rev. Entomol. 25, 447–477.

Edwards, P.A., Ericsson, J., 1999. Sterols and isoprenoids: signaling molecules derived from the cholesterol biosynthetic pathway. Annu. Rev. Biochem. 68, 157–185.

Ehrlich, P.R., Raven, P.H., 1964. Butterflies and plants – a study in coevolution. Evolution 18, 586–608.

Farrell, B.D., 1998. Inordinate fondness explained – why are there so many beetles. Science 281, 555–559.

Feld, B.K., Pasteels, J.M., Boland, W., 2001. *Phaedon cochleariae* and *Gastrophysa viridula* (*Coleoptera*: *Chrysomelidae*) produce defensive iridoid monoterpenes *de novo* and are able to sequester glycosidically bound terpenoid precursors. Chemoecology 11, 191–198.

Fernandez, P., Hilker, M., 2007. Host plant location by *Chrysomelidae*. Basic Appl. Ecol. 8, 97–116.

Friesen, J., Rodwell, V. 2004. The 3-hydroxy-3-methylglutaryl coenzyme-A (HMG-CoA) reductases. Genome Biol 5, 248.1–248.7.

Gilg, A.B., Bearfield, J.C., Tittiger, C., Welch, W.H., Blomquist, G.J., 2005. Isolation and functional expression of an animal geranyl diphosphate synthase and its role in bark beetle pheromone biosynthesis. Proc. Natl. Acad. Sci. USA 102, 9760–9765.

Gillespie, J.J., Kjer, K.M., Duckett, C.N., Tallamy, D.W., 2003. Convergent evolution of cucurbitacin feeding in spatially isolated rootworm taxa (*Coleoptera*: *Chrysomelidae*; *Galerucinae*, *Luperini*). Mol. Phylogenet. Evol. 29, 161–175.

Goldstein, J.L., Brown, M.S., 1990. Regulation of the mevalonate pathway. Nature 343, 425–430.

Gross, J., Fatouros, N.E., Neuvonen, S., Hilker, M., 2004. The importance of specialist natural enemies for *Chrysomela lapponica* in pioneering a new host plant. Ecol. Entomol. 29, 584–593.

Hartmann, T., 1999. Chemical ecology of pyrrolizidine alkaloids. Planta 207, 483–495.

Hartmann, T., 2004. Plant-derived secondary metabolites as defensive chemicals in herbivorous insects: a case study in chemical ecology. Planta 219, 1–4.

Hartmann, T., Ober, D., 2000. Biosynthesis and metabolism of pyrrolizidine alkaloids in plants and specialized insect herbivores. Top. Curr. Chem. 209, 207–243.

Hartmann, T., Ober, D., 2008. Defense by pyrrolizidine alkaloids: developed by plants and recruited by insects. In: Schaller, A. (Ed.), Induced Plant Resistance to Herbivory. Springer Science+Business Media B.V., pp. 213–231.

Hartmann, T., Witte, L., Ehmke, A., Theuring, C., Rowellrahier, M., Pasteels, J.M., 1997. Selective sequestration and metabolism of plant derived pyrrolizidine alkaloids by chrysomelid leaf beetles. Phytochemistry 45, 489–497.

Hartmann, T., Theuring, C., Schmidt, J., Rahier, M., Pasteels, J.M., 1999. Biochemical strategy of sequestration of pyrrolizidine alkaloids by adults and larvae of chrysomelid leaf beetles. J. Insect Physiol. 45, 1085–1095.

Hartmann, T., Theuring, C., Witte, L., Pasteels, J.M., 2001. Sequestration, metabolism and partial synthesis of tertiary pyrrolizidine alkaloids by the neotropical leaf-beetle *Platyphora boucardi*. Insect Biochem. Mol. Biol. 31, 1041–1056.

Hartmann, T., Theuring, C., Witte, L., Schulz, S., Pasteels, J.M., 2003. Biochemical processing of plant acquired pyrrolizidine alkaloids by the neotropical leaf-beetle *Platyphora boucardi*. Insect Biochem. Mol. Biol. 33, 515–523.

Hilker, M., Schulz, S., 1994. Composition of larval secretion of *Chrysomela lapponica* (*Coleoptera*, *Chrysomelidae*) and its dependence on host plant. J.Chem. Ecol. 20, 1075–1093.

Istvan, E.S., Deisenhofer, J., 2001. Structural mechanism for statin inhibition of HMG-CoA reductase. Science 292, 1160–1164.

Kuhn, J., Pettersson, E.M., Feld, B.K., Burse, A., Termonia, A., Pasteels, J.M., Boland, W., 2004. Selective transport systems mediate sequestration of plant glucosides in leaf beetles: a molecular basis for adaptation and evolution. Proc. Natl. Acad. Sci. USA 101, 13808–13813.

Kuhn, J., Pettersson, E.M., Feld, B.K., Nie, L., Tolzin-Banasch, K., Machkour M'Rabet, S., Pasteels, J.M., Boland, W., 2007. Sequestration of plant-derived phenolglucosides by larvae of the leaf beetle *Chrysomela lapponica*: thioglucosides as mechanistic probes. J. Chem. Ecol. 33, 5–24.

Kunert, M., Soe, A., Bartram, S., Discher, S., Tolzin-Banasch, K., Nie, L., David, A., Pasteels, J.M., Boland, W., 2008. *De novo* biosynthesis versus sequestration: a network of transport systems supports in iridoid producing leaf beetle larvae both modes of defense. Insect Biochem. Mol. Biol. 38, 895–904.

Laurent, P., Braekman, J.C., Daloze, D., Pasteels, J., 2003a. Biosynthesis of defensive compounds from beetles and ants. Eur. J. Org. Chem. 15, 2733–2743.

Laurent, P., Dooms, C., Braekman, J.C., Daloze, D., Habib-Jiwan, J.L., Rozenberg, R., Termonia, A., Pasteels, J.M., 2003b. Recycling plant wax constituents for chemical defense: hemi-biosynthesis of triterpene saponins from beta-amyrin in a leaf beetle. Naturwissenschaften 90, 524–527.

Laurent, P., Braekman, J.-C., Daloze, S., 2005. Insect chemical defense. In: Schulz, S. (Ed.), Chemistry of Pheromones and Other Semi Chemicals II, vol. 240. Springer, Berlin/Heidelberg, pp. 167–229.

Liang, P.H., Ko, T.P., Wang, A.H.J., 2002. Structure, mechanism and function of prenyltransferases. Eur. J. Biochem. 269, 3339–3354.

Lorenz, M., Boland, W., Dettner, K., 1993. Biosynthesis of iridodials in the defense glands of beetle larvae (*Chrysomelinae*). Angew. Chem., Int. Ed. 32, 912–914.

Macias, F.A., Galindo, J.L.G., Galindo, J.C.G., 2007. Evolution and current status of ecological phytochemistry. Phytochemistry 68, 2917–2936.

Meinwald, J., Jones, T.H., Eisner, T., Hicks, K., 1977. New methylcyclopentanoid terpenes from the larval defensive secretion of a chrysomelid beetle (*Plagiodera versicolora*). Proc. Natl. Acad. Sci. USA 74, 2189–2193.

Michalski, C., Mohagheghi, H., Nimtz, M., Pasteels, J.M., Ober, D., 2008. Salicyl alcohol oxidase of the chemical defense secretion of two chrysomelid leaf beetles – molecular and functional characterization of two new members of the glucose–methanol–choline oxidoreductase gene family. J. Biol. Chem. 283, 19219–19228.

Narberhaus, I., Papke, U., Theuring, C., Beuerle, T., Hartmann, T., Dobler, S., 2004a. Direct evidence for membrane transport of host-plant-derived pyrrolizidine alkaloid *N*-oxides in two leaf beetle genera. J. Chem. Ecol. 30, 2003–2022.

Narberhaus, I., Theuring, C., Hartmann, T., Dobler, S., 2004b. Time course of pyrrolizidine alkaloid sequestration in *Longitarsus flea* beetles (*Coleoptera*, *Chrysomelidae*). Chemoecology 14, 17–23.

O'Donnell, M.J., Rheault, M.R., 2005. Ion-selective microelectrode analysis of salicylate transport by the Malpighian tubules and gut of *Drosophila melanogaster*. J. Exp. Biol. 208, 93–104.

Oldham, N.J., Veith, M., Boland, W., Dettner, K., 1996. Iridoid monoterpene biosynthesis in insects – evidence for a *de novo* pathway occurring in the defensive glands of *Phaedon armoraciae* (Chrysomelidae) leaf beetle larvae. Naturwissenschaften 83, 470–473.

Pasteels, J.M., Rowell-Rahier, M., 1989. Defensive glands and secretions as taxonomical tools in the Chrysomelidae. Entomography 6, 423–432.

Pasteels, J.M., Braekman, J.C., Daloze, D., Ottinger, R., 1982. Chemical defence in chrysomelid larvae and adults. Tetrahedron 38, 1891–1897.

Pasteels, J.M., Rowell-Rahier, M., Braekman, J.C., Dupont, A., 1983. Salicin from host plant as precursor of salicyl aldehyde in defensive secretion of chrysomeline larvae. Physiol. Entomol. 8, 307–314.

Pasteels, J.M., Duffey, S., Rowell-Rahier, M., 1990. Toxins in chrysomelid beetles, possible evolutionary sequence from *de novo* synthesis to derivation from food-plant chemicals. J. Chem. Ecol. 16, 211–222.

Pasteels, J.M., Termonia, A., Windsor, D.M., Witte, L., Theuring, C., Hartmann, T., 2001. Pyrrolizidine alkaloids and pentacyclic triterpene saponins in the defensive secretions of *Platyphora* leaf beetles. Chemoecology 11, 113–120.

Pasteels, J.M., Theuring, C., Witte, L., Hartmann, T., 2003. Sequestration and metabolism of protoxic pyrrolizidine alkaloids by larvae of the leaf beetle *Platyphora boucardi* and their transfer via pupae into defensive secretions of adults. J. Chem. Ecol. 29, 337–355.

Renner, K., 1970. Über die ausstülpbaren Hautblasen der Larven von *Gastroidea viridula* De Geer und ihre ökologische Bedeutung (*Coleoptera*: *Chrysomelidae*). Beitr. Entomol. 20, 527–533.

Schulz, S., 1998. Insect–plant interactions – metabolism of plant compounds to pheromones and allomones by lepidoptera and leaf beetles. Eur. J. Org. Chem. 1, 13–20.

Schulz, S., Gross, J., Hilker, M., 1997. Origin of the defensive secretion of the leaf beetle *Chrysomela lapponica*. Tetrahedron 53, 9203–9212.

Seybold, S.J., Tittiger, C., 2003. Biochemistry and molecular biology of *de novo* isoprenoid pheromone production in the Scolytidae. Annu. Rev. Entomol. 48, 425–453.

Soe, A.R.B., Bartram, S., Gatto, N., Boland, W., 2004. Are iridoids in leaf beetle larvae synthesized *de novo* or derived from plant precursors? A methodological approach. Isot. Environ. Health Stud. 40, 175–180.

Termonia, A., Pasteels, J.M., 1999. Larval chemical defence and evolution of host shifts in *Chrysomela* leaf beetles. Chemoecology 9, 13–23.

Termonia, A., Hsiao, T.H., Pasteels, J.M., Milinkovitch, M.C., 2001. Feeding specialization and host-derived chemical defense in Chrysomeline leaf beetles did not lead to an evolutionary dead end. Proc. Natl. Acad. Sci. USA 98, 3909–3914.

Veith, M., Lorenz, M., Boland, W., Simon, H., Dettner, K., 1994. Biosynthesis of iridoid monoterpenes in insects – defensive secretions from larvae of leaf beetles (*Coleoptera*, *Chrysomelidae*). Tetrahedron 50, 6859–6874.

Veith, M., Dettner, K., Boland, W., 1996. Stereochemistry of an alcohol oxidase from the defensive secretion of larvae of the leaf beetle *Phaedon armoraciae* (*Coleoptera*, *Chrysomelidae*). Tetrahedron 52, 6601–6612.

Veith, M., Oldham, N.J., Dettner, K., Pasteels, J.M., Boland, W., 1997. Biosynthesis of defensive allomones in leaf beetle larvae – stereochemistry of salicylalcohol oxidation in *Phratora vitellinae* and comparison of enzyme substrate and stereospecificity with alcohol oxidases from several iridoid producing leaf beetles. J. Chem. Ecol. 23, 429–443.

Willinger, G., Dobler, S., 2001. Selective sequestration of iridoid glycosides from their host plants in *Longitarsus flea* beetles. Biochem. Syst. Ecol. 29, 335–346.

Zvereva, E.L., Rank, N.E., 2003. Host plant effects on parasitoid attack on the leaf beetle *Chrysomela lapponica*. Oecologia 135, 258–267.

Zvereva, E.L., Rank, N.E., 2004. Fly parasitoid *Megaselia opacicornis* uses defensive secretions of the leaf beetle *Chrysomela lapponica* to locate its host. Oecologia 140, 516–522.

Antje Burse (born 1973, Germany) obtained her B.Sc. and M.Sc. (1999) degrees at the Friedrich Schiller University of Jena. She received her Ph.D. (2003) at the Philipps University of Marburg/Lahn. The corresponding research in the field of phytopathology was performed at the Max Planck Institute for Terrestrial Microbiology, Marburg/Lahn. She analyzed the impact of multi-drug efflux proteins on the pathogenesis of fire blight bacteria. With the studies on sequestration strategies in leaf beetle she is continuing to investigate transport processes. The current research is performed in the Prof. Dr. W. Boland's group at the Max Planck Institute for Chemical Ecology, Jena.

5.3 MANUSCRIPT 3

PRECISE RNAI-MEDIATED SILENCING OF METABOLICALLY ACTIVE PROTEINS IN THE DEFENSE SECRETIONS OF JUVENILE LEAF BEETLES

PROCEEDINGS OF THE ROYAL SOCIETY B BIOLOGICAL SCIENCES

Precise RNAi-mediated silencing of metabolically active proteins in the defence secretions of juvenile leaf beetles

René Roberto Bodemann, Peter Rahfeld, Magdalena Stock, Maritta Kunert, Natalie Wielsch, Marco Groth, Sindy Frick, Wilhelm Boland and Antje Burse

Proc. R. Soc. B 2012 **279**, doi: 10.1098/rspb.2012.1342 first published online 8 August 2012

PROCEEDINGS OF THE ROYAL SOCIETY B

CrossMark click for updates

Proc. R. Soc. B (2012) **279**, 4126–4134
doi:10.1098/rspb.2012.1342
Published online 8 August 2012

Precise RNAi-mediated silencing of metabolically active proteins in the defence secretions of juvenile leaf beetles

René Roberto Bodemann[1,†], Peter Rahfeld[1,†], Magdalena Stock[1], Maritta Kunert[1], Natalie Wielsch[1], Marco Groth[2], Sindy Frick[1], Wilhelm Boland[1] and Antje Burse[1,*]

[1]*Max Planck Institute for Chemical Ecology, Beutenberg Campus, Hans-Knoell-Str. 8, 07745 Jena, Germany*
[2]*Leibniz Institute for Age Research – Fritz Lipmann Institute, Beutenbergstr. 11, 07745 Jena, Germany*

Allomones are widely used by insects to impede predation. Frequently these chemical stimuli are released from specialized glands. The larvae of Chrysomelina leaf beetles produce allomones in gland reservoirs into which the required precursors and also the enzymes are secreted from attached gland cells. Hence, the reservoirs can be considered as closed bio-reactors for producing defensive secretions. We used RNA interference (RNAi) to analyse *in vivo* functions of proteins in biosynthetic pathways occurring in insect secretions. After a salicyl alcohol oxidase was silenced in juveniles of the poplar leaf beetles, *Chrysomela populi*, the precursor salicyl alcohol increased to 98 per cent, while salicyl aldehyde was reduced to 2 per cent within 5 days. By analogy, we have silenced a novel protein annotated as a member of the juvenile hormone-binding protein superfamily in the juvenile defensive glands of the related mustard leaf beetle, *Phaedon cochleariae*. The protein is associated with the cyclization of 8-oxogeranial to iridoids (methylcyclopentanoid monoterpenes) in the larval exudates made clear by the accumulation of the acylic precursor 5 days after RNAi triggering. A similar cyclization reaction produces the secologanin part of indole alkaloids in plants.

Keywords: RNAi; insects; leaf beetle; secretome; salicyl alcohol oxidase; monoterpene cyclization

1. INTRODUCTION

Insects are extraordinarily inventive when it comes to producing defensive compounds for repelling their enemies. To circumvent auto-intoxicative effects, these natural products frequently originate in the epidermis-derived exocrine glands [1]. The gland cells produce secretions that are fortified with defensive compounds [2,3]. It has been demonstrated that insects convert either intrinsic precursors or food-derived compounds into biologically active allelochemicals [4–7]. The precursors can be activated in the defensive glands or in the secretions. Immature leaf beetles of the subtribe Chrysomelina, for example, produce their deterrents in biphasic secretions, and store them in nine unique pairs of impermeable reservoirs in their backs [8,9]. The larval exudates containing salicyl aldehyde (**3**) have been of particular interest [10,11]. The hydrophobic aldehyde forms an organic layer, accounting for 15 per cent of the total discharge volume, while the aqueous phase constitutes 85 per cent [12]. The latter contains the precursor salicyl alcohol (**2**) and a flavine-dependent salicyl alcohol oxidase (SAO); the SAO uses molecular oxygen as an electron acceptor for alcohol oxidation, yielding the aldehyde and hydrogen peroxide [12–14] (figure 1). Salicyl aldehyde is considered as a potent repellent against generalist predators [11,15] and as an antimicrobial agent [16]. The larvae feed on salicaceous plants and sequester the secondary metabolite salicin (**1**) [17–19]. After shuttling salicin to the defensive glands, the glucoside is cleaved by a β-glucosidase into **2** and glucose for further metabolism [20] (figure 1). According to phylogenetic analyses, the synthesis of **3** from sequestered precursors has evolved from the de novo production of defensive iridoids (methylcyclopentanoid monoterpenes containing an iridane skeleton) [21]. Also the last steps of the iridoid pathway in the secretions are thought to be similar to those found in sequestering species [20] (figure 1). At first, the sugar moiety is cleaved from 8-hydroxygeraniol-8-*O*-β-D-glucoside (**4**), and an oxygen-dependent oxidase converts the aglucone into 8-oxogeranial (**6**) [20,22–24]. A subsequent cyclization reaction yields iridoids (**7**) [25].

Despite the many current genome- and transcriptome-sequencing projects, up to now it has only been shown for SAO sequences to be entangled in allomone production in the defensive secretions of the leaf beetle species *Chrysomela tremulae*, *Chrysomela populi*, *Chrysomela lapponica* and *Phratora vitellinae* [13,14,26]. To demonstrate the *in vivo* relevance of a target sequence, gene silencing by RNA interference (RNAi) is a suitable method. RNAi is an endogenous mechanism, derived from an anti-viral immune response [27], and can be found virtually in all eukaryotic species. It can be triggered artificially by double-stranded RNA (dsRNA), whose nucleotide sequence is identical to that of the target gene [28]. The

* Author for correspondence (aburse@ice.mpg.de).
† These authors contributed equally to the study.

Electronic supplementary material is available at http://dx.doi.org/10.1098/rspb.2012.1342 or via http://rspb.royalsocietypublishing.org.

Received 12 June 2012
Accepted 17 July 2012

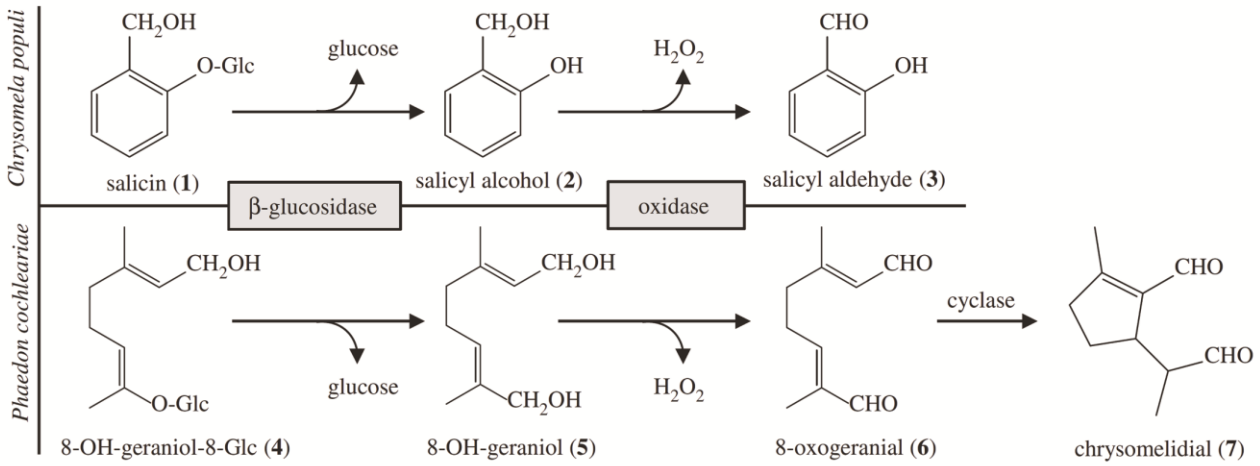

Figure 1. Enzymatic reactions in the defensive secretions of juvenile *C. populi* and *P. cochleariae* adapted from Michalski *et al.* [14]. Glc, Glucose.

RNAi effect is attended by decreased transcript and protein levels, and consequently by loss-of-function phenotypes. In addition to embryogenesis, pattern formation, reproduction and behaviour, RNAi allows biosynthetic pathways in insects to be successfully analysed [29–31].

Here, we describe how RNAi can be used to target the biosynthesis of discrete components in the defensive discharges of juvenile Chrysomelina. We first validated this technique by silencing the known *SAO* sequence in the sequestering species *C. populi* (*CpopSAO*). After knocking down the SAO, the alcohol precursor of **3** accumulated in the gland. This showed that we are able to interrupt the deterrent biosynthesis *in vivo*. Next, we extended the method to the related de novo iridoid-producing species, *P. cochleariae*. In the secretions of its larvae C_{10}-precursors are converted to the methylcyclopentanoid monoterpene chrysomelidial. Particularly, the cyclization mechanism is of importance because it occurs not only in insects but also in plants. Here, the cyclization leads ultimately to secologanin, one of the building blocks for more than 2500 indole alkaloids that have been isolated mainly from three plant families [32]. Although an enzyme with cyclase activity for secologanin biosynthesis has long been predicted, a corresponding sequence has yet to be published. In the *P. cochleariae* secretome, we identified a novel protein which is involved in the cyclization reaction of the monoterpenoid 8-oxogeranial to chrysomelidial.

2. MATERIAL AND METHODS

See electronic supplementary material for complete secretome analyses by data-independent liquid chromatography/mass spectrometry detection (LC/MS^E), cloning procedures, detailed quantitative real-time PCR procedure (qPCR), all primer sequences and accession numbers.

(a) *Beetle rearing and secretion analyses*

Chrysomela populi (L.) was collected near Dornburg, Germany (latitude 51.015, longitude 11.64), on *Populus maximowiczii*×*Populus nigra*. In the laboratory, beetles were kept in a 16 L : 8 D cycle, 18 ± 2°C in light and 13 ± 2°C in darkness. *Phaedon cochleariae* (F.) was laboratory-reared on *Brassica oleracea* convar. *capitata* var. *alba* (Gloria F1) in 16 L : 8 D cycle conditions and 15 ± 2°C. According to [33], we obtained the relative growth rate (RGR) of six biological replicates of each group of five larvae by RGR = [(final weight − weight of neonate larva)/(weight of neonate larva × developmental time (days))]. Each replicate group was weighed every 24 ± 3 h and data were compared with two-tailed *t*-test. Larval secretions were collected in glass capillaries (inner diameter, 0.28 mm; outer diameter, 0.78 mm, length 100 mm; Hirschmann, Eberstadt, Germany). Sealed capillaries containing samples were stored at −20°C until needed. Secretions were weighed in the sealed capillaries on an ultra-microbalance (Mettler-Toledo, Greifensee, Switzerland) three times; the weight of the capillaries was subtracted and the final weight was averaged.

(b) *Production of double-stranded RNA*

Sequenced plasmids pIB-*CpopSAO* (GeneBank: HQ245 154.1) and pIB-*PcTo-like* (GeneBank: JQ728549) were used to amplify a 1.5 kb *CpopSAO* fragment and a 450 bp *PcTo-like* fragment, respectively. The *gfp* sequence was amplified from pcDNA3.1/CT- GFP-TOPO (Life Technology, Darmstadt, Germany). The amplicons were subject to *in vitro* transcription assays according to instructions from the Ambion MEGAscript RNAi kit (Life Technologies, Darmstadt, Germany). The resulting dsRNA was eluted after nuclease digestion three times with 50 µl of injection buffer (3.5 mM Tris–HCl, 1 mM NaCl, 50 nM Na_2HPO_4, 20 nM KH_2PO_4, 3 mM KCl, 0.3 mM EDTA, pH 7.0). The concentration of dsRNA was calculated with A = 1 = 45 mg ml^{-1} and adjusted to 1 µg $µl^{-1}$. The quality of dsRNA was checked by TBE-agarose-electrophoresis.

(c) *Injection of double-stranded RNA*

First instar of *C. populi* with 5 mm body length was injected with 0.1–3 µg of dsRNA approximately 10 days after hatching. *Phaedon cochleariae* second instar with 4 mm body length was injected with 0.3 µg of dsRNA approximately 5 days after hatching. Injections were accomplished with ice-chilled larvae using a Nano2000 injector (WPI, Sarasota, FL, USA) directed by a three-axis micromanipulator. The larvae were injected parasagittally between the pro- and mesothorax.

(d) *Off-target prediction*

According to the mechanism of RNAi [28], the top and bottom strands of dsRNAs of *CpopSAO*, *PcTo-like* and *gfp* were diced *in silico* into all possible 21 bp fragments [34]. The resulting siRNAs were subjected to BLASTn

(stand-alone NCBI-BLAST) [35] by invoking BLASTALL v. 2.2.21 (parameters: -p blastn -e 1e-1 -G 7 -T -b 80 -v 80) searching against our in-house transcriptome databases of *C. populi* and *P. cochleariae*. Hits less than 20 nts in length were ignored and hits more than or equal to 20 nts were considered as putative off targets.

(e) CpopSAO *and* PcTo-like *transcript abundance*

Cq values of genes of interest from three biological replicates were normalized by *CpRPL45* and *CpActin* for *C. populi* and *PcRP-L8* and *PcRP-S18* for *P. cochleariae*, respectively. Real-time PCR data were acquired on an Mx3000P Real-Time PCR system using Brilliant II SYBR Green qPCR Master Mix (Agilent, Santa Clara, CA, USA).

(f) *Gas chromatography/mass spectrometry analysis of low-molecular-weight compounds in chrysomelid secretions*

Secretions of *C. populi* were diluted in 1 : 150 (w/v) ethyl acetate and secretions of *P. cochleariae* were diluted in 1 : 100 (w/v) dichloromethane. Of each diluted secretion, 1 µl was subjected to GC/EIMS analysis (ThermoQuest Finnigan Trace GC/MS 2000, Frankenhorst, Germany) equipped with Phenomenex (Aschaffenburg, Germany) ZB−5−W/Guardian−column, 25 m. Substances were separated using helium as a carrier (1.5 ml min^{-1}). Conditions for *C. populi* secretions: 50°C (1 min), 10°C per minute to 80°C, 60°C per minute to 280°C (1 min). Inlet temperature was 220°C, transfer line was 280°C. Substances were identified according to standard substances **2** and **3**. Conditions for *P. cochleariae* secretions: 50°C (2 min), 10°C per minute to 80°C, 5°C per minute to 200°C, 30°C per minute to 300°C (1 min). Inlet temperature was 220°C and transfer line was 280°C. Substances were identified according to [36] and the reference compounds 8-oxogeranial and chrysomelidial. The synthesis of 8-oxogeranial and chrysomelidial was carried out as in [25,37], respectively. Peak areas from GC-chromatograms were obtained using an ICIS-algorithm (XCALIBUR BUNDLE v. 2.0.7, Thermo Scientific).

(g) *Statistical analyses*

Two-tailed Student's *t*-tests for unequal variation were used to value the significance levels of transcript abundances and to weight differences comparing values of three different biological replicates from the non-injected control (NIC) group with those of either the RNAi group or the *gfp* control. Multi-dimensional ANOVA tests were carried out to validate significant differences in time series and between different RNAi treatments. The level of significance was reached at a *p*-value of 0.05. Calculations were done with R (http://www.r-project.org/).

3. RESULTS

(a) *Targeting the defensive glands of juvenile poplar leaf beetles by RNA interference*

Recently, a 1872-bp *CpopSAO* cDNA (Genbank/HQ245154.1) encoding a 69 kDa protein for conversion of **2** into **3** was identified from the larval defensive glands of *C. populi* [13,14] (figure 2*a*). It belongs to the glucose−methanol−choline (GMC) family of oxido-reductases [38]. Given that the expression of *CpopSAO* was detectable exclusively in glandular tissues (figure 2*b*), silencing this gene would affect only the process of glandular biosynthesis.

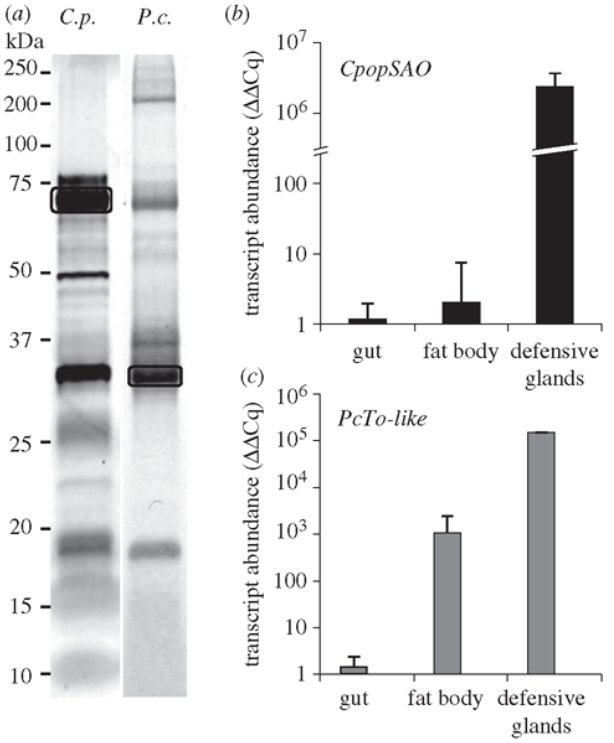

Figure 2. Protein and transcript abundance in juvenile leaf beetles. (*a*) Proteins in defensive exudates separated by one-dimensional SDS−PAGE. left: 1 mg secretions of *C. populi* (*C.p.*), silver stained, box marks *Cpop*SAO; right: 0.65 mg secretions of *P. cochleariae* (*P.c.*), Coomassie stained, box marks *Pc*To-like. (*b*) Expression pattern of *CpopSAO* ±s.d. in different *C. populi* tissues, $n = 3$. (*c*) Expression pattern of *PcTo-like* ±s.d. in different *P. cochleariae* tissues, $n = 2$. Both *y*-axes are in $\log_{10}$ scale.

To induce RNAi in *C. populi* larvae, we injected 1.0 µg of 1.5 kb *CpopSAO* dsRNA into late first instar. A 719-bp dsRNA fragment of *gfp* served as a control for effects caused by dsRNA; although the RNAi machinery will be induced, genes should not be silenced. Furthermore, we included an NIC group in our experiments. By monitoring the developmental traits and the secretion production in *C. populi* and comparing the results with those from control groups, we found that silencing *CpopSAO* did not influence either growth rate or pupae weight (see the electronic supplementary material, figure S1*a*). But the larvae treated with *CpopSAO* dsRNA produced slightly more secretions than did the larvae of the control groups (see the electronic supplementary material, figure S1*b*), which might be owing to the different osmotic characteristics between **2** and **3** [12]. Because we did not detect significant differences between NIC and *gfp* controls in any experiments delineated below, we continue showing only the data of the *gfp* controls.

Transcript abundance was measured in glandular tissue using qPCR after 1, 3 and 12 days. Comparing tissue from these samples to tissue from the *gfp* controls, we noticed significant reductions to 7.6 per cent mRNA level ($p = 0.002$) just 24 h after injection. After day 3, the transcript level was diminished to 1.6 per cent ($p = 0.004$), and after day 12, to 0.5 per cent (figure 3*a*).

In accordance with the literature, SAO corresponds to the dominant band at 70 kDa in the secretions of

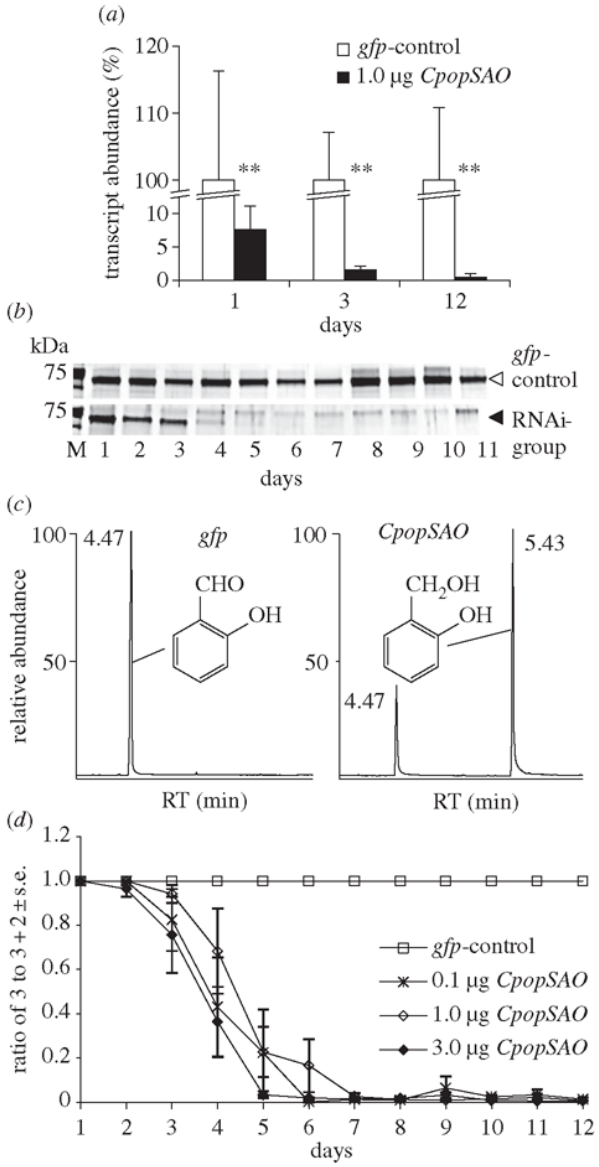

Figure 3. RNAi effects in juvenile *C. populi*. (*a*) White bars: transcript abundance of *CpopSAO* after injecting 1.0 µg *gfp* dsRNA, $n = 3 \pm$ s.d.. Black bars: transcript abundance of *CpopSAO* after injecting 1.0 µg *CpopSAO* dsRNA, $n = 3$. 100% = ΔCq of *gfp* control. Asterisks indicate level of significance: $^{**}p < 0.01$ (*b*) *Cpop*SAO protein abundance in defence secretions was monitored over time. A total of 0.85 mg secretions per lane was separated on silver-stained SDS gels. The 70-kDa band corresponds to *Cpop*SAO. Secretions originating from control treatment with 1 µg dsRNA of *gfp* (white arrowhead) and RNAi treatment with 1 µg dsRNA of *CpopSAO* (black arrowhead) are shown. (*c*) GC-chromatogram of secretions on day 5 after treatment; left: injecting 1.0 µg *gfp* dsRNA resulted in the production of **3**, right: injecting 1.0 µg *CpopSAO* dsRNA resulted in the production of **2** and **3**. (*d*) GC-chromatogram peak-area-based plot of secretions after dsRNA injection of *gfp* and different amounts of *CpopSAO* ($n = 5$).

C. populi (figure 2*a*) [12,14]. The composition of the secretome after dsRNA treatment was monitored in a time series in silver-stained one-dimensional SDS gels. Owing to the silencing effect, the quantity of *Cpop*SAO was apparently reduced just 2 days after dsRNA injection and the protein was barely visible after day 5 (figure 3*b*).

The effects on the biosynthesis of **3** in the defensive secretions were determined by GC/MS analysis. For these experiments, 0.1, 1.0 and 3.0 µg of *CpopSAO* dsRNA were injected into larvae from the same clutch. As in the protein reduction, we detected **2** in the defensive secretions just 2 days after the injection of 3.0 µg *CpopSAO* dsRNA (figure 3*c*). Compound **2** was not detectable in *gfp* control secretions. In addition, no unexpected chemical compound arose owing to the dsRNA treatments. By setting the peak area of **3** in ratio equalling the sum of the main peak areas, a diagram of the RNAi-dependent reduction of **3** can be plotted (figure 3*d*). We have tested dsRNA amounts ranging from 0.1 to 3.0 µg. After RNAi induction, significantly less aldehyde was observed for the 3.0 µg *CpopSAO* group ($p = 0.015$) on the 4th day and for all tested *CpopSAO* groups on the 5th day (0.1 µg, $p = 0.016$; 1 µg, $p = 0.002$; 3 µg, $p = \ll 0.001$). Biological variation prevented us from observing dose-dependent RNAi effects in these experiments; the amount of **2** did not differ significantly between the RNAi samples.

(b) *Off-target prediction and validation for* CpopSAO

Owing to strong sequence identities, co-silencing non-target genes can cause unintended side-effects [39,40]. Therefore, we performed off-target predictions for the desired dsRNA sequences of *CpopSAO* and *gfp*. Predicted off-target genes were validated by qPCR using cDNA derived from successful RNAi experiments. Because of a lack of genome sequences, the potential silencing effects of targeting the nucleus where fragments of the long dsRNA may bind to non-transcribed regulatory sequences [41] or introns [42] could be neither predicted nor validated.

For *gfp* dsRNA, no critical candidates were detected in the transcriptome library of *C. populi*. Off-target analyses in the *C. populi* sequence library, however, identified 25–21 bp contiguous regions of *CpopSAO* dsRNA that were identical to sequences of eight unique transcripts (see the electronic supplementary material, table ST2 for putative off-target hits). Three of them encode putative proteins having the GMC-oxidoreductase motif in the C-terminal region (*Cp*GMClike I-III) and five were annotated as hypothetical proteins (*Cp*COMP3092; *Cp*COMP6024; *Cp*COMP36289; *Cp*COMP38777; *Cp*COMP51471).

CpopSAO shares with *CpGMClike-I* two similar regions spanning 22 and 25 nucleotides (nts) each; these regions are interrupted by one mismatch (22/1 and 25/1) and, with *CpGMClike-III*, one similar sequence stretch without mismatch (24/0). *CpGMClike-II* and the five remaining transcripts possess sequence regions of 22/0 to 20/0 nts identical to *CpopSAO*. In all tissues, all putative off-target genes exhibited generally low expression levels with relative Cq values median less than 2×10^{-3}. qPCR assays were carried out for all eight targets 12 days after larvae were treated with 1.0 µg 1500-bp *CpopSAO* dsRNA; only for the *CpGMClike-I* and *CpGMClike-II* did these treatments reveal significant differences of transcript level in the gut tissue ($p = 0.049$; $p = 0.032$). No other tested transcripts showed changes of mRNA abundance in the examined tissues

(see the electronic supplementary material, figure S2). Since *C. populi* larvae transport the plant-derived precursor into the defensive glands for final transformation, we assume that the off-target effects on the putative GMC-oxidoreductases in gut tissue of unknown function do not distort the RNAi effects observed in the secretions.

(c) *Identification of unknown proteins in the defence-related secretome of* Phaedon cochleariae

After successfully introducing the 'lack-of-function approach' to the defensive secretions of *C. populi* by silencing an enzyme for which we had a clear expectation of the resulting phenotype, we used the method to identify proteins in unknown secretions. For this reason, we chose the larval exudates from the related de novo iridoid-producing species *P. cochleariae*. We assigned to the abundant 35-kDa band a putative protein whose deduced sequence contains 243 amino acids and a 22 amino acid signal peptide; the existence of such a sequence suggests that the mature protein is secreted (figure 2*a*). It possesses a conserved domain (pfam06585) characteristic for the juvenile hormone-binding protein (JHBP) superfamily. Sequence comparisons using the BLAST algorithm [35] revealed that the *P. cochleariae* amino acid sequence shares only very limited identity with functionally characterized insect proteins, for example, 12 per cent identity with the JHBP from *Bombyx mori* [43] and 16 per cent with the takeout (To) 1 from *Epiphyas postvittana* [44] (figure 2*a*). Higher identities up to 25 per cent were found only with insect proteins not yet fully characterized in their functions, such as those with the To-like protein (NP_001191952) from *Acyrtosyphon pisum* or the JHBP-like (XP_001359416) from *Drosophila pseudoobscura pseudoobscura*. None of the mentioned insect species is known to produce cyclic monoterpenoids.

The JHBP superfamily combines both the To protein family and the JHBP family. There are two major differences between the families: one is the number of disulphide bonds (To proteins have one and JHBPs have two) and the second are the conserved C-terminal sequence motives that are only present in To proteins. *In silico* analyses predicted in the *P. cochleariae* sequence seven N-glycosylation sites and only one disulphide bond. Along with identifying the two To-specific motives [45] (figure 4) in the C-terminal region, we conclude that our protein can be attributed to the To family. Therefore, we named it *Pc*To-like.

Despite the generally low sequence similarity, most To proteins and JHBPs are classified as ligand-binding proteins for juvenile hormones or similar hydrophobic terpenoids [44,46–49]. Because the precursor of the cyclic iridoid is also a terpenoid, we hypothesize that the putative protein could be involved in the iridoid biosynthesis in the defensive secretions. The assumption that the putative protein has relevance in the defensive glands is corroborated by the high transcript level which has been detected mainly in the glandular tissue of juvenile mustard leaf beetles (figure 2*c*). Low mRNA levels were also detectable in the fat body tissue.

(d) *RNA interference effects in larvae of* Phaedon cochleariae

A total of 0.3 µg of dsRNA derived from a 450-bp fragment of the *PcTo-like* sequence was injected into second instars of *P. cochleariae*. Transcript quantification 5 days after dsRNA injection confirmed a significant reduction of the mRNA in glandular tissue ($p = 0.043$) down to 1.0 per cent ($\pm 0.9\%$) compared with mRNA levels in *gfp* injections (figure 5*a*).

Phenotypic analyses after injection of dsRNA on the composition of low-molecular-weight compounds in the secretions were carried out by using GC/MS. The quality of the metabolites in samples collected 1 and 2 days after *Pc*To-like RNAi induction did not vary from the quality of the metabolites in those collected from *gfp* controls. In both treatments, we detected only the end-product **7**. The first deviation in the composition of the secretions was measured 3 days after dsRNA injection. Only in samples triggered by *PcTo-like* RNAi did minor amounts of the postulated intermediate **6** in addition to **7** emerge. After 5 days, however, **6** clearly accumulated in addition to **7** owing to the RNAi effect (figure 4*b*). Therefore, we conclude that the *Pc*To-like has to be involved in the cyclization of monoterpene precursors into iridoids.

Off-target effects were predicted using the method described for *CpopSAO*, and predicted off-target effects were avoided from final dsRNA sequence by choosing the template for dsRNA outside of areas of predicted off-target effects.

4. DISCUSSION

The results of our larval RNAi experiments clearly demonstrate selective excision of a component in a biosynthetic pathway. To the best of our knowledge, RNAi has never been used to target enzymes in insect defensive secretions. Owing to the silencing of *Cpop*SAO, the chemical composition in the larval exudates of *C. populi* was massively altered, starting as early as 48 h after treatment. This shows a distinct function of this enzyme *in vivo*. Before, Kirsch *et al.* [13] showed activity only in *in vitro* assays. Evidently, RNAi is a valuable technique for identifying *in vivo* relevance for unknown proteins in defensive glands. Although insects contain a large number of exocrine glands in which bioactive compounds are produced, to date few studies have relied on RNAi to provide evidence for the *in vivo* function of enzymes in insect glands. One example is the production of sex pheromones in special glands of the silkmoth *Bombyx mori*. By injecting the pupae with dsRNA, Ohnishi *et al.* [50,51] were able to dissect the components of the biosynthetic pathway as well as assign a function to a transport protein within the glands of adults. Another RNAi target was the production of pheromone in jewel wasps, *Nasonia vitripennis*. Silencing an epoxide hydrolase in these insects resulted in pheromone reduction by 55 per cent and suppressed the targeted gene transcripts by 95 per cent [52]. Freshly emerged males were injected and 2 days later levels of transcript and pheromones were analysed. As our results demonstrate, RNAi effects are easily detectable in exocrine glands. In the secretions of immature *P. cochleariae*, we were able to assign *in vivo* relevance to a cDNA encoding a protein which is important for the cyclization of iridoids. The iridoid pathway in insects was already proposed by using deuterium labelled precursors by Weibel *et al.* [53]. In his work, the stereospecifity of the cyclization was analysed and allocated to an enzymatic conversion. However, to date JHBPs and

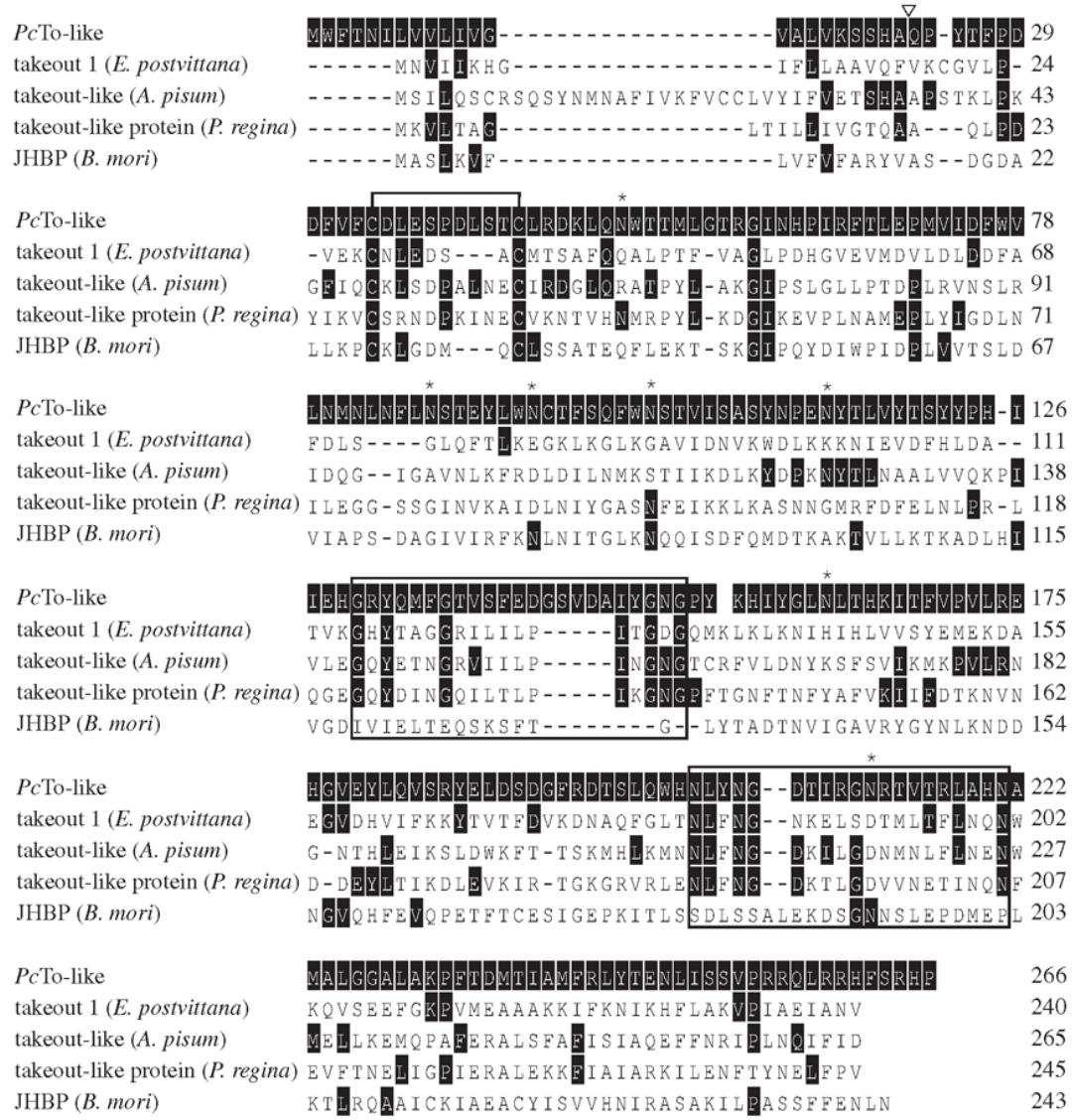

Figure 4. Amino acid alignments (ClustalW) of *Pc*To-like from *P. cochleariae* and other members from the To/JHBP family (*Epiphyas postvittana* To1: GeneBank: ACF39401; *Acyrthosiphon pisum* To-like: GeneBank: XP_001952685; *Phormia regina* To-like protein: GeneBank: BAD83405; *Bombyx mori* JHBP: GeneBank: AAF19267). Solid black shading depicts amino acids identical to *Pc*To-like sequence. White inverted triangles indicate the predicted signal peptide of *Pc*To-like. Asterisks mark the predicted N-glycosylation sites. Conserved cysteine residues that form disulphide bonds are marked with a bracket above the sequence. The two black boxes show the location of the To-typical motives.

To proteins have been established as being carriers of hydrophobic ligands [44,48]. Several lines of evidence indicate that JHBPs form complexes with juvenile hormones (JHs) which provide protection of the chemically labile JHs against nonspecific enzymatic degradation and/or adsorption to lipophilic surfaces during the delivery process from the production site to the target tissue [46,47,49]. Up to now only the crystal structure of To 1 from *E. postvittana* with ubiquinone provided direct evidence for ligand binding in To proteins [44]. Most of the putative To proteins await elucidation of their mode of action. Therefore, the actual mechanism how *Pc*To-like acts in the defensive exudates has to be analysed *in vitro* with purified recombinant protein. On-going experiments will reveal more functional enzymes in Chrysomelina and clarify the molecular machinery for the biosynthesis of deterrents in larval defence secretions.

To perform RNAi experiments, it is essential to ensure the specificity. Off-target effects can arise when siRNAs diced from long dsRNA fragments possess sufficient sequence similarity to non-target mRNA and thus triggering degradation of similar sequences [39]. For sequenced organisms, genome-scale off-target prediction programs are available [34]. These approaches are not suitable for organisms whose genomes have yet to be sequenced. In the last few years, several approaches have been used to detect off targets for those species, such as screening for target specificity by rapidly amplifying cDNA ends [54]. Another approach has used microarrays to compare the cDNAs from treated groups with those from non-treated groups; such comparisons offer proof of differentially expressed transcripts *via* qPCR [55]. Transcriptome sequences have rarely been used for approaches based on local alignment algorithms but represent an economical

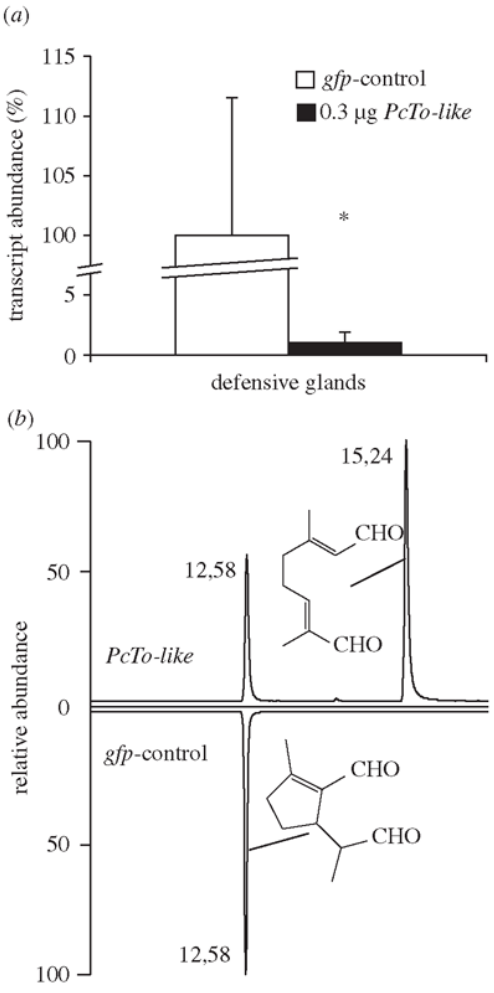

Figure 5. RNAi effects in juvenile *P. cochleariae*. (*a*) White bars: transcript abundance of *PcTo-like* after injecting 0.3 µg *gfp* dsRNA, $n = 3$ ±SD. Black bars: transcript abundance of *PcTo-like* after injecting 0.3 µg *PcTo-like* dsRNA, $n = 3$. 100% = ΔCq of *gfp*-control. Asterisks indicate level of significance: $*p < 0.05$. (*b*) GC-chromatogram of diluted secretions on day 5 after treatment, above: injecting 0.3 µg *PcTo-like* dsRNA resulted in the production of **6** and **7**; below: injecting 0.3 µg *gfp* dsRNA resulted in the production of **7**.

way to make off-target predictions [56]. In our case, we showed that *in silico* dicing of long dsRNA pieces to 21-bp fragments and subsequent BLASTn searches in our transcriptome libraries also lead to the identification of putative off-target transcripts. Subsequent qPCR analysis after successful RNAi induction revealed the co-silencing of predicted transcripts in *C. populi*. Two of eight mRNAs were significantly altered in gut tissue (see the electronic supplementary material, figure S2). But the observed off-target silencing could be assigned neither to the length of the fragments nor to the amount of pmol of the putative siRNAs (see the electronic supplementary material, table ST2). Furthermore, the composition and internal stability of the sequence fragments are supposed to have an impact on successful RNAi triggering [57] and could be included in the prediction. Although publications concerning off-target prediction have increased in the last 2 years, as yet no standard method is available. But as our results indicate, off-target validation is crucial for a realistic discussion of RNAi effects.

The authors would like to express their gratitude to Heiko Vogel for making available 454-sequences from *P. cochleariae*. We also gratefully acknowledge Angelika Berg, Kerstin Ploss, Gerhard Pauls and Antje Loele for technical assistance. We thank Gregor Bucher for helpful discussions on aspects of this work. Very special thanks are due to Prof. Jacques M. Pasteels and Emily Wheeler for their critical reading of the manuscript. This work was supported by the Deutsche Forschungsgemeinschaft (BU 1862/2-1) and the Max Planck Society.

R.R.B., P.R., M.S., M.K., N.W., W.B. and A.B. designed study. R.R.B. established RNAi in leaf beetles and performed RNAi treatments of *Cpop*SAO and its control treatments, performed off-target validation, collected all corresponding data except the off-target prediction and analysed output data. P.R. identified *PcTo-like*, performed RNAi treatments of *PcTo-like* and control treatments, collected all corresponding data and analysed output data. S.F., M.S. and M.G. generated transcriptome libraries. M.S. established and performed off-target prediction and contributed to interpretation of LC/MS^E output data. M.K. designed GC/MS assays, synthesized **6** and **7** and contributed to interpretation of output data. N.W. performed LC/MS^E analysis, collected and contributed to interpretation of output data. W.B. and A.B. contributed substantially to interpretation of all output data. R.R.B., P.R. and A.B. wrote first draft of the manuscript, and all authors contributed substantially to revisions.

REFERENCES

1 Quennedey, A. 1998 Insect epidermal gland cells: ultrastructure and morphogenesis. In *Microscopic anatomy of invertebrates, vol. 11A: insecta* (eds W. H. Harrison & M. Locke) pp. 177–207. New York: Wiley-Liss.
2 Dettner, K. 1987 Chemosystematics and evolution of beetle chemical defenses. *Annu. Rev. Entomol.* **32**, 17–48. (doi:10.1146/annurev.en.32.010187.000313)
3 Pasteels, J. M., Gregoire, J. C. & Rowell-Rahier, M. 1983 The chemical ecology of defense in arthropods. *Annu. Rev. Entomol.* **28**, 263–289. (doi:10.1146/annurev.en.28.010183.001403)
4 Burse, A., Frick, S., Discher, S., Tolzin-Banasch, K., Kirsch, R., Strauss, A., Kunert, M. & Boland, W. 2009 Always being well prepared for defense: the production of deterrents by juvenile Chrysomelina beetles (Chrysomelidae). *Phytochemistry* **70**, 1899–1909. (doi:10.1016/j.phytochem.2009.08.002)
5 Duffey, S. S. 1980 Sequestration of plant natural-products by insects. *Annu. Rev. Entomol.* **25**, 447–477. (doi:10.1146/annurev.en.25.010180.002311)
6 Opitz, S. E. W. & Mueller, C. 2009 Plant chemistry and insect sequestration. *Chemoecology* **19**, 117–154. (doi:10.1007/s00049-009-0018-6)
7 Laurent, P., Braekman, J. C., Daloze, D. & Pasteels, J. 2003 Biosynthesis of defensive compounds from beetles and ants. *Eur. J. Org. Chem.* 2733–2743. (doi:10.1002/ejoc.200300008)
8 Hinton, H. E. 1951 On a little-known protective device of some chrysomelid pupae (Coleoptera). *Proc. R. Entomol. Soc. A* **26**, 67–73. (doi:10.1111/j.1365-3032.1951.tb00123.x)
9 Pasteels, J. M. & Rowell-Rahier, M. 1989 Defensive glands and secretions as taxonomical tools in the Chrysomelidae. *Entomography* **6**, 423–432.
10 Pasteels, J. M., Daloze, D. & Rowell-Rahier, M. 1986 Chemical defense in chrysomelid eggs and neonate larvae. *Physiol. Entomol.* **11**, 29–37. (doi:10.1111/j.1365-3032.1986.tb00388.x)

11 Pasteels, J. M., Rowell-Rahier, M., Braekman, J. C. & Dupont, A. 1983 Salicin from host plant as precursor of salicyl aldehyde in defensive secretion of chrysomeline larvae. *Physiol. Entomol.* **8**, 307–314.

12 Brueckmann, M., Termonia, A., Pasteels, J. M. & Hartmann, T. 2002 Characterization of an extracellular salicyl alcohol oxidase from larval defensive secretions of *Chrysomela populi* and *Phratora vitellinae* (Chrysomelina). *Insect Biochem. Mol. Biol.* **32**, 1517–1523. (doi:10.1016/S0965-1748(02)00072-3)

13 Kirsch, R., Vogel, H., Muck, A., Reichwald, K., Pasteels, J. M. & Boland, W. 2011 Host plant shifts affect a major defense enzyme in *Chrysomela lapponica*. *Proc. Natl Acad. Sci. USA* **108**, 4897–4901. (doi:10.1073/pnas.1013846108)

14 Michalski, C., Mohagheghi, H., Nimtz, M., Pasteels, J. M. & Ober, D. 2008 Salicyl alcohol oxidase of the chemical defense secretion of two chrysomelid leaf beetles—molecular and functional characterization of two new members of the glucose–methanol–choline oxidoreductase gene family. *J. Biol. Chem.* **283**, 19 219–19 228. (doi:10.1074/jbc.M802236200)

15 Wallace, J. B. & Blum, M. S. 1969 Refined defensive mechanisms in *Chrysomela scripta*. *Ann. Entomol. Soc. Am.* **62**, 503–506.

16 Gross, J., Podsiadlowski, L. & Hilker, M. 2002 Antimicrobial activity of exocrine glandular secretion of *Chrysomela* larvae. *J. Chem. Ecol.* **28**, 317–331. (doi:10.1023/a:1017934124650)

17 Rowell-Rahier, M. & Pasteels, J. M. 1986 Economics of chemical defense in Chrysomelinae. *J. Chem. Ecol.* **12**, 1189–1203. (doi:10.1007/bf01639004)

18 Kuhn, J., Pettersson, E. M., Feld, B. K., Burse, A., Termonia, A., Pasteels, J. M. & Boland, W. 2004 Selective transport systems mediate sequestration of plant glucosides in leaf beetles: a molecular basis for adaptation and evolution. *Proc. Natl Acad. Sci. USA* **101**, 13 808–13 813. (doi:10.1073/pnas.0402576101)

19 Discher, S., Burse, A., Tolzin-Banasch, K., Heinemann, S. H., Pasteels, J. M. & Boland, W. 2009 A versatile transport network for sequestering and excreting plant glycosides in leaf beetles provides an evolutionary flexible defense strategy. *ChemBioChem* **10**, 2223–2229. (doi:10.1002/cbic.200900226)

20 Pasteels, J. M., Duffey, S. & Rowell-Rahier, M. 1990 Toxins in chrysomelid beetles possible evolutionary sequence from de novo synthesis to derivation from food-plant chemicals. *J. Chem. Ecol.* **16**, 211–222. (doi:10.1007/bf01021280)

21 Termonia, A., Hsiao, T. H., Pasteels, J. M. & Milinkovitch, M. C. 2001 Feeding specialization and host-derived chemical defense in Chrysomeline leaf beetles did not lead to an evolutionary dead end. *Proc. Natl Acad. Sci. USA* **98**, 3909–3914. (doi:10.1073/pnas.061034598)

22 Daloze, D. & Pasteels, J. M. 1994 Isolation of 8-hydroxygeraniol-8-O-beta-D-glucoside, a probable intermediate in biosynthesis of iridoid monoterpenes, from defensive secretions of *Plagiodera versicolora* and *Gastrophysa viridula* (Coleoptera, Chrysomelidae). *J. Chem. Ecol.* **20**, 2089–2097. (doi:10.1007/BF02066245)

23 Soetens, P., Pasteels, J. M. & Daloze, D. 1993 A simple method for *in vivo* testing of glandular enzymatic activity on potential precursors of larval defensive compounds in *Phratora* species (Coleoptera, Chrysomelinae). *Experientia* **49**, 1024–1026. (doi:10.1007/BF02125653)

24 Veith, M., Oldham, N. J., Dettner, K., Pasteels, J. M. & Boland, W. 1997 Biosynthesis of defensive allomones in leaf beetle larvae—stereochemistry of salicylalcohol oxidation in *Phratora vitellinae* and comparison of enzyme substrate and stereospecificity with alcohol oxidases from several iridoid producing leaf beetles. *J. Chem. Ecol.* **23**, 429–443. (doi:10.1023/B:JOEC.0000006369.26490.c6)

25 Veith, M., Lorenz, M., Boland, W., Simon, H. & Dettner, K. 1994 Biosynthesis of iridoid monoterpenes in insects—defensive secretions from larvae of leaf beetles (Coleoptera, Chrysomelidae). *Tetrahedron* **50**, 6859–6874. (doi:10.1016/S0040-4020(01)81338-7)

26 Kirsch, R., Vogel, H., Muck, A., Vilcinskas, A., Pasteels, J. M. & Boland, W. 2011 To be or not to be convergent in salicin-based defence in chrysomeline leaf beetle larvae: evidence from *Phratora vitellinae* salicyl alcohol oxidase. *Proc. R. Soc. B* **278**, 3225–3232. (doi:10.1098/rspb.2011.0175)

27 Ding, S.-W., Li, H., Lu, R., Li, F. & Li, W.-X. 2004 RNA silencing: a conserved antiviral immunity of plants and animals. *Virus Res.* **102**, 109–115. (doi:10.1016/j.virusres.2004.01.021)

28 Fire, A., Xu, S. Q., Montgomery, M. K., Kostas, S. A., Driver, S. E. & Mello, C. C. 1998 Potent and specific genetic interference by double-stranded RNA in *Caenorhabditis elegans*. *Nature* **391**, 806–811. (doi:10.1038/35888)

29 Belles, X. 2010 Beyond *Drosophila*: RNAi *in vivo* and functional genomics in insects. *Annu. Rev. Entomol.* **55**, 111–128. (doi:10.1146/annurev-ento-112408-085301)

30 Mito, T., Nakamura, T., Bando, T., Ohuchi, H. & Noji, S. 2011 The advent of RNA interference in entomology. *Entomol. Sci.* **14**, 1–8. (doi:10.1111/j.1479-8298.2010.00408.x)

31 Terenius, O. *et al.* 2011 RNA interference in Lepidoptera: an overview of successful and unsuccessful studies and implications for experimental design. *J. Insect Physiol.* **57**, 231–245. (doi:10.1016/j.jinsphys.2010.11.006)

32 Szabo, L. F. 2008 Rigorous biogenetic network for a group of indole alkaloids derived from strictosidine. *Molecules* **13**, 1875–1896. (doi:10.3390/molecules13081875)

33 Kuhnle, A. & Muller, C. 2011 Responses of an oligophagous beetle species to rearing for several generations on alternative host–plant species. *Ecol. Entomol.* **36**, 125–134. (doi:10.1111/j.1365-2311.2010.01256.x)

34 Naito, Y., Yamada, T., Matsumiya, T., Ui-Tei, K., Saigo, K. & Morishita, S. 2005 dsCheck: highly sensitive off-target search software for double-stranded RNA-mediated RNA interference. *Nucleic Acids Res.* **33**, W589–W591. (doi:10.1093/nar/gki419)

35 Altschul, S. F., Madden, T. L., Schaeffer, A. A., Zhang, J., Zhang, Z., Miller, W. & Lipman, D. J. 1997 Gapped BLAST and PSI-BLAST: a new generation of protein database search programs. *Nucleic Acids Res.* **25**, 3389–3402. (doi:10.1093/nar/25.17.3389)

36 Oldham, N. J., Veith, M., Boland, W. & Dettner, K. 1996 Iridoid monoterpene biosynthesis in insects—evidence for a de novo pathway occurring in the defensive glands of *Phaedon armoraciae* (Chrysomelidae) leaf beetle larvae. *Naturwissenschaften* **83**, 470–473. (doi:10.1007/BF01144016)

37 Uesato, S., Ogawa, Y., Doi, M. & Inouye, H. 1987 Biomimetic synthesis of (±)-chrysomelidial, (±)-dehydroiridoidal, and (±)-iridoidal. *J. Chem. Soc.-Chem. Commun.* 1020–1021. (doi:10.1039/c39870001020)

38 Cavener, D. R. 1992 GMC oxidoreductases: a newly defined family of homologous proteins with diverse catalytic activities. *J. Mol. Biol.* **223**, 811–814. (doi:10.1016/0022-2836(92)90992-s)

39 Jackson, A. L., Bartz, S. R., Schelter, J., Kobayashi, S. V., Burchard, J., Mao, M., Li, B., Cavet, G. & Linsley, P. S. 2003 Expression profiling reveals off-target gene

regulation by RNAi. *Nat. Biotechnol.* **21**, 635–637. (doi:10.1038/nbt831)
40 Seinen, E., Burgerhof, J. G. M., Jansen, R. C. & Sibon, O. C. M. 2011 RNAi-induced off-target effects in *Drosophila melanogaster*: frequencies and solutions. *Brief. Funct. Genom.* **10**, 206–214. (doi:10.1093/bfgp/elr017)
41 Morris, K. V., Chan, S. W. L., Jacobsen, S. E. & Looney, D. J. 2004 Small interfering RNA-induced transcriptional gene silencing in human cells. *Science* **305**, 1289–1292. (doi:10.1126/science.1101372)
42 Bosher, J. M., Dufourcq, P., Sookhareea, S. & Labouesse, M. 1999 RNA interference can target pre-mRNA: consequences for gene expression in a *Caenorhabditis elegans* operon. *Genetics* **153**, 1245–1256.
43 Vermunt, A. M. W., Kamimura, M., Hirai, M., Kiuchi, M. & Shiotsuki, T. 2001 The juvenile hormone binding protein of silkworm haemolymph: gene and functional analysis. *Insect Mol. Biol.* **10**, 147–154. (doi:10.1046/j.1365-2583.2001.00249.x)
44 Hamiaux, C., Stanley, D., Greenwood, D. R., Baker, E. N. & Newcomb, R. D. 2009 Crystal structure of *Epiphyas postvittana* takeout 1 with bound ubiquinone supports a role as ligand carriers for takeout proteins in insects. *J. Biol. Chem.* **284**, 3496–3503. (doi:10.1074/jbc.M807467200)
45 So, W. V., Sarov-Blat, L., Kotarski, C. K., McDonald, M. J., Allada, R. & Rosbash, M. 2000 Takeout, a novel *Drosophila* gene under circadian clock transcriptional regulation. *Mol. Cell. Biol.* **20**, 6935. (doi:10.1128/MCB.20.18.6935-6944.2000)
46 deKort, C. A. D. & Granger, N. A. 1996 Regulation of JH titers: the relevance of degradative enzymes and binding proteins. *Arch. Insect Biochem. Physiol.* **33**, 1–26. (doi:10.1002/(sici)1520-6327(1996)33:1<1::aid-arch1>3.0.co;2-2)
47 Prestwich, G. D., Wojtasek, H., Lentz, A. J. & Rabinovich, J. M. 1996 Biochemistry of proteins that bind and metabolize juvenile hormones. *Arch. Insect Biochem. Physiol.* **32**, 407–419. (doi:10.1002/(sici)1520-6327(1996)32:3/4<407::aid-arch13>3.0.co;2-g)
48 Suzuki, R., Fujimoto, Z., Shiotsuki, T., Tsuchiya, W., Momma, M., Tase, A., Miyazawa, M. & Yamazaki, T. 2011 Structural mechanism of JH delivery in hemolymph by JHBP of silkworm, *Bombyx mori*. *Sci. Rep.* **1**, 133. (doi:10.1038/srep00133)
49 Winiarska, B., Dwornik, A., Debski, J., Grzelak, K., Bystranowska, D., Zalewska, M., Dadlez, M., Ozyhar, A. & Kochman, M. 2011 N-linked glycosylation of *G. mellonella* juvenile hormone binding protein—Comparison of recombinant mutants expressed in *P. pastoris* cells with native protein. *Biochim. Biophys. Acta: Proteins Proteom.* **1814**, 610–621. (doi:10.1016/j.bbapap.2011.02.002)
50 Ohnishi, A., Hashimoto, K., Imai, K. & Matsumoto, S. 2009 Functional characterization of the *Bombyx mori* fatty acid transport protein (BmFATP) within the silkmoth pheromone gland. *J. Biol. Chem.* **284**, 5128–5136. (doi:10.1074/jbc.M806072200)
51 Ohnishi, A., Hull, J. J. & Matsumoto, S. 2006 Targeted disruption of genes in the *Bombyx mori* sex pheromone biosynthetic pathway. *Proc. Natl Acad. Sci. USA* **103**, 4398–4403. (doi:10.1073/pnas.0511270103)
52 Abdel-Latief, M., Garbe, L. A., Koch, M. & Ruther, J. 2008 An epoxide hydrolase involved in the biosynthesis of an insect sex attractant and its use to localize the production site. *Proc. Natl Acad. Sci. USA* **105**, 8914–8919. (doi:10.1073/pnas.0801559105)
53 Weibel, D. B., Oldham, N. J., Feld, B., Glombitza, G., Dettner, K. & Boland, W. 2001 Iridoid biosynthesis in staphylinid rove beetles (Coleoptera : Staphylinidae, Philonthinae). *Insect Biochem. Mol. Biol.* **31**, 583–591. (doi:10.1016/s0965-1748(00)00163-6)
54 Sabirzhanov, B., Sabirzhanova, I. B. & Keifer, J. 2011 Screening target specificity of siRNAs by rapid amplification of cDNA ends (RACE) for non-sequenced species. *J. Mol. Neurosci.* **44**, 68–75. (doi:10.1007/s12031-011-9514-6)
55 Lew-Tabor, A. E., Kurscheid, S., Barrero, R., Gondro, C., Moolhuijzen, P. M., Valle, M. R., Morgan, J. A. T., Covacin, C. & Bellgard, M. I. 2011 Gene expression evidence for off-target effects caused by RNA interference-mediated gene silencing of *Ubiquitin-63E* in the cattle tick *Rhipicephalus microplus*. *Int. J. Parasitol.* **41**, 1001–1014. (doi:10.1016/j.ijpara.2011.05.003)
56 Qiu, S., Adema, C. M. & Lane, T. 2005 A computational study of off-target effects of RNA interference. *Nucleic Acids Res.* **33**, 1834–1847. (doi:10.1093/nar/gki324)
57 Reynolds, A., Leake, D., Boese, Q., Scaringe, S., Marshall, W. S. & Khvorova, A. 2004 Rational siRNA design for RNA interference. *Nat. Biotechnol.* **22**, 326–330. (doi:10.1038/nbt936)

ELECTRONIC SUPPLEMENTARY MATERIAL

(I) Materials and Methods

All chemicals are purchased from Sigma-Aldrich (St. Louis, MO, USA), Carl Roth (Karlsruhe, Germany) or Serva (Heidelberg, Germany), if not stated other.

(a) Secretome analysis by LC-MS/MS and data processing. Larval secretions samples of *P. cochleariae* were separated by any-kD gradient gels (Bio-Rad Laboratories, Munich, Germany) in SDS-PAGE [1]. Protein bands of Coomassie Brilliant blue R250 stained gels were cut from the gel matrix and tryptic digestion was carried out as described by Shevchenko et al. [2]. Samples were separated using a nanoUPLC system (Waters, Manchester, UK). A mobile phase of 0.1% aqueous formic acid was used to concentrate and desalt the sample on a Symmetry C18 trap-column (20 x 0.18 mm, 5 µm particle size) at a flow rate of 15 µL/min. Subsequently, peptides were separated by in-line gradient elution onto a nanoAcquity C18 column (200 mm ×75 µm ID, C18 BEH 130 material, 1.7 µm particle size) at a flow rate of 0.350 µl/min using an increasing acetonitrile gradient from 1-95% B over 90 min (Buffers: A, 0.1% formic acid in water; B: 100% acetonitrile in 0.1% formic acid). The eluted peptides were transferred to the nanoelectrospray source of a Synapt HDMS tandem mass spectrometer (Waters, Manchester, UK) equipped with a metal-coated nanoelectrospray tip (Picotip, 50 ×0.36 mm, 10 µm internal diameter, New Objective, Woburn, USA). The source temperature was set to 80°C, cone gas flow 20 L/h, and the nanoelectrospray voltage was 3.2 kV. For all measurements, the mass spectrometer was operated in V-mode with a resolving power of at least 10,000 FWHM. All analyses were performed in positive ESI mode. A 650 fmol/µL human Glu-fibrinopeptide B in 0.1% formic acid/acetonitrile (1:1 v/v) was infused at a flow rate of 0.5 µL min-1 through the

reference NanoLockSpray source every 30 seconds to compensate for mass shifts in MS and MS/MS fragmentation mode.

LC-MS data were collected using data-independent LC-MS^E analysis [3]. Full scan LC-MS data were collected using alternating mode of acquisition: low energy (MS) and elevated energy (MS^E) mode over 1.5 sec intervals in the range m/z of 50-1700 with an interscan delay of 0.2 sec. In low energy mode, data were collected at constant collision energy of 4 eV set on the trap T-wave device and ramped during scan from 15 to 40 eV in elevated MS^E mode.

The continuum LC-MS^E data were processed by PLGS 2.5 software (Waters). Baseline-subtracted, smoothed, deisotoped, and lockmass-corrected spectra were aligned according to the ion accounting algorithm [4]. The processed data were searched against the *P. cochleariae* protein subdatabases constructed from in-house transcriptome-database by their translation from all six reading frames. In order to increase the complexity of the searched database it was appended with Swissprot database downloaded on 13 August, 2011. Automatic settings for precursor and product ion tolerance were used for database searching, with a maximum false positive rate of 4%. Ion accounting search parameter were: minimum of 1 peptide matches per protein, with a minimum of 5 consecutive fragment ions per peptide, and minimum number of product ion matches per protein, 7. The acquired data were searched with a fixed carbamidomethylation of cysteine, along with variable oxidation of methionine residues.

(b) Cloning of *CpopSAO* and *PcTo-like*. Tissue samples from beetles were collected as described by Burse et al. [5]. Total RNA was extracted from insect tissue with the RNAqueous Micro Kit (Ambion, Life Technologies) according to the manufacturers' instructions except that 1% (v/v) ExpressArt NucleoGuard (Amplification technologies, Hamburg, Germany) was added to the lysis buffer. For method establishment, the integrity of RNA purified this way, was validated by electrophoresis on RNA 6000 Nano labchips on a Bioanalyzer 2100 (Agilent

Technologies). No RNA degradation products were observed. A RNA-integrity number could not be determined, as insects 28S-RNA breaks up in the purification process and accumulates around the 18S-RNA [6]. In on-going experiments RNA integrity was evaluated by TBE-gels and measurement of 260:280 nm absorbance ratios. RNA concentrations were determined employing a NanoView (GE-Healthcare, Little Chalfont, UK). Up to 5 µg of the RNA was reverse transcribed at 50°C for 60 min. using SuperScript III and Oligo(dT)$_{12-18}$ primer (both, Invitrogen, Life Technologies).

Full length cDNA sequence of *CpopSAO* and *PcTo-like* were amplified by the high fidelity *Pfx*-Polymerase (Invitrogen, Life Technologies) (for Primers see supplemental table ST1). After purification with PCR-purification Kit (Roche, Basel, Switzerland) the resulting fragments were cloned into T7-promotor site free pIB/V5-HIS-TOPO vectors (Invitrogen, Life Technologies). Further, the pIB-CpopSAO and pIB-PcTo-like vectors, isolated from transformed *E. coli* TOP10 cells, were sequenced to confirm the presence of unaltered *CpopSAO* and *PcTo-like*. Functional allocations were performed with pfam-search (http://pfam.sanger.ac.uk/). The signal peptides were predicted using SignalP 3.0 [7] (http://www.cbs.dtu.dk/services/SignalP/), for N-glycosylation site prediction NetNGlyc 1.0 (http://www.cbs.dtu.dk/services/NetNGlyc/) was used.

(b) Quantitative Real-time PCR. Real-time PCR was employed for relative quantification [8]. Two technical replicates were performed from three biological replicates each. Technical replicates with a Cq difference of >1 were repeated. To normalize the PCRs for the amount of cDNA template added to the reactions, *CpRP-L45* and *CpActin* were chosen as reference genes in *C. populi* and *PcRP-L8* and *PcRP-S18* were chosen for *P. cochleariae*, respectively. Primers were designed using primer3PLUS:

http://www.bioinformatics.nl/cgi-bin/primer3plus/primer3plus.cgi (See supplemental table ST1 for primer sequences). Real-time PCR data were acquired on an Mx3000P Real-Time PCR system (Stratagene, Agilent Technologies) using Brilliant II SYBR Green qPCR Master Mix (Agilent Technologies). These assays were performed following the MIQE-guidelines [9].

References

1. Sambrook J., Russell D.W. 2001 *Molecular cloning: A laboratory manual*, Cold Spring Harbor Laboratory Press {a} , 10 Skyline Drive, Plainview, NY, 11803-2500, USA.
2. Shevchenko A., Tomas H., Havlis J., Olsen J.V., Mann M. 2006 In-gel digestion for mass spectrometric characterization of proteins and proteomes. *Nat. Prot.* **1**(6), 2856-2860. (doi:10.1038/nprot.2006.468).
3. Levin Y., Hradetzky E., Bahn S. 2011 Quantification of proteins using data-independent analysis (MSE) in simple and complex samples: A systematic evaluation. *Proteomics* **11**(16), 3273-3287. (doi:10.1002/pmic.201000661).
4. Li G.Z., Vissers J.P.C., Silva J.C., Golick D., Gorenstein M.V., Geromanos S.J. 2009 Database searching and accounting of multiplexed precursor and product ion spectra from the data independent analysis of simple and complex peptide mixtures. *Proteomics* **9**(6), 1696-1719. (doi:10.1002/pmic.200800564).
5. Burse A., Schmidt A., Frick S., Kuhn J., Gershenzon J., Boland W. 2007 Iridoid biosynthesis in Chrysomelina larvae: Fat body produces early terpenoid precursors. *Insect Biochem. Mol. Biol.* **37**(3), 255-265. (doi:10.1016/j.ibmb.2006.11.011).
6. Krupp G. 2005 Stringent RNA quality control using the Agilent 2100 bioanalyzer. In *www.Agilent.com/chem/labonachip* (01.02.2005 ed.
7. Bendtsen J.D., Nielsen H., von Heijne G., Brunak S. 2004 Improved prediction of signal peptides: SignalP 3.0. *J. Mol. Biol.* **340**(4), 783-795.
8. Livak K.J., Schmittgen T.D. 2001 Analysis of relative gene expression data using real-time quantitative PCR and the 2-DELTADELTACT method. *Methods (Orlando)* **25**(4), 402-408. (doi:10.1006/meth.2001.1262).
9. Bustin S.A., Benes V., Garson J.A., Hellemans J., Huggett J., Kubista M., Mueller R., Nolan T., Pfaffl M.W., Shipley G.L., et al. 2009 The MIQE Guidelines: Minimum Information for Publication of Quantitative Real-Time PCR Experiments. *Clin. Chem.* **55**(4), 611-622. (doi:10.1373/clinchem.2008.112797).

Table ST1

List of primers used for cloning, dsRNA synthesis and quantitative Real-Time PCR (qPCR)

Gene name used in this study		Cloning Primers
CpopSAO	fwd:	ATGTAGGAGTTAGTTTTATTATT
GeneBank: HQ245154.1	rev:	TCACATTCCGTAGTCTTTTT
PcTo-like	fwd:	GTAAAATCAAGTCATGCTCAACCATATAC
GeneBank: JQ728549	rev:	CTAAGGATGTCTGGAGAAATGTCTGCG
		Primers for dsRNA
CpopSAO	fwd:	TAATACGACTCACTATAGGGAACTTGATAATGAGTTGTCTGG
	rev:	TAATACGACTCACTATAGGGTTTTTGCATGGCAGGAGTTC
PcTo-like	fwd:	GTAATACGACTCACTATAGGGAGGGTTCTAAACATGAACCTGA ACTTTTTG
	rev:	GTAATACGACTCACTATAGGGAGACGAATAGTGTCACCATTGT ATAAGTTATG
gfp	fwd:	TAATACGACTCACTATAGGGAGATGGCTAGTAAGGGA
UniProtKB: P42212.1	rev:	TAATACGACTCACTATAGGGAGATTATTTGTAGAGTTC
		qPCR-primers
CpopSAO	fwd:	CCATGCAAAAATATAATCCAACGA
GeneBank: HQ245154.1	rev:	TACTTCTGATACCACATTCCCAA
CpRPL45	fwd:	CACTGGAATCCAAAGTGGAAACTG
GeneBank: JX 122918	rev:	CTGCCTTTCAACCCATGGTC
CpActin	fwd:	ACGTGGACATCAGGAAGGAC
GeneBank: JX122919	rev:	ACATCTGCTGGAAGGTGGAC
CpGMClike-I	fwd:	ACAATCAAACAGGGGTAATG
GeneBank: JX122924	rev:	CAAGGCTTTTTGTTAGCACT
CpGMClike-II	fwd:	TGACGTCTATGTTGTCTGGA
GeneBank: JX122922	rev:	CATCCAAAATCCAAAGGATA
CpGMClike-III	fwd:	TTTTTGCATAGTGGGAGTTT
GeneBank: JX122928	rev:	TTGAACTGAAATCGGCTAAT
Cp-comp3092	fwd:	ACTACTGCCGAGTGAAAAAG
GeneBank: JX122926	rev:	TGAACAATTGCATTGTGAAT
Cp-comp6204	fwd:	ATATCTTGCTTGGGAATTGA
GeneBank: JX122923	rev:	AGCGGAACCTGAAGATTTAT
Cp-comp36289	fwd:	TTGAAAACTGATTCTGTGGA
GeneBank: JX136676	rev:	TAGGAGTTGAAACCCAAAAA
Cp-comp38777	fwd:	TCATTGGGGAAAAATACAAC
GeneBank: JX122927	rev:	TGAAGGGGATAGGAATTATG
Cp-comp51471	fwd:	TGCAATATTGATTTCAAAGGT
GeneBank: JX122925	rev:	AATGATATCACCCCATGGTA
PcTo-like	fwd:	CTTACTACCCCCACATCATC
GeneBank: JQ728549	rev:	CTGGGACGAAGGTTATTTTGTG
PcRPL8	fwd:	CATGCCTGAAGGTACTATAGTGTG
GeneBank: JX122920	rev:	GCAATGACAGTGGCATAGTTACC
PcRPS18	fwd:	ATGCTCCGATGAAGAAGTCG
GeneBank: JX122921	rev:	GCCTATTCAAGAACCAGTCAGG

(II) Results

Table ST2

Off-target prediction for dsRNA sequence of *CpopSAO*. Putative siRNAs are labelled as length of sequence/mismatch.

Query id	Subject	% identity	mismatch	gap opening	Subject start	Subject end	putative siRNAs
CpopSAO dsRNA	CpGMClike-I	95.24	1	0	324	304	22/1
CpopSAO dsRNA	CpGMClike-I	95.24	1	0	325	305	25/1
		95.24	1	0	331	311	
		95.24	1	0	332	312	
		95.24	1	0	333	313	
		95.24	1	0	334	314	
		95.24	1	0	335	315	
CpopSAO dsRNA	CpGMClike-II	95.24	1	0	605	625	21/1
CpopSAO dsRNA	CpGMClike-III	100.00	0	0	822	841	24/0
		100.00	0	0	821	841	
		100.00	0	0	820	840	
		100.00	0	0	819	839	
		100.00	0	0	818	838	
		100.00	0	0	818	837	
CpopSAO dsRNA	CpCOMP3092	95.24	1	0	94	74	21/1
CpopSAO dsRNA	CpCOMP6204	95.24	1	0	1377	1357	22/1
		95.24	1	0	420	400	
CpopSAO dsRNA	CpCOMP36289	95.24	1	0	167	147	21/1
CpopSAO dsRNA	CpCOMP38777	100.00	0	0	295	275	22/0
		100.00	0	0	294	274	
CpopSAO dsRNA	CpCOMP38777	100.00	0	0	295	276	20/0
		100.00	0	0	293	274	
CpopSAO dsRNA	CpCOMP51471	100.00	0	0	231	212	20/0

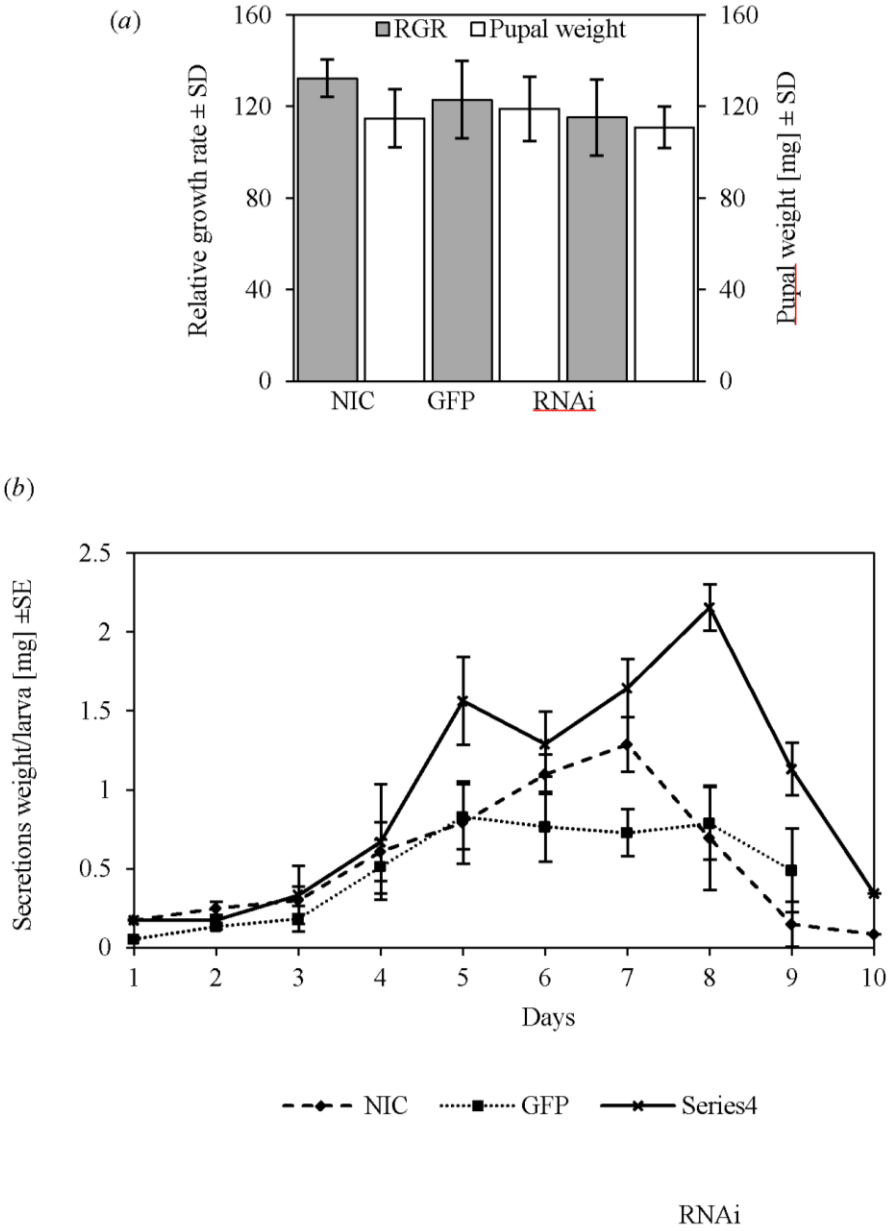

Figure S1

Developmental and metabolic effects of RNAi treatments. (*a*) Relative growth rate (RGR) and pupae weight of non-injected control (NIC), 1.0 µg dsRNA of *gfp*-treated groups (GFP), and 1.0 µg dsRNA of *CpopSAO*-treated groups (RNAi), n=6, (*b*) Produced secretions per day and larva, n=6.

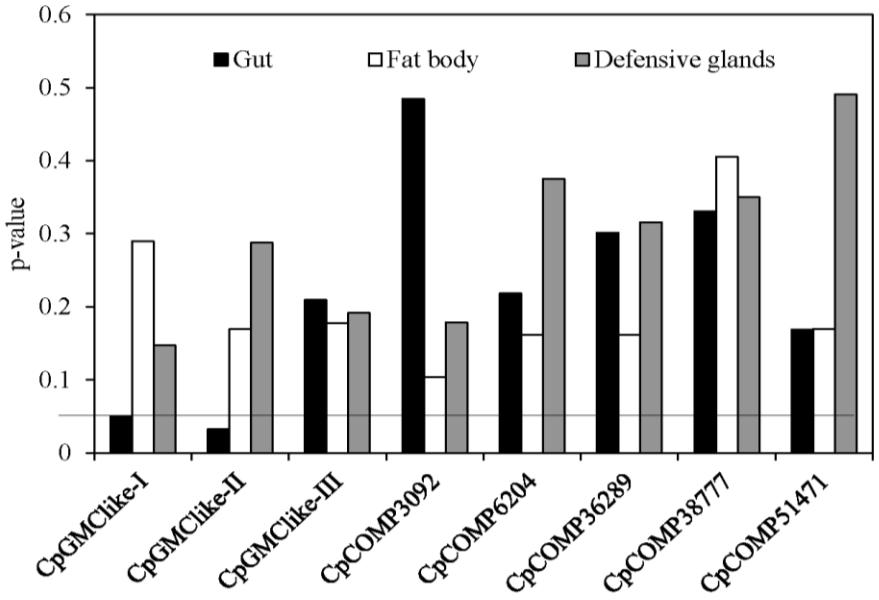

Figure S2

Significance of off-target-validation in *C. populi* larvae. Expression level was measured by qPCR 12 days after RNAi induction. Cq-values of off-target-genes were normalized using *CpRPL45* and *CpActin* and tested for significance by student's t-test; test compared expression levels between dsRNA injections of *gfp* and those of *CpopSAO*, respectively, n=3. Threshold line indicates p-value of 0.05, n=3.

5.4 MANUSCRIPT 4

METAL IONS CONTROL PRODUCT SPECIFICITY OF ISOPRENYL DIPHOSPHATE SYNTHASES IN THE INSECT TERPENOID PATHWAY

Metal ions control product specificity of isoprenyl diphosphate synthases in the insect terpenoid pathway

Sindy Frick[a], Raimund Nagel[b], Axel Schmidt[b], René R. Bodemann[a], Peter Rahfeld[a], Gerhard Pauls[a], Wolfgang Brandt[c], Jonathan Gershenzon[b], Wilhelm Boland[a], and Antje Burse[a,1]

Departments of [a]Bioorganic Chemistry and [b]Biochemistry, Max Planck Institute for Chemical Ecology, Beutenberg Campus, D-07745 Jena, Germany; and [c]Department of Bioorganic Chemistry, Leibniz Institute of Plant Biochemistry, D-06120 Halle/Saale, Germany

Edited by Jerrold Meinwald, Cornell University, Ithaca, NY, and approved January 29, 2013 (received for review December 12, 2012)

Isoprenyl diphosphate synthases (IDSs) produce the ubiquitous branched-chain diphosphates of different lengths that are precursors of all major classes of terpenes. Typically, individual short-chain IDSs (scIDSs) make the C_{10}, C_{15}, and C_{20} isoprenyl diphosphates separately. Here, we report that the product length synthesized by a single scIDS shifts depending on the divalent metal cofactor present. This previously undescribed mechanism of carbon chain-length determination was discovered for a scIDS from juvenile horseradish leaf beetles, *Phaedon cochleariae*. The recombinant enzyme *P. cochleariae* isoprenyl diphosphate synthase 1 (*Pc*IDS1) yields 96% C_{10}-geranyl diphosphate (GDP) and only 4% C_{15}-farnesyl diphosphate (FDP) in the presence of Co^{2+} or Mn^{2+} as a cofactor, whereas it yields only 18% C_{10} GDP but 82% C_{15} FDP in the presence of Mg^{2+}. In reaction with Co^{2+}, *Pc*IDS1 has a K_m of 11.6 μM for dimethylallyl diphosphate as a cosubstrate and 24.3 μM for GDP. However, with Mg^{2+}, *Pc*IDS1 has a K_m of 1.18 μM for GDP, suggesting that this substrate is favored by the enzyme under such conditions. RNAi targeting *Pc*IDS1 revealed the participation of this enzyme in the de novo synthesis of defensive monoterpenoids in the beetle larvae. As an FDP synthase, *Pc*IDS1 could be associated with the formation of sesquiterpenes, such as juvenile hormones. Detection of Co^{2+}, Mn^{2+}, or Mg^{2+} in the beetle larvae suggests flux control into C_{10} vs. C_{15} isoprenoids could be accomplished by these ions in vivo. The dependence of product chain length of scIDSs on metal cofactor identity introduces an additional regulation for these branch point enzymes of terpene metabolism.

cobalt | kinetic | prenyltransferase | secretions | silencing

Terpenes are an extensive group of natural products serving essential biological functions in Eukaryota, Bacteria, and Archaea. The more than 55,000 terpenes identified thus far are crucial components of intracellular signal-transduction pathways, electron transport chains, and membranes, or they can function as hormones, photosynthetic pigments, and semiochemicals (1, 2). Despite their structural diversity, terpenes are derived from the universal linear C_{10}, C_{15}, C_{20}, and larger diphosphate intermediates whose synthesis is catalyzed by isoprenyl diphosphate synthases (IDSs), also known as prenyltransferases (3). Depending on the stereochemistry of the double bond of the reaction product, these enzymes are classified as either *trans*-IDSs or *cis*-IDSs (4, 5).

Here, we focus on *trans*-IDSs, which can be further divided into enzymes producing short-chain (C_{10}–C_{20}), medium-chain (C_{25}–C_{35}), and long-chain (C_{40}–C_{50}) IDS products (6). Short-chain IDSs (scIDSs) are named for their main end products. Geranyl diphosphate synthases (GDPSs; EC 2.5.1.1) catalyze the alkylation of the homoallylic isopentenyl diphosphate (C_5-IDP) by the allylic dimethylallyl diphosphate (C_5-DMADP) resulting in geranyl diphosphate (GDP), the ubiquitous C_{10}-building block of many monoterpenes. Farnesyl diphosphate synthases (FDPSs; EC 2.5.1.10) form farnesyl diphosphate (FDP), the C_{15} precursor of sesquiterpenes, and geranylgeranyl diphosphate synthases (GGDPSs; EC 2.5.1.29) produce geranylgeranyl diphosphate (GGDP), the C_{20} backbone of diterpenes.

Whereas FDPSs and GGDPSs occur nearly ubiquitously in plants, animals, fungi, and bacteria, GDPSs have mainly been described in plants and insects to date (7). In plants, they participate in the biosynthesis of defenses against herbivores and pathogens, as well as in the formation of attractants for pollinators and seed-dispersing animals (1). Most plant GDPSs make GDP as a single product (8). However, occasionally, the enzymes are bifunctional and also produce FDP [*Pb*GDPS from the orchid *Phalaenopsis bellina* (9)] or GGDP [*Pa*IDS1 from the spruce *Picea abies* (10)] in addition to GDP. So far, only a few GDPSs have been characterized in insects (7). Strikingly, most of them have the ability to form multiple products.

The GDPSs cloned from the bark beetle *Ips pini*, for example, displayed prenyltransferase and terpene synthase activity in succession (11), resulting in the formation of precursors for the de novo synthesis of monoterpenoid aggregation pheromones such as ipsdienol, which coordinates the colonization of coniferous trees (12). Bifunctionality was also observed from the scIDSs characterized from different aphid species (13–17). Here, the recombinant proteins generated both GDP and FDP in parallel, and hence may be involved in the biosynthesis of either aphid sex pheromones or the sesquiterpene (*E*)-β-farnesene, the most common component of alarm pheromones. How nature accomplishes mixed-product formation by scIDSs in insects as well as in plants is still poorly understood.

Generally, catalysis by scIDSs follows a sequential mechanism called "head-to-tail alkylation." During chain elongation, the allylic cosubstrate (DMADP or GDP) undergoes coupling with IDP through electrophilic alkylation at its carbon-carbon double bond (18, 19). The reaction depends for activation on a trinuclear metal cluster, usually containing Mg^{2+} or Mn^{2+} (20). Based on earlier studies describing the role of metal cofactors for scIDS catalysis, we tested the product composition of a unique scIDS discovered from juvenile horseradish leaf beetles, *Phaedon cochleariae*, in the presence of different metal ions. To our surprise, we found that the enzyme *P. cochleariae* isoprenyl diphosphate synthase 1 (*Pc*IDS1) possesses an unusual product regulation mechanism not previously described for scIDSs. It alters the chain length of its products depending on the cofactor: The protein yields C_{10}-GDP in the presence of Co^{2+} or Mn^{2+}, whereas it produces the longer C_{15}-FDP in the presence of Mg^{2+}. GDP is needed for the de novo synthesis of the cyclopentanoid monoterpene iridoids, defensive compounds that are produced during the entire larval stage of *P. cochleariae* (21, 22) (Fig. 1). On the

Author contributions: S.F., A.S., J.G., W. Boland, and A.B. designed research; S.F., R.N., R.R.B., P.R., and G.P. performed research; J.G., W. Boland, and A.B. contributed new reagents/analytic tools; S.F., R.N., A.S., R.R.B., P.R., G.P., W. Brandt, and A.B. analyzed data; and S.F., A.S., J.G., W. Boland, and A.B. wrote the paper.

The authors declare no conflict of interest.

This article is a PNAS Direct Submission.

Data deposition: The *Pc*IDS1 sequence reported in this paper has been deposited in the GenBank database (accession no. KC109782) and the *Pc*IDS1 model has been deposited in the Protein Model DataBase (ID code PM0078683).

[1]To whom correspondence should be addressed. E-mail: aburse@ice.mpg.de.

This article contains supporting information online at www.pnas.org/lookup/suppl/doi:10.1073/pnas.1221489110/-/DCSupplemental.

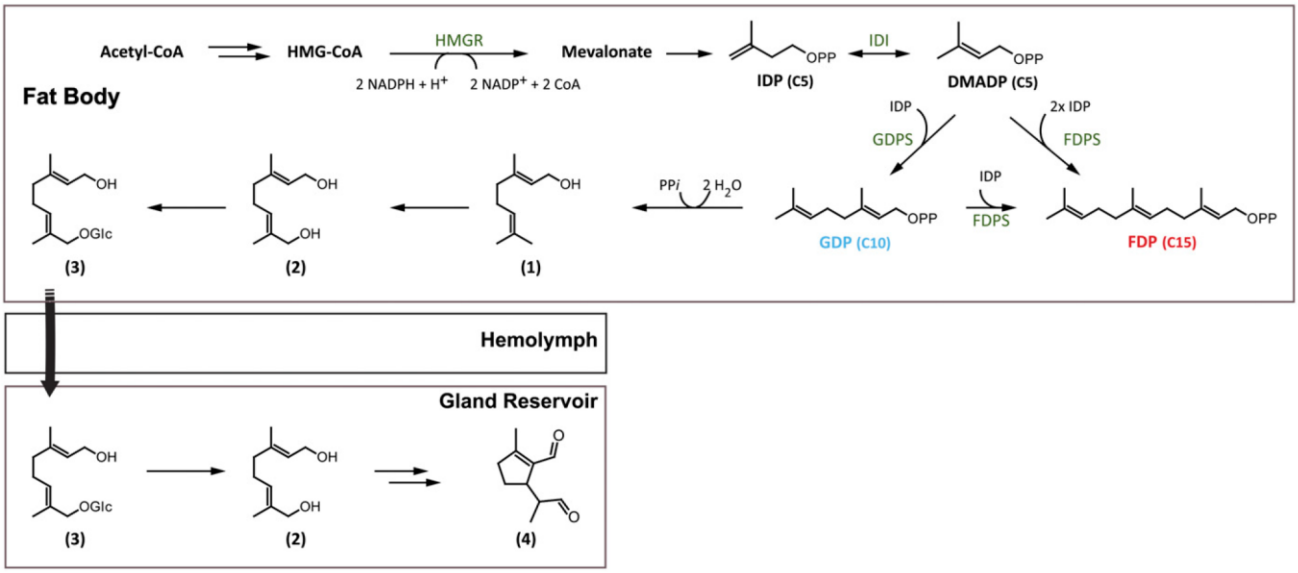

Fig. 1. Biosynthesis of iridoid monoterpene defenses in juvenile *P. cochleariae*: (1) geraniol, (2) 8-hydroxygeraniol, (3) 8-hydroxygeraniol-glucoside, (4) chrysomelidial. HMGR, 3-hydroxy-3-methyl-glutaryl-CoA reductase; IDI, isopentenyl diphosphate isomerase.

other hand, FDP serves as precursor for various primary metabolites and juvenile required hormone. The identification of Co^{2+}, Mn^{2+}, and Mg^{2+} in the juvenile beetles supports the notion that these organisms may control the product specificity of scIDSs by means of changes in local concentrations of these metal ions. Hence, the direction of flux at a branch point in terpene metabolism between defense and primary metabolism is regulated by an unprecedented IDS control mechanism.

Results

Identification and Tissue Distribution of a scIDS in Juvenile *P. cochleariae*. The use of degenerate primers allowed the amplification of a cDNA that encodes a protein of 430 aa (49.3 kDa, pI of 8.63) referred to here as *Pc*IDS1. ClustalW alignments revealed a high amino acid sequence identity of *Pc*IDS1 in relation to other functionally characterized insect scIDSs and showed all the conserved regions known for prenyltransferases (3, 23) (Fig. S1). The sequence also contains an RxxS motif (R_{67}–S_{70}), which could be the cleavage site for a mitochondrial targeting sequence already known from other identified scIDSs (11, 24).

Quantitative real-time assays revealed that *Pc*IDS1 transcripts are generally present in all analyzed larval tissues (Fig. S2*A*). However, the highest transcript abundance was observed in fat body tissue, which had a 5.6-fold higher transcript level compared with gut tissue. The transcript abundance was also reflected in protein level, because *Pc*IDS1 was detectable in all tested tissues, with the strongest signal derived from fat body tissue (Fig. S2*B*). Additionally, overall scIDS activity was determined in all crude extracts of the different larval tissues (Fig. 2*A*). In contrast to the trace amounts of FDP produced by extracts of every tissue tested, GDP-forming activity followed a different pattern. Compared with gut tissue, GDP formation was 141-fold higher in fat body tissue. Our results are consistent with recent findings on the distribution of the pathway to the iridoid defense compounds in *P. cochleariae* larvae. The early steps leading to the formation of the intermediate 8-hydroxygeraniol-glucoside are most likely localized in the fat body tissue. The glucoside is then transferred from there via the hemolymph into the defense glands, where the later steps in formation of chrysomelidial are located (25) (Fig. 1).

***Pc*IDS1 Is Involved in the Production of Defensive Monoterpenoids in Juvenile *P. cochleariae*.** RNAi experiments were performed with *P. cochleariae* to demonstrate the in vivo relevance of *Pc*IDS1. There were no significant differences in the relative growth rate between insects injected with a *PcIDS1*-dsRNA probe or with a control *Gfp* dsRNA probe and noninjected controls (NICs) (Fig. S3). However, transcript quantification 5 d after injection confirmed a significant *PcIDS1* mRNA reduction in fat body tissue (by 95%; $P < 0.001$) in comparison to *PcIDS1* mRNA levels in *Gfp*-treated larvae and NICs (Fig. 2*B*). Accordingly, 5 d after injection, the relative weight of defensive secretions decreased (by 52%; $P < 0.001$) in larvae challenged by *PcIDS1* dsRNA. This reduction continued until by day 13, a defenseless phenotype appeared that lacked secretions. The *Gfp* controls and NICs, on the other hand, produced unaltered amounts of defensive secretions (Fig. 2*C*). Detailed analyses of the relative amount of chrysomelidial per larva revealed a significant decline of this iridoid (by 78%; $P < 0.001$) in *PcIDS1*-treated larvae compared with the *Gfp* group and NICs after 5 d; this decline proceeded until there was a complete loss of secretions (Fig. 2*F*).

To determine if the chrysomelidial reduction is correlated with a decrease of the precursor, 8-hydroxygeraniol-glucoside, we analyzed the hemolymph and fat body tissue of larvae treated with *PcIDS1* dsRNA, *Gfp* dsRNA, and NICs. Seven days after *PcIDS1*-dsRNA injection, the level of precursor in the hemolymph was significantly reduced (by 89%; $P < 0.001$) compared with corresponding *Gfp* controls and NICs. This effect continued further with a reduction of 97% on day 11 (Fig. 2*E*). A similar effect was observed in the fat body tissue, where the amount of 8-hydroxygeraniol-glucoside was diminished (by 64.5 ± 14.08%) after 7 d. In addition to the reduction of chrysomelidial and 8-hydroxygeraniol-glucoside, we observed a significant loss of the overall scIDS activity (by 93%; $P < 0.001$) in the fat body tissue of *PcIDS1*-silenced larvae 7 d after injection compared with *Gfp* controls and NICs (Fig. 2*D*).

Recombinant *Pc*IDS1 Shows Metal Cofactor-Dependent Product Formation. Our results suggest that *Pc*IDS1 is involved in the biosynthesis of the monoterpenoid precursors needed for formation of the defensive compound chrysomelidial. Next, *Pc*IDS1 was expressed in *Escherichia coli* after truncation of the signal sequence at the 5′-end of the coding region, and the enzymatic activity of the purified recombinant protein was studied in vitro.

Like other scIDS proteins, *Pc*IDS1 was inactive without adding divalent metal cations, such as Mg^{2+} or Mn^{2+}. As recent

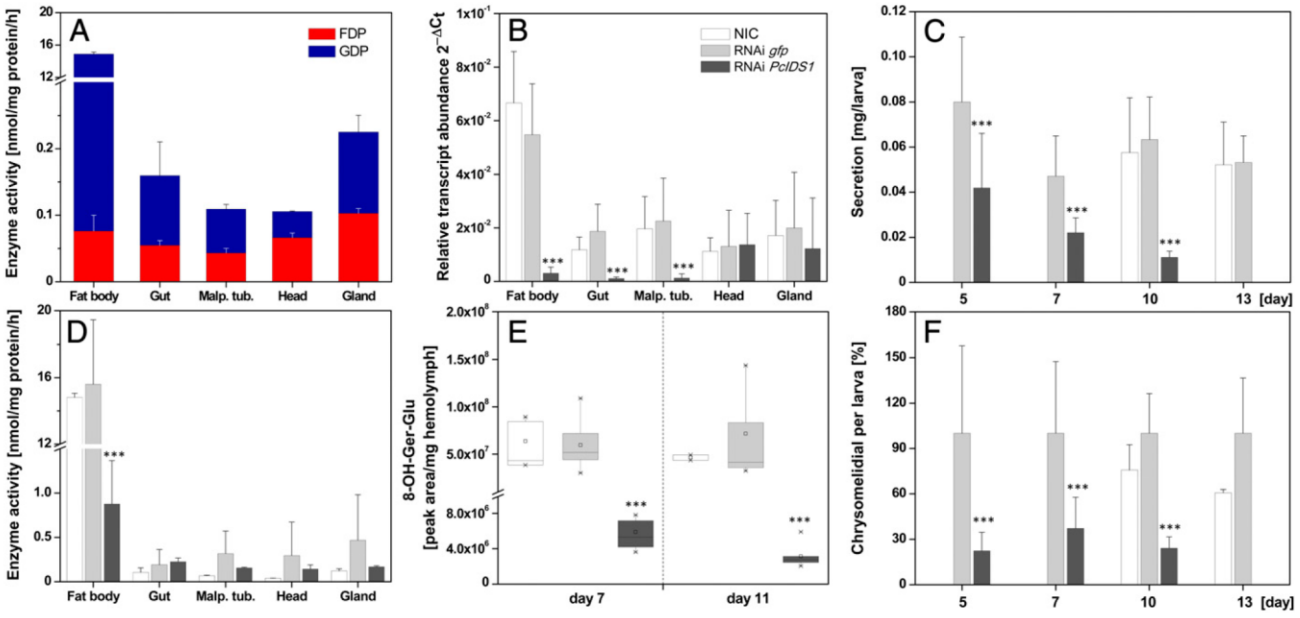

Fig. 2. Silencing *Pc*IDS1 in juvenile *P. cochleariae* by RNAi. (*A*) scIDS activity in tissue extracts of NICs: 10 μg of protein was incubated with 50 μM IDP, 50 μM DMADP, and 10 mM Mg^{2+} for 60 min ($n = 3$). (*B*) Relative transcript abundance ($2^{-\Delta Ct}$) of *Pc*IDS1 in different larval tissues 5 d after dsRNA injection ($n = 3$, ±SD). (*C*) Relative weight of larval secretions observed at different time points after dsRNA injection ($n = 3$, ±SD). (*D*) scIDS activity in tissues extracts 7 d after dsRNA injection. Ten micrograms of protein was incubated with 50 μM IDP, 50 μM DMADP, and 10 mM Mg^{2+} for 60 min ($n = 3$, ±SD). (*E*) Amount of 8-hydroxygeraniol-glucoside (8-OH-Ger-Glu) in hemolymph by HPLC analyses after dsRNA injection ($n = 3$, ±SD). (*F*) GC-MS analyses of chrysomelidial after dsRNA injection ($n = 3$, ±SD). Malp. tub., Malpighian tubules. ***, $p < 0.001$.

studies show, scIDS activity can be modulated by these metal ion cofactors (7, 15, 16, 26, 27); we therefore tested *Pc*IDS1 activity with IDP and two different allylic substrates, DMADP and GDP, in the presence of five different divalent cations. Each ion was tested separately at comparable concentration ranges.

In our assays with DMADP, the maximum overall enzyme activity for each cation was observed at 5 mM for Mg^{2+}, 0.5 mM for Co^{2+} and Mn^{2+}, and 0.1 mM for Ni^{2+} and Zn^{2+} (Fig. 3*A*, Fig. S4*A*, and Table S1). *Pc*IDS1 was far more active with Co^{2+} as an additive than with any other tested metal ion. Intriguingly, not only the overall enzyme activity but the product specificity varied considerably according to the different ions. In the presence of Co^{2+} or Mn^{2+}, with DMADP as a cosubstrate, *Pc*IDS1 produced about 96% GDP and only 4% FDP. In contrast, with Mg^{2+} as an additive, *Pc*IDS1 produced 18% GDP and 82% FDP.

Moreover, the optimal ion concentration changed depending on the allylic substrates. After GDP was substituted for DMADP, leading to the production of FDP, we observed *Pc*IDS1 being most active by addition of 0.5 mM Mg^{2+} compared with any other tested cofactor (Fig. 3*B*, Fig. S4*B*, and Table S1). Overall, Mg^{2+}, Mn^{2+}, and Co^{2+} represent the cofactors most favored in *Pc*IDS1 catalysis. Because Co^{2+} and Mg^{2+} resulted in the highest levels of *Pc*IDS1 activity, we used these cofactors in the following experiments.

In a first approach with DMADP, a constant Co^{2+} concentration of 0.5 mM was complemented with an ascending concentration of Mg^{2+} in a range of 0.001–10 mM (Fig. 4*A*). *Pc*IDS1 formed mainly GDP and only minor amounts of FDP, suggesting that Co^{2+} is the dominant metal ion independent of the tested Mg^{2+} concentration.

In a second approach with DMADP, we measured the enzyme activity with Mg^{2+} constant at 5 mM and an ascending concentration of Co^{2+} in the range of 0.001–10 mM (Fig. 4*B*). At Co^{2+} concentrations lower than 0.05 mM, FDP was the main product, accompanied by a 50% reduction in enzyme activity. However, if Co^{2+} concentrations exceeded 0.1 mM, *Pc*IDS1 activity clearly increased. Simultaneously, a shift from FDP to the reduced chain length of GDP was observed. Even if Mg^{2+} was 100-fold more abundant in the mixture, the enzyme definitely showed a preference for Co^{2+}.

With GDP as a cosubstrate, a constant 0.5 mM Co^{2+}, and an ascending Mg^{2+} concentration, *Pc*IDS1 displayed low FDP-forming activity (Fig. 4*C*). If Mg^{2+} is constant at 5 mM and Co^{2+} concentrations vary, we observed high FDP production only at Co^{2+} concentrations below 0.1 mM. However, as soon as the Co^{2+} concentration ascends, the FDP-forming activity decreases dramatically (Fig. 4*D*). Our findings indicate that the Mg^{2+}-catalyzed activity of *Pc*IDS1 is abolished as soon as Co^{2+} reaches its optimal concentration.

To determine the conformational state of *Pc*IDS1 quaternary structure, size exclusion chromatography was performed. Fig. S5 shows the relative retention volumes of the apoprotein without adding cofactors and *Pc*IDS1 in presence of Co^{2+} (0.5 mM) or Mg^{2+} (5 mM). Surprisingly, we found an obvious difference in the elution volume among the apoprotein (without divalent metal), the *Pc*IDS1-Mg^{2+} complex, and the *Pc*IDS1-Co^{2+} complex. The apoprotein eluted from the column at a retention volume of 76.36 mL (corresponding to 74.6 kDa), whereas *Pc*IDs1-Mg^{2+} and *Pc*IDS1-Co^{2+} eluted at 73.65 mL (corresponding to 93.8 kDa) and 74.46 mL (corresponding to 87.6 kDa), respectively. Given the calculated monomeric mass of 45.8 kDa, this indicates on one hand that the enzyme is always present as a dimer regardless of added cofactor. On the other hand, the difference in the elution volume reflects a change in the hydrodynamic volume of the protein caused by the divalent metal. In the case of Mg^{2+}, the dimeric protein possesses the largest volume, most likely due to a more relaxed conformation. With Co^{2+}, *Pc*IDS1 seems to have a more compact conformation, which may be responsible for the change in product spectrum. As a control, we also analyzed the metal influence on the standard proteins and observed no obvious difference in the elution volume with addition of various amounts of Mg^{2+} or Co^{2+}.

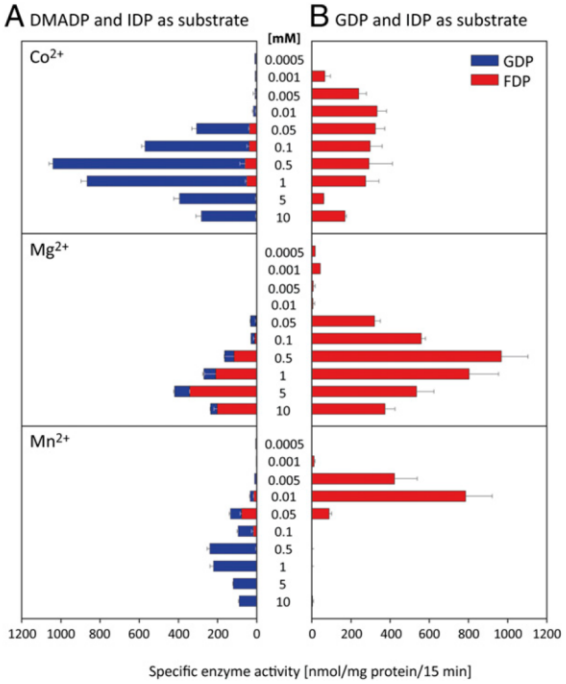

Fig. 3. Effect of metal cofactors on enzyme activity and product formation of *Pc*IDS1. (*A*) Different concentrations of Co^{2+}, Mg^{2+}, and Mn^{2+} were added to *Pc*IDS1 and incubated with 50 μM IDP and 50 μM DMADP ($n = 3$, ±SD). (*B*) Different concentrations of Co^{2+}, Mg^{2+}, and Mn^{2+} were added to *Pc*IDS1 and incubated with 50 μM IDP and 50 μM GDP ($n = 3$, ±SD).

Kinetic Analyses of Purified *Pc*IDS1. All kinetic parameters measured for *Pc*IDS1 are displayed in Table 1. In combination with Co^{2+} and fixed IDP, *Pc*IDS1 has a K_m of 11.6 μM for DMADP (Fig. S6*A*) and a K_m of 24.3 μM for GDP (Fig. S6*E*), suggesting that DMADP is the preferred substrate compared with GDP. Significant differences in the V_{max} were not observed. With Co^{2+} and DMADP fixed at 50 μM, *Pc*IDS1 has a K_m of 0.8 μM for IDP and substrate inhibition at higher concentrations with a K_i of 46.6 μM (Fig. S6*B*). No inhibitory effect of IDP was observed with GDP fixed at 50 μM (Fig. S6*F*).

In combination with Mg^{2+} and fixed IDP, *Pc*IDS1 displayed atypical kinetics for DMADP that resulted in a biphasic curve (Fig. S6*C*). In the first part of the curve from 0.1 to 100 μM DMADP, the reaction seems to follow a Michaelis–Menten kinetic. However, the curve displays a different slope as soon as the DMADP concentration exceeds 50 μM. The K_m for GDP was 1.2 μM with a slight substrate inhibition (Fig. S6*G*). With Mg^{2+} and DMADP fixed at 50 μM, *Pc*IDS1 has a K_m of 11.8 μM for IDP with a slight substrate inhibition (Fig. S6*D*), and with GDP fixed at 50 μM, the K_m of IDP was 7.1 μM (Fig. S6*H*). Analyses of the calculated V_{max} show that Mn^{2+} gave generally lower reaction velocities than did Co^{2+}.

The kinetic parameters substantiate our previous observations that *Pc*IDS1 has a preference for Co^{2+} with DMADP as an allylic cosubstrate giving the C_{10} product GDP. If Mg^{2+} is the metal cofactor, GDP is the favored cosubstrate affording the C_{15} product FDP.

Metal Cofactors Identified in *P. cochleariae* Larvae Have Different Affinities in the Enzyme Complex. Inductively coupled plasma-MS analysis of *P. cochleariae* larvae showed an overall concentration of Co^{2+} in the fat body tissue at ≥0.24 μg/g of dry weight (DW) or 4 nmol/g of DW, and an overall concentration of Mn^{2+} at ≥16.6 μg/g of DW or 0.3 μmol/g of DW, whereas Mg^{2+} was found at a concentration of 2,223 μg/g of DW or 91 μmol/g of DW in the fat body (Table S2).

Quantum mechanical calculations revealed reaction energies of about 40 kcal/mol lower for the formation of complexes containing Co^{2+} or Mn^{2+} compared with those containing Mg^{2+} for association with the diphosphate of DP^{3-} or the aspartate residues of the enzyme (mimicked by propionic acid anions) (Tables S3 and S4). In all cases, the affinity of the metal cations for the diphosphate was more than 200 kcal/mol higher than for the aspartate residues. Based on these gas phase calculations, the deduced minimum equilibrium constant for formation of the diphosphate metal complex is at least 10^{28}-fold higher for Co^{2+} or Mn^{2+} than for Mg^{2+}, which suggests that *Pc*IDS1 may have a considerably higher affinity for Co^{2+} or Mn^{2+} than for Mg^{2+}, although the magnitude of this difference may be reduced somewhat by solvation effects not considered here. Hence, the low concentrations of Co^{2+} or Mn^{2+} in the larval tissue in comparison to Mg^{2+} may be compensated for by their greater complex formation ability with diphosphate. On the other hand, if one compares the affinities of either the metal ion-complexed diphosphate with the aspartate (assuming the metal cations are delivered to the binding site together with the substrate) or, alternatively, the metal-complexed aspartates with the diphosphate (Tables S5 and S6), in both cases, the affinities for Co^{2+} or Mn^{2+} are lower than the affinity for Mg^{2+} in nice agreement with the measured lower $K_{m\,(GDP)}$ (higher affinity) ($Mg^{2+} = 1.18$ μM, $Co^{2+} = 24.3$ μM) and might be an explanation for the experimental differences in product specificity with different divalent metal ions. Note, one order of magnitude in K_m represents 1.4 kcal/mol (ΔG) in interaction energies.

Discussion

Understanding the mechanism of chain-length determination of scIDSs has been a major challenge for researchers of terpene biosynthetic enzymes, and much has been learned about active site features that restrict the length of the enzyme products. The determination of product carbon length by the identity of the metal cofactor apparently provides an alternative mechanism to the regulation of product formation by scIDS. Given that plants possess a number of genes encoding IDSs [e.g., at least 10 in *Arabidopsis thaliana* (8)], whereas insects possess only a few [e.g., 3 in *Bombyx mori* (28)], insects may compensate for this disparity by generating different chain-length products in other ways. In our case, the metal ion-mediated product differences enable the *P. cochleariae* beetles to supply precursors for two terpene pathways, one for monoterpene metabolism (synthesis of chemical defenses) and one for sesquiterpene metabolism (juvenile hormone formation), using only a single enzyme. Instead of "inventing" a new IDS, insects appear to use different cofactors to add an additional product to an enzyme's repertoire, thereby lowering metabolic costs. Such a regulation mechanism may allow faster adaptation to developmental or environmental changes that insects may face, such as metamorphosis or host plant shifts. Due to differences in metal ion identity and concentration, shifts in overall scIDS activity have previously been observed for enzymes from plants [e.g., *Abies grandis* (29)] and for enzymes from insects [e.g., *Myzus persicae* (15), *Choristoneura fumiferana* (30)], but without alterations in product chain length. However, Sen et al. (26) report cofactor-dependent changes of product chain length in crude homogenates of the *corpora allata* of the lepidopteran *Manduca sexta*. The product ratios formed during the coupling of DMADP with IDP by means of scIDS activity showed that FDP formation was stimulated by adding Mg^{2+}, whereas GDP formation increased in the presence of Mn^{2+}. Taken together with our results, these findings should motivate researchers to test alternative cofactors with scIDSs in the future.

*Pc*IDS1 produces mainly GDP (95%) in the presence of Co^{2+} (or Mn^{2+}) with IDP and DMADP as substrates and produces only minor amounts of FDP (4%). In contrast, with Mg^{2+}, the predominant product was FDP (82%); only minor amounts of GDP (18%) were produced. Our kinetic data for *Pc*IDS1 support the observation that the regulation of product distribution by these metal cofactors is biochemically relevant. Comparisons

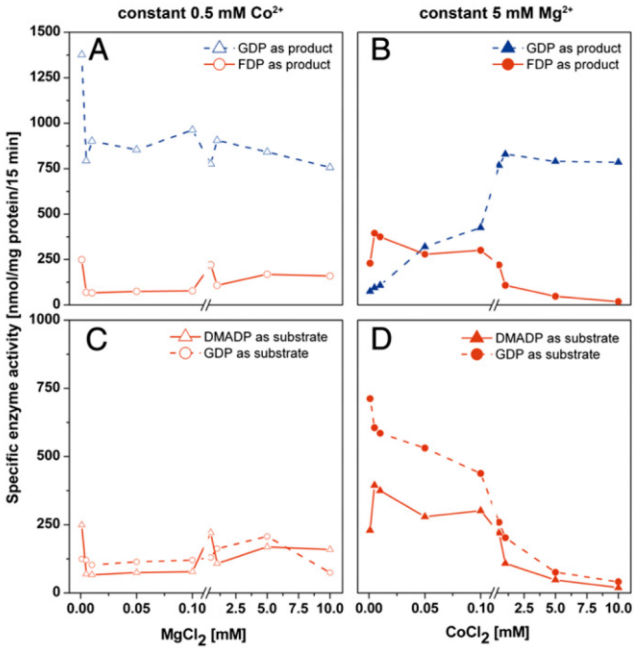

Fig. 4. Effect of mixtures of divalent metal ion cofactors on enzyme activity and product formation of *Pc*IDS1. (*A*) Constant 0.5 mM Co^{2+} with an ascending Mg^{2+} concentration in a range of 0.001 mM up to 10 mM with 50 μM IDP or 50 μM DMADP ($n = 2$). (*B*) Constant 5 mM Mg^{2+} with an ascending Co^{2+} concentration from 0.001 mM up to 10 mM with 50 μM IDP or 50 μM DMADP ($n = 2$). (*C*) FDP formation at constant 0.5 mM Co^{2+} with an ascending Mg^{2+} concentration with 50 μM GDP or 50 μM DMADP ($n = 2$). (*D*) FDP formation at constant 5 mM Mg^{2+} with an ascending Co^{2+} concentration with 50 μM GDP or 50 μM DMADP ($n = 2$).

with kinetic data available from plant GDPSs in the presence of DMADP revealed that the $K_{m(DMADP)}$ of *Pc*IDS1 (11.6 μM) with Co^{2+} corresponds to the K_m of the enzyme from *Anthirrhium majus* (24.1 μM) (31) or *Anthirrhium grandis* (16.7 μM) (29). $K_{m(DMADP)}$ values from insect scIDSs have so far been determined only for the bifunctional GDPSs of *M. persicae* *Mp*IPPS1-S (28.6 μM) (17) and *Mp*IPPS2-S (24.2 μM) (17), as well as *Aphis gossypii* (39.2 μM) (14), and for the FDPS from *Drosophila melanogaster* *Dm*FPPS-1b (33.5 μM) (32). The K_m of *Pc*IDS1 is found within the range of literature values. The combination of DMADP with Mg^{2+} did not allow a K_m calculation due to the biphasic progression of the kinetic curve. Although DMADP reacts initially with IDP to form GDP, in later catalytic cycles, the GDP formed can compete with another molecule of DMADP at the allylic binding site of *Pc*IDS1. If GDP is the preferred allylic substrate in combination with Mg^{2+}, it can lead to the formation of FDP.

The K_m values of *Pc*IDS1 for GDP, which are 24.3 μM and 1.1 μM in the presence of Co^{2+} and Mg^{2+}, respectively, are in the range of K_m values for previously described insect scIDSs, such as those of *A. gossypii* (12.6 μM) (14), *D. melanogaster* FPPS-1b (7 μM) (32), *M. sexta* (0.8 μM) (27), and *M. persicae* (*Mp*IPPS1-S, 25.4 μM; *Mp*IPPS2-S, 15.4 μM) (17). The difference in the *Pc*IDS1 K_m values for different metal cofactors suggests that the enzyme favors GDP as a substrate with Mg^{2+}. The alteration of IDS product specificity by metal ions has so far been described only for long-chain IDSs from microbes. In the presence of Co^{2+} or Mn^{2+}, octaprenyl-, solanesyl-, and decaprenyl-diphosphate synthases gave a variety of polyprenyl products whose chains were longer by up to two isoprene units than those of the products formed in the presence of Mg^{2+} (33–35).

IDS structure elucidation in combination with mutagenesis studies has suggested that product chain length is determined by the size of the hydrophobic pocket in the active center. In particular, the amino acids in the vicinity of the conserved first and second aspartate-rich regions (FARM and SARM motifs, respectively) form a steric hindrance that terminates chain elongation (3, 23, 36, 37). The van der Waals radii of Co^{2+} and Mn^{2+} are 1.73 Å and 1.9 Å, respectively, both of which are larger than that of Mg^{2+} at 0.96 Å (38). These differences may lead to conformational changes of *Pc*IDS1 or to rearrangements of substrate position in the enzymes that influence chain-length elongation. First hints toward conformational changes were obtained by size exclusion chromatography that revealed differences in the quaternary structure due to complex formation with different metal ions. Further homology modeling in combination with site-directed amino acid mutagenesis is needed to explain more fully how changes in cofactors influence the chain-length determination mechanism for *Pc*IDS1.

Mg^{2+} and Mn^{2+} are well-known cofactors for scIDS activity; however, in our biochemical characterization, *Pc*IDS1 showed the highest GDP synthase activity in the presence of Co^{2+}. Despite its rare occurrence in nature, Co^{2+} plays a role as a cofactor in a number of proteins (e.g., methionine aminopeptidase, glucose isomerase) (39). To balance the need for cobalt with its intrinsic toxicity, nature has evolved trafficking systems to maintain metal homeostasis (40). For example, in the transcriptome from *P. cochleariae*, we have identified a transport protein that shows high similarity to the cobalt uptake protein Cot 1 of *Saccharomyces cerevisiae* (41). This finding and the calculated high affinity of Co^{2+} to *Pc*IDS1 underline the possibility that Co^{2+} is an available as well as biologically relevant cofactor for this enzyme despite its low concentration in the larvae.

Using an RNAi approach, we were able to show that the *Pc*IDS1-catalyzed formation of GDP is involved in the production of monoterpenoid defensive compounds in *P. cochleariae* larvae. However, we could not detect a phenotype arising from the loss of formation of the alternate product, FDP. In insects, FDP is the essential precursor for the synthesis of juvenile hormones (42), and it is localized in the *corpora allata* complex found in the head posterior to the brain. Given that RNAi efficiency can differ from tissue to tissue as well as from gene to gene (43), the lack of a phenotype caused by low FDP levels might be attributed to ineffective silencing in the larval head. However, even more important may be the existence of additional prenyltransferases. Aphids, coleopterans, and lepidopterans are known to possess up to three scIDSs, and we are currently searching for additional scIDSs in *P. cochleariae*, which, like many other

Table 1. Kinetic constants for *P. cochleariae* *Pc*IDS1 depend on the identity of both the metal cofactor and allylic substrate

	Co^{2+}				Mg^{2+}			
Fixed substrate	$IDP_{(15\ \mu M)}$	$IDP_{(50\ \mu M)}$	$DMADP_{(50\ \mu M)}$	$GDP_{(50\ \mu M)}$	$IDP_{(50\ \mu M)}$	$IDP_{(50\ \mu M)}$	$DMADP_{(50\ \mu M)}$	$GDP_{(50\ \mu M)}$
Substrate	DMADP	GDP	IDP	IDP	DMADP	GDP	IDP	IDP
$K_{m\ (substrate)}$, μM	11.60	24.31	0.84	1.46	~1103	1.19	11.79	7.08
V_{max}, μmol·min^{-1}·mg^{-1} of protein	0.44	0.41	0.67	0.23	~2.39	0.12	0.17	0.20
$K_{i\ (substrate)}$, μM	n.d.	n.d.	46.62	n.d.	n.d.	1,047	572.7	322.1

n.d., not detectable.

enzymes of this class, may make more than one product. Our work shows that enzymes with an intrinsic promiscuity may also use exogenous factors, such as metal cofactors, to regulate product synthesis. It also serves as a reminder that neither substrate specificity nor product profiles can always be predicted by sequence similarity. Instead, rigorous biochemical testing is needed to establish enzyme function, especially among enzymes of terpene metabolism.

Materials and Methods

A scIDS from *P. cochleariae* was isolated with a degenerated PCR approach and RACE amplification. For further biochemical characterization, heterologous expression in *E. coli* Bl21 star (DE3) and protein purification were performed by affinity chromatography with Ni-nitrilotriacetric acid agarose columns. RNAi techniques were used to determine in vivo relevance, followed by quantitative real-time PCR, the quantification of 8-hydroxygeraniol via liquid chromatography (LC)-tandem MS (MS/MS), the relative quantification of chrysomelidial with GC-MS, and *Pc*IDS1 activity measurements determined by LC-MS/MS. Kinetic analyses and product determination were realized by LC-MS/MS, and calculations were performed with GraphPad Prism (GraphPad Software). Details of beetle rearing, reagents, protein purification/sequencing, antibody production, RNAi techniques, LC-MS/MS, GC-MS, quantitative PCR, sequence analyses, and other methods used in this study are described in *SI Materials and Methods*.

ACKNOWLEDGMENTS. We thank Dr. Dirk Merten for the element analysis and Angelika Berg and Dr. Maritta Kunert for technical assistance. We thank Prof. Jacques M. Pasteels for helpful discussions on aspects of this work and Emily Wheeler for critically reading of the manuscript. This work has been supported by the Deutsche Forschungsgemeinschaft (Grant BU 1862/2-1) and the Max Planck Society.

1. Gershenzon J, Dudareva N (2007) The function of terpene natural products in the natural world. *Nat Chem Biol* 3(7):408–414.
2. Pichersky E, Noel JP, Dudareva N (2006) Biosynthesis of plant volatiles: Nature's diversity and ingenuity. *Science* 311(5762):808–811.
3. Wang KC, Ohnuma S (2000) Isoprenyl diphosphate synthases. *Biochim Biophys Acta* 1529(1-3):33–48.
4. Kharel Y, Koyama T (2003) Molecular analysis of cis-prenyl chain elongating enzymes. *Nat Prod Rep* 20(1):111–118.
5. Liang PH (2009) Reaction kinetics, catalytic mechanisms, conformational changes, and inhibitor design for prenyltransferases. *Biochemistry* 48(28):6562–6570.
6. Gershenzon J, Kreis J (1999) Biochemistry of terpenoids: Monoterpenes, sesquiterpenes, diterpenes, sterols, cardiac glycosides, and steroid saponins. *Biochemistry of Plant Secondary Metabolism*, ed Wink M (Sheffield Academic, Sheffield, UK), pp 222–299.
7. Vandermoten S, Haubruge E, Cusson M (2009) New insights into short-chain prenyltransferases: Structural features, evolutionary history and potential for selective inhibition. *Cell Mol Life Sci* 66(23):3685–3695.
8. Tholl D, Lee S (2011) Terpene specialized metabolism in *Arabidopsis thaliana*. *The Arabidopsis Book*, ed Last R (American Society of Plant Biologists, Rockville, MD), Vol 9, pp e0143.
9. Hsiao YY, et al. (2008) A novel homodimeric geranyl diphosphate synthase from the orchid Phalaenopsis bellina lacking a DD(X)2-4D motif. *Plant J* 55(5):719–733.
10. Schmidt A, et al. (2010) A bifunctional geranyl and geranylgeranyl diphosphate synthase is involved in terpene oleoresin formation in *Picea abies*. *Plant Physiol* 152(2):639–655.
11. Gilg AB, Bearfield JC, Tittiger C, Welch WH, Blomquist GJ (2005) Isolation and functional expression of an animal geranyl diphosphate synthase and its role in bark beetle pheromone biosynthesis. *Proc Natl Acad Sci USA* 102(28):9760–9765.
12. Blomquist GJ, et al. (2010) Pheromone production in bark beetles. *Insect Biochem Mol Biol* 40(10):699–712.
13. Lewis MJ, Prosser IM, Mohib A, Field LM (2008) Cloning and characterisation of a prenyltransferase from the aphid *Myzus persicae* with potential involvement in alarm pheromone biosynthesis. *Insect Mol Biol* 17(4):437–443.
14. Ma G-Y, Sun XF, Zhang YL, Li ZX, Shen ZR (2010) Molecular cloning and characterization of a prenyltransferase from the cotton aphid, *Aphis gossypii*. *Insect Biochem Mol Biol* 40(7):552–561.
15. Vandermoten S, et al. (2008) Characterization of a novel aphid prenyltransferase displaying dual geranyl/farnesyl diphosphate synthase activity. *FEBS Lett* 582(13): 1928–1934.
16. Vandermoten S, et al. (2009) Structural features conferring dual geranyl/farnesyl diphosphate synthase activity to an aphid prenyltransferase. *Insect Biochem Mol Biol* 39(10):707–716.
17. Zhang Y-L, Li Z-X (2012) Functional analysis and molecular docking identify two active short-chain prenyltransferases in the green peach aphid, *Myzus persicae*. *Arch Insect Biochem Physiol* 81(2):63–76.
18. Oldfield E, Lin FY (2012) Terpene biosynthesis: Modularity rules. *Angew Chem Int Ed Engl* 51(5):1124–1137.
19. Brandt W, et al. (2009) Molecular and structural basis of metabolic diversity mediated by prenyldiphosphate converting enzymes. *Phytochemistry* 70(15-16):1758–1775.
20. Aaron JA, Christianson DW (2010) Trinuclear metal clusters in catalysis by terpenoid synthases. *Pure Appl Chem* 82(8):1585–1597.
21. Pasteels JM, Braekman JC, Daloze D, Ottinger R (1982) Chemical defence in chrysomelid larvae and adults. *Tetrahedron* 38(13):1891–1897.
22. Termonia A, Hsiao TH, Pasteels JM, Milinkovitch MC (2001) Feeding specialization and host-derived chemical defense in Chrysomeline leaf beetles did not lead to an evolutionary dead end. *Proc Natl Acad Sci USA* 98(7):3909–3914.
23. Tarshis LC, Proteau PJ, Kellogg BA, Sacchettini JC, Poulter CD (1996) Regulation of product chain length by isoprenyl diphosphate synthases. *Proc Natl Acad Sci USA* 93(26):15018–15023.
24. von Heijne G (1990) The signal peptide. *J Membr Biol* 115(3):195–201.
25. Burse A, et al. (2008) Implication of HMGR in homeostasis of sequestered and *de novo* produced precursors of the iridoid biosynthesis in leaf beetle larvae. *Insect Biochem Mol Biol* 38(1):76–88.
26. Sen SE, Brown DC, Sperry AE, Hitchcock JR (2007) Prenyltransferase of larval and adult M. sexta corpora allata. *Insect Biochem Mol Biol* 37(1):29–40.
27. Sen SE, Sperry AE (2002) Partial purification of a farnesyl diphosphate synthase from whole-body Manduca sexta. *Insect Biochem Mol Biol* 32(8):889–899.
28. Kaneko Y, Kinjoh T, Kiuchi M, Hiruma K (2011) Stage-specific regulation of juvenile hormone biosynthesis by ecdysteroid in *Bombyx mori*. *Mol Cell Endocrinol* 335(2): 204–210.
29. Tholl D, Croteau R, Gershenzon J (2001) Partial purification and characterization of the short-chain prenyltransferases, geranyl diphosphate synthase and farnesyl diphosphate synthase, from Abies grandis (grand fir). *Arch Biochem Biophys* 386(2):233–242.
30. Sen SE, et al. (2007) Purification, properties and heteromeric association of type-1 and type-2 lepidopteran farnesyl diphosphate synthases. *Insect Biochem Mol Biol* 37(8): 819–828.
31. Tholl D, et al. (2004) Formation of monoterpenes in *Antirrhinum majus* and *Clarkia breweri* flowers involves heterodimeric geranyl diphosphate synthases. *Plant Cell* 16(4):977–992.
32. Sen SE, Trobaugh C, Béliveau C, Richard T, Cusson M (2007) Cloning, expression and characterization of a dipteran farnesyl diphosphate synthase. *Insect Biochem Mol Biol* 37(11):1198–1206.
33. Ohnuma S, Koyama T, Ogura K (1992) Chain length distribution of the products formed in solanesyl diphosphate synthase reaction. *J Biochem* 112(6):743–749.
34. Ohnuma S, Koyama T, Ogura K (1993) Alteration of the product specificities of prenyltransferases by metal ions. *Biochem Biophys Res Commun* 192(2):407–412.
35. Fujii H, et al. (1980) Variable product specificity of solanesyl pyrophosphate synthetase. *Biochem Biophys Res Commun* 96(4):1648–1653.
36. Chen AJ, Kroon PA, Poulter CD (1994) Isoprenyl diphosphate synthases: Protein sequence comparisons, a phylogenetic tree, and predictions of secondary structure. *Protein Sci* 3(4):600–607.
37. Szkopińska A, Plochocka D (2005) Farnesyl diphosphate synthase; regulation of product specificity. *Acta Biochim Pol* 52(1):45–55.
38. Heuts JPA, Schipper E, Piet P, German AL (1995) Molecular mechanics calculations on cobalt phthalocyanine dimers. *Theochem-J Mol Struct* 333(1-2):39–47.
39. Kobayashi M, Shimizu S (1999) Cobalt proteins. *Eur J Biochem* 261(1):1–9.
40. Okamoto S, Eltis LD (2011) The biological occurrence and trafficking of cobalt. *Metallomics* 3(10):963–970.
41. Conklin DS, McMaster JA, Culbertson MR, Kung C (1992) COT1, a gene involved in cobalt accumulation in Saccharomyces cerevisiae. *Mol Cell Biol* 12(9):3678–3688.
42. Bellés X, Martín D, Piulachs MD (2005) The mevalonate pathway and the synthesis of juvenile hormone in insects. *Annu Rev Entomol* 50:181–199.
43. Terenius O, et al. (2011) RNA interference in Lepidoptera: An overview of successful and unsuccessful studies and implications for experimental design. *J Insect Physiol* 57(2):231–245.

Supporting Information

Frick et al. 10.1073/pnas.1221489110

SI Materials and Methods

Beetle Rearing and Secretion Collection. *Phaedon cochleariae* (F.) was laboratory-reared as continuous cultures (York chamber, 15 °C and 16-h/8-h light/dark period) on leaves of *Brassica rapa* spp. Larval secretion was collected in glass capillaries (inner diameter = 0.28 mm, outer diameter = 0.78 mm, length = 100 mm; Hirschmann Laborgeraete, Eberstadt, Germany). Sealed capillaries containing samples were stored at −20 °C until needed. Secretions were weighed in the sealed capillaries on an ultramicrobalance (Mettler–Toledo) three times; the weight of empty capillaries was subtracted, and the final weight was averaged.

Isolation and Cloning of a cDNA encoding the *Phaedon cochleariae* isoprenyl diphosphate synthase 1 (*Pc*IDS1). Tissue samples from the head, gut, fat body, Malpighian tubules, and defensive glands were taken from third-instar larvae dissected in Ringer's solution (1) and directly transferred in liquid nitrogen-cooled reaction tubes. Total RNA was extracted with the RNeasy Micro Kit (Qiagen) according to the manufacturer's instructions. Complete removal of DNA was achieved using the RNase-free DNase Set (Qiagen). The quality of the RNA was evaluated by measuring the 260:280-nm absorbance ratio, and the integrity of 18S and 28S ribosomal RNA bands was assessed by electrophoresis on RNA 6000 Nano labchips (Agilent Technologies). RNA concentrations were determined from absorbance values at a wavelength of 260 nm. First-strand cDNA was subsequently transcribed from total RNA using SuperScript III reverse transcriptase (Life Technologies). Up to 1 μg of total RNA was reverse-transcribed according to the manufacturer's instructions using oligo(dT)$_{12–18}$ primer. Degenerated primers were designed against the highly conserved regions of previously identified short-chain isoprenyl diphosphate synthases (scIDSs) from *Myzus persicae*, *Aphis gossypii*, *Agrotis ipsilon*, and *Anthonomus grandis*. PCR amplification using Taq DNA Polymerase (Promega) of a 686-bp core fragment was performed with the primer pair FWD_211_geranyl diphosphate synthase (GDPS) (5′-TTC ATG G(AC)(ACT)(GT)(GT)(GC)TTCCC(AGC)GA-3′) and REV_903_GDPS (5′-GAAGTCAT(CT)(CT)TGA(AC)(CT)TTG-3′). The following cycling profile was carried out in an Eppendorf thermal cycler: 3 min at 94 °C; 35 cycles of 30 s at 94 °C, 30 s at 45 °C, and 1 min at 72 °C; and a final 10-min extension at 72 °C. PCR products were purified using QiaEx II (Qiagen), ligated into pCR2.1-TOPO vector (Life Technologies), and sequenced. To obtain full-length cDNA sequence of *P. cochleariae* isoprenyl diphosphate synthase (IDS), a BD SMART RACE cDNA Amplification Kit (BD Biosciences) was used. For amplification of the 5′-end, site sequence-specific reverse primers were designed as followed: RACE_5_214_Rev (5′-CCCTAGGATGCCGGCCAATCTCACG-3′) and nested primer RACE_5_140_Rev (5′-GTGGACAGGCCCCTGGTCTTCTTGC-3′). The sequence-specific primers for the 3′-end site were RACE_3_447_FWD (5′-GACCAACATGGGCCAATCTTTAGACGC-3′) and nested primer RACE_3_483_FWD (5′-GAAGGATGGGAGGCCCATATTGAGCC-3′). The 5′ and 3′ RACE products were cloned and sequenced. The resulting assembled cDNA sequence contained a 1,290-bp open-reading frame that encodes an IDS similar protein of 430 aa referred to here as *P. cochleariae* isoprenyl diphosphate synthase 1 (*Pc*IDS1). This sequence of *Pc*IDS1was registered at GenBank (accession no. KC109782).

Functional Expression and Purification of Recombinant *Pc*IDS1. The entire encoding sequence of *Pc*IDS1 lacking the predicted signal peptide (based on analysis with SignalP 4.1 (2), available at the prediction servers of the Center for Biological Sequence Analysis, Technical University of Denmark, Lyngby, Denmark) was amplified with the following primers that included the start and stop codons for translation in an *Escherichia coli*-based heterologous expression system: *Pc*IDS1-forward (5′-CACCAGGGCCCTCTCCACGATC-3′) and *Pc*IDS1-reverse (5′-CTATGCATCCCTCTTGTAAATCTTCTT-3′). Template cDNA was synthesized by RT from RNA of whole-body *P. cochleariae* larvae, except for the gut tissue. PCR was performed using an Expand High Fidelity PCR system (Roche Applied Science). PCR was performed for 3 min at 94 °C for denaturation, followed by 10 cycles of 15 s at 94 °C, 30 s at 55 °C, and 90 s at 72 °C; 20 cycles of 15 s at 94 °C, 30 s at 55 °C, and 90 s plus 5 s of elongation for each cycle at 72 °C; and a final extension for 7 min at 72 °C. The resulting cDNA fragment was purified with the Zymoclean Gel DNA Recovery Kit (Zymo) and cloned in the expression vector pET100/D-TOPO (Invitrogen), which has a 6 × His-tag on the N terminus. Plasmids were transferred into the strain *E. coli* TOP10F (Life Technologies) and sequenced. Positive constructs were then transferred into different expression strains, including BL21(DE3) star (Invitrogen), BL21(DE3) pLysS (Life Technologies), and Rosetta (DE3; Novagen), but strain BL21(DE3) star produced the highest amount of soluble and active protein of long and short *Pc*IDS1. Bacterial precultures of 20 mL were grown over 3 d at 18 °C under continuous rotation on LB with 50 μg/mL carbenicillin. Afterward, the cells were pelleted and used to inoculate the 200-mL expression culture. There, we used the Overnight Express Autoinduction System 1 (Novagen) and let them grow over 2 d at 18 °C under continuous rotation to stationary phase according to the manufacturer's recommendations. Bacterial pellets were resuspended in 2 mL of assay buffer containing 25 mM 3-(*N*-morpholino)-2-hydroxypropanesulfonic acid (MOPSO; pH 7.3), 10% (vol/vol) glycerol, and 150 mM NaCl. The suspension was sonicated using a Sonopuls HD2070 (Bandelin) for 4 min, cycle 2, at 60% power. The overexpressed His-tagged proteins were subsequently column-purified by affinity chromatography with Ni-nitrilotriacetic acid agarose columns (Qiagen) using a stepwise imidazole gradient from 10 to 500 mM. The purity of the recombinant proteins was evaluated by SDS/PAGE gel electrophoresis, followed by colloidal Coomassie staining (Roti-Blue Colloidal Coomassie Staining; Carl Roth). The purified *Pc*IDS1 migrated at ∼45.8 kDa (399 aa). Fractions that contained the highest amount of pure recombinant protein were pooled and desalted in assay buffer with a PD-10 Desalting column (Amersham Biosciences) to remove the imidazole.

To see if the affinity tag influenced the enzyme activity, the fusion protein *Pc*IDS1 was subsequently cleaved using the highly specific serine protease EnterokinaseMax (Life Technologies) according to the manufacturer's instructions. After purification and removal of the affinity tag, cleavage was checked by SDS/PAGE and Western blotting using the anti-His antibody. The fusion protein and the cleaved protein were tested for their enzyme activity. Because cleavage of the tag altered neither the activity nor the product profile, the truncated His-tagged fusion protein *Pc*IDS1 was used in all following experiments.

To determine the conformational state of the *Pc*IDS1 quaternary structure, size exclusion chromatography was performed. The protein was added to running buffer [25 mM MOPSO (pH 7.3), 10% (vol/vol) glycerol, and 150 mM NaCl] in the presence of either 5 mM $MgCl_2$ or 0.5 mM $CoCl_2$ and incubated for 10

min at 4 °C. To confirm the overall conformation of the protein with the different metal cofactors, an aliquot of each solution was separated on a SuperdexHiLoad 16/60 200 prep grade (GE Healthcare) column at a flow rate of 1 mL/min. The retention volume of *Pc*IDS1 was detected via its absorption at 280 nm. To calibrated the column, we used cytochrome *c* from horse heart (12.4 kDa), carbonic anhydrase from bovine erythrocytes (29 kDa), BSA (66 kDa), alcohol dehydrogenase from yeast (150 kDa), and β-amylase from sweet potato (200 kDa) in the presence of 10 mM $CoCl_2$ or 10 mM $MgCl_2$. The molecular weight for *Pc*IDS1 was calculated by the formula received from the corresponding standard curve. Without cofactor, $y = -27.133x + 128.38$ ($R^2 = 0.9925$); with Co^{2+}, $y = -27.133x + 128.21$ ($R^2 = 0.9927$); and with Mg^{2+}, $y = -27.122x + 128.26$ ($R^2 = 0.9921$).

Prenyltransferase Assay and Product Distribution Analyses. For kinetic analyses, enzyme assays of *Pc*IDS1 were carried out in a final volume of 200 μL containing 25 mM MOPSO (pH 7.3), 10% (vol/vol) glycerol, 150 mM NaCl, and 5 mM Mg^{2+} or 1 mM Co^{2+}, respectively. As substrates and countersubstrates, isopentenyl diphosphate (IDP), dimethylallyl diphosphate, and geranyl diphosphate (GDP; Sigma–Aldrich) were used. The countersubstrate concentration was kept constant at 50 μM; different experimental conditions are mentioned separately. The analyzed substrate ranged from 0.1 μM up to 100 μM. The reaction was heated to 30 °C and initiated by adding 0.2 μg of protein for Co^{2+} assays or 2 μg of protein for Mg^{2+} assays of the recombinant protein, and it was then incubated further at 30 °C. The water phase was analyzed by direct injection of 1 μL into the HPLC system at different time points from the same reaction mixture to identify the linear reaction velocity for every parameter. Calculation of the kinetic parameters was performed with GraphPad Prism version 5.04 (GraphPad Software) using the built-in enzyme kinetics module.

The pH optimum for the catalytic activity of *Pc*IDS1 was determined to be 7.0–7.5 in the presence of Mg^{2+} or Co^{2+}. However, the enzyme activity was quite stable over a broad range, from pH 4 to pH 8. Even the temperature optimum was not delimited to a narrow range. Acceptable activity with Mg^{2+} or Co^{2+} was measured from 15 °C up to 45 °C, whereas the optimum resided at 28 °C to 32 °C.

Activity testing of purified full-length *Pc*IDS1 in the presence of Mg^{2+} or Co^{2+} showed only about 5% of the activity in both cases in comparison to its truncated form, which lacks the predicted signal sequence.

For enzyme assay from larvae material, the samples were obtained by macerating different tissues with a 2-mL Potter–Elvehjem grinder with a Teflon pestle for 2 min at 4 °C with 300 μL of assay buffer. The suspension was centrifuged at 20,000 × *g*, and the protein concentration of the supernatant was determined. Ten micrograms of protein was used for standard assays and incubated at 30 °C for 60 min. The assays were stopped by adding 500 μL of chloroform and by mixing for 20 s, followed by centrifugation for 5 min at 5,000 × *g*. Subsequently, the water phase was transferred to a glass vial and measured directly by injecting 1 μL into the HPLC system. Protein concentrations were measured according to Bradford and Williams (3) and Bradford (4), using the Coomassie Plus Protein Assay Kit (Thermo Scientific Pierce) with BSA as a standard.

Liquid Chromatography-Tandem MS Method for *Pc*IDS1 Assay Product Determination. Analysis of isoprenoid diphosphates (IDS) was performed according to a modified method (5) on an Agilent 1260 HPLC system (Agilent Technologies) coupled to an API 5000 triple-quadrupole mass spectrometer (AB Sciex Instruments). For separation, a ZORBAX Extended C-18 column (1.8 μm, 50 mm × 4.6 mm; Agilent Technologies) was used. The mobile phase consisted of 5 mM ammonium bicarbonate in water as solvent A and acetonitrile as solvent B, with the flow rate set at 1.2 mL/min and the column temperature kept at 20 °C. Separation was achieved by using a gradient starting at 0% B, increasing to 90% B in 3 min and 100% B in 3.1 min (1-min hold), followed by a change to 0% B in 0.5 min (2.5-min hold) before the next injection. The injection volume for samples and standards [GDP and farnesyl diphosphate (FDP) from Sigma–Aldrich] was 1 μL; autosampler temperature was either 30 °C for assays without or 4 °C for assays with chloroform extraction. The mass spectrometer was used in the negative electrospray ionization (EI) mode. Optimal settings were determined using standards. Levels of ion source gases 1 and 2 were set at 60 and 70 psi, respectively, with a temperature of 700 °C. Curtain gas was set at 30 psi and collision gas was set at 7 psi, with all gases being nitrogen. Ion spray voltage was maintained at −4,200 V. Multiple-reaction monitoring (MRM) was used to monitor analyte parent ion-to-product ion formation: *m/z* 312.9/79 for GDP and *m/z* 380.9/79 for (*E,E*)-FDP. *Cisoid* products like neryl-diphosphate, (*Z,E*)-FDP, or (*Z,Z*)-FDP were not detected. Detection of GDP was omitted when used as substrate. Data analysis was performed using Analyst Software 1.6 Build 3773 (AB Sciex).

***Pc*IDS1 Antibody Production and Immunoblot Analysis.** For synthesis of polyclonal antibodies, a 16-aa peptide (HDLFFKIMKKIY-KRDA) from the N-terminal end of the protein was used. The antibody was affinity-purified with 3 mg epoxy-immobilized antigen that was used for immunization (Davids Biotechnologie).

For immunoblot analysis, crude protein from different larval tissue was extracted in assay buffer as described above. Equal amounts of 5 μg of total protein of each tissue were separated by SDS/PAGE using any-KD acrylamide gels (BIO-RAD). Afterward, the proteins were transferred electrophoretically onto nitrocellulose membranes (BIO-RAD). Membranes were blocked with TBST [20 mM Tris (pH 7.5), 150 mM NaCl, 0.1% (vol/vol) Tween 20] and 10% nonfat milk, followed by incubation with 1:100 of the polyclonal anti-*Pc*IDS1 antibody at 16 °C overnight. After washing with blocking solution and a subsequent incubation with anti-rabbit HRP-conjugated secondary antibody, a final TBST washing was carried out. Signal detection was achieved by enhanced chemiluminescence (Thermo Scientific) and Amersham Hyperfilm ECL (GE Healthcare).

Sequence Comparison and Homology Modeling. Sequence similarity searches were performed using the alignment tool BLAST (6). Nucleotide sequences of different organisms were downloaded from the National Center for Biotechnology Information. To determine the degree of similarity between the members of insect scIDS and full-length *Pc*IDS1, sequence analysis was performed using the ClustalW tool (Lasergene 10 Core Suite; DNASTAR).

The 3D structure of truncated *Pc*IDS1 was modeled using the molecular modeling software YASARA (7). YASARA identified 15 templates based on alignment scores and low E-values suitable for homology modeling. Altogether, 32 models were automatically created and subsequently refined. The model based on the X-ray structure of FDP synthase from *Homo sapiens* deposited in the protein database (1zw5; see www.rcsb.org) (8, 9) appeared to be the most useful one. The structure of the model of *Pc*IDS1 has been deposited at the Protein Model DataBase (http://mi.caspur.it/PMDB/main.php) (10) and has been assigned the ID code PM0078683 for free download. The Mg^{2+} and the ligand binding position of IDP were automatically imported from the template's X-ray structure. The artificial cocrystallized zoledronic acid, [1-hydroxy-2-(1H-imidazol-1-yl)ethane-1,1-diyl]bis(phosphonic acid), was manually replaced by GDP. This model was then refined with the md-refinement tool of YASARA (7). The quality of the final model was checked with PROSA II (11) and PROCHECK (12). The graphical analysis with PROSA II showed one small loop (10 aa) area in positive energy range out-

side the active site. A combined energy z-score of −9.83 clearly indicated a native-like folded structure. Analysis of the calculated model with PROCHECK evaluated the consistency of all stereochemical parameters, such as the Ramachandran plot quality (92.3% of the backbone dihedral angles in most favored areas).

To investigate influences by the replacement of Mg^{2+} with Co^{2+}, the TRIPOS force field was used first (13). Thus, the atom types of Mg^{2+} were modified to Co^{2+}, and short molecular dynamics simulations (10 ps, 300 K) with subsequent energy minimization of GDP in the active site were performed. The Co^{2+} and the interacting side chains of all remaining amino acids except this ligand were kept fixed because the TRIPOS force field is not suitable for protein structure refinement. To estimate the interaction energies of different ions with the diphosphate moiety and aspartate side chains, density functional theory (DFT) B3LYP 6-311G++ calculations were performed using Gaussian 03 (14).

Tissue-Specific Expression of *Pc*IDS1. Quantitative real-time PCR was used for relative quantification (15). cDNA was synthesized from DNA-digested RNA and purified from three larvae per biological replicate using the RNAqueous Micro Kit (Life Technologies). Three biological replicates were analyzed twice. If technical replicates had a difference in the quantification cycle value greater than 1, the assay was repeated. Reference genes [*Pc*RPL8 (EMBL: AFQ22729.1) and *Pc*RPS3 (GenBank: KC109783)] were chosen. Real-time PCR data were acquired on an Mx3000P Real-Time PCR system (Agilent) using Brilliant III SYBR Green qPCR Master Mix (Agilent) according to the manufacturer's instructions. These analyses were performed following the minimum information for publication of quantitative real-time PCR experiments guidelines (16, 17).

RNAi in *P. cochleariae* Larvae. dsRNA was synthesized using the Megascript RNAi kit (Life Technologies) with altering of the elution buffer to 3.5 mM Tris·HCl, 1 mM NaCl, 50 nM Na_2HPO_4, 20 nM KH_2PO_4, 3 mM KCl, and 0.3 mM EDTA (pH 7.0). Off-target prediction was performed for highly specific silencing according to Bodemann et al. (18). The ORFs of full-length *PcIDS1* and *Gfp* were analyzed for off-target prediction by dicing the sequences *in silico* (19) and using the resulting putative 21-nt siRNAs for a BLASTn search linked to our transcriptome database of *P. cochleariae*. No putative off-target effects with other transcripts are predicted with the chosen dsRNA sequences on a critical value of at least 20 continuous nucleotides that have to be identical. The dsRNA synthesis templates with opposite T7-promotor sites were amplified out of sequenced plasmid pIB/V5-His (Life Technologies) containing full-length *PcIDS1* for 850 bp of *PcIDS1* using IDS1_FWD_T7_RNA (5′-TAATACGACTCACTATAGGGAGATCAAGCCAGTCTCCT-3′) as forward primer and IDS1_REV_T7_RNA (5′-TAATACGACTCACTATAGGGAGACTAAGCATCCCTCTTG-3′) as reverse primer and pCR3.1/CT-GFP-TOPO (Life Technologies) for 720 bp of *Gfp* (for primer, see ref. 18), respectively. The concentration of dsRNA was adjusted to 2 μg/μL, and for all injections, 250 nL (500 ng) of dsRNA solution was used.

Late first-instar larvae of *P. cochleariae* were used for injections. These were collected 5 d after hatching and were put in an incubator set to 16 h of light at 14 °C and 8 h of darkness at 12 °C for slow larval development after treatment. A Nano2000 injector (WPI) on a three-axis micromanipulator was used for injecting ice-chilled larvae parasagittal between the pro- and mesothorax.

Relative Quantification of 8-Hydroxygeraniol-Glucoside in *P. cochleariae* Fat Body and Hemolymph. Analysis was done on an Agilent 1260 HPLC system (Agilent Technologies) coupled to an API 5000 triple-quadrupole mass spectrometer (AB Sciex Instruments). For separation, a ZORBAX Eclipse XDB-C-18 column (1.8 μm, 50 mm × 4.6 mm; Agilent Technologies) was used. The mobile phase consisted of 20 mM ammonium formate in water as solvent A and acetonitrile as solvent B, with the flow rate set at 1.0 mL/min and the column temperature kept at 20 °C. Separation was achieved by using a gradient starting at 10% solvent B, increasing to 95% solvent B in 5 min (1-min hold), followed by a change to 10% solvent B in 1 min (1-min hold) before the next injection. Injection volume for samples and standards was 5 μL; the autosampler temperature was 4 °C. The mass spectrometer was used in negative EI mode. Optimal settings were determined using a standard. Ion source gases 1 and 2 were set at 70 psi, with a temperature of 700 °C. Curtain gas was set at 25 psi and collision gas was set at 6 psi, with all gases being nitrogen. Ion spray voltage was maintained at −3000 V. The monitored MRM transition was *m/z* 377.3/331.2. Data analysis was performed using Analyst Software 1.6 Build 3773 (AB Sciex).

Relative Quantification of Chrysomelidial in Defense Secretions of *P. cochleariae*. Secretions were collected and weighed in pulled-out glass capillaries from different instar stages of treated larvae, and they were then diluted 1:200 (wt/vol) in ethyl acetate supplemented with 100 μg/mL methyl benzoate as an internal standard. One microliter was subjected to GC-EI-MS analysis [ThermoQuest Finnigan ITQ GC-MS 2000 (quadrupole) equipped with Phenomenex ZB-5-W/Guardian-column, 25 m (10-m Guardian precolumn) × 0.25 mm, film thickness of 0.25 μm]. Substances were separated splitless using helium as a carrier (1.5 mL/min). Conditions were set as follows: 50 °C (2 min), 20 °C/min to 130 °C, 40 °C/min to 200 °C, 20 °C/min to 220 °C, and 40 °C/min to 300 °C (1 min). Inlet temperature was 220 °C, and transfer line temperature was 280 °C. Chrysomelidial was identified according to Oldham et al. (20). The peak areas were obtained using the Interactive Chemical Information System algorithm that is implemented in the Xcalibur bundle (version 2.0.7; Thermo Scientific). The relative amount of chrysomelidial per larva has been calculated with the following equation, in which *mChry* is the relative amount of chrysomelidial per larva, *AoChry* is the peak area of chrysomelidial, *AoMB* is the peak area of methyl benzoate, and *mSec* is the average mass of secretion per larva:

$$mChry = \left(\frac{AoChry}{AoMB} * dilution\right) * mSec.$$

Fitness Measurements. The development of larval weight was documented using five replicates of three larvae. Larval weight was measured per replicate on an ultramicrobalance in a 24-h ± 3-h period. In accordance with the method used by Kuehnle and Mueller (21), the relative growth rate was calculated using the weight of freshly emerged pupae as the final larval developmental stage.

1. Discher S, et al. (2009) A versatile transport network for sequestering and excreting plant glycosides in leaf beetles provides an evolutionary flexible defense strategy. *ChemBioChem* 10(13):2223–2229.
2. Petersen TN, Brunak S, von Heijne G, Nielsen H (2011) SignalP 4.0: Discriminating signal peptides from transmembrane regions. *Nat Methods* 8(10):785–786.
3. Bradford MM, Williams WL (1976) New, rapid, sensitive method for protein determination. *Fed Proc* 35(3):274.
4. Bradford MM (1976) A rapid and sensitive method for the quantitation of microgram quantities of protein utilizing the principle of protein-dye binding. *Anal Biochem* 72(1-2):248–254.
5. Nagel R, Gershenzon J, Schmidt A (2012) Nonradioactive assay for detecting isoprenyl diphosphate synthase activity in crude plant extracts using liquid chromatography coupled with tandem mass spectrometry. *Anal Biochem* 422(1):33–38.

6. Altschul SF, Lipman DJ (1990) Protein database searches for multiple alignments. *Proc Natl Acad Sci USA* 87(14):5509–5513.
7. Krieger E, et al. (2009) Improving physical realism, stereochemistry, and side-chain accuracy in homology modeling: Four approaches that performed well in CASP8. *Proteins* 77(Suppl 9):114–122.
8. Kavanagh KL, Dunford JE, Bunkoczi G, Russell RG, Oppermann U (2006) The crystal structure of human geranylgeranyl pyrophosphate synthase reveals a novel hexameric arrangement and inhibitory product binding. *J Biol Chem* 281(31):22004–22012.
9. Kavanagh KL, et al. (2006) The molecular mechanism of nitrogen-containing bisphosphonates as antiosteoporosis drugs. *Proc Natl Acad Sci USA* 103(20): 7829–7834.
10. Castrignanò T, De Meo PD, Cozzetto D, Talamo IG, Tramontano A (2006) The PMDB Protein Model Database. *Nucleic Acids Res* 34:D306–D309.
11. Sippl MJ (1990) Calculation of conformational ensembles from potentials of mean force. An approach to the knowledge-based prediction of local structures in globular proteins. *J Mol Biol* 213(4):859–883.
12. Laskowski RA, MacArthur MW, Moss DS, Thornton JM (1993) PROCHECK—A program to check the stereochemical quality of protein structures. *J Appl Cryst* 26(2):283–291.
13. Clark M, Cramer RD, Van Opdenbosch N (1989) Validation of the General Purpose Tripos 5.2 Force Field. *J Comp Chem* 10(8):982–1012.
14. Frisch MJ, et al. (2004) Gaussian 03, Revision C.02. (Gaussian, Wallingford CT).
15. Livak KJ, Schmittgen TD (2001) Analysis of relative gene expression data using real-time quantitative PCR and the $2^{(-\Delta\Delta C(T))}$ Method. *Methods* 25(4):402–408.
16. Bustin SA, et al. (2010) MIQE précis: Practical implementation of minimum standard guidelines for fluorescence-based quantitative real-time PCR experiments. *BMC Mol Biol* 11:74–78.
17. Bustin SA, Johnson G, Agrawal SG (2012) [MIQE—Guidelines for developing robust real-time PCR assays]. *Mycoses* 55(Suppl 2):30–34. German.
18. Bodemann RR, et al. (2012) Precise RNAi-mediated silencing of metabolically active proteins in the defence secretions of juvenile leaf beetles. *Proc Biol Sci* 279(1745):4126–4134.
19. Naito Y, et al. (2005) dsCheck: Highly sensitive off-target search software for double-stranded RNA-mediated RNA interference. *Nucleic Acids Res* 33(Web Server issue): W589-91.
20. Oldham NJ, Veith M, Boland W, Dettner K (1996) Iridoid monoterpene biosynthesis in insects—Evidence for a *de novo* pathway occurring in the defensive glands of *Phaedon armoraciae* (Chrysomelidae) leaf beetle larvae. *Naturwissenschaften* 83(10): 470–473.
21. Kuehnle A, Mueller C (2011) Responses of an oligophagous beetle species to rearing for several generations on alternative host-plant species. *Ecol Entomol* 36(2):125–134.

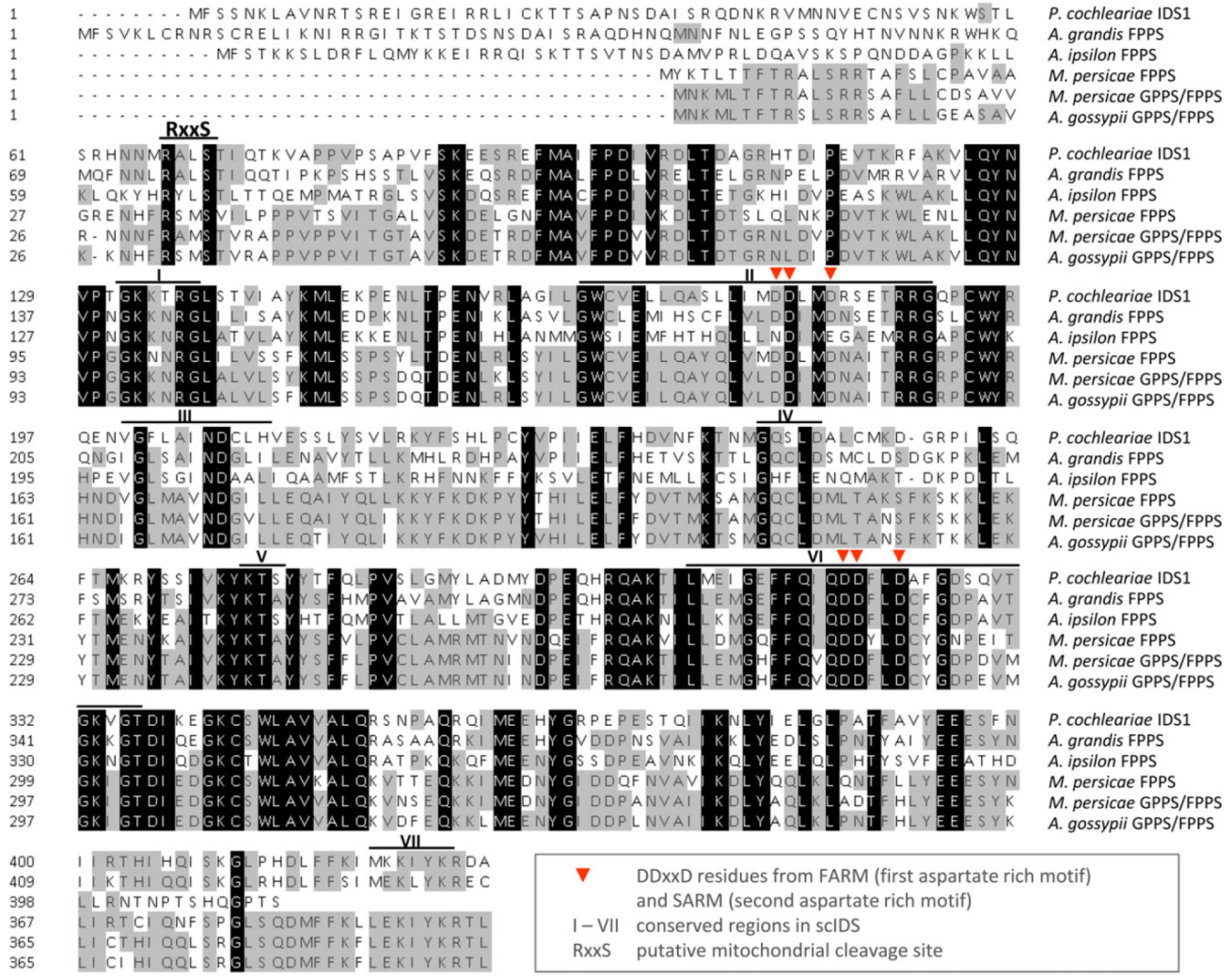

Fig. S1. Amino acid alignment (ClustalW) of full-length *Pc*IDS1 from *P. cochleariae* with other insect scIDSs. Sequence identity to other farnesyl diphosphate synthases (FDPSs): *Anthonomus grandis* (54.1%) (GenBank: AAX78434), *Myzus persicae* (45.4%) (GenBank: ABY19313), and *Agrotis ipsilon* (45.2%) (GenBank CAA08918). Sequence identity to bifunctional FDPSs/GDPSs: *Aphis gossypii* (48.6%) (EMBL: ACT79808) and *M. persicae* (48.4%) (EMBL: ABY19312). (Residues in black are identical in all sequences; gray residues are >50% identical in aligned sequences.)

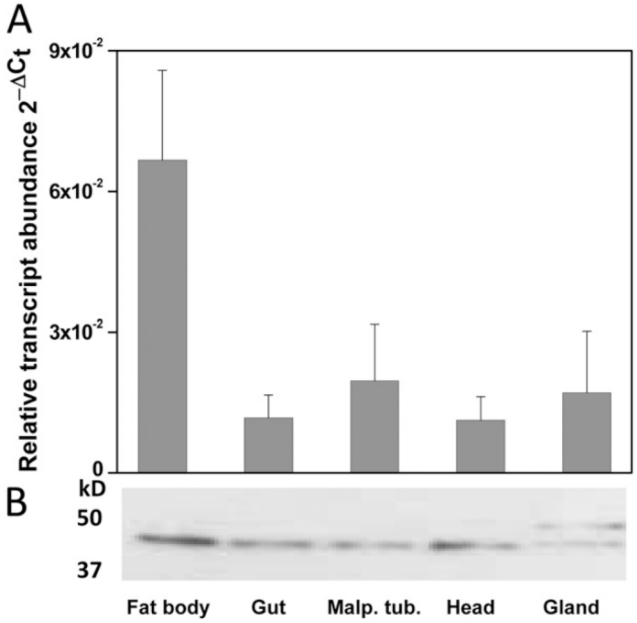

Fig. S2. (*A*) Relative transcript abundance ($2^{\Delta Ct}$) of *PcIDS1* in different larval tissues. (*B*) Western blot analyses of 5 μg of protein per lane probed with sequence-specific antibodies against *Pc*IDS1, followed by ECL detection. Malp. tub, Malpighian tubules.

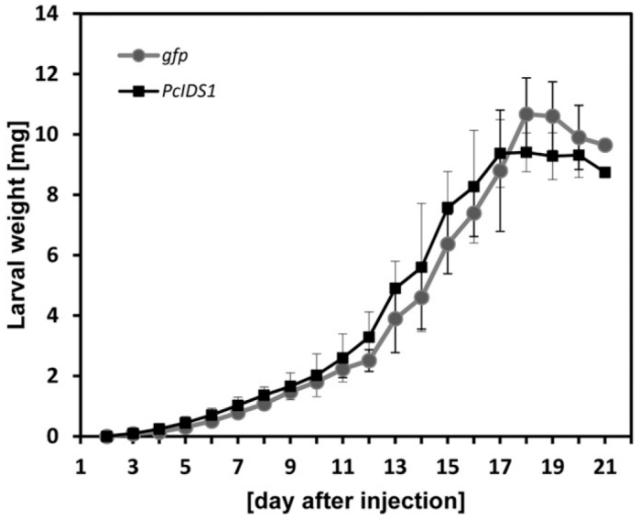

Fig. S3. Relative growth rate of RNAi-induced larvae from *P. cochleariae*. The development of larval weight was documented and measured in a 24-h ± 3-h period. No significant differences in the relative growth rate were observed between *Gfp*- and *PcIDS1*-injected larvae. The final larval developmental stage was the weight of freshly emerged pupae (n = 15, ±SD).

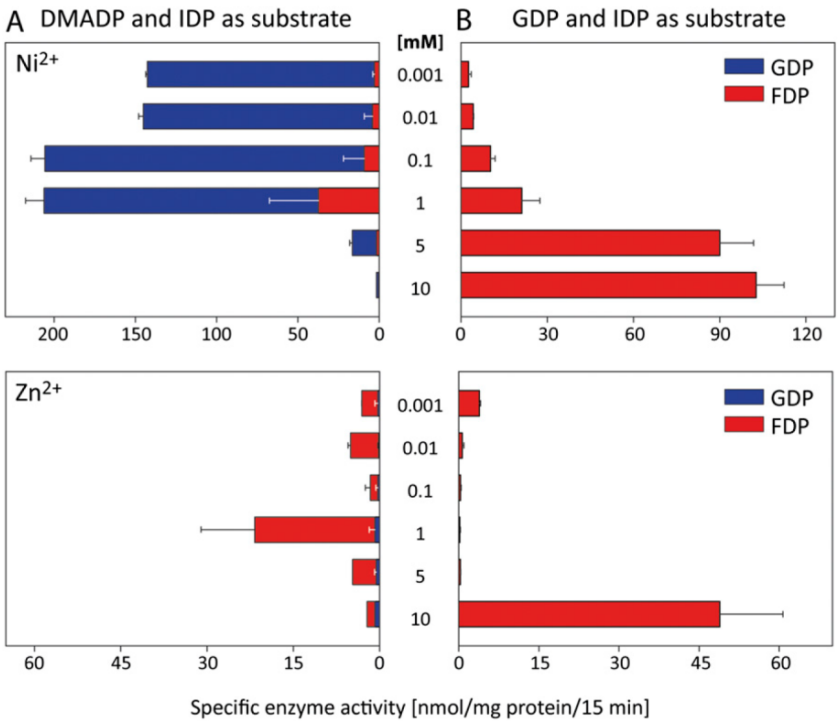

Fig. S4. Effect of metal cofactors regarding product formation and enzyme activity of *Pc*IDS1. (*A*) Different concentrations of Ni^{2+} and Zn^{2+} were added to *Pc*IDS1 and incubated with 50 μM IDP and 50 μM dimethylallyl diphosphate (DMADP; $n = 3$, ±SD). (*B*) Different concentrations of Ni^{2+} and Zn^{2+} were added to *Pc*IDS1 and incubated with 50 μM IDP and 50 μM GDP ($n = 3$, ±SD).

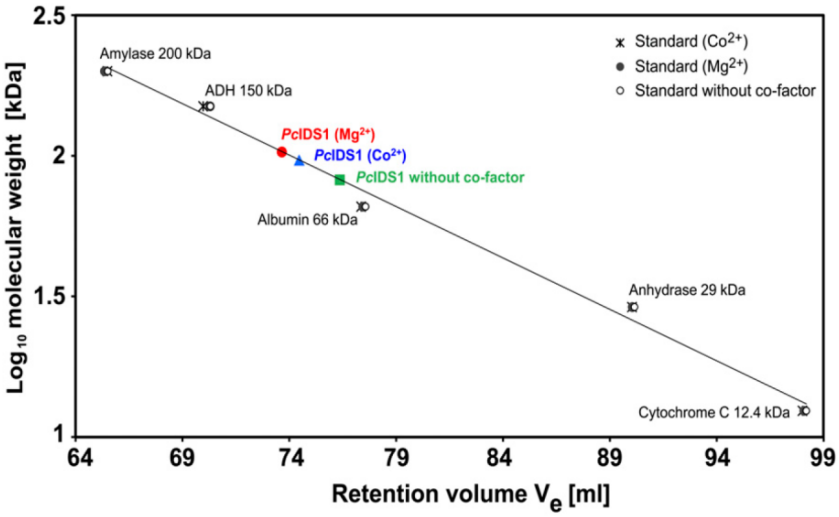

	Elution volume			MW log10			calc. MW (kDa)		
	No co-factor	Co^{2+}	Mg^{2+}	No co-factor	Co^{2+}	Mg^{2+}	No co-factor	Co^{2+}	Mg^{2+}
*Pc*IDS1	76.3	74.4	73.6	1.91	1.98	2.01	74.6	87.6	93.8
Amylase	65.5	65.4	65.3	2.31	2.31	2.31	207.5	204.9	208.5
ADH	70.3	69.9	70.2	2.14	2.14	2.13	138.1	140.1	137.2
Albumin	77.5	77.3	77.4	1.87	1.87	1.87	74.5	74.8	74.7
Anhydrase	90.1	90.0	90.0	1.40	1.40	1.40	25.6	25.5	25.6
Cytochrome C	98.1	98.0	98.0	1.11	1.11	1.11	12.9	12.9	12.9

Fig. S5. Analytical size exclusion chromatography of *Pc*IDS1. The plot shows the relative retention volumes of the protein molecular weight standards and the calculated standard curve by linear regression dependent on the divalent ions. The relative retention volumes of the apoprotein *Pc*IDS1 are shown by the green rectangle. The shifts of the retention volume dependent on the divalent metal cofactor are represented by the red dot in the presence of Mg^{2+} and the blue triangle in the presence of Co^{2+}.

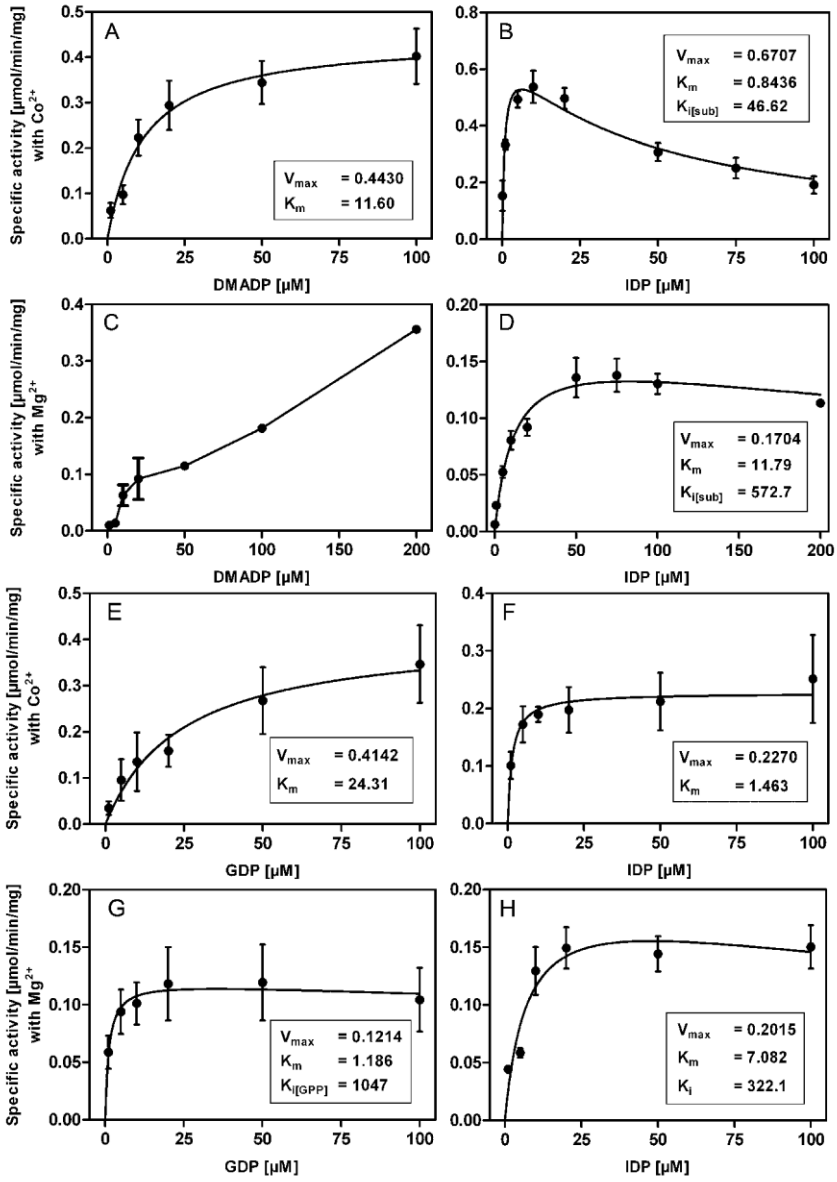

Fig. S6. Kinetic analyses of *Pc*IDS1 with nonlinear regression and built-in function calculated with GraphPad Prism version 5.04. (*A*) Calculation according to the Michaelis–Menten kinetic of $K_{m(DMADP)}$ with Co^{2+} and 15 µM IDP. (*B*) Calculation with substrate inhibition of $K_{m(IDP)}$ with Co^{2+} and 50 µM dimethylallyl diphosphate (DMADP). (*C*) Enzyme activity data with variable DMADP in the presence of Mg^{2+} and 50 µM IDP. (*D*) Calculation with substrate inhibition of $K_{m(IDP)}$with Mg^{2+} and 50 µM DMADP. (*E*) Calculation according to the Michaelis–Menten kinetic of $K_{m(GDP)}$ with Co^{2+} and 50 µM IDP as countersubstrate. (*F*) Calculation according to the Michaelis–Menten kinetic of $K_{m(IDP)}$ with Co^{2+} and 50 µM GDP as countersubstrate. (*G*) Calculation with substrate inhibition of $K_{m(GDP)}$ with Mg^{2+} and 50 µM IDP as countersubstrate. (*H*) Calculation with substrate inhibition of $K_{m(IDP)}$ with Mg^{2+} and 50 µM GDP as countersubstrate.

Table S1. Enzyme activity of *Pc*IDS1 with different metal cofactors

Substrate	Ion	Optimal cofactor concentration, mM	Total activity, nmol/mg of protein per 15 min (±SD)	GDP activity, % of total activity
DMADP	Co^{2+}	0.5	1,022.33 (±72.2)	95.9
	Mg^{2+}	5	418.85 (±6.2)	18.3
	Mn^{2+}	0.5	239.66 (±16.2)	98.8
	Ni^{2+}	0.1	206.8 (±41.3)	81.9
	Zn^{2+}	0.1	21.69 (±24.1)	96.3
GDP	Co^{2+}	0.01	333.56 (±48.13)	
	Mg^{2+}	0.5	967.25 (±136.4)	
	Mn^{2+}	0.01	785.07 (±136.5)	
	Ni^{2+}	0.001	102.68 (±9.6)	
	Zn^{2+}	0.001	48.90 (±11.8)	

DMADP, dimethylallyl diphosphate.

Table S2. ICP-OES and ICP-MS analyses of fat body and gut tissue of *P. cochleariae* larvae

		Fat body 1		Fat body 2		Gut	
Element	Method	DW, µg/g (±SD)	DW, µmol/g	DW, µg/g (±SD)	DW, µmol/g	DW, µg/g (±SD)	DW, µmol/g
Ca	ICP-OES	753.2 (±0.3)	18.7	788 (±16)	19.6	893 (±12)	22.2
Co	ICP-MS	0.243 (±0.005)	0.0041	0.198 (±0.005)	0.0033	0.297 (±0.001)	0.005
Cu	ICP-MS	14.09 (±0.07)	0.221	14.9 (±0.2)	0.234	12.88 (±0.03)	0.203
Fe	ICP-MS	41.7 (±0.1)	0.746	41.8 (±0.5)	0.748	92.6 (±0.04)	1.658
K	ICP-OES	12,075 (±274)	308.8	12,112 (±71)	309.8	18,299 (±4)	468
Mg	ICP-OES	2,223 (±41)	91.4	2,255.5 (±0.5)	92.8	2,205.2 (±0.4)	90.7
Mn	ICP-MS	16.51 (±0.04)	0.301	16.706 (±0.002)	0.304	47.3 (±0.4)	0.861
Na	ICP-OES	462 (±11)	20.1	463 (±5)	20.1	499.2 (±0.4)	21.7
Ni	ICP-MS	0.36 (±0.01)	0.0061	0.3598 (±0.0007)	0.0061	0.88 (±0.08)	0.0149
Zn	ICP-MS	62.3 (±0.3)	0.952	62.66 (±0.02)	0.958	141.1 (±0.03)	2.158

DW, dry weight; ICP-MS, inductively coupled plasma mass spectrometry; ICP-OES, inductively coupled plasma optical emission spectrometry.

Table S3. Energies of the compounds and resulting reaction energies for the formation of diphosphate metal complexes in kilocalories per mole calculated with density functional theory (DFT) B3LYP 6-311G++ (d.p)

	Products energy	Educts energy			
X	X-DP^{3-}	X	DP^{3-}	Reaction energy	Δ to Mg^{2+}
Mg^{2+}	−885,175.2	−125,023.7	−759,218.5	−933.0	0
Co^{2+}	−16,277,257.6	−867,059.6	−759,218.5	−979.6	−46.6
Mn^{2+}	−1,481,820.2	−721,619.3	−759,218.5	−982.4	−49.4

X, metal cation.

Table S4. Energies of the compounds and resulting reaction energies for the formation of propionic acid metal complexes in kilocalories per mole calculated with DFT B3LYP 6-311G++ (d.p)

	Products energy	Educts energy			
X	$X(CH_3CH_2COO^-)_2$	X	$(CH_3CH_2COO^-)_2$	Reaction energy	Δ to Mg^{2+}
Mg^{2+}	−461,861.2	−125,023.7	−336,166.4	−671.1	0
Co^{2+}	−1,203,933.8	−867,059.6	−336,166.4	−712.6	−41.5
Mn^{2+}	−1,058,498.3	−721,619.3	−336,166.4	−707.8	−36.7

X, metal cation.

Table S5. Energies of the compounds and resulting reaction energies for the formation of metal complexes with both propionic acid and diphosphate using the metal cation diphosphate complex as educt in kilocalories per mole calculated with DFT B3LYP 6-311G++ (d.p)

	Products energy	Educts energy			
X	$CH_3CH_2COO^- \times (P_2O_7H_3)^-$	$X\ (P_2O_7H_3)^-$	$CH_3CH_2COO^-$	Reaction energy	Δ to Mg^{2+}
Mg^{2+}	−1,054,033.6	−885,711.5	−168,083.2	−238.9	0
Co^{2+}	−1,796,098.5	−1,627,782.5	−168,083.2	−232.8	6.1
Mn^{2+}	−1,650,660.9	−1,482,341.6	−168,083.2	−236.1	2.8

X, metal cation.

Table S6. Energies of the compounds and resulting reaction energies for the formation of metal complexes with both propionic acid and diphosphate using the metal cation propionic acid complex as educt in kilocalories per mole calculated with DFT B3LYP 6-311G++ (d.p)

	Products energy	Educts energy			
X	$CH_3CH_2COO^- \times (P_2O_7H_3)^-$	$(P_2O_7H_3)^-$	$CH_3CH_2COO^-\ X$	Reaction energy	Δ to Mg^{2+}
Mg^{2+}	−1,054,033.6	−760,331.1	−293,532.0	−170.5	0
Co^{2+}	−1,796,098.5	−760,331.1	−1,035,599.4	−168.0	2.5
Mn^{2+}	−1,650,660.9	−760,331.1	−890,171.2	−158.6	11.9

X, metal cation.

6 General Discussion

In the published findings of my thesis I investigated important enzymes regarding the *de-novo* biosynthesis of iridoids in Chrysomelina larvae. The outcomes are discussed in detail in each manuscript. Therefore, I want to create an overview on the current state of research and discuss my findings in general concerning regulatory mechanisms of branch point enzymes within terpene biosynthesis.

The relevance of warfare between organisms is an important impulsion for the development of ingenious defense strategies. Plants for example were challenged during evolution to "fight" against herbivores. Thus, various phytochemicals, like phenolic glucosides or terpenoids, produced by plants are major constraints that can influence the feeding behavior of herbivores and were scrutinized by researchers since decades. Analogous to plant´s defenses, insects also developed robust physical attributes for defense, such as strong dermis but also chemicals, like alkaloids, phenolics, glucosinolates or terpenes. Due to the fact that plants developed phytochemicals to avoid feeding, herbivores had to deal with them. Specialists are not only in the position to live and feed on those plants; they are sometimes also able to incorporate these compounds in their own defense system.

Perfectly adapted to plants and their defensive chemicals are the Chrysomelidae. There are more than 37.000 described species subdivided into 19 subfamilies which are mostly phytophagous (154, 155). Especially, the subtribe Chrysomelina spends their entire lifetime on the leaf surface of the same plant. Hence, they are highly exposed to a multiplicity of predators like ants, spiders, birds and microorganisms (156). Particularly in larvae, a multitude of chemical defense strategies against their enemies developed during evolution (122, 132-135, 157-159). Within the subtribe Chrysomelina, three evolutionary related modes regarding biosynthesis of defensive compounds were postulated.

1. *De-novo* biosynthesis of cyclopentanoic monoterpenes displays the ancestral strategy. This endogenous production of deterrents is independent from plant derived precursors (58, 119, 121, 130, 132, 135, 137-139, 141-145).
2. Sequestration as a more evolved approach is found in *Phratora vitellinae* and the genus *Chrysomela* living on Salicaceae. They sequester plant-derived phenolic

glucosides present in Salicaceae as salicin and convert it within the defensive secretions to salicylaldehyd. (119, 121, 129, 130, 135, 151, 160, 161).

3. The most evolved species is the *interrupta* group of the *Chrysomela* which exhibits a combination of the two previous described mechanisms. The larvae are able to sequester plant-derived phenolic glucosides and produce butyryl-ester with endogenously synthesized compounds (133-136).

6.1 SEQUESTRATION - OLD ENDOWMENT OR NEW DEVELOPMENT

In the past, research revealed that classification of Chrysomelina in three distinct biosynthetic groups is not that strict. For instance, *Plagiodera versicolora* and various *Phratora* species except *P. vitellinae* live on salicaceous plants and do not sequester phenolic glucosides to incorporate them into their defensive secretions. They still produce cyclopentanoic iridoids *de-novo* (151, 162). Quite contrary observations are made for *P. vitellinae* which belongs phylogenetically to the group of *de-novo* producers. Besides the genus *Chrysomela* those larvae are also able to produce salicylaldehyde, even though they are not closely related. Older phylogenetic and biochemical analyzes favored the hypothesis of a convergent origin of salicin-based defense strategy (119, 126, 130, 146). However, newer findings support the hypothesis that sequestration has a single origin. Genetic evaluations of the salicyl alcohol oxidase (SAO) of both species show that the enzyme is not recruited independently from the oxidase repertoire of the iridoid producers. Both enzymes seem to share a common ancestor in the GMC oxidoreductases multi-gene family (163, 164).

Even more fascinating are the results received from different feeding experiment with *de-novo* producer species. They clearly indicate that *Phratora laticollis, Plagiodera versicolora*, *Phaedon cochleariae* and *Gastrophysa viridula* are able to successfully sequester hydrolysis-resistant Ger-8-*S*-Glc as well as the naturally occurring Ger-8-*O*-Glc (130, 152, 153). Further feeding experiments with ^{13}C-DOX pre-incubated plants were performed. This led to the production of labeled plant derived precursors *via* the MEP pathway. Larvae of *Pl. versicolora* and *Prathora laticollis* fed on these ^{13}C-plants clearly showed the uptake of ^{13}C-labeled precursors due to detectable amount of ^{13}C-iridoids in the secretions (139). In contrast, *G. viridula* and *P. cochleariae*

secretions contain no detectable ^{13}C-labeled iridoids. Analyzes of the different host plants concerning the availability of related precursor displayed highly diverse terpenoid contents. The leaves of *Salix fragilis* and *Populus canadensis* contain small amounts of Ger-8-*O*-Glc, whereas the host plants of *G. viridula* and *P. cochleariae* do not. Anyway, also these larvae possess the ability to sequester, shown by feeding experiments with d_5-Ger-8-*O*-Glc painted on host plants. After feeding, secretions contained a high amount of d_5-labeled chrysomelidial (153)(Manuscript 2). Physiological analysis of transport mechanisms displayed that the uptake of plant derived glucosides by the gut epithelium into the hemolymph is non-selective. If mixtures of Ger-8-*O*-Glc and salicin had been present in the food, both of them could be detected in the hemolymph later on. Interestingly, the uptake of Ger-8-*O*-Glc was higher even in the salicin sequestering species *C. populi.* However, the import of the glucose precursors into the glandular system is highly specific! Injection experiments clearly showed that, if mixtures of glucosides had been present in the hemolymph, only the genuine precursors of the defensive compound were transported into the glands. It therefore seems likely, that the uptake of precursors is accomplished by glucose transport proteins. (130, 131, 152).

In total, these observations indicate common principles concerning chemical defense in all Chrysomelina larvae.

i) All larvae represent a uniform architecture and morphology of the defensive system.
ii) All larvae use glucosidically bound precursors for the biosynthesis of their defensive secretions.
iii) All groups, even the ancestral beetles, possess the potential to sequester non-specific plant derived glucosides from the gut epithelium into the hemolymph.
iv) All larvae transport glucosidically bound precursors *via* the hemolymph to the glandular reservoir indicating a complex transport guided mechanism.
v) All larvae show a highly selective and substrate specific transport into the glandular system.

Possessing transport mechanisms for sequestration of plant derived precursors opens the way to switch the biosynthetic strategy from *de-novo* production to

sequestration if appropriate substrates are available. While *de-novo* biosynthesis facilitates a host plant switch without losing defense, sequestration enables the larvae to save costs and energy and leads to increased fitness (130, 136, 152). Hence, identification of similarities in sequestration processes strongly implicate that the larvae may employ both, endogenous and exogenous pools of the iridoid precursors.

However, biosynthetic mechanisms highly depend on the need and supply of precursors. Therefore, the development of a regulatory system is indispensable to gain a benefit from plant derived substrates. Consequently, regulation mediated by plant-derived precursors could then function as a switcher between different biosynthetic routes.

6.2 Regulation processes in terms of sequestration

To gain a benefit, geraniol, Ger-8-OH or Ger-8-*O*-Glc should display a regulatory impact on upstream processes of the biosynthesis of defensive secretions to save costs by the feedback inhibition of the whole pathway. HMGR seems therefore a good target. As key enzyme of the MVA pathway, it is strongly involved in the *de-novo* biosynthesis of defensive iridoids due to production of the early precursors IDP and DMADP (142, 143)(Manuscript 1 and 2).

Former localization studies of MVA derived compounds elucidated fundamental strategies in precursor production. An increased HMGR transcript abundance correlated to increased enzyme activity was only observed in the fat body tissue of *de-novo* producers (141). Another important enzyme of deterrent biosynthesis is a GDPS, due to the fact that Ger-8-*O*-Glc derives from the monoterpenoid precursor GDP. Similar results regarding product formation, transcript abundance and enzyme activity are obtained for a putative GDPS, which emphasize earlier findings that precursor production is located in the fat body tissue (141) (Manuscript 2 and 4). Additionally, this correlates with the identification of Ger-8-*O*-Glc in high amounts in the fat body tissue and hemolymph of *de-novo* producers (141) (manuscript 4). All together, these conclusively demonstrate that the early biosynthetic steps are located in the fat body and, therefore, regulatory processes should take place there.

REGULATORY IMPACT OF SEQUESTERED COMPOUNDS ON KEY ENZYME HMGR

HMGR is highly regulated on transcriptional, translational as well as on protein level (66). It is known that farnesol, farnesol derivatives or homologs can accelerate the degradation of HMGR (70, 165-170). Also an impact of mevalonate-derived non-sterols at translational level occurs (171). Furthermore, it was shown that geraniol can suppress HMGR activity by the down-regulation of transcription and translation (172). However, in insects HMGR regulation received only limited attention although it is highly important in the biosynthesis of the acyclic sesquiterpenoid JHs. Belles *et al*. already showed a positive transcriptional regulation of HMGR triggered by JH. Application of JH III to larvae of the bark beetles (Scolytidae) *Ips pini*, *Dendroctonus jeffreyi* and *Ips paraconfusus* causes a significant increase of HMGR transcript abundance and enzyme activity. This in turn corresponds to a higher pheromone production (173-180). Nevertheless, the regulatory mechanisms are not clarified yet.

The capability to sequester, shown for *de-novo* producers, clearly forced us to analyze Ger-8-*S*-Glc, Ger-8-OH and geraniol for their regulatory impact. And indeed, HMGR activity in crude enzyme extracts of larval fat body from *P. cochleariae* indicates a 50% inhibition by Ger-8-OH with a concentration of 2 mM. Furthermore, an inhibition of 25- 35% was achieved by geraniol even though at a higher concentration of 5 mM. No detectable inhibition was perceived for Ger-8-*S*-Glc. The thioglucoside was used to prevent hydrolysis by *β*-glucosidases present in the crude extract (Manuscript 1 and 2).

For profound understanding of regulatory mechanisms we further analyzed the influence of these compounds on the heterologous expressed catalytic domain of HMGR from *P. cochleariae*. Interestingly, an inhibition for the isolated catalytic domain was observed only for Ger-8-OH (Manuscript 1 and 2). This lack of inhibition by geraniol could be explained by at least two factors. First, the crude enzyme extract of the fat body tissue still contained the whole bunch of enzymes involved in the biosynthesis of Ger-8-*O*-Glc. Therefore, the oxidation of geraniol producing Ger-8-OH, by a suggested P450 enzyme, could occur in parallel and the inhibiting effect is caused indirectly *via* Ger-8-OH and not by geraniol. A second reason could be the truncated form of the overexpressed protein. HMGR possesses different domains which are subjected to various regulation mechanisms: For example, degradation associated with the membrane spanning domain (49, 181, 182) or activity loss due to phosphorylation of

the catalytic domain (183, 184). Consequently, due to truncation of the protein potential interacting motifs, like linker region or membrane spanning domain, might be absent and thus no inhibition by geraniol occurs.

The ineffectiveness of Ger-8-*O*-Glc in both approaches seems not coherent with respect to analyzes of the host plant derived compounds. There, the glucoside was supposed to be the sequestered compound and therefore suggested as the main regulatory factor. But following the route of ingested plant material, it was revealed that not only Ger-8-*O*-Glc can reach the hemolymph and fat body cell, but also Ger-8-OH, produced by hydrolytically cleavage of the glucose moiety, can pass the gut barrier to attenuate HMGR activity. Furthermore, cleavage of Ger-8-*O*-Glc after uptake in the fat body cell or hemolymph may occur and lead to production of Ger-8-OH which in turn can regulate the HMGR (141, 153). However, until now only the influence on HMGR was analyzed but almost certainly it might be possible that regulation processes of other upstream enzymes are also present (Fig. 9 dotted lines). Regulation which works as a progressive feedback inhibition system might be conceivable. Therefore, Ger-8-*O*-Glc might be also influenced by the Glycosyltransferase. Ger-8-OH in turn can inhibit the P-450 oxygenase or the GDPS directly. This series of reactions can go further until the formation of GDP is selectively inhibited. Furthermore, taking into account where HMGR is localized within terpenoids biosynthesis it seems likely that a fast shut down could also affects other terpenoid pathways like JH production. Therefore, the calculated higher IC_{50} for Ger-8-OH of 1.2 mM, compared to the human IC_{50} of 28 nM, seems reasonable. Although this could be attributed to the truncation of the protein, I would suppose that HMGR has to have a high tolerance threshold regarding Ger-8-OH to ensure the refill of the reservoir expeditiously after loss of secretions. As already mentioned, we found enormous amounts of precursors in both, fat body tissue and hemolymph (Manuscript 1 and 4). This is not astonishing due to the huge quantities of secretions produced by the larvae even in very short time periods. Therefore, regulation of HMGR has to be clearly verified and an inhibition *via* Ger-8-OH at very low concentrations would make no sense. However, homology modeling and docking experiments of *P. cochleariae* HMGR emphasize our observations by considering Ger-8-OH as a possible competitive inhibitor. It appeared that the docking position of Ger-8-OH is almost identical to the binding position of HMG in the X-ray structure of human HMGR. The perfect fit of Ger-8-OH within the active center of HMGR clearly emphasizes the possible

regulatory impact as competitive inhibitor for the *de-novo* biosynthesis in *P. cochleariae* (Manuscript 1).

Concluding, Ger-8-OH can act as a competitive inhibitor at higher concentrations to down-regulate HMGR activity. Therefore, HMGR represents a regulatory element of the early biosynthesis of iridoids in maintaining homeostasis between *de-novo* produced and sequestered metabolites (Fig. 9). But it further seems reasonable that HMGR cannot be the only regulatory element. Hence, additional mechanisms may exist controlling exclusively the pathway for defensive secretions.

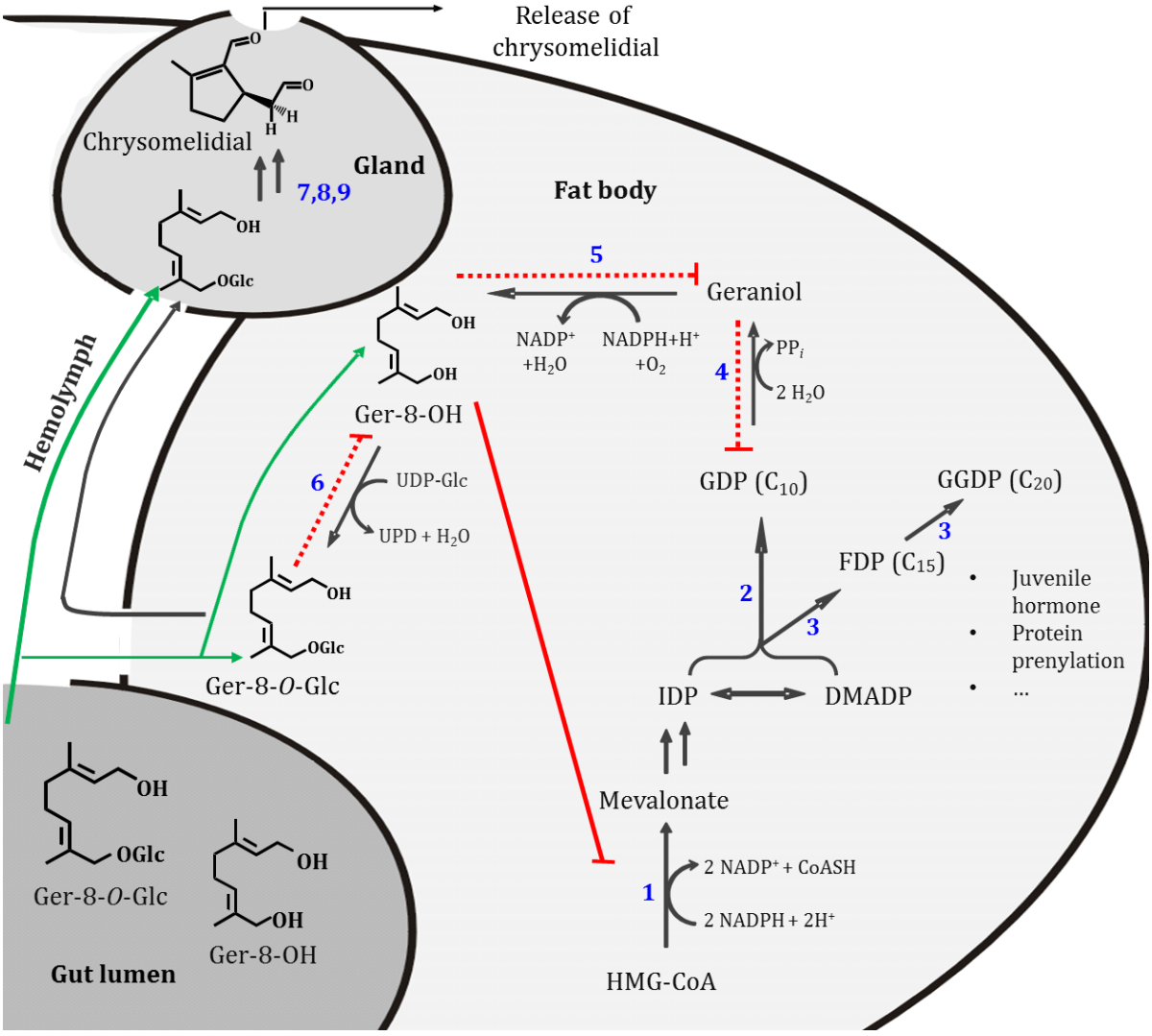

Fig. 9 Biosynthesis of defensive secretions in the larvae of *P. cochleariae* considering regulatory mechanisms. 1, HMGR; 2, GDPS; 3, scIDS; 4, Phosphatase; 5, Cytochrome P-450 mixed function Oxygenase; 6, Glycosyltransferase; 7, *β*-D-Glucosidase; 8, Oxidase; 9, Cyclase. Green arrows indicate the possibility of sequestration and the supposed regulatory route of sequestered compounds. Dotted red lines indicate possible inhibitory mechanisms. Red lines indicate the negative feedback inhibition of Ger-8-OH on HMGR (adapted from (58)).

6.3 RNAi-MEDIATED SILENCING TO IDENTIFY ENZYME CORRELATED TO DEFENSIVE SECRETIONS

Interfering RNA (RNAi) has become a valuable research "tool" due to the highly selective induced suppression of specific genes of interest. Most research using RNAi was done to investigate developmental processes in insects. However, RNAi decreases transcript and protein levels and seems a suitable method to demonstrate and proof *in-vivo* relevance of specific enzymes for particular metabolic pathways (185-187).

This technique was established for leaf beetle larvae because of two reasons. First, to identify enzymes involved in the biosynthesis of deterrent secretions even if *in-vitro* analyzes are not established yet. Second, it is used to demonstrate *in-vivo* relevance of target sequences, which are already identified and biochemically characterized *in-vitro* (Manuscript 3). Validation of this method was accomplished for a known SAO derived from *C. populi* (163, 164) (Manuscript 3). RNAi of SAO leads to accumulation of salicyl alcohol due to an interruption of the last oxidative step, normally producing salicyl aldehyde. Also, for the *de-novo* producer *P. cochleariae* the method was functionally investigated. Novel proteins were identified in the secretome of *P. cochleariae* which could be involved in the cyclisation reaction to form chrysomelidial. Knock down of a putative cyclase resulted in accumulation of non-cyclized 8-oxogeranial in addition to chrysomelidial (Manuscript 3).

RNAi experiments of *Pc*IDS1 clearly demonstrated *in-vivo* relevance regarding defensive secretions. After a couple of days *Pc*IDS1 knock down species developed a defenseless phenotype. Reduced transcript level and enzyme activity correspond to a significant reduction of Ger-8-*O*-Glc in the fat body tissue and hemolymph. An impact on the larval development was not observed; indicating that biosynthesis of JHs was not affected. This could be addressed to different reasons. One could be that *Pc*IDS1 is not involved in JHs biosynthesis. Second, one could assume that RNAi is not equally efficient in all tissues. Significant reduction of transcripts was observed in fat body tissue, whereas in the head tissue apparently no silencing occurred. JH biosynthesis of insects is known to be located in the corpora allata (CA) a pair of small, compact glandular organs located behind the brain. Therefore, JH biosynthesis could remain unaffected if silencing

of *Pc*IDS1 is insufficient in the CA. Anyway, the results indicate that *Pc*IDS1 is involved in the biosynthesis of the deterrent compound chrysomelidial.

The consolidated view indicates that RNAi is a reliable method to provide new evidence for *in-vivo* relevance of newly discovered proteins and their allocation to a specific metabolic process (manuscript 3).

6.4 *Isoprenyl diphosphate synthases control terpenoid fluxes*

Due to the fact that HMGR produces very early terpenoid precursors, I additionally investigated another branch point enzyme of further downstream reactions. GDPS appeared to be a good candidate simply because Ger-8-*O*-Glc exclusively derives from GDP (142, 143). Further, I already showed that RNAi of *Pc*IDS1 has an impact on the biosynthesis of chrysomelidial. Manuscript 4 additionally depicts a new opportunity to regulate *sc*IDSs in general. I propose *Pc*IDS1 as a very precisely regulated target within the biosynthesis of iridoids.

The condensation of allylic DMADP and homoallylic IDP to produce GDP is catalyzed by GDPS (102, 188, 189) belonging to the family of *sc*IDSs. Whereas, FDPSs and GGDPSs occur nearly ubiquitously, GDPS was mainly described in plants and few insects until now (14). *Sc*IDSs function as branch points within terpenoid biosynthesis due to synthesizing universal precursors with different chain-length for all classes of terpenes. Together with terpene synthases, *sc*IDS play an important regulatory role in controlling the metabolic fluxes of different terpenoid pathways (1, 42, 47, 190). Insect isoprenoids are highly important for the production of e.g. JHs, sex pheromones or defensive compounds, like *(E)*-β-farnesene. Research regarding aphid sex pheromones (monoterpenoids) is highly investigated due to their economic importance as main insect pest of northern European agriculture. The first characterized pheromone is the cyclopentanoic monoterpenes nepetalactone from the vetch aphid *Megura viciae* (191). Among others, this importance of terpenes has promoted research on terpenoid biosynthesis to clarify the principal regulatory mechanisms of *sc*IDSs.

Commonly, most *sc*IDSs generate a single product (192). However, some enzymes identified so far are promiscuous and produce intermediates of different chain-length. For instance, GDPS of *Phalaenopsis bellina* (*Pb*GDPS) (193) or *Picea abies* (*Pa*IDS1)(194)

produce next to GDP also FDP or GGDP, respectively. In insects, only few GDPSs are identified whereas most of them are poorly characterized (82). Strikingly, most of them show promiscuity and form FDP next to GDP. Conspicuously in this context, plants possess a huge number of genes encoding for different *sc*IDSs, at least 15 are known in *Arbidopsis thaliana* (192), whereas insects only possess a few, e.g. three in *Bombyx mori* (195). This phenomenon of bi-functionality may compensate the disparity of the numbers of *sc*IDSs by generating different chain-lengths with only one enzyme.

Also, the larvae of *P. cochleariae* possess at least two *sc*IDSs whereof one of them (*Pc*IDS1) could be isolated and characterized profoundly. Thus, I was able to observe an efficient and up to now not-described mechanism of regulation. There, the divalent metal co-factors regulate the final chain-length of the *Pc*IDS1 product. The recombinant protein produces either GDP or FDP depending on the co-factor provided. However, this has to be precisely regulated to provide the appropriate precursor, needed for different terpenoid pathways. Especially in *P. cochleariae*, regulation concerning product formation is important to clearly define which metabolic pathway is served by the enzyme. The immense amount of GDP, needed for *de-novo* production, has to be allocated fast, highly specific and in large quantities. However, at the same time biosynthesis of FDP derived compounds have to be secured and should not suffer from the enormous GDP consuming pathway due to the usage of the same MVA derived intermediates IDP and DMADP.

6.4.1 Regulation of product specificity of *PcIDS1* by the metal cofactor

Understanding the mechanism of chain-length determination in IDSs has been a challenge for many researchers since decades. By analyzing substrate and product specificity of isolated IDSs a lot has been learned about active site features that restrict product length. Typically, IDSs have a specific product and substrate spectrum determined by the deepness of the hydrophobic pocket of the active center. Amino acid residues, mainly located in proximity of the FARM region, define the pocket size. The residues simply cause a steric hindrance in the cavity which accommodates the growing carbon chain (Fig, (1, 40, 47, 80, 81, 94, 196). The increasing numbers of identified IDSs also gain new knowledge concerning chain-length determination factors besides simple

steric hindrance. For instance, purified long chain IDSs requires phospholipids or detergents for efficient turnover. However, the stimulatory effect seems to be enzyme-dependent. Furthermore, these detergents affect not only enzyme activity, but also product specificity by influencing the final chain-length (197). Alterations of enzymatic activity in case of different metal co-factors are also observed. Literature declares Mg^{2+} as the common co-factor for IDSs but also Mn^{2+}, Zn^{2+}, Ni^{2+} and Co^{2+} confer enzyme activity (86, 87) in plants (e.g. *Abies grandis* (88)) or in insects (*Myzus persicae* (80) or *Choristoneura fumiferana* (84)). However, these examples show no alteration in chain-length besides the impact on general enzyme activity. This is in contrast to some older observation of long chain IDSs isolated from microbes which produce a variety of polyprenyl products. In the presence of Co^{2+} or Mn^{2+}, polyprenyl diphosphate synthases still produced multi-products in which the longest chain shifted to one or two C_5 units longer products compared to those formed with Mg^{2+} (110).

In our case, *Pc*IDS1 shows a highly adjustable and co-factor mediated product pattern switch. Surprisingly, the promiscuous enzyme produces nearly exclusively GDP (95%) if Co^{2+} was used as co-factor, whereas in case of Mg^{2+} mainly FDP (82%) was observed (Manuscript 4). Profound analyzes of kinetic parameters display the biochemical relevance of this regulation. The calculated k_m values for the different substrates in matters of the metal co-factors go ahead with known literature values. In case of Mg^{2+} the preferred substrate is GDP, whereas in case of Co^{2+} the K_m for DMADP was lower than for GDP. These results are re-emphasized by the calculated enzyme activity. If DMADP was used in combination with Mg^{2+}, *Pc*IDS1 showed a reduced FDP forming activity compared to the values obtained with the allylic precursor GDP. The contrary was observed if Co^{2+} was present as co-factor. There, the highest activity was achieved with DMADP resulting in GDP formation, whereas GDP as substrate resulted in a significantly decreased FDP formation (Manuscript 4).

Emphasizing the regulatory possibility of HMGR activity by host plant derived compounds; this was also proven for *Pc*IDS1. Admittedly, this does not lead to any detectable influences (unpublished data). However, the observed influence on product specificity mediated by metal co-factors displays an even more specific regulatory process. Here, the flux control is highly independent from negative feedback inhibition mediated by precursors which furthermore was not specific for deterrent production in case of HMGR.

While searching for enzymes evolved for the specific isoprenoid biosynthesis, we rather found one enzyme developed for serving several terpenoid pathways by occupying switchable product specificity. The regulation, simply by use of different co-factors, enables the larvae of the leaf beetles to supply precursors for at least two different pathways. GDP is needed as precursor for defensive secretions and, therefore, used for monoterpenoid metabolism and FDP for the sesquiterpenoid pathway to synthesize e.g. JH.

6.4.2 Prediction of function and product specificity of IDS

Functional annotation is highly important to get usable information out of thousands of new sequences. It is the first hint for which kind of protein the sequence could code for. Assigning function, especially concrete product profiles to biochemically unknown IDSs, is in the main focus of recent research. Recently, Wallrapp *et al.* described a large-scale bioinformatics study on over 5,000 putative IDSs. They further biochemically characterized the product specificity of 79 members and determined structures by crystallization for some of these enzymes. Finally, they showed that a specific chain-length was predicted for 63.2% of the functional annotated IDSs. However, these predictions based on pure sequence homology and, therefore, the prognosticated chain-length are often incorrect. Taking into account that only 125 sequences out of over 5,000 have been biochemically characterized, it seems likely that not all determining mechanisms are uncovered yet (94). Therefore, the common idea of the "molecular ruler"-mechanism for chain-length determination might be incomplete due to still unknown factors.

The bi-functionality of some IDSs challenges researchers additionally to annotate the correct functionality. Promiscuity arouses *in-vitro* by different buffer components, substrates ratios of IDP/allylic precursor or co-factors (80, 81, 85, 108, 110, 197-201) (Manuscript 4). This raised the question regarding the determining factors regulating the adjustable functionality. Wallrapp *et al*. showed, mainly bioinformatically proposed, that steric hindrance mediated by defined residues within the conserved domains causes chain-length specificity. However, they also clearly depict that the products/intermediates itself occupy the ability to force residues to move out of the

ligands way. Consequently, residues located in the neighborhood of the catalytic cavity can finally determine the chain-length (94). Moreover, newer findings emphasize that also the dimer interface and, thereby, amino acid residues from the associated monomer influence product chain-length (94, 98, 107).

How metal ions modify the product range of *Pc*IDS1 is still under investigation. Without profound biochemical experiments, important findings like the influence of metal ions on product formation as a novel "control element" would not have been discovered. Therefore, experimental settings should always include biochemical and bioinformatical approaches.

6.4.3 Catalytic promiscuity - Evolution of metabolic diversity

As already mentioned, up to date more than 55.000 structures have been identified belonging to the group of terpenes (1). But, considering the abundance of terpenoid products this can only be the tip of an iceberg. The huge variety of the terpenome derives from different modifications of a small amount of common backbone structures. The genome, transcriptome and metabolome data revealed that the number of compounds exceed by far the number of possible genes and proteins which have to be involved in their biosynthesis. Even if regulatory mechanisms, like different reading frames, alternative splicing and post-translational modification, are taken into account, the system of one protein-one product seems not feasible! In the last years, lots of proteins have been identified which show promiscuity regarding their substrate and product specificity. Astonishing examples can be found in the biosynthesis of sesquiterpenes, probably the most complex reactions in biology. *Mt*TPS5, a terpene synthases isolated from *Medicaco truncatula*, displays a product spectrum of at least 27 different compounds in *in-vitro* analyzes. Those all derive from FDP, 17 are definitely sesquiterpenes and 10 are sesquiterpene alcohols. Comparative studies of *in-vivo* and *in-vitro* data show differences in some extend concerning the product profile of both approaches. This indicates possible regulatory mechanisms taking place on the protein level (202, 203). *M*tTPS5 also shows divalent metal co-factor dependent product specificity. If Mn^{2+} was used instead of Mg^{2+}, the product pattern shifted into the direction of the terpene alcohols. More precisely, with Mg^{2+} 32% of overall products are

terpene alcohols and in case of Mn^{2+} over 69%. An almost similar effect was observed for the amorphadiene synthase from *Artemisia annua,* converting FDP mainly into amorpha-4,11-diene next to other compounds like terpene alcohols. Here, terpene alcohols are drastically increased in case of Mn^{2+} or Co^{2+} compared to Mg^{2+} (204). There are more examples known within terpenoid synthases own a co-factor mediated product specificity (110, 205, 206). However, the mechanism behind this reaction determination is not understood yet. But it seems likely that, besides the different calculated affinities, also the varying atomic radii of the metal ions do have an impact. They probably change spatial structures of the enzyme or the substrates position within the active pocket. These influences can result, for example, in altered steric hindrance with different interacting residues, which in turn prevents or allows the additional condensation of a further C_5 unit and hence promote the production of GDP or FDP (Manuscript 4). Some researchers suggest that the metal ions influence the transmission of protons to the intermediate. But, influences on the geometry of the internal coordination of all reaction partners as well as alterations of the quaternary protein structure are also conceivable (207) (Manuscript 4).

In my opinion, these examples clearly support the hypothesis that increasing metabolome diversity does not simply correlates with an increase of the numbers of genes or proteins. Rather, it is associated with an increase of “unspecific” enzyme activity finally resulting in promiscuous enzymes which indeed elevate metabolic diversity. External stimuli, like pH, temperature, co-factors or substrates availability, channeling the promiscuous activity to receive the specific enzyme activity needed to produce distinct products. The combination of highly adjustable enzymes, regulated by various parameters, leads to the enormous variety of different product specificities. Therefore, promiscuous activities of enzymes provide the opportunity for the development of new biosynthetic pathways and therefore, promote the evolution of organisms.

7 FUTURE PERSPECTIVES

Considering the fact that controlling mechanisms of terpenoid biosynthesis in insects are not well understood, the achieved results clearly promote profound knowledge of possible regulatory processes.

When I started with my thesis nearly no data concerning enzymes involved in monoterpene biosynthesis in *Phaedon cochleariae* were available. Therefore, we established, besides other approaches, transcriptome data from a variety of Chrysomelina larvae in order to identify new key enzymes of deterrent biosynthesis. Due to highly diverse protein spectra that furthermore possess diverse product and substrate specificity, we were forced to investigate new methods like RNAi to determine metabolic affiliation. The findings of enzymatic analysis regarding HMGR and *Pc*IDS1 broadened not only the knowledge concerning deterrent biosynthesis, but also display newly-discovered processes supporting the hypothesis of the origin of metabolic diversity. Especially, how the huge variety of the terpenome might be enabled and specifically regulated. However, to proof our suggestions and to uncover further defined regulatory mechanisms we actually need more data. Therefore, I would like to depict some future projects supported by already obtained data.

7.1 EVALUATION OF THE MECHANISM OF METAL CO-FACTOR MEDIATED PRODUCT SPECIFICITY

A high quality homology model of *Pc*IDS1 with IDP and GDP implemented in the active site was already generated. Comparative studies concerning Mg^{2+} and Co^{2+} as co-factors using molecular dynamic simulations and energy minimization revealed small but significant changes. The analysis of the active site, in complex with Mg^{2+}, displays GDP proper bound to the hydrophobic residues. There, GDP is located already near the bottom of the binding pocket, generated by Asparagine (N) 244 and Methionine (M) 178. For Co^{2+} essential changes in the conformation of the diphosphate moiety as well as movement of GDP deeper into the binding pocket were observed. Hence, movement of GDP closer to the bottom results in a steric conflict with N244 and partly with M178 (Fig. 10) (unpublished data).

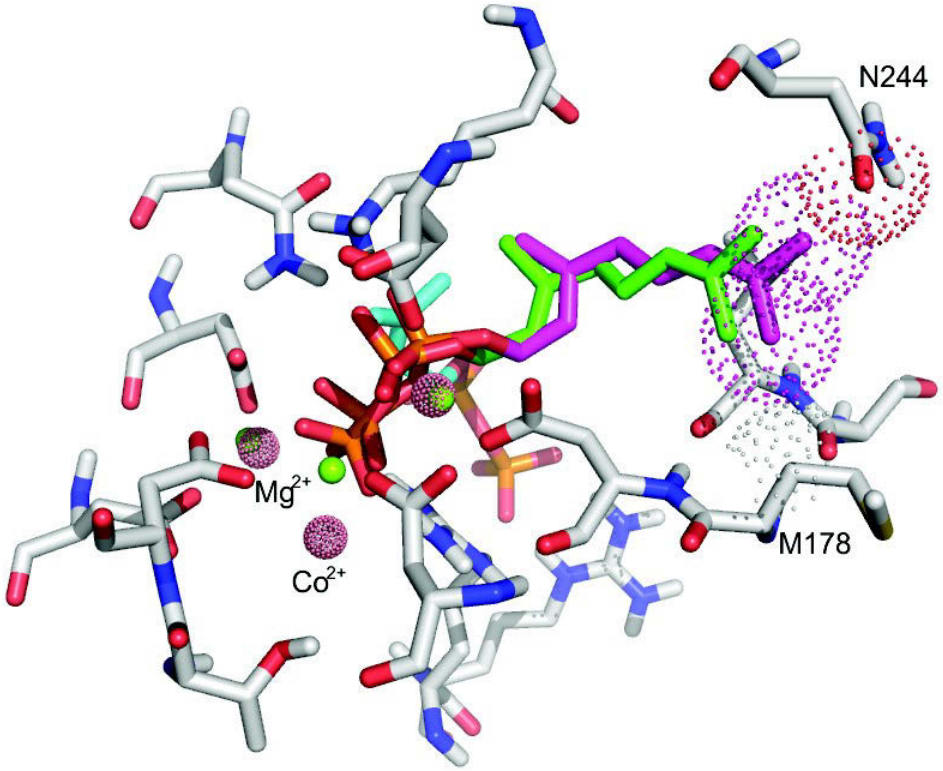

Fig. 10: Comparison of GDP located in *PcIDS1* with different metal co-factors. Mg^{2+} ions (green balls and green prenyl chain) and Co^{2+} (dotted balls and magenta prenyl chain) are fitted into the homology model of *Pc*IDS1. The larger van der Waals radius of Co^{2+} (1.73 Å) in comparison to Mg^{2+} (0.96 Å) causes movement of GDP deeper into the binding pocket. The possible steric conflict with N244 and partly M178 in turn causes repulsion, indicated by the dotted spheres.

It can be suggested, that rearrangements occur due to the bigger van der Waals radius of Co^{2+} (1.73 Å) compared to that of Mg^{2+} (0.96 Å.). The allocation of GDP in turn prevents the Co^{2+}-bound enzyme to add an additional IDP unit to form FDP and, therefore, promotes the release of GDP.

7.2 Analysis of mutants to identify chain-length determination factors

A widely-used method to characterize enzyme specificity is the biochemical analysis of mutants. Therefore, bioinformatics data of well characterized scIDSs were already compiled. Furthermore, we analysed sequence data and X-ray structures and compared them with *Pc*IDS1. Concluding this analysis, I want to suggest which amino

acid residues might be important for co-factor binding, substrate positioning and product specificity. The outcome of this comprehensive analysis will be used to design different mutants of *Pc*IDS1 and to proof the hypothesis of steric hindrance due to a shift of GDP. A first trial with a double mutant of *Pc*IDS1 were both amino acids, N244 and M178, are mutated to the short amino acid alanine (A), already achieved surprising results concerning chain-length determination (Fig. 11) (unpublished data). After abolishment of steric hindrance caused by N244 and M178 the expected product of *Pc*IDS1 was FDP. However, the mutated enzyme produced mainly GDP independently of the co-factor (Mg^{2+} or Co^{2+}).

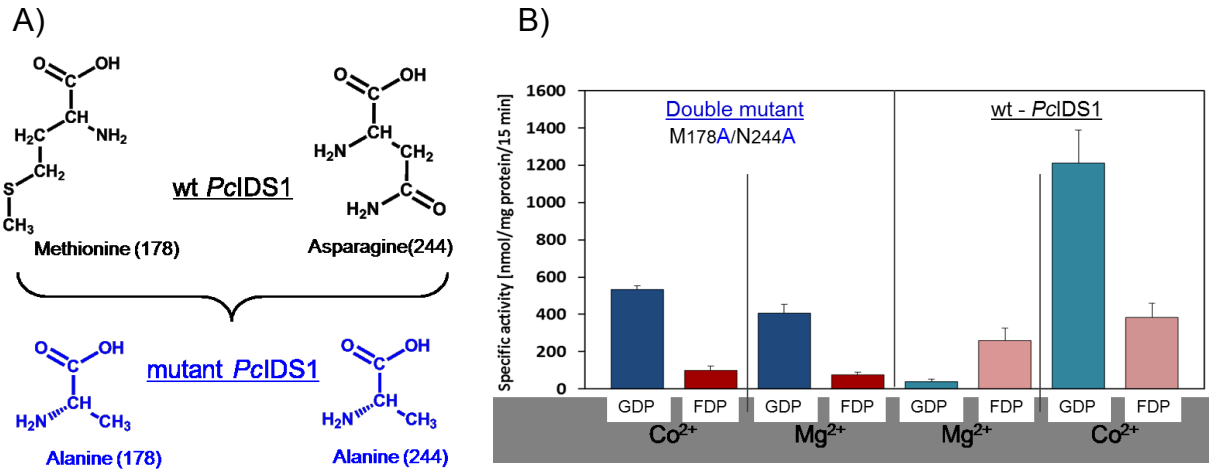

Fig. 11: Enzyme activity of double mutant *Pc*IDS1 and wt *Pc*IDS1 dependent on the metal co-factor Co^{2+} or Mg^{2+}. A) Structures of amino acids are shown which were mutated in the double mutant of *Pc*IDS1. B) Specific enzyme activity of wt-*Pc*IDS1 compared to double mutant *Pc*IDS1 concerning the influence of metal co-factor on product specificity.

How does this result match with our hypothesis? If the whole dimer structure is considered for explanation, it will match. Both amino acids, N244 and M178, seem to provide enough space within the active cavity, for either GDP or FDP production depending on the co-factor. Nevertheless, it seems that the replacements of both residues by the smaller alanine do not provide additional space. Apparently, quite the contrary happened in the mutated *Pc*IDS1. Analysis of the dimer structure gives the impression that N244 and M178 keep residues from the interacting monomer at a defined distance. The mutation to N244A and M178A in turn enables contiguous residues from the other monomer to move closer and, thereby, narrows the catalytic cavity (Fig. 12). Consequently, only GDP as product fits in the remaining space,

attributed to the even greater steric hindrance of the amino acids from the contiguous monomer. Accordingly, non-active site residues are now directly responsible for product specificity in determining the final chain-length independently from metal co-factors (unpublished results). However, if this is the final explanation this has to be investigated by other mutants as well (in preparation).

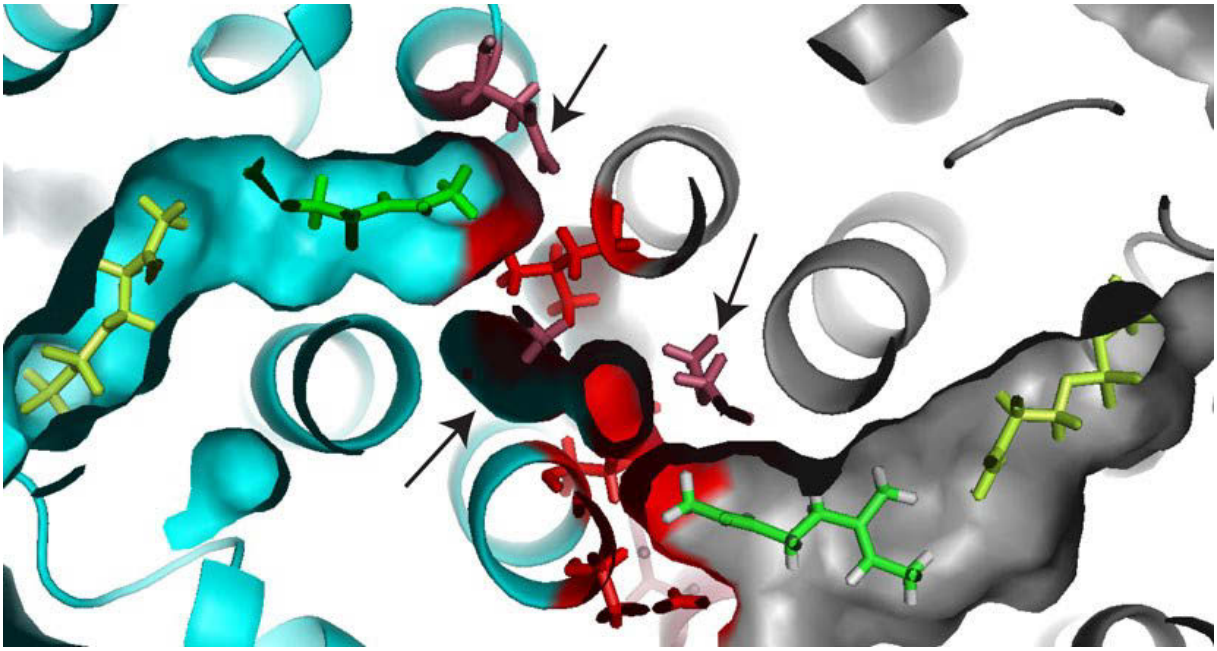

Fig. 12: Insight view on the dimer interface of *Pc*IDS1 with regard to amino acids contributing to the catalytic cavity. IDP (light green) and GDP (green) are illustrated. Blue helices display one monomer and gray the contributing monomer. Residues colored in pink and indicated with an arrow represent amino acids which arouse the steric conflict in the corresponding monomer by the use of Co^{2+} as co-factor. Residues colored in red represent putative interacting amino acids from the adjacent monomer which arouses a potential steric conflict after the mutations of M178A and N244A.

7.3 Identification of *sc*IDS in Chrysomelina larvae and other insects

Aphids, coleopterans and lepidopterans are known to possess up to three *sc*IDS (78, 80, 83, 195, 208). To investigate the impact of this newly identified regulatory mechanism of *Pc*IDS1 it is highly important to characterize other *sc*IDS as well. I already identified homologous sequences, functionally annotated as FDPS, within the Chrysomelina species *P. cochleariae* (one additional), *C. populi* (two in total) and *C. lapponica* (two in total). Furthermore, I tried to determine the product specificity of enzymes isolated from other insects like aphids, Lepidoptera or Hymenoptera. The biochemical characterization is currently under investigation. Certainly, first results

show that some *sc*IDSs, isolated from other leaf beetle larvae, are also able to switch product specificity e.g. *C. lapponica*. Whereas, the results obtained from Hymenoptera are contrary. Here, the product pattern seems stable and *sc*IDS produces FDP with both co-factors Co^{2+} or Mg^{2+} (unpublished data).

Nevertheless, for a final decision these observations have to be reproduced and investigated in more detail. But taking these results into account and comparing them with the analysis of the mutants, the findings will definitely increase the knowledge of the chain-length determination mechanism.

7.4 Co-localization of *Pc*IDS1 and metal co-factors in *P. cochleariae*

The accumulation of metals is often reported for specialized plant species living on soil polluted or infiltrated with high concentrations of metals. In connection with research concerning phytoremediation, where plants are used to remove metals from soil, analyses of metal distribution and transportation in plants were performed. Since this research field in insects is not as well investigated as for plants, it is difficult to identify exceptional elevated levels of trace metals. Some publications dealing with resistance and accumulation of metals in insects, feeding on hyper-accumulating plants or contaminated soil, indicate how heavy metals might be distributed in insects (209-212). I was able to observe an overall availability of the metal ions Mg^{2+}, Co^{2+} and Mn^{2+} in the larval tissue as well as in the host plant *Armoracia rusticana* (horseradish) (Manuscript 4). However, this does not give a clear evidence for the discrete local distribution of the metals within the tissue or cells. An intriguing question which has to be answered is: Do we find a correlation between local distribution of *Pc*IDS1 and the metal co-factors such as Mg^{2+} and Co^{2+}/Mn^{2+}? The investigation of such relationships can be achieved by the combination of different high resolution analysis. On one hand, the local distribution of *Pc*IDS1 has to be determined by using specific antibodies. On the other hand, the accumulation of different metal ions has to be examined by using e.g. NanoSIMS or microPIXE technology (211, 213-215). NanoSIMS is a unique ion microprobe optimized Secondary Ion Mass Spectrometry (SIMS) analysis which allows, with 50 nm lateral resolution, imaging and quantification of trace elements. Particle-induced X-ray emission (PIXE) is a non-destructive method to determine the elemental composition of samples. There, metals are exposed to an ion beam and resulting

interactions give off electromagnetic (EM) radiation. The wavelengths are highly specific for each element. A tightly focused beam down to 1 µm will achieve the capability of microscopic analysis of trace element localisation. Comparing the results of both approaches should generate a defined picture of distinct local distribution and accumulation of *Pc*IDS1 and the corresponding metal co-factor.

7.5 IDENTIFICATION OF COBALT TRANSPORTERS IN CHRYSOMELINA

Cobalt was shown to be a regulatory co-factor in terpenoid biosynthesis. It is less frequently encountered in metalloenzymes than iron, manganese or zinc. However, it is also known as an important co-factor in almost all living organisms, for example in vitamin B12-dependent enzymes or methionine aminopeptidase or glucose isomerase (216, 217). However, like all redox-active metal ions Co^{2+} is highly toxic at elevated intracellular concentration. Intoxication is associated with various diseases in humans such as contact dermatitis, pneumonia, allergic asthma and lung cancer (218). Toxicity mainly arises from its competition with the regular metal ions of the enzymes. Binding of Co^{2+} instead of the physiologically correct metal ion can thereby inhibit proper enzyme functions.

However, to gain access to metals, they have to be specifically transported into the cells/compartment where it is needed. To balance the need for Co^{2+} with its intrinsic toxicity, nature had to developed distinct trafficking systems to maintain metal homeostasis (219). However, it is known that cation transporters often possess a broader substrate spectrum for different ions. Therefore, I assume a specialized transport system involved in Co^{2+}/Mn^{2+} transfer and homeostasis. In the transcriptome of *P. cochleariae,* I have identified a putative transport protein (unpublished data) showing high similarity to the cobalt uptake protein Cot 1 of *Saccharomyces cerevisiae* (220). Sequence similarity and conserved domain analyzes display motifs of the Superfamily cl00316 defined as cation efflux family. These proteins are thought to be involved in ion transport and metabolism. Members of this family are integral membrane proteins that increase the tolerance to divalent metal ions such as cobalt, cadmium and zinc. These findings enforce the possibility of Co^{2+} as a relevant co-factor regulating terpenoid biosynthesis.

8 SUMMARY

Chrysomelina larvae possess a sophisticated strategy in terms of chemical defense eminently adapted to their natural habitat. In case of predatory attack, the deterrent secretions are released from dorsal thoracic and abdominal glands. The source of the deterrent compound for this ingenious mechanism depends on different biosynthetic strategies and subdivides the Chrysomelina in three different groups. The ancestral strategy represents the *de-novo* production of iridoids. Species belonging to this group e.g. *Phaedon cochleariae* and *Gastrophysa viridula* produce the deterrent compound independently of host plant derived precursors. More evolved species of the *Chrysomela* as well as *Phratora vitellinae* use the approach of sequestering phenol glucosides to produce salicylaldehyde. Based on the precursor salicin, this defense strategy is highly adapted to the secondary metabolites of the salicaceous plant which restricts the larvae in their forage. The third group is represented by several species of the *interrupta*-group belonging to the genus *Chrysomela*. They exhibit a combined biosynthetic strategy by using *de-novo* produced and phytogenic derived precursors to generate butyrate-esters as defensive compounds. Irrespective of different deterrent substances, the defensive systems of all groups exhibit *per se* a uniform architecture and morphology. Together with the self-contained biosynthesis of these compounds, the Chrysomelina larvae represent an excellent system to analyze regulatory processes as well as uncover evolutionary relationships regarding the defensive system.

In the present thesis, I identified and characterized enzymes essentially involved in the *de-novo* biosynthesis of the defensive compound Chrysomelidial of *P. cochleariae*.

8.1 REGULATION OF THE DE-NOVO BIOSYNTHESIS MEDIATED BY HMGR INHIBITION

Former feeding experiments with Ger-8-*S*-Glc and d_5-Ger-8-*O*-Glc clearly displayed that even *de-novo* producers are able to sequester precursors and incorporate them in the defensive secretions. This in turn implies the existence of regulatory mechanisms within *de-novo* biosynthesis to gain a benefit from sequestration. Therefore, geraniol, Ger-8-OH and Ger-8-*S*-Glc were tested regarding their regulatory impact on HMGR of *P. cochleariae* (*Pc*HMGR), one of the key enzymes within *de-novo* biosynthesis. Enzyme

assays with raw enzyme extract from fat body tissue display a strong inhibition of *Pc*HMGR by Ger-8-OH. The same result was obtained by using the heterologously expressed catalytic domain of *Pc*HMGR. Profound docking analysis on the basis of a high quality model of *Pc*HMGR re-emphasized our observations. The most preferred docking arrangement of Ger-8-OH appeared to be almost identical to the binding site of the natural substrate HMG. This in turn defined Ger-8-OH as competitive inhibitor for *Pc*HMGR and to regulate terpenoid biosynthesis *via* feedback inhibition.

Altogether, it can be noted that *Pc*HMGR represents an excellent target to regulate terpenoid biosynthesis and to mediate the homeostasis between *de-novo* produced and sequestered precursors. The ability of *de-novo* production promotes, in an evolutionary view, host plant switches without losing chemical defense. Consequently, new host plant species which might produce suitable precursors to sequester could be colonized. Therefore, regulation of *de-novo* biosynthesis and sequestration offers the larvae the possibility to adjust deterrent production *via* feedback inhibition on given biosynthetic demands. Sequestration enables a switch from an endogenous strategy to an energy saving tactic to decrease metabolic costs and to gain a benefit without developing new enzymes or mechanisms in comparison to the general *de-novo* production.

However, as a general control element *Pc*HMGR seems to be not selectively enough to specifically regulate deterrent biosynthesis. Given the circumstance that all terpenes are built up from the same precursors IDP and DMADP, provided by the mevalonate pathway, it is assumable that feedback inhibition of *Pc*HMGR also down-regulates other terpenoid pathways, like juvenile hormone biosynthesis. Therefore, more specific regulatory mechanisms have to be available to control and channel precursor production for different terpenoid fluxes within the larval metabolism

8.2 Co-factor mediated product specificity of PcIDS1

To ensure a highly efficient Chrysomelidial production, common as well as more selective regulatory processes within terpenoid biosynthesis are indispensable. Precursors for different terpenoid pathways need to be channeled to regulate the terpenoid metabolism on demand. Consequently, the influence of further downstream

processes, specifically involved in Chrysomelidial production, might be a more precise regulatory target. Therefore, I identified and characterized a short-chain isoprenyl diphosphate synthase (*sc*IDS) which catalyzes the production of terpenoid precursors. Besides terpene synthases IDSs are one of the most important branch points within terpenoid biosynthesis to regulate the huge variety of the terpenome.

RNAi, targeting the identified *sc*IDS from *P. cochleariae* (*Pc*IDS1), revealed direct participation of this enzyme in terpenoid biosynthesis due to a significant reduction of Ger-8-*O*-Glc as well as of defensive secretions. Enzymatic analysis of RNAi treated larvae simultaneously revealed a significant reduction of GDPS activity in the fat body tissue.

Interestingly, heterologously expressed *Pc*IDS1 possesses a promiscuous enzyme activity adjustable by external factors. Divalent metal ions, indispensable for enzyme activity, influence the product pattern significantly. If Mg^{2+} as co-factor and DMADP as substrate were used, a moderate FDP forming activity was observed. While providing GDP as allylic substrate a significantly higher FDPS activity was revealed. Astonishingly, product specificity of *Pc*IDS1 was shifted to an excellent GDPS activity when Co^{2+} was present as co-factor together with DMADP as substrate. Furthermore, several experiments clearly indicated that Co^{2+} dominates Mg^{2+} and binds with a higher affinity to *Pc*IDS1 even if Mg^{2+} is more than 1.000 times higher concentrated.

Kinetic data of *Pc*IDS1 in matters of the influence of Mg^{2+} and Co^{2+} show a significant shift regarding substrate affinity. The parameters substantiate our previous observations that the enzyme preferred DMADP as allylic substrate if Co^{2+} was given due to the lower K_m compared to GDP. Additionally, in the same experimental design we observed substrate inhibition of *Pc*IDS1 for IDP with a $K_{i[sub]}$ of 46.62 µM. It can be assumed that substrate inhibition is a further biologically relevant mechanism concerning self-regulation of *Pc*IDS1 (221). This ensures that *Pc*IDS1 does not extract undue quantities of IDP from the system, which in turn decreases DMADP and thereby destabilizes homeostasis. However, this effect was only observed in the combination of Co^{2+} and DMADP. Kinetic data of *Pc*IDS1 in combination with Mg^{2+} clearly show that GDP is the preferred allylic substrate. Measured data for DMADP resulted in a biphasic curve and did not allow a K_m calculation. An explanation could be that initially DMADP reacts with IDP to produce GDP, whereas in a subsequent reaction GDP competes with DMADP for binding at *Pc*IDS1. But due to the higher binding affinity, in combination with Mg^{2+}, GDP will bind to *Pc*IDS1 leading to the production of FDP.

The minimum equilibrium constant is at least 10^{28}-fold higher for Co^{2+} than for Mg^{2+}. Even if solvation effects may reduce the magnitude of this difference it still would be higher for Co^{2+} than for Mg^{2+}. In addition, quantum mechanical calculations, gas phase calculations as well as docking studies clearly emphasize that Co^{2+} compared to Mg^{2+} exhibits the significant higher binding affinity to both substrates and *Pc*IDS1.

The discovery of metal dependent product specificity of *Pc*IDS1 revealed a new type of metabolic regulation. In contrast to inventing new proteins or using alternative splicing to broaden enzyme spectra, co-factor mediated product specificity allows the highly selective control of metabolic fluxes by only one single enzyme (Fig. 13).

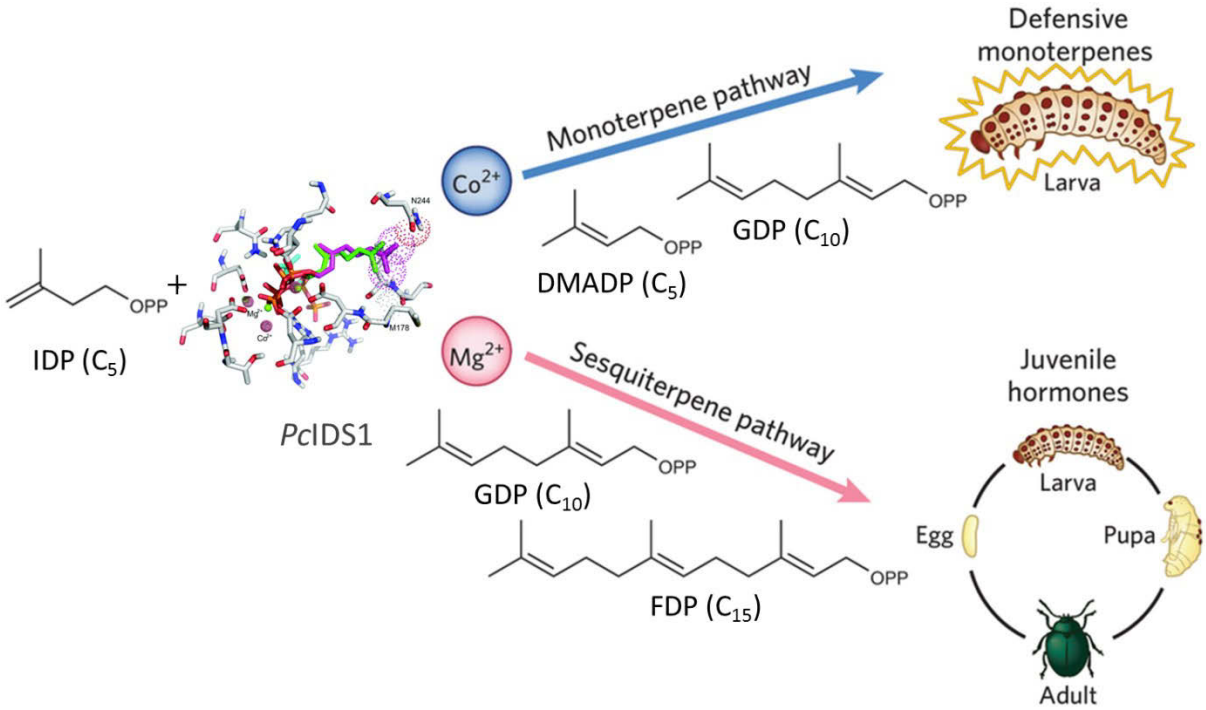

Fig. 13: Regulation of terpenoid pathways by metal co-factors. *Pc*IDS1 alters product specificity dependent on the present metal co-factor. If Co^{2+} is used as co-factor *Pc*IDS1 will prefer IDP and DMADP as substrate and produce the C_{10} compound GDP which is the precursor for chrysomelidial production. With Mg^{2+} as co-factor *Pc*IDS1 favors IDP and GDP to form FDP the C_{15} backbone of sesquiterpenes which are involved for example in the biosynthesis of juvenile hormones. (modified by (222))

9 Zusammenfassung

Larven des Subtribus Chrysomelina besitzen eine faszinierende, spezifisch an ihre Umwelt angepasste chemische Verteidigungsstrategie. Im Falle eines Angriffes von potentiellen Fraßfeinden setzen die Larven aus dorsalen Drüsen ein abschreckendes Wehrsekret frei. Aufgrund der ausgeklügelten Strategien der Wehrchemiebiosynthese werden die Chrysomelina-Larven in drei Gruppen unterteilen. Die basale Strategie basiert im Wesentlichen auf der wirtspflanzenunabhängigen *de-novo*-Biosynthese von Iridoiden, welche unter anderem bei *Phaedon cochleariae* und *Gastrophysa viridula* zu finden ist. Hiervon abgeleitete Arten, wie z.B. *Chrysomela populi,* nutzen hingegen die energetisch günstigere, jedoch wirtspflanzenabhängige Strategie der Sequestrierung von phenolischen Glukosiden. Hierbei wird die Vorstufe Salicin über die Nahrung aufgenommen und effizient im Drüsenreservoir zu Salicylaldehyd umgebaut. Die Wehrchemie ist somit stark an die Sekundärmetabolite der Pflanze angepasst und beschränkt die Larven in ihrem Lebensraum auf salicinhaltige Wirtspflanzen. Als dritte Strategie weist die sogenannte *interrupta*-Gruppe der Gattung *Chrysomela* eine Mischform aus *de-novo*-Produktion und Sequestrierung auf. Diese Larven sequestrieren glukosidisch gebundene Vorstufen und verestern diese mit *de-novo*-produzierten Aminosäure-Derivaten zu Butyrat-Estern. Trotz unterschiedlicher Zusammensetzung des Wehrsekretes weisen die Larven einen hohen Grad an Übereinstimmung hinsichtlich des morphologischen Aufbaus des Verteidigungsapparates auf. In Kombination mit der in sich abgeschlossenen Biosynthese stellen die Chrysomelina Larven daher ein einzigartiges Untersuchungsobjekt dar. Hierdurch können gezielt regulative Prozesse innerhalb der Wehrsekretbiosynthese als auch evolutionäre Zusammenhänge der chemischen Verteidigung untersucht werden.

In der vorliegenden Arbeit wurden regulatorische Enzyme, involviert in die *de-novo*-Synthese von Chrysomelidial, bei *Phaedon cochleariae* identifiziert und eingehend biochemisch charakterisiert

9.1 Regulation der De-Novo-Biosynthese mittels Inhibierung der HMGR

Vorangegangene Fütterungsexperimente mit Ger-8-*S*-Glc und d_5-Ger-8-*O*-Glc zeigten eindeutig die Aufnahme bzw. den Einbau dieser Vorstufen in das Wehrsekret und belegen, dass bereits in der basalen Gruppe der *de-novo*-Produzenten die Fähigkeit der Sequestrierung angelegt ist (58, 153). Diese Beobachtungen implizieren jedoch, dass innerhalb der *de-novo*-Biosynthese regulative Elemente vorhanden sein müssen, um aus sequestrierten Vorstufen einen energetischen Nutzen zu ziehen.

Es wurde daher der regulative Einfluss von Ger-8-*S*-Glc, Ger-8-OH und Geraniol auf die HMGR von *P. cochleariae* (*Pc*HMGR) untersucht, welches eines der Schlüsselenzyme innerhalb der Iridoid-Biosynthese darstellt. Dabei zeigte sich für Ger-8-OH eine inhibierende Wirkung auf *Pc*HMGR im Rohenzymextrakt des Fettkörpergewebes, der Hauptsyntheseort der Wehrsekretvorstufen. Im vergleichenden Experiment mit der rekombinant hergestellten katalytischen Domäne von *Pc*HMGR konnte die regulative Interaktion ebenfalls gezeigt werden. Diese Ergebnisse wurden zudem durch Docking-Studien mit Ger-8-OH an dem homologen Modell von *Pc*HMGR unterstützt. Hierbei zeigte sich, dass Ger-8-OH ähnlich wie das natürliche Substrat HMG an das katalytische Zentrum bindet und dabei als kompetitiver Inhibitor fungiert.

Im Gesamtbild lässt sich daher festhalten, dass HMGR von *P. cochleariae* bei der Homöostase zwischen *de-novo*-produzierten und möglichen sequestrierten Vorstufen regulativ fungieren kann. Die Fähigkeit der wirtspflanzenunabhängigen *de-novo*-Produktion erleichtert zudem einen Wirtspflanzenwechsel ohne direkten Verlust der chemischen Abwehr. Wohingegen die Fähigkeit zur Sequestrierung von nutzbaren Vorstufen, wenn sie in der Wirtspflanze vorhanden sind, einen Wechsel der Synthesestrategie ermöglichen. Die Kombination aus *de-novo*-Biosynthese und Sequestrierung eröffnet den Larven somit die Möglichkeit, ihre biochemische Wehrstrategie mittels regulatorischer Inhibierung an die gegebenen Bedingungen anzupassen. Der daraus resultierende energetische Nutzen würde den Larven einen deutlichen Vorteil gegenüber der reinen *de-novo*-Produktion bringen.

Als alleiniges Stellglied innerhalb der Iridoid-Biosynthese ist *Pc*HMGR allerdings nicht selektiv genug. Die Inhibierung von *Pc*HMGR würde möglicherweise nicht nur die Produktion von Chrysomelidial drosseln, sondern alle Terpenbiosynthesen. So würde

auch die Juvenilhormon Biosynthese, auf Grund ihrer allgemeinen Abhängigkeit von den Substraten IDP und DMADP, welche über den Mevalonatweg generiert werden, inhibiert werden.

9.2 *Cofaktoren vermittelte Regulation der Produktspezifität von PcIDS1*

Um eine effiziente Chrysomelidial-Produktion zu gewährleisten, sollten sowohl prinzipielle als auch selektiv wirkende Mechanismen vorliegen, welche die Vorstufen für die Terpenbiosynthesen bedarfsgenau im larvalen Metabolismus regulieren und kanalisieren. Die Beeinflussung von Enzymen, die spezifisch an der Produktion von Chrysomelidial beteiligt sind, erfordert eine stark gerichtete Regulation. Da es sich bei Chrysomelidial um ein Monoterpen handelt, stellen die *„short-chain"*-Isoprenyldiphosphatsynthasen (*sc*IDS) ein weiteres regulatorisches Stellglied dar. Sie katalysieren die Produktion der Terpenvorstufen und gelten neben den Terpensynthasen als eine der wichtigsten Regulationsebenen innerhalb der Terpenbiosynthese, um die Vielfalt des Terpenoms zu kanalisieren.

Die identifizierte *Pc*IDS1 aus *P. cochleariae* konnte mittels RNAi-Analysen in einen direkten Zusammenhang mit der Synthese von Ger-8-*O*-Glc gesetzt werden. Das *„silencing"* von *Pc*IDS1 führte sowohl zu einem deutlichen Rückgang der Vorstufe Ger-8-*O*-Glc als auch des Wehrsekretes an sich. Zudem weisen RNAi behandelten Larven einen signifikanten Verlust an GDPS-Aktivität im Fettkörpergewebe im Vergleich zu unbehandelten Larven auf und unterstützten damit vorangegangenen Beobachtungen.

Die fundierte Analyse der rekombinant hergestellten *Pc*IDS1 zeigt erstaunlicherweise eine promiskuitive Enzymaktivität. Das Produktprofil von *Pc*IDS1 kann signifikant durch den Einsatz verschiedener, essentieller, metallischer Cofaktoren beeinflusst werden. Nutzt das Enzym Mg^{2+} als Cofaktor und DMADP als Substrat, so erzeugt es in einer moderaten Enzymaktivität FDP als Hauptprodukt. Setzt man hingegen GDP als Substrat ein, kann eine gesteigerte FDPS-Aktivität beobachtet werden. Die geänderte Produktspezifität wird bei *Pc*IDS1 durch den Einsatz von Co^{2+}/Mn^{2+} als Cofaktor erzeugt. *Pc*IDS1 agiert, wenn DMADP als Substrat vorliegt als hoch effiziente GDPS. Des Weiteren konnte in verschiedensten Versuchen eindeutig gezeigt werden,

dass Co^{2+} dominant gegenüber Mg^{2+} ist. Co^{2+} wurde hierbei mit einer deutlich größeren Affinität von *Pc*IDS1 gebunden, auch wenn Mg^{2+} im 1000-fachen Überschuss vorlag.

Kinetische Analysen von *Pc*IDS1 hinsichtlich der Substrataffinität zeigen eine signifikante Abhängigkeit von Mg^{2+} und Co^{2+}. Im Fall von Mg^{2+} ist GDP als bevorzugtes Substrat bestimmt worden, wobei die Messungen für DMADP eine biphasische Aktivitätskurve zeigten. Es lässt sich hierbei vermuten, dass zwei Reaktionen stattfinden. In der ersten Phase wird DMADP als Substrat gebunden, wobei GDP als Produkt entsteht. Überschreitet GDP einen gewissen Schwellenwert wird es in der zweiten Phase, auf Grund der höheren Bindeaffinität zu *Pc*IDS1, zum präferiertes Substrat und weiter zu FDP umgesetzt. IDP erzeugt in Kombination mit Co^{2+} eine Substratinhibierung bei *Pc*IDS1, wenn DMADP als allylisches Substrat vorlag. Substratinhibierung könnte eine mögliche Selbstregulation von *Pc*IDS1 darstellen, um zu verhindern, dass dem System zu viel IDP entzogen wird. Dies wiederum hätte einen Rückgang von DMADP zur Folge, dass aus IDP gebildet wird. Im Vergleich der K_m-Werte für die Substrate DMADP und GDP zeigte sich für DMADP ein niedrigerer Wert, was die Produktspezifität von *Pc*IDS1 bereits vermuteten ließ. Thermodynamischen Berechnungen, sowie Docking-Studien am homologen Modell von *Pc*IDS1 zeigen übereinstimmend signifikant höherer Bindungsenergien und somit eine eindeutige Prävalenz für Co^{2+} als Cofaktor. Gasphasen-Kalkulationen ergaben, dass die Gleichgewichtskonstante für Co^{2+} im Vergleich zu Mg^{2+} um mehr als das 10^{28}-fache höher liegt. Selbst im Hinblick auf mögliche Solvatisierungseffekte würde ein Affinitätsvorteil für Co^{2+} bestehen bleiben und unterstreicht die gemessenen *in-vitro*-Daten.

Zusammenfassend lässt sich daher sagen, dass die Metallionenabhängige Produktspezifität von *Pc*IDS1 eine neue Art der metabolischen Regulation innerhalb des Terpenstoffwechsels ist. Im Unterschied zum alternativen Spleißen oder Genduplikationen, welches neue enzymatische Proteine zur Erweiterung des Produktspektrums hervorbringt, erlaubt die Cofaktor vermittelte Regulation mittels eines einzelnen Enzyms eine Kosten sparende und zugleich selektive Kontrolle von metabolischen Flüssen (Fig. 14).

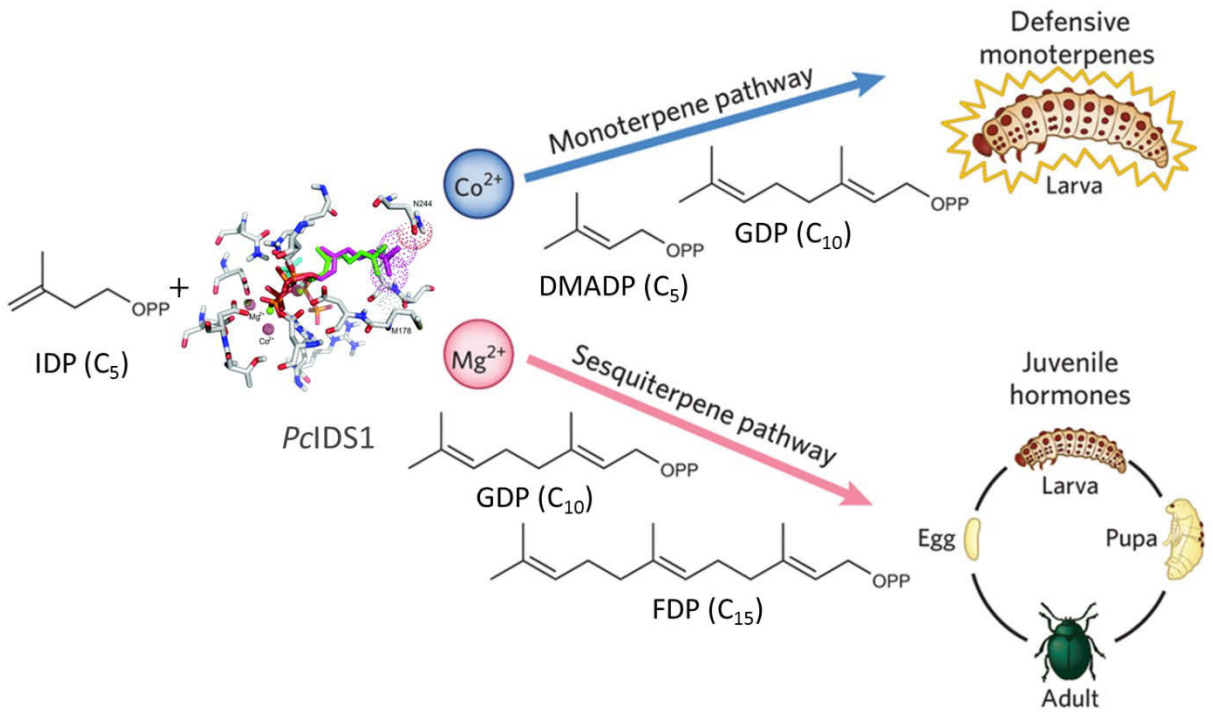

Fig. 14: Regulation der Terpenoid-Biosynthese unter dem Einfluss verschiedener metallischer Cofaktoren. *Pc*IDS1 kann seine Produktspezifität in Abhängigkeit von Metallionen verändern. Im Fall von Co^{2+} präferiert es die Substrate IDP und DMADP und produziert die C_{10}-Verbindung GDP. GDP dient als Vorstufe für die Biosynthese des pentazyklischen Monoterpens Chrysomelidial, der Abwehrstoff gegen potentielle Fraßfeinde. Wird Mg^{2+} als Cofaktor zugesetzt, sind IDP und GDP die favorisierten Substrate und *Pc*IDS1 produziert fast ausschließlich die C_{15}-Verbindung FDP. FDP dient als Vorstufe für die Biosynthese der Sesquiterpene, zu denen unter Anderem das JH zählt (modifiziert nach (222)).

10 CITATIONS

1. Oldfield E & Lin F-Y (2012) Terpene Biosynthesis: Modularity Rules. *Angewandte Chemie-International Edition* 51(5):1124-1137.
2. Kannenberg EL & Poralla K (1999) Hopanoid Biosynthesis and Function in Bacteria. *Naturwissenschaften* 86(4):168-176.
3. Espenshade PJ & Hughes AL (2007) Regulation of Sterol Synthesis in Eukaryotes. *Annual Review of Genetics* 41(1):401-427.
4. Matsumi R, Atomi H, Driessen AJM, & Oost Jvd (2011) Isoprenoid biosynthesis in Archaea - Biochemical and evolutionary implications. *Res. Microbiol.* 162(1):39-52.
5. Yalovsky S (2011) *Protein Prenylation CaaX Processing in Plants* (Elsevier Science Bv Sara Burgerhartstraat 25, Po Box 211, 1000 Ae Amsterdam, Netherlands,) pp 163-182
6. Zverina EA, Lamphear CL, Wright EN, & Fierke CA (2012) Recent advances in protein prenyltransferases: substrate identification, regulation, and disease interventions. *Current opinion in chemical biology* 16(5-6):544-552.
7. Bueno E, Mesa S, Bedmar EJ, Richardson DJ, & Delgado MJ (2012) Bacterial adaptation of respiration from oxic to microoxic and anoxic conditions: Redox control. *Antioxidants & Redox Signaling* 16(8):819-852.
8. Piller LE, Abraham M, Dormann P, Kessler F, & Besagni C (2012) Plastid lipid droplets at the crossroads of prenylquinone metabolism. *Journal of Experimental Botany* 63(4):1609-1618.
9. Shibata M*, et al.* (2004) Chlorophyll formation and photosynthetic activity in rice mutants with alterations in hydrogenation of the chlorophyll alcohol side chain. *Plant Science* 166(3):593-600.
10. Cazzonelli CI & Pogson BJ (2010) Source to sink: regulation of carotenoid biosynthesis in plants. *Trends in Plant Science* 15(5):266-274.
11. Hedden P & Thomas SG (2012) Gibberellin biosynthesis and its regulation. *Biochemical Journal* 444(1):11-25.
12. Belles X, Martin D, & Piulachs M-D (2005) The mevalonate pathway and the synthesis of juvenile hormone in insects. *Annual Review of Entomology* 50(1):181-199.
13. Hu J, Zhang Z, Shen W-J, & Azhar S (2010) Cellular cholesterol delivery, intracellular processing and utilization for biosynthesis of steroid hormones. *Nutrition & Metabolism* 7.
14. Gershenzon J & Dudareva N (2007) The function of terpene natural products in the natural world. *Nature Chemical Biology* 3(7):408-414.
15. Pichersky E, Noel JP, & Dudareva N (2006) Biosynthesis of plant volatiles: Nature's diversity and ingenuity. *Science* 311(5762):808-811.
16. Wallach O (1887) Zur Kenntniss der Terpene und ätherischen Oele. *Justus Liebigs Annalen der Chemie* 238(1-2):78-89.
17. Christmann M (2010) Otto Wallach: Founder of Terpene Chemistry and Nobel Laureate 1910. *Angewandte Chemie International Edition* 49(50):9580-9586.
18. Lynen F, Eggerer H, Henning U, & Kessel I (1958) Farnesyl-pyrophosphat und 3-Methyl-Δ3-butenyl-1-pyrophosphat, die biologischen Vorstufen des Squalens. Zur Biosynthese der Terpene, III. *Angewandte Chemie* 70(24):738-742.
19. Ruzicka L (1953) The isoprene rule and the biogenesis of terpenic compounds. *Experientia* 9(10):357-367.
20. Bloch K, Chaykin S, Phillips AH, & de Waard A (1959) Mevalonic acid pyrophosphate and isopentenylpyrophosphate. *Journal of Biological Chemistry* 234(10):2595-2604.
21. Gao Y, Honzatko RB, & Peters RJ (2012) Terpenoid synthase structures: a so far incomplete view of complex catalysis. *Nat. Prod. Rep.* 29(10):1153-1175.
22. Ruzicka L (1963) Perspektiven der Biogenese und der Chemie der Terpene. in *Justus Liebig's Annalen der Chemie*, pp 493–523.
23. Semmler FW (1910) Zur Kenntnis der Bestandteile ätherischer Öle (Tetrahydro-santalen, C15H28). *Berichte der deutschen chemischen Gesellschaft* 43(1):445-448.

24. Kerschbaum M (1913) Über den aliphatischen Sesquiterpen-Alkohol Farnesol. *Berichte der deutschen chemischen Gesellschaft* 46(2):1732-1737.
25. Lange BM, Rujan T, Martin W, & Croteau R (2000) Isoprenoid biosynthesis: The evolution of two ancient and distinct pathways across genomes. *Proceedings of the National Academy of Sciences of the United States of America* 97(24):13172-13177.
26. Rohmer M (1999) The mevalonate-independent methylerythritol 4-phosphate (MEP) pathway for isoprenoid biosynthesis, including carotenoids. *Pure Appl. Chem.* 71(12):2279-2284.
27. Rohmer M (1999) The discovery of a mevalonate-independent pathway for isoprenoid biosynthesis in bacteria, algae and higher plants. *Nat. Prod. Rep.* 16(5):565-574.
28. Kim DY, Bochar DA, Stauffacher CV, & Rodwell VW (1999) Expression and characterization of the HMG-CoA reductase of the thermophilic archaeon Sulfolobus solfataricus. *Protein Expression and Purification* 17(3):435-442.
29. Wilding EI*, et al.* (2000) Identification, evolution, and essentiality of the mevalonate pathway for isopentenyl diphosphate biosynthesis in gram-positive cocci. *Journal of Bacteriology* 182(15):4319-4327.
30. Eisenreich W, Bacher A, Arigoni D, & Rohdich F (2004) Biosynthesis of isoprenoids via the non-mevalonate pathway. *Cellular and Molecular Life Sciences* 61(12):1401-1426.
31. Chappell J (1995) The biochemistry and molecular-biology of isoprenoid metabolism. *Plant Physiol* 107(1):1-6.
32. McGarvey DJ & Croteau R (1995) Terpenoid Metabolism. *Plant Cell* 7(7):1015-1026.
33. Ferguson JJ, Durr IF, & Rudney H (1959) The biosynthesis of mevalonic acid. *Proceedings of the National Academy of Sciences* 45(4):499-504.
34. Lynen F, Agranoff BW, Eggerer H, Henning U, & Moslein EM (1959) Gamma-gamma-dimethyl-allyl-pyrophosphate and geranyl-pyrophosphate, biological preliminary stages of squalene .6. Biosynthesis of terpenes. *Angewandte Chemie-International Edition* 71(21):657-663.
35. Agranoff BW, Eggerer H, Henning U, & Lynen F (1960) Biosynthesis of terpenes .7. Isopentenyl pyrophosphate isomerase. *Journal of Biological Chemistry* 235(2):326-332.
36. Tchen TT (1958) Mevalonic kinase - purification and properties. *Journal of Biological Chemistry* 233(5):1100-1103.
37. Poulter CD & Rilling HC (1976) Prenyltransferase - mechanism of reaction. *Biochemistry* 15(5):1079-1083.
38. Poulter CD, Argyle JC, & Mash EA (1977) Prenyltransferase - new evidence for an "ionization-condensation-elimination mechanism with 2-fluorogeranyl pyrophosphate. *Abstr. Pap. Am. Chem. Soc.* 173(MAR20):7-7.
39. Croteau R & Purkett PT (1989) Geranyl pyrophosphate synthase - characterization of the enzyme and evidence that this chain-length specific prenyltransferase is associated with monoterpene biosynthesis in sage (salvia-officinalis). *Archives of Biochemistry and Biophysics* 271(2):524-535.
40. Wang KC & Ohnuma S (2000) Isoprenyl diphosphate synthases. *Biochimica et Biophysica Acta-Molecular and Cell Biology of Lipids* 1529(1-3):33-48.
41. Kharel Y & Koyama T (2003) Molecular analysis of cis-prenyl chain elongating enzymes. *Nat. Prod. Rep.* 20(1):111-118.
42. Liang PH (2009) Reaction kinetics, catalytic mechanisms, conformational changes, and inhibitor design for prenyltransferases. *Biochemistry* 48(28):6562-6570.
43. Schilmiller AL*, et al.* (2009) Monoterpenes in the glandular trichomes of tomato are synthesized from a neryl diphosphate precursor rather than geranyl diphosphate. *Proceedings of the National Academy of Sciences* 106(26):10865-10870.
44. Schilmiller AL, Schauvinhold I, Charbonneau A, Last RL, & Pichersky E (2009) A new route for monoterpene biosynthesis in tomato glandular trichomes: the use of neryl diphosphate rather than geranyl diphosphate as substrate. *Plant Biology (Rockville)* 2009(Suppl. S):378.
45. Schulbach MC, Brennan PJ, & Crick DC (2000) Identification of a Short (C15) ChainZ-Isoprenyl Diphosphate Synthase and a Homologous Long (C50) Chain Isoprenyl

Diphosphate Synthase inMycobacterium tuberculosis. *Journal of Biological Chemistry* 275(30):22876-22881.

46. Ambo T, Noike M, Kurokawa H, & Koyama T (2008) Cloning and functional analysis of novel short-chain cis-prenyltransferases. *Biochemical and Biophysical Research Communications* 375(4):536-540.
47. Liang PH, Ko TP, & Wang AHJ (2002) Structure, mechanism and function of prenyltransferases. *European Journal of Biochemistry* 269(14):3339-3354.
48. Tholl D (2006) Terpene synthases and the regulation, diversity and biological roles of terpene metabolism. *Current Opinion in Plant Biology* 9(3):297-304.
49. Friesen JA & Rodwell VW (2004) The 3-hydroxy-3-methylglutaryl coenzyme-A (HMG-CoA) reductases. *Genome Biol.* 5(11).
50. Bochar DA, Stauffacher CV, & Rodwell VW (1999) Sequence comparisons reveal two classes of 3-hydroxy-3-methylglutaryl coenzyme A reductase. *Molecular Genetics and Metabolism* 66(2):122-127.
51. Rodwell VW, *et al.* (2000) 3-hydroxy-3-methylglutaryl-CoA reductase. *Branched-Chain Amino Acids, Pt B,* Methods in Enzymology, (Academic Press Inc, San Diego), Vol 324, pp 259-280.
52. Lawrence CM, Rodwell VW, & Stauffacher CV (1995) Crystal-structure of pseudomonas-mevalonii hmg-coa reductase at 3.0 angstrom resolution. *Science* 268(5218):1758-1762.
53. Beach MJ & Rodwell VW (1989) Cloning, sequencing, and overexpression of mvaa, which encodes pseudomonas-mevalonii 3-hydroxy-3-methylglutaryl coenzyme-a reductase. *Journal of Bacteriology* 171(6):2994-3001.
54. Istvan ES & Deisenhofer J (2000) The structure of the catalytic portion of human HMG-CoA reductase. *Biochimica Et Biophysica Acta-Molecular and Cell Biology of Lipids* 1529(1-3):9-18.
55. Istvan ES, Palnitkar M, Buchanan SK, & Deisenhofer J (2000) Crystal structure of the catalytic portion of human HMG-CoA reductase: insights into regulation of activity and catalysis. *EMBO Journal* 19(5):819-830.
56. Liscum L, *et al.* (1985) Domain-structure of 3-hydroxy-3-methylglutaryl coenzyme-a reductase, a glycoprotein of the endoplasmic-reticulum. *Journal of Biological Chemistry* 260(1):522-530.
57. Frimpong K & Rodwell VW (1994) Catalysis by syrian-hamster 3-hydroxy-3-methylglutaryl-coenzyme-a reductase - proposed roles of histidine-865, glutamate-558, and aspartate-766. *Journal of Biological Chemistry* 269(15):11478-11483.
58. Burse A, *et al.* (2008) Implication of HMGR in homeostasis of sequestered and *de-novo* produced precursors of the iridoid biosynthesis in leaf beetle larvae. *Insect Biochemistry & Molecular Biology* 38(1):76-88.
59. Burg JS & Espenshade PJ (2011) Regulation of HMG-CoA reductase in mammals and yeast. *Progress in Lipid Research* 50(4):403-410.
60. Osborne TF, Gil G, Goldstein JL, & Brown MS (1988) Operator constitutive mutation of 3-hydroxy-3-methylglutaryl coenzyme-a reductase promoter abolishes protein-binding to sterol regulatory element. *Journal of Biological Chemistry* 263(7):3380-3387.
61. Rajavashisth TB, Shukla AK, & Shah PK (2000) HMG-CoA reductase inhibitors downregulate M-CSF expression in vascular endothelial cells. *Molecular Biology of the Cell* 11:26A-27A.
62. Rosenthal RS & Rodwell VW (1998) Purification and characterization of the heteromeric transcriptional activator MvaT of the Pseudomonas mevalonii mvaAB operon. *Protein Science* 7(1):178-184.
63. Nakanishi M, Goldstein JL, & Brown MS (1988) Multivalent control of 3-hydroxy-3-methylglutaryl coenzyme-a reductase - mevalonate-derived product inhibits translation of messenger-rna and accelerates degradation of enzyme. *Journal of Biological Chemistry* 263(18):8929-8937.
64. Peffley D & Sinensky M (1985) Regulation of 3-hydroxy-3-methylglutaryl coenzyme-a reductase synthesis by a non-sterol mevalonate-derived product in mev-1 cells - apparent translational control. *Journal of Biological Chemistry* 260(18):9949-9952.

65. Tanaka RD, Edwards PA, & Fogelman AM (1983) Regulation of Hmg-Coa Reductase by 25-Hydroxycholesterol. *Journal of Lipid Research* 24(10):1414-1414.
66. Goldstein JL & Brown MS (1990) Regulation of the Mevalonate Pathway. *Nature* 343(6257):425-430.
67. Skalnik DG, Narita H, Kent C, & Simoni RD (1988) The membrane domain of 3-hydroxy-3-methylglutaryl-coenzyme-a reductase confers endoplasmic-reticulum localization and sterol-regulated degradation onto beta-galactosidase. *Journal of Biological Chemistry* 263(14):6836-6841.
68. Radhakrishnan A, Ikeda Y, Kwon HJ, Brown MS, & Goldstein JL (2007) Sterol-regulated transport of SREBPs from endoplasmic reticulum to Golgi: Oxysterols block transport by binding to Insig. *Proceedings of the National Academy of Sciences* 104(16):6511-6518.
69. Gardner R, Cronin S, Leder B, Rine J, & Hampton R (1999) Sequence determinants for regulated degradation of yeast 3-Hydroxy-3-Methylglutaryl-CoA reductase, an integral endoplasmic reticulum membrane protein (vol 9, pg 2611, 1999). *Molecular Biology of the Cell* 10(3).
70. Gardner RG & Hampton RY (1999) A highly conserved signal controls degradation of 3-hydroxy-3-methylglutaryl-coenzyme A (HMG-CoA) reductase in eukaryotes. *Journal of Biological Chemistry* 274(44):31671-31678.
71. Janssens V & Goris J (2001) Protein phosphatase 2A: a highly regulated family of serine/threonine phosphatases implicated in cell growth and signalling. *Biochem. J.* 353(3):417-439.
72. Hemmerlin A, Rivera SB, Erickson HK, & Poulter CD (2003) Enzymes encoded by the farnesyl diphosphate synthase gene family in the big sagebrush artemisia tridentata ssp. Spiciformis. *Journal of Biological Chemistry* 278(34):32132-32140.
73. Attucci S, Aitken SM, Gulick PJ, & Ibrahim RK (1995) Farnesyl pyrophosphate synthase from white lupin - molecular-cloning, expression, and purification of the expressed protein. *Archives of Biochemistry and Biophysics* 321(2):493-500.
74. Attucci S, Aitken SM, Ibrahim RK, & Gulick PJ (1995) A cDNA encoding farnesyl pyrophosphate synthase in white lupin. *Plant Physiol* 108(2):835-836.
75. Cunillera N, *et al.* (1996) Arabidopsis thaliana contains two differentially expressed farnesyl-diphosphate synthase genes. *Journal of Biological Chemistry* 271(13):7774-7780.
76. Gupta P, Akhtar N, Tewari SK, Sangwan RS, & Trivedi PK (2011) Differential expression of farnesyl diphosphate synthase gene from Withania somnifera in different chemotypes and in response to elicitors. *Plant Growth Regulation* 65(1):93-100.
77. Schmidt A, *et al.* (2011) Induction of isoprenyl diphosphate synthases, plant hormones and defense signalling genes correlates with traumatic resin duct formation in Norway spruce (Picea abies). *Plant Mol.Biol* 77(6):577-590.
78. Cusson M, *et al.* (2006) Characterization and tissue-specific expression of two lepidopteran farnesyl diphosphate synthase homologs: Implications for the biosynthesis of ethyl-substituted juvenile hormones. *Proteins-Structure Function and Bioinformatics* 65(3):742-758.
79. Zhang Y-L & Li Z-X (2012) Functional analysis and molecular docking identify two active short-chain prenyltransferases in the green peach aphid, *Myzus persicae*. *Archives of Insect Biochemistry and Physiology* 81(2):63-76.
80. Vandermoten S, *et al.* (2008) Characterization of a novel aphid prenyltransferase displaying dual geranyl/farnesyl diphosphate synthase activity. *FEBS Lett.* 582(13):1928-1934.
81. Vandermoten S, *et al.* (2009) Structural features conferring dual Geranyl/Farnesyl diphosphate synthase activity to an aphid prenyltransferase. *Insect Biochemistry and Molecular Biology* 39(10):707-716.
82. Vandermoten S, Haubruge E, & Cusson M (2009) New insights into short-chain prenyltransferases: structural features, evolutionary history and potential for selective inhibition. *Cellular and Molecular Life Sciences* 66(23):3685-3695.

83. Ma G-Y, Sun X-F, Zhang Y-L, Li Z-X, & Shen Z-R (2010) Molecular cloning and characterization of a prenyltransferase from the cotton aphid, *Aphis gossypii*. *Insect Biochemistry and Molecular Biology* 40(7):552-561.
84. Sen SE*, et al.* (2007) Purification, properties and heteromeric association of type-1 and type-2 lepidopteran farnesyl diphosphate synthases. *Insect Biochemistry and Molecular Biology* 37(8):819-828.
85. Sen SE, Trobaugh C, Beliveau C, Richard T, & Cusson M (2007) Cloning, expression and characterization of a dipteran farnesyl diphosphate synthase. *Insect Biochemistry and Molecular Biology* 37(11):1198-1206.
86. Ishii K, Sagami H, & Ogura K (1985) Decaprenyl pyrophosphate synthetase from *Paracoccus denitrificans*. *Biochimica et Biophysica Acta* 835(2):291-297.
87. Sagami H, Ogura K, Weiner A, & Poulter CD (1984) Effect of zinc ions on farnesyl pyrophosphate synthetase-activity. *Biochemistry International* 8(5):661-667.
88. Tholl D, Croteau R, & Gershenzon J (2001) Partial purification and characterization of the short-chain prenyltransferases, geranyl diphosphate synthase and farnesyl diphosphate synthase, from abies grandis (grand fir). *Archives of Biochemistry and Biophysics* 386(2):233-242.
89. Gershenzon J & Kreis J (1999) Biochemistry of terpenoids: monoterpenes, sesquiterpenes, diterpenes, sterols, cardiac glycosides, and steroid saponins. *Biochemistry of Plant Secondary Metabolism*, ed Wink M (Sheffield Academic Press, Sheffield, UK), pp 222–299.
90. Poulter CD & Rilling HC (1981) Prenyl transferases and isomerase. *Biosynthesis of Isoprenoid Compounds* 1:161-224.
91. Poulter CD (1995) Mechanistic studies of the prenyl transfer reaction. *Abstracts of Papers American Chemical Society* 209(1-2):ORGN 140.
92. Thulasiram HV & Poulter CD (2006) Farnesyl diphosphate synthase: The art of compromise between substrate selectivity and stereoselectivity. *Journal of the American Chemical Society* 128(49):15819-15823.
93. Tarshis LC, Yan MJ, Poulter CD, & Sacchettini JC (1994) Crystal-structure of recombinant farnesyl diphosphate synthase at 2.6-angstrom resolution. *Biochemistry* 33(36):10871-10877.
94. Wallrapp FH*, et al.* (2013) Prediction of function for the polyprenyl transferase subgroup in the isoprenoid synthase superfamily. *Proceedings of the National Academy of Sciences of the United States of America* 110(13):E1196-E1202.
95. Aaron JA & Christianson DW (2010) Trinuclear metal clusters in catalysis by terpenoid synthases. *Pure Appl. Chem.* 82(8):1585-1597.
96. Brandt W*, et al.* (2009) Molecular and structural basis of metabolic diversity mediated by prenyldiphosphate converting enzymes. *Phytochemistry* 70(15-16):1758-1775.
97. Guo RT*, et al.* (2005) Crystal structures of undecaprenyl pyrophosphate synthase in complex with magnesium, isopentenyl pyrophosphate, and farnesyl thiopyrophosphate - Roles of the metal ion and conserved residues in catalysis. *Journal of Biological Chemistry* 280(21):20762-20774.
98. Ogawa T, Yoshimura T, & Hemmi H (2011) Connected cavity structure enables prenyl elongation across the dimer interface in mutated geranylfarnesyl diphosphate synthase from Methanosarcina mazei. *Biochemical and Biophysical Research Communications* 409(2):333-337.
99. Narita K, Ohnuma S, & Nishino T (1999) Protein design of geranyl diphosphate synthase. Structural features that de line the product specificities of prenyltransferases. *Journal of Biochemistry* 126(3):566-571.
100. Ohnuma S*, et al.* (1996) A role of the amino acid residue located on the fifth position before the first aspartate-rich motif of farnesyl diphosphate synthase on determination of the final product. *Journal of Biological Chemistry* 271(48):30748-30754.
101. Vandermoten S, Cusson M, Francis F, & Haubruge E (2008) Isoprenoid metabolism in aphids: a new target for bio-insecticides development? *Biotechnologie Agronomie Societe Et Environnement* 12(4):451-460.

102. Kellogg BA & Poulter CD (1997) Chain elongation in the isoprenoid biosynthetic pathway. *Current Opinion in Chemical Biology* 1(4):570-578.
103. Tarshis LC, Proteau PJ, Kellogg BA, Sacchettini JC, & Poulter CD (1996) Regulation of product chain length by isoprenyl diphosphate synthases. *Proceedings of the National Academy of Sciences, USA* 93(26):15018-15023.
104. Fernandez SMS, Kellogg BA, & Poulter CD (2000) Farnesyl diphosphate synthase. Altering the catalytic site to select for geranyl diphosphate activity. *Biochemistry* 39(50):15316-15321.
105. Koyama T (1999) Molecular analysis of prenyl chain elongating enzymes. *Biosci. Biotechnol. Biochem.* 63(10):1671-1676.
106. Ohnuma S*, et al.* (1998) A pathway where polyprenyl diphosphate elongates in prenyltransferase - Insight into a common mechanism of chain length determination of prenyltransferases. *Journal of Biological Chemistry* 273(41):26705-26713.
107. Chang T-H*, et al.* (2010) Structure of a heterotetrameric geranyl pyrophosphate synthase from mint (mentha piperita) reveals intersubunit regulation. *Plant Cell* 22(2):454-467.
108. Ohnuma S, Koyama T, & Ogura K (1992) Chain-length distribution of the products formed in solanesyl diphosphate synthase reaction. *Journal of Biochemistry* 112(6):743-749.
109. Ohnuma S, Koyama T, & Ogura K (1993) Solanesyl diphosphate synthase reaction with artificial substrates - formation of r-enantiomers and s-enantiomers of 4-methyl and 8-methyl derivatives of geranylgeranyl diphosphate. *Bioorg. Med. Chem. Lett.* 3(12):2733-2738.
110. Ohnuma S, Koyama T, & Ogura K (1993) Alteration of the product specificities of prenyltransferases by metal-ions. *Biochemical and Biophysical Research Communications* 192(2):407-412.
111. Fujii H, Sagami H, Koyama T, Ogura K, & Seto S (1980) Variable product specificity of solanesyl pyrophosphate synthetase. *Biochemical and Biophysical Research Communications* 96(4):1648-1653.
112. Gilg AB, Tittiger C, & Blomquist GJ (2009) Unique animal prenyltransferase with monoterpene synthase activity. *Naturwissenschaften* 96(6):731-735.
113. Gilg AB, Bearfield JC, Tittiger C, Welch WH, & Blomquist GJ (2005) Isolation and functional expression of an animal geranyl diphosphate synthase and its role in bark beetle pheromone biosynthesis. *Proceedings of the National Academy of Sciences, USA* 102(28):9760-9765.
114. Song M*, et al.* (2013) Functional characterization of myrcene hydroxylases from two geographically distinct Ips pini populations. *Insect Biochemistry and Molecular Biology* 43(4):336-343.
115. Fernandez-Grandon GM, Woodcock CM, & Poppy GM (2013) Do asexual morphs of the peach-potato aphid, Myzus persicae, utilise the aphid sex pheromone? Behavioural and electrophysiological responses of M. persicae virginoparae to (4aS,7S,7aR)-nepetalactone and its effect on aphid performance. *Bulletin of entomological research* 103(4):466-472.
116. Birkett MA & Pickett JA (2003) Aphid sex pheromones: from discovery to commercial production. *Phytochemistry* 62(5):651-656.
117. Stewart-Jones A*, et al.* (2007) Structure, ratios and patterns of release in the sex pheromone of an aphid, Dysaphis plantaginea. *J. Exp. Biol* 210(24):4335-4344.
118. Vandermoten S, Mescher MC, Francis F, Haubruge E, & Verheggen FJ (2012) Aphid alarm pheromone: An overview of current knowledge on biosynthesis and functions. *Insect Biochemistry and Molecular Biology* 42(3):155-163.
119. Termonia A, Hsiao TH, Pasteels JM, & Milinkovitch MC (2001) Feeding specialization and host-derived chemical defense in Chrysomeline leaf beetles did not lead to an evolutionary dead end. *Proceedings of the National Academy of Sciences of the United States of America* 98(7):3909-3914.
120. Daloze D & Pasteels JM (1979) Production of cardiac-glycosides by chrysomelid beetles and larvae. *Journal of Chemical Ecology* 5(1):63-77.

121. Pasteels JM, Braekman JC, Daloze D, & Ottinger R (1982) Chemical defense in chrysomelid larvae and adults. *Tetrahedron* 38(13):1891-1897.
122. Pasteels JM, Daloze D, & Rowellrahier M (1986) Chemical defense in chrysomelid eggs and neonate larvae. *Physiological Entomology* 11(1):29-37.
123. Hinton H (1951) On a little-known protective device of some Chrysomelid pupae (Coleoptera). *Pros. R. Ent. Soc. Lond.* 26:4-6.
124. Renner K (1970) Über die ausstülpbaren Hautblasen der Larven von Gastroidea viridula De Geer und ihre ökologische Bedeutung. 20(5):527-533.
125. Garb G (1915) The eversible glands of a Chrysomelid larva, *Melasoma lapponica*. *J. Entomol. Zool.* 8:88-97.
126. Pasteels JM, Duffey S, & Rowellrahier M (1990) Toxins in chrysomelid beetles - possible evolutionary sequence from denovo synthesis to derivation from food-plant chemicals. *Journal of Chemical Ecology* 16(1):211-222.
127. Rowellrahier M & Pasteels JM (1986) Economics of chemical defense in chrysomelinae. *Journal of Chemical Ecology* 12(5):1189-1203.
128. Pasteels JM, Gregoire JC, & Rowellrahier M (1983) The Chemical Ecology of Defense in Arthropods. *Annual Review of Entomology* 28:263-289.
129. Pasteels JM, Rowellrahier M, Braekman JC, & Dupont A (1983) Salicin from host plant as precursor of salicylaldehyde in defensive secretion of chrysomeline larvae. *Physiological Entomology* 8(3):307-314.
130. Kuhn J, *et al.* (2004) Selective transport systems mediate sequestration of plant glucosides in leaf beetles: A molecular basis for adaptation and evolution. *Proceedings of the National Academy of Sciences of the United States of America* 101(38):13808-13813.
131. Discher S, *et al.* (2009) A versatile transport network for sequestering and excreting plant glycosides in leaf beetles provides an evolutionary flexible defense strategy. *Chembiochem* 10(13):2223-2229.
132. Blum MS, Brand JM, Wallace JB, & Fales HM (1972) Chemical characterization of defensive secretion of a chrysomelid larva. *Life Sciences Pt-2 Biochemistry General and Molecular Biology* 11(10):525-&.
133. Schulz S, Gross J, & Hilker M (1997) Origin of the defensive secretion of the leaf beetle Chrysomela lapponica. *Tetrahedron* 53(27):9203-9212.
134. Hilker M & Schulz S (1994) Composition of larval secretion of Chrysomela lapponica (coleoptera, chrysomelidae) and its dependence on host-plant. *Journal of Chemical Ecology* 20(5):1075-1093.
135. Termonia A & Pasteels JM (1999) Larval chemical defence and evolution of host shifts in Chrysomela leaf beetles. *Chemoecology* 9(1):13-23.
136. Kuhn J, *et al.* (2007) Sequestration of plant-derived phenolglucosides by larvae of the leaf beetle Chrysomela lapponica: Thioglucosides as mechanistic probes. *Journal of Chemical Ecology* 33(1):5-24.
137. Meinwald J, Jones TH, Eisner T, & Hicks K (1977) Defense-mechanisms of arthropods .56. New methylcyclopentanoid terpenes from larval defensive secretion of a chrysomelid beetle (plagiodera-versicolora). *Proceedings of the National Academy of Sciences of the United States of America* 74(6):2189-2193.
138. Blum MS, *et al.* (1978) Chrysomelidial in defensive secretion of leaf beetle gastrophysa-cyanea melsheimer. *Journal of Chemical Ecology* 4(1):47-53.
139. Soe ARB, Bartram S, Gatto N, & Boland W (2004) Are iridoids in leaf beetle larvae synthesized *de-novo* or derived from plant precursors? A methodological approach. *Isotopes in Environmental and Health Studies* 40(3):175-180.
140. Frick S, *et al.* (2013) Metal ions control product specificity of isoprenyl diphosphate synthases in the insect terpenoid pathway. *Proceedings of the National Academy of Sciences* 110(11):4194-4199.
141. Burse A, *et al.* (2007) Iridoid biosynthesis in Chrysomelina larvae: Fat body produces early terpenoid precursors. *Insect Biochemistry & Molecular Biology* 37(3):255-265.

142. Veith M, Lorenz M, Boland W, Simon H, & Dettner K (1994) Biosynthesis of iridoid monoterpenes in insects - defensive secretions from larvae of leaf beetles (coleoptera, chrysomelidae). *Tetrahedron* 50(23):6859-6874.
143. Lorenz M, Boland W, & Dettner K (1993) Biosynthesis of iridodials in the defense glands of beetle larvae (chrysomelinae). *Angewandte Chemie-International Edition in English* 32(6):912-914.
144. Daloze D & Pasteels JM (1994) Isolation of 8-Hydroxygeraniol-8-O-Beta-D-Glucoside, a Probable Intermediate in Biosynthesis of Iridoid Monoterpenes, from Defensive Secretions of Plagiodera-Versicolora and Gastrophysa-Viridula (Coleoptera, Chrysomelidae). *Journal of Chemical Ecology* 20(8):2089-2097.
145. Veith M, Dettner K, & Boland W (1996) Stereochemistry of an alcohol oxidase from the defensive secretion of larvae of the leaf beetle Phaedon armoraciae (Coleoptera: Chrysomelidae). *Tetrahedron* 52(19):6601-6612.
146. Veith M, Oldham NJ, Dettner K, Pasteels JM, & Boland W (1997) Biosynthesis of defensive allomones in leaf beetle larvae: Stereochemistry of salicylalcohol oxidation in Phratora vitellinae and comparison of enzyme substrate and stereospecificity with alcohol oxidases from several iridoid producing leaf beetles. *Journal of Chemical Ecology* 23(2):429-443.
147. Oldham NJ & Boland W (1996) Chemical ecology: Multifunctional compounds and multitrophic interactions. *Naturwissenschaften* 83(6):248-254.
148. Oldham NJ, Veith M, Boland W, & Dettner K (1996) Iridoid monoterpene biosynthesis in insects: Evidence for a *de-novo* pathway occurring in the defensive glands of Phaedon armoraciae (Chrysomelidae) leaf beetle larvae. *Naturwissenschaften* 83(10):470-473.
149. Laurent P, Braekman JC, Daloze D, & Pasteels J (2003) Biosynthesis of defensive compounds from beetles and ants. *European Journal of Organic Chemistry* (15):2733-2743.
150. Soetens P, Pasteels JM, & Daloze D (1993) A simple method for in-vivo testing of glandular enzymatic-activity on potential precursors of larval defensive compounds in phratora-species (coleoptera, chrysomelinae). *Experientia* 49(11):1024-1026.
151. Bruckmann M, Termonia A, Pasteels JM, & Hartmann T (2002) Characterization of an extracellular salicyl alcohol oxidase from larval defensive secretions of Chrysomela populi and Phratora vitellinae (Chrysomelina). *Insect Biochemistry & Molecular Biology* 32(11):1517-1523.
152. Feld BK, Pasteels JM, & Boland W (2001) Phaedon cochleariae and Gastrophysa viridula (Coleoptera : Chrysomelidae) produce defensive iridoid monoterpenes *de-novo* and are able to sequester glycosidically bound terpenoid precursors. *Chemoecology* 11(4):191-198.
153. Kunert M*, et al.* (2008) *De-novo* biosynthesis versus sequestration: A network of transport systems supports in iridoid producing leaf beetle larvae both modes of defense. *Insect Biochemistry & Molecular Biology* 38(10):895-904.
154. Hilker M (1993) Chemische Ökologie juveniler Entwicklungsstadien der Blattkäfer (Coleoptera, Chrysomelindae). Habitilationsschrift (Universität Bayreuth, Verlag: Bayreuther Forum Ökologie, Bayreuth).
155. Jolivet P, Petitpierre E, & Hsiao TH (1988) *Biology of Chrysomelidae* (Springer Netherlands).
156. Rowell-Rahier M, Pasteels JM, Alonso-Media A, & Brower LP (1995) Relative unpalatability of leaf beetles with either biosynthesized or sequestered chemical defence. *Animal Behaviour* 49(3):709-714.
157. Denno RF, Larsson S, & Olmstead KL (1990) Role of enemy-free space and plant-quality in host-plant selection by willow beetles. *Ecology* 71(1):124-137.
158. Pasteels JM, Rowellrahier M, Braekman JC, Daloze D, & Duffey S (1989) Evolution of Exocrine Chemical Defense in Leaf Beetles (Coleoptera, Chrysomelidae). *Experientia* 45(3):295-300.
159. Gross J, Fatouros NE, & Hilker M (2004) The significance of bottom-up effects for host plant specialization in Chrysomela leaf beetles. *Oikos* 105(2):368-376.

160. Pasteels JM, Braekman JC, Daloze D, & Ottinger R (1982) Chemical defence in chrysomelid larvae and adults. *Tetrahedron* 38(13):1891-1897.
161. Pasteels JM, Rowellrahier M, Braekman JC, & Daloze D (1984) Chemical Defenses in Leaf Beetles and Their Larvae - the Ecological, Evolutionary and Taxonomic Significance. *Biochemical Systematics and Ecology* 12(4):395-406.
162. Kopf A*, et al.* (1998) The evolution of host-plant use and sequestration in the leaf beetle genus phratora (coleoptera, chrysomelidae). *Evolution* 52(2):517-528.
163. Kirsch R*, et al.* (2011) Host plant shifts affect a major defense enzyme in Chrysomela lapponica. *Proceedings of the National Academy of Sciences of the United States of America* 108:4897 - 4901.
164. Kirsch R, Vogel H, Pasteels J, & Boland W (2011) To be or not to be convergent in salicin-based defense in chrysomeline leaf beetle larvae: Evidence from Phratora vitellinae SAO. *Proceedings of the Royal Society of London Series B-Biological Sciences* 278:3225 - 3232.
165. Correll CC & Edwards PA (1994) Mevalonic acid-dependent degradation of 3-hydroxy-3-methylglutaryl-coenzyme-a reductase in-vivo and in-vitro. *Journal of Biological Chemistry* 269(1):633-638.
166. Meigs TE, Roseman DS, & Simoni RD (1996) Regulation of 3-hydroxy-3-methylglularyl-coenzyme A reductase degradation by the nonsterol mevalonate metabolite farnesol *in-vivo*. *Journal of Biological Chemistry* 271(14):7916-7922.
167. Meigs TE & Simoni RD (1997) Farnesol as a regulator of HMG-CoA reductase degradation: Characterization and role of farnesyl pyrophosphatase. *Archives of Biochemistry and Biophysics* 345(1):1-9.
168. Bradfute DL & Simoni RD (1994) Nonsterol compounds that regulate cholesterogenesis - analogs of farnesyl pyrophosphate reduce 3-hydroxy-3-methylglutaryl-coenzyme-a reductase levels. *Journal of Biological Chemistry* 269(9):6645-6650.
169. Kumagai H, Chun KT, & Simoni RD (1995) Molecular dissection of the role of the membrane domain in the regulated degradation of 3-hydroxy-3-methylglutaryl coenzyme-a reductase. *Journal of Biological Chemistry* 270(32):19107-19113.
170. Pearce BC*, et al.* (1994) Inhibitors of cholesterol-biosynthesis .2. Hypocholesterolemic and antioxidant activities of benzopyran and tetrahydronaphthalene analogs of the tocotrienols. *J. Med. Chem.* 37(4):526-541.
171. Peffley DM & Gayen AK (1997) Inhibition of squalene synthase but not squalene cyclase prevents mevalonate-mediated suppression of 3-hydroxy-3-methylglutaryl coenzyme A reductase synthesis at a posttranscriptional level. *Archives of Biochemistry and Biophysics* 337(2):251-260.
172. Peffley DM & Gayen AK (2003) Plant-derived monoterpenes suppress hamster kidney cell 3-hydroxy-3-methylglutaryl coenzyme A reductase synthesis at the transcriptional level. *Journal of Nutrition* 133(1):38-44.
173. Tittiger C, Blomquist GJ, Ivarsson P, Borgeson CE, & Seybold SJ (1999) Juvenile hormone regulation of HMG-R gene expression in the bark beetle Ips paraconfusus (Coleoptera : Scolytidae): implications for male aggregation pheromone biosynthesis. *Cellular and Molecular Life Sciences* 55(1):121-127.
174. Tittiger C*, et al.* (2000) Isolation and endocrine regulation of an HMG-CoA synthase cDNA from the male Jeffrey pine beetle, Dendroctonus jeffreyi (Coleoptera : Scolytidae). *Insect Biochemistry and Molecular Biology* 30(12):1203-1211.
175. Tittiger C, Barkawi LS, Bengoa CS, Blomquist GJ, & Seybold SJ (2003) Structure and juvenile hormone-mediated regulation of the HMG-CoA reductase gene from the Jeffrey pine beetle, Dendroctonus jeffreyi. *Molecular and Cellular Endocrinology* 199(1-2):11-21.
176. Hall GM*, et al.* (2002) Midgut tissue of male pine engraver, Ips pini, synthesizes monoterpenoid pheromone component ipsdienol *de-novo*. *Naturwissenschaften* 89(2):79-83.
177. Hall GM*, et al.* (2002) Male Jeffrey pine beetle, Dendroctonus jeffreyi, synthesizes the pheromone component frontalin in anterior midgut tissue. *Insect Biochemistry & Molecular Biology* 32(11):1525-1532.

178. Blomquist GJ*, et al.* (2010) Pheromone production in bark beetles. *Insect Biochemistry and Molecular Biology* 40(10):699-712.
179. Keeling CI, Bearfield JC, Young S, Blomquist GJ, & Tittiger C (2006) Effects of juvenile hormone on gene expression in the pheromone-producing midgut of the pine engraver beetle, Ips pini. *Insect Molecular Biology* 15(2):207-216.
180. Keeling CI, Blomquist GJ, & Tittiger C (2004) Coordinated gene expression for pheromone biosynthesis in the pine engraver beetle, Ips pini (Coleoptera : Scolytidae). *Naturwissenschaften* 91(7):324-328.
181. Chun KT & Simoni RD (1992) The role of the membrane domain in the regulated degradation of 3-hydroxy-3-methylglutaryl coenzyme A reductase. *Journal of Biological Chemistry* 267(6):4236-4246.
182. Gil G, Faust JR, Chin DJ, Goldstein JL, & Brown MS (1985) Membrane-bound domain of HMG CoA reductase is required for sterol-enhanced degradation of the enzyme. *Cell* 41(1):249-258.
183. Sato R, Goldstein JL, & Brown MS (1993) Replacement of Serine-871 of Hamster 3-Hydroxy-3-Methylglutaryl-Coa Reductase Prevents Phosphorylation by Amp-Activated Kinase and Blocks Inhibition of Sterol Synthesis Induced by Atp Depletion. *Proceedings of the National Academy of Sciences of the United States of America* 90(20):9261-9265.
184. Omkumar RV, Darnay BG, & Rodwell VW (1994) Modulation of Syrian-Hamster 3-Hydroxy-3-Methylglutaryl-Coa Reductase-Activity by Phosphorylation - Role of Serine-871. *Journal of Biological Chemistry* 269(9):6810-6814.
185. Belles X (2010) Beyond drosophila: Rnai *in-vivo* and functional genomics in insects. *Annual Review of Entomology,* Annual Review of Entomology), Vol 55, pp 111-128.
186. Mito T, Nakamura T, Bando T, Ohuchi H, & Noji S (2011) The advent of rna interference in entomology. *Entomological Science* 14(1):1-8.
187. Terenius O*, et al.* (2011) RNA interference in Lepidoptera: An overview of successful and unsuccessful studies and implications for experimental design. *J. Insect Physiol* 57(2):231-245.
188. Ogura K (1975) Prenyltransferase. *Seikagaku* 47(9):808-820.
189. Ogura K & Koyama T (1998) Enzymatic aspects of isoprenoid chain elongation. *Chemical Reviews* 98(4):1263-1276.
190. Tholl D*, et al.* (2004) Formation of monoterpenes in *Antirrhinum majus* and *Clarkia breweri* flowers involves heterodimeric geranyl diphosphate synthases. *Plant Cell* 16(4):977-992.
191. Dawson GW*, et al.* (1987) Identification of an aphid sex-pheromone. *Nature* 325(6105):614-616.
192. Tholl D & Lee S (2011) Terpene specialized metabolism in *Arabidopsis thaliana*. *The Arabidopsis Book*, ed Last R (The American Society of Plant Biologists, Rockville, MD, USA), Vol 9, p e0143.
193. Hsiao YY*, et al.* (2008) A novel homodimeric geranyl diphosphate synthase from the orchid Phalaenopsis bellina lacking a DD(X)(2-4)D motif. *Plant Journal* 55(5):719-733.
194. Schmidt A*, et al.* (2010) A bifunctional geranyl and geranylgeranyl diphosphate synthase is involved in terpene oleoresin formation in picea abies. *Plant Physiol* 152(2):639-655.
195. Kaneko Y, Kinjoh T, Kiuchi M, & Hiruma K (2011) Stage-specific regulation of juvenile hormone biosynthesis by ecdysteroid in *Bombyx mori*. *Molecular and Cellular Endocrinology* 335(2):204-210.
196. Wang K & Ohnuma S (1999) Chain-length determination mechanism of isoprenyl diphosphate synthases and implications for molecular evolution. *Trends in Biochemical Sciences* 24(11):445-451.
197. Pan J-J, Ramamoorthy G, & Poulter CD (2013) Dependence of the product chain-length on detergents for long-chain e-polyprenyl diphosphate synthases. *Biochemistry* 52(29):5002-5008.
198. Pan JJ, Kuo TH, Chen YK, Yang LW, & Liang PH (2002) Insight into the activation mechanism of Escherichia coli octaprenyl pyrophosphate synthase derived from pre-

steady-state kinetic analysis. *Biochimica Et Biophysica Acta-Protein Structure and Molecular Enzymology* 1594(1):64-73.
199. Sen SE, Brown DC, Sperry AE, & Hitchcock JR (2007) Prenyltransferase of larval and adult *Manduca sexta* corpora allata. *Insect Biochemistry and Molecular Biology* 37(1):29-40.
200. Sen SE, Ewing GJ, & Childress M (1996) An *in-vitro* assay for monitoring prenyl transferase activity in lepidopteran corpora allata. *J. Agric. Food Chem.* 44(2):472-476.
201. Sen SE & Sperry AE (2002) Partial purification of a farnesyl diphosphate synthase from whole-body Manduca sexta. *Insect Biochemistry and Molecular Biology* 32(8):889-899.
202. Boland W & Garms S (2010) Induced volatiles of Medicago truncatula: molecular diversity and mechanistic aspects of a multiproduct sesquiterpene synthase from M. truncatula. *Flavour and Fragrance Journal* 25(3):114-116.
203. Garms S, Köllner TG, & Boland W (2010) A multiproduct terpene synthase from Medicago truncatula generates cadalane sesquiterpenes via two different mechanisms. *J. Org. Chem.* 75:5590 - 5600.
204. Picaud S, Olofsson L, Brodelius M, & Brodelius PE (2005) Expression, purification, and characterization of recombinant amorpha-4,11-diene synthase from Artemisia annua L. *Archives of Biochemistry and Biophysics* 436(2):215-226.
205. Landmann C, *et al.* (2007) Cloning and functional characterization of three terpene synthases from lavender (Lavandula angustifolia). *Archives of Biochemistry and Biophysics* 465(2):417-429.
206. Köllner TG, Schnee C, Gershenzon J, & Degenhardt J (2004) The variability of sesquiterpenes emitted from two zea mays cultivars is controlled by allelic variation of two terpene synthase genes encoding stereoselective multiple product enzymes. *The Plant Cell Online* 16(5):1115-1131.
207. Garms S (2010) Mechanistic studies on terpenoid synthases from Medicago truncatula. Ph.D. Thesis (Friedrich-Schiller-Universität Jena).
208. Kinjoh T, *et al.* (2007) Control of juvenile hormone biosynthesis in Bombyx mori: Cloning of the enzymes in the mevalonate pathway and assessment of their developmental expression in the corpora allata. *Insect Biochemistry and Molecular Biology* 37(8):808-818.
209. Boyd RS (2009) High-nickel insects and nickel hyperaccumulator plants: A review. *Insect Science* 16(1):19-31.
210. Boyd RS, Wall MA, & Jaffre T (2006) Nickel levels in arthropods associated with Ni hyperaccumulator plants from an ultramafic site in New Caledonia. *Insect Science* 13(4):271-277.
211. Gramigni E, *et al.* (2013) Ants as bioaccumulators of metals from soils: Body content and tissue-specific distribution of metals in the ant Crematogaster scutellaris. *European Journal of Soil Biology* 58(0):24-31.
212. Popham HR, Sun R, Shelby K, & Robertson JD (2012) Changes in trace metals in hemolymph of baculovirus-infected noctuid larvae. *Biol Trace Elem Res* 146(3):325-334.
213. Mesjasz-Przybyłowicz J & Przybyłowicz WJ (2011) PIXE and metal hyperaccumulation: from soil to plants and insects. *X-Ray Spectrometry* 40(3):181-185.
214. Smart KE, *et al.* (2010) High-resolution elemental localization in vacuolate plant cells by nanoscale secondary ion mass spectrometry. *The Plant Journal* 63(5):870-879.
215. Moore K, Lombi E, Zhao F-J, & Grovenor CM (2012) Elemental imaging at the nanoscale: NanoSIMS and complementary techniques for element localisation in plants. *Anal Bioanal Chem* 402(10):3263-3273.
216. Kobgyashi M (2001) Cobalt proteins involved in nitrile metabolism. *Journal of Inorganic Biochemistry* 86(1):63-63.
217. P. S, *et al.* (2010) A preliminary study on susceptibility of Escherichia coli strain nissle 1917 to transition metal stress. *Bio Science Research Bulletin* 26(2): 75-81.
218. Barceloux DG (1999) Cobalt. *Journal of Toxicology-Clinical Toxicology* 37(2):201-216.
219. Okamoto S & Eltis LD (2011) The biological occurrence and trafficking of cobalt. *Metallomics* 3(10):963-970.

220. Conklin DS, McMaster JA, Culbertson MR, & Kung C (1992) Cot1, a gene involved in cobalt accumulation in Saccharomyces cerevisiae. *Mol. Cell. Biol.* 12(9):3678-3688.
221. Reed MC, Lieb A, & Nijhout HF (2010) The biological significance of substrate inhibition: A mechanism with diverse functions. *BioEssays* 32(5):422-429.
222. Snyder JH & Qi XQ (2013) Biosynthesis metal matters. *Nature Chemical Biology* 9(5):295-296.

11 TABLE OF FIGURES

12 ACKNOWLEDGEMENTS

At this point I would like to express my gratitude to Prof. Dr. Wilhelm Boland, Dr. Antje Burse and Dr. Axel Schmidt for the excellent supervision of my work and the unquestionable confidence and liberty you offered me to follow my scientific ideas! You always share your creativity advices to support my projects and you were always helpful in profound discussions which lay the foundation of new ideas.

I thank Prof. Dr. Jonathan Gershenzon for kindly supporting me in revising our manuscripts, for very fruitful cooperation's and giving me the opportunity to perform huge amount of HPLC-Tandem MS measurements in his department (Biochemistry).

A special note of thanks I want to express to PD. Dr. Wolfgang Brandt from the Leibniz Institute of Plant Biochemistry (Halle) for the excellent collaboration regarding homology modeling, docking studies and the considerable calculations of all parameters which finally ended in a very good manuscript. I hope this good cooperation will continue in future.

In particular I want to express my heartfelt thanks to Raimund Nagel for a brilliant collaboration and for providing his skilled help with (the unbelievable amounts of nearly 10.000) HPLC-Tandem MS measurements (also during the night) and for lots of fruitful discussions.

I would like to thank all past and present members of the Department of Bioorganic chemistry for their support in any questions and for contributing to a productive atmosphere. In particular I am very thankful to:

Dr. Stefan Garms, Dr. Stefan Bartram and Abith Vattekkatte for remarkably help in terpene related questions,
Angelika Berg for rearing the beetles and being always a kind-hearted co-worker,
Kerstin Ploß for technical assistance in measuring of GC-MS samples,
Grit Winnefeld for always being helpful with administrative issues as the heart and soul of the department

I extend special thanks to the unexcelled “Beetle group” accompanying my way and providing a creative working atmosphere over the last years as well as supported substantially with their consolidated knowledge, advices, help and discussions at work and also aside research life. Therefore, simply thanks for being a friend Magdalena, Gerhard, Peter, Anja, Rene, Ding, Karla, Maritta, Matthias, Roy, Sabrina, Tobias.

I am thankful to Prof. Jacques M. Pasteels, an outstanding expert of the Biology of Chrysomelidae, for sending several beetles.

I thank all the little helpers (bachelor and HIWI´s) over the past years doing a fantastic job and promote my work a lot!

I thank the IT department, especially Marcel, the library team, especially Linda, and the administrative staff of the MPI for always uncomplicated and excellent help.

I want to address my thanks to all of my friends outside of the Institute to enrich my social life substantially. Thanks for being my companion Bianca, Heike, Uli, Nici, Rese, Katja, Ju, and all other marvelously friends who are not explained here in detail, you are too much :-)

An dieser Stelle möchte ich meine unbeschreibliche Dankbarkeit gegenüber meinen Eltern, Katrin Frick, Bernd Frick und Volker Wötzel, meinem Bruder Ronny Frick sowie meiner **gesamten** Familie aussprechen. Ihr standet in allen erdenklichen Lebenslagen stets hinter mir und meinen Entscheidungen. Ihr habt immer geholfen soweit es in eurer Macht stand und darüber hinaus! Vor allem in weitaus wichtigeren Belangen als reine finanzielle Unterstützung! Ihr habt einen grundlegenden Anteil am Gelingen der Promotion und habt mir so manchen Schnitzer in der letzten Zeit nicht krumm genommen. - **Danke!**

Daniel Rosenberger zusammen mit unserem Sohn Wendelin danke ich ganz Besonderes. Ich danke dir für die gemeinsamen Jahre, für uneingeschränktes Verständnis, das du immer da bist, wenn es brenzlig wird und ihr zusammen mein Leben bereichert mit Lebenslust, Frohsinn und Energie! Ohne deine Unterstützung wäre diese Arbeit wohl kaum möglich gewesen. Ich liebe euch!

13 SELBSTSTÄNDIGKEITSERKLÄRUNG

Hiermit erkläre ich, dass mir die geltende Promotionsordnung (§ 5 PromO) der Biologisch-Pharmazeutischen Fakultät der Friedrich Schiller Universität Jena bekannt ist. Die vorliegende Arbeit wurde selbständig und ohne unzulässige Hilfe oder Benutzung anderer als der angegebenen Hilfsmittel angefertigt. Übernommene Inhalte aus anderen Quellen und von anderen Personen, das in dieser Arbeit Verwendung fanden oder auf welche direkt Bezug genommen wird, sind als solches eindeutig kenntlich gemacht. Insbesondere wurden alle Personen genannt, die direkt an der Entstehung der vorliegenden Arbeit und den publizierten Manuskripten beteiligt waren.
Ich versichere, dass weder ein Promotionsberater in Anspruch genommen wurde, noch das Dritte unmittelbar noch mittelbar von mir geldwerte Leistungen für Arbeiten erhalten haben, die im Zusammenhang mit dem Inhalt der vorgelegten Dissertation stehen. Die vorgelegte Arbeit wurde zu keinem früheren Zeitpunkt, weder im Inland noch im Ausland in gleicher oder ähnlicher Form an einer anderen Prüfungsbehörde zum Zweck einer Promotion oder eines anderen Prüfungsverfahrens eingereicht.

Sindy Frick
Jena, den

14 Curriculum Vitae

Personal

Name:	Sindy Frick
Current address:	Camburger Strasse 36
	07743 Jena - Germany
Date of Birth:	06.02.1981
City of Birth:	Jena
Sex:	Female
Marital status:	single, 1 child
Nationality:	German

Academic Education

2011 –2013	Doctoral student
2007 – 2009	at Max Plank Institute for Chemical Ecology, Jena
	Department of Bioorganic Chemistry
	First supervisor: Prof. Boland
2006 – 2007	Diploma thesis
	at Max Plank Institute for Chemical Ecology, Jena
	Department of Bioorganic Chemistry
	First supervisor: Prof. Boland
2000 – 2007	Studies in Biology at Friedrich Schiller University, Jena (FSU Jena)
1999 - 2000	Studies in Biotechnology at Jena University of Applied Science (EAH Jena)

SCIENTIFIC PUBLICATION

JOURNAL ARTICLES

Frick S., Nagel R., Schmidt A., Bodemann R. R., Rahfeld P., Pauls G., Brandt W. G., Gershenzon J., Boland W., Burse A. (2013) Metal ions control product specificity of isoprenyl diphosphate synthases in the insect terpenoid pathway. *Proceedings of the National Academy of Sciences* 110(11):4194-4199.

Bodemann R. R., Rahfeld P., Stock M., Kunert M., Wielsch N., Groth M., **Frick S.**, Boland W., Burse A. (2012) Precise RNAi-mediated silencing of metabolically active proteins in the defence secretions of juvenile leaf beetles. *Proceedings. Biological sciences / The Royal Society* 279(1745):4126-4134.

Burse A., **Frick S.**, Discher S., Tolzin-Banasch K., Kirsch R., Strauß A., Kunert M., Boland W. (2009). Always being well prepared for defense: The production of deterrents by juvenile Chrysomelina beetles (Chrysomelidae). *Phytochemistry* 70: 1899-1909.

Burse A., **Frick S.**, Schmidt A., Buechler R., Kunert M., Gershenzon J., Brandt W. G., Boland W. (2008) Implication of HMGR in homeostasis of sequestered and *de-novo* produced precursors of the iridoid biosynthesis in leaf beetle larvae. *Insect Biochemistry & Molecular Biology* 38 (1): 76-88.

Burse A., Schmidt A., **Frick S.**, Kuhn J., Gershenzon J. and Boland W. (2007) Iridoid biosynthesis in Chrysomelina larvae: Fat body produces early terpenoid precursors. *Insect Biochemistry & Molecular Biology* 37(3): 255-265.

ORAL PRESENTATIONS

Frick S. (2013) Metal ions control chain-length specificity of isoprenyl diphosphate synthases in insects. *TERPNET 2013 - 11th International Meeting on Biosynthesis, Function and Biotechnology of Isoprenoids in Terrestrial and Marine Organisms; COST Action FA1006 "Plant Engine"; COST Action FA1106 "QualityFruit"; EU-SMARTCELL,* Kolympari, Crete GR

Frick S. (2012) Iridoid biosynthesis in leaf beetle larvae - Metal cofactors control chain-length of an Isoprenyl diphosphate synthase from *Phaedon cochleariae*. *28th ISCE Meeting, International Society of Chemical Ecology*, Vilnius LT

Frick S. (2012) Metal cofactors control chain-length of an Isoprenyl diphosphate synthase from the horseradish leaf beetle *43. Doktorandenworkshop Naturstoffe: Chemie, Biologie und Ökologie*, Halle (Saale) DE

Frick S. (2008) Identification of branch point enzymes within the iridoid biosynthesis in Chrysomelina larvae *Phaedon cochleariae*. *36. Doktorandenworkshop: Naturstoffe: Chemie, Biologie und Ökologie,* Universität Würzburg, Würzburg DE

Frick S. (2008) *De-novo* biosynthesis versus sequestration: Regulation of iridoid biosynthesis in leaf beetles. *ICE Symposium*, MPI for Chemical Ecology, Jena DE

Frick S. (2008) Identification of branch point enzymes within the iridoid biosynthesis in Chrysomelina larvae *Phaedon cochleariae 6. Kurt-Mothes-Workshop "Sekundär-stoffwechsel"* MPI for Chemical Ecology, Jena DE

Frick S. (2008) Identification of Branch Point Enzymes within the Iridoid Biosynthesis in Chrysomelina Larvae *Phaedon cochleariae*. *24th ISCE Meeting, International Society of Chemical Ecology*, State College US

Frick S. (2007) Implication of HMGR in homoeostasis of sequestered and *de-novo* produced precursors of the iridoid biosynthesis in leaf beetle larvae. *34. Doktorandenworkshop: Naturstoffe: Chemie, Biologie und Ökologie*, Halle (Saale) DE

Poster Presentations

Frick S., Nagel R., Rahfeld P., Schmidt A., Brandt W., Gershenzon J., Boland W., Burse A., (2013) Metal ions control chain-length specificity of isoprenyl diphosphate synthases in insects. *25. Irseer Naturstofftage*, Irsee DE,

Frick S., Kunert M., Boland W., Burse A., (2012) Terpenoid biosynthesis in leaf beetle larvae. *SAB Meeting 2012*, MPI for Chemical Ecology, Jena DE

Frick S., Kunert M., Boland W. (2011) Chemical defense: Terpenoid biosynthesis in leaf beetle larvae. *ICE Symposium*, MPI for Chemical Ecology, Jena DE

Burse A., **Frick S.,** Bodemann RR., Kirsch R., Kunert M., Pauls G., Shaheed M., Stock M., Strauß A., Tolzin-Banasch K., Boland W. (2010) Leaf beetles – Adaptation to their host plants and exploitation of phytochemicals. *SAB Meeting 2010*, MPI for Chemical Ecology, Jena DE

Frick S., Burse A., Schmidt A., Boland W. (2009) HMG-CoA-Reductase and Isoprenyl Diphosphate Synthase Regulate Iridoid Biosynthesis in Chrysomelina Larvae. *25th ISCE Meeting, International Society of Chemical Ecology*, Neuchâtel CH

Frick S., (2009) HMG-CoA-reductase and isoprenyl diphosphate synthase regulate iridoid biosynthesis in Crysomelina larvae. *ICE Symposium*, MPI for Chemical Ecology, Jena DE

Burse A., **Frick S.**, Discher S., Kirsch R., Kunert M., Stock M., Strauss A., Tolzin K., Boland W. (2009) Chemical Defense in Leaf Beetle Larvae. *ICE Symposium*, MPI for Chemical Ecology, Jena DE

Frick S., Burse A., Schmidt A., Boland W. (2009) HMG-CoA-reductase and isoprenyl diphosphate synthase regulates iridoid biosynthesis in Chrysomelina larvae. *TERPNET 2009 - 9th International Meeting: Biosynthesis and Function of Isoprenoids in Plants, Microorganisms and Parasites*, The University of Tokyo, Graduate School of Pharmaceutical Sciences, Tokyo JP

Frick S., Kunert M., Burse A., Bartram S., Boland W. (2008) *De-novo* synthesis versus sequestration of defensive compounds in leaf beetle larvae. *SAB Meeting 2008*, MPI for Chemical Ecology, Jena DE

Frick S., Schmidt A., Kunert M., Büchler R., Boland W., Burse A. (2007) Iridoid biosynthesis in leaf beetle larvae – regulation of HMG-CoA reductase by biosynthesis metabolites and plant derived compounds. *Herbsttagung der Gesellschaft für Biochemie und Molekularbiologie*, Hamburg DE

Frick S., Schmidt A., Kunert M., Büchler R., Boland W., Burse A. Iridoid biosynthesis in leaf beetle larvae – regulation of HMG-CoA reductase by biosynthesis metabolites and plant derived compounds. *23rd ISCE Meeting, International Society of Chemical Ecology*, Jena DE